Title
ON THE NATURE OF THE SECONDARY STRUCTURE OF SINGLE-STRAND RNA

Author
Jaskunas, Stanley Richard

Publication Date
1968-03-01

UCRL-18136
ej. 2

University of California

Ernest O. Lawrence Radiation Laboratory

ON THE NATURE OF THE SECONDARY STRUCTURE OF SINGLE-STRAND RNA

Stanley Richard Jaskunas, Jr.

March 1968

DISCLAIMER

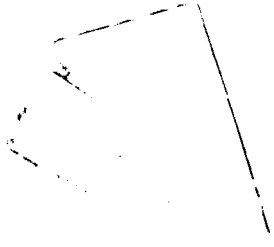

UCRL-18136

UNIVERSITY OF CALIFORNIA

Lawrence Radiation Laboratory
Berkeley, California

AEC Contract No. W-7405-eng-48

ON THE NATURE OF THE SECONDARY STRUCTURE OF SINGLE-STRAND RNA

Stanley Richard Jaskunas, Jr.

(Ph. D. Thesis)

March 1968

Acknowledgements

My association with Dr. I. Tinoco, Jr., during the course of my graduate studies has been very stimulating and rewarding. I am especially grateful to him for awakening in me a latent fascination for nucleic acids and suggesting possible directions for fruitful research.

All of the experiments described in Part III of this dissertation were made possible by the generosity of Dr. Michael Chamberlin. He provided laboratory space, the seed DNAs, a seemingly inexhaustible supply of RNA polymerase and DNA polymerase, and the necessary technical information and guidance.

We are grateful to Dr. Stanley Mandeles for the procedures used in the preparation of oligoribonucleotides by specific enzymatic hydrolysis and column chromatography. He has also given us generous amounts of oligoribonucleotides and TMV RNA on several occasions.

Dr. John Hearst, Dr. Horace Gray, and Mr. Frank Rinehart have liberally given of their time and knowledge in helping us determine molecular weights by equilibrium sedimentation.

We have benefited from fruitful collaboration with Dr. Charles Cantor and Dr. David McMullen. Numerous discussions with Dr. Robert Davis, Mr. David Lloyd, Mr. Barrett Tomlinson, Dr. Sunil Podder, Dr. Myron Warshaw, Dr. Marc Maestre, Dr. Curtis Johnson, Dr. Martin Itzkowitz, Mr. Dana Carroll, Dr. Steve Davis, Mr. Jean Thiery,

Miss Arlene Blum, and Dr. Rodney Biltonen have also been stimulating and helpful.

We are grateful to Dr. Robert Davis for giving us the unpublished data from his studies on the temperature dependence of the ORD of dimers and monomers. Dr. Tom Mahan wrote the Fortran programs so that we could calculate the ORD of single-strand polyribonucleotides as a function of temperature from the data on the dimers and monomers.

F2 RNA, R17 RNA, and RF-MS2 RNA were gifts from Dr. M. Takanami, P. Kaesberg, and H. Kamen, respectively.

Expert technical assistance has been provided by Mrs. Barbara Dengler in the preparation of oligoribonucleotides and polynucleotide phosphorylase. Mrs. Susan Dreyfuss Emberton has also been helpful, especially in the smoothing of innumerable optical rotation spectra by hand.

We would also like to acknowledge the expert assistance given by Mrs. Nancy Monroe in the preparation of this dissertation. She has carefully prepared all the figures and typed the final manuscript.

Finally, I would like to express my great appreciation to my wife, Sharron, whose love has made the writing of this dissertation and the research that preceded it a true joy.

Table of Contents

Table of Contents (Continued)

Table of Contents (Continued

Table of Contents (Continued)

Table of Contents (Continued)

On The Nature Of The Secondary Structure of Single-Strand RNA

Stanley Richard Jaskunas, Jr.

ABSTRACT

Base stacking and base pairing in single-strand RNA have been investigated. The ultraviolet optical rotatory dispersion of tobacco mosaic virus RNA, F2 RNA, R17 RNA, and mixed yeast tRNA have been measured in the presence and absence of salt at 25°C, pH 7. The optical rotatory dispersion of tobacco mosaic virus RNA has also been measured as a function of temperature at four different ionic strengths. All of these optical rotation spectra have been compared with that expected for a random coil in which there is no preferred orientation of neighboring bases and with that expected for a single-strand helix with stacked bases. The optical rotation spectra of all the RNA samples in the absence of salt are close to the calculated spectra of the stacked conformation. For tobacco mosaic virus RNA, agreement with these calculations has been found at low ionic strengths and high temperatures. The lowest temperature for which there is agreement increases with increasing ionic strength. These results indicate that, in the absence of hydrogen-bonded base pairs, the bases in single-strand RNA are stacked. The stacked conformation approaches a random coil as the temperature is increased.

Nevertheless, the bases still have a preferred orientation at 80°C. The deviations from the expected optical rotatory dispersion of the stacked conformation at low temperature and high ionic strength appear to be the result of A-U and G-C base pairs.

Attempts have been made to study the optical and thermodynamic sequential properties of double-strand RNA using specific 1:1 complexes of complementary oligoribonucleotides. Several pairs of complementary oligoribonucleotides have been mixed under conditions favorable for intermolecular association. Interaction between GpGpC and GpCpC has been observed. Other pairs of complementary oligoribonucleotides have been mixed under similar conditions but no interaction has been observed. These included ApCpU and ApGpU, ApGpC and GpCpU, and ApApApA and UpUpUpU. Self-aggregation has been observed with GpGpC and ApGpC. These results suggest the ribosome or tRNA structure must help to stabilize complexes between the anticodon and mRNA. Calculation of the stability of triple-strand regions in tRNA like $(GpGpC)_2$:GpCpC indicate such structures could exist.

The sequential properties of double-strand RNA can also be studied with 1:1 complexes of complementary polyribonucleotides containing repeating sequences. Poly rAC and poly rUG have been prepared by RNA polymerase transcription of poly dAC:dTC, one strand at a time. Preliminary optical rotation and absorption properties of poly rAC at pH 7

indicate it has a stacked conformation. Poly rUG at pH 7, however, may contain U-G base pairs.

INTRODUCTION

Our ability to control life for good or evil depends on our understanding of the forces that affect it and how they are applied. Scientists have found it useful to approximate the whole by the sum of the parts. Thus, we see life as a complex of matter and energy precisely organized in space and time and regulated by the same forces as affect inanimate matter. Understanding life in this context requires an understanding of the specificity of biological molecules and the reactions in which they participate.

In a general way the work that is described in this dissertation has as its goal an understanding of the specificity of tRNA. The actual goal is to aid in the understanding of the secondary structure of single-strand RNA, including rRNA and mRNA as well as tRNA.* Secondary structure refers to the relative spatial orientation of residues that are close to one another along the chain. For us, it shall refer to the stacking of adjacent bases and the base pairs that form when a polynucleotide chain folds back upon itself. Tertiary structure shall refer to the relative orientation of the loops that are held together by these short double-strand helical regions. We justify

---

*Abbreviations used in this dissertation can be found in Appendix A.

our experiments as being particularly relevant for tRNA because the importance of structure for specificity is more clearly understood for tRNA than for mRNA or rRNA.

Every tRNA molecule is specific for a particular amino acid.[1] It will only accept that amino acid from an amino acyl synthetase and it will then transfer that amino acid to a growing polypeptide chain in an order dictated by mRNA. How does a tRNA molecule distinguish between an amino acyl synthetase carrying that amino acid and enzymes carrying any other amino acid? How does the mRNA determine the order in which amino acids are transferred to a growing polypeptide chain?

We already have a good understanding of how mRNA dictates the sequence of amino acids in a polypeptide. The genetic message of mRNA is read as a sequence of nonoverlapping triplets[2] starting from some beginning point[3-5] to an end.[6] Transfer RNA molecules recognize the triplet that corresponds to their amino acid.[5] The mechanism of recognition is thought to be the base pairs that form between the codon triplet and a special triplet on the tRNA called the anticodon or nodoc. According to the Wobble hypothesis of Crick,[7] the first two bases of the codon triplet, in the direction that the message is read, form normal Watson-Crick base pairs, A-U, G-C, and I-C, with two bases of the anticodon. The third base of the codon also forms a base pair with the third base of the anticodon. Non-Watson-Crick base pairs are possible in this position

because of the wobble or additional freedom of the third base of the anticodon. Fuller and Hodgson[8] have recently suggested a molecular bases for the wobble. In summary, we have a good understanding of the molecular basis for the specific interaction of tRNA and mRNA.

By contrast, we have no satisfying explanation of the specificity in the reaction of tRNA and amino acyl synthetases. Experiments by Hayashi and Miura[9] indicate that the amino acyl synthetase recognizes the anticodon. They found that oligoribonucleotides that are complementary to the codons for a particular amino acid competitively inhibit the interaction of the tRNA and amino acyl synthetase for that amino acid. The oligomer is presumably competing with the anticodon of the tRNA for a site on the enzyme. Experiments with polynucleotides by Deutscher[10] and Letendre et al.[11] have not confirmed this hypothesis. They found that a polynucleotide complementary to the codon of some amino acid does not always inhibit the transfer of that amino acid more than other polynucleotides. Letendre et al.[11] found that poly G inhibits more strongly than poly A, poly C, and poly U for all the transfer reactions that were studied. Perhaps the best experiment to determine whether the anticodon is the recognition site would be with a homogeneous tRNA preparation in which only the anticodon has been modified. Unfortunately, chemical or genetic methods are not yet available to selectively modify one or two residues in a tRNA.

It appears that tRNAs differ from one another in their interaction with mRNA because they have different sequences of bases in a position on the molecule called the anticodon. They may differ from one another in their interaction with amino acyl synthetases for the same reason. In other words, the specificity of tRNA molecules may be determined directly by their primary structure.

Nevertheless, there is evidence that a correct three-dimension structure of tRNA is essential for its biological functions. Fresco and collaborators[12-14] have trapped a leucine tRNA from yeast in a structure that is inactive when assayed *in vitro* for leucine acceptance activity, terminal adenosine acceptance activity, and transfer of leucine to a growing polypeptide chain. Biologically active leucine tRNA is converted to the inactive or denatured state by heating at 60°C in the presence of EDTA. The transformation does not involve any change in the primary structure since it is reversible by heating at 60°C in the presence of excess magnesium ions. The sedimentation and viscosity properties of the native and denatured states show that the native state is more compact. The denatured tRNA apparently has a shape that cannot be recognized by leucine amino acyl synthetase, the tRNA adenylyltransferase, and the ribosome-mRNA complex. An arginine tRNA from yeast has also been trapped in the denatured state. Also, tRNAs from *E. coli* for glutamine, histidine, tryptophan, glutamic acid, and possibly leucine have been caught in inactive structures.

All of these tRNAs are inactive to amino acid acceptance when they are in the denatured state. Only leucine tRNA from yeast has been assayed for its ability to transfer its amino acid to a growing polypeptide chain. Suioka and collaborators[15a,15b] have found a tryptophan tRNA from E.coli that can also be caught in an inactive state. These experiment have been sufficiently universal and unambiguous to convince us that a precise three-dimensional structure is essential for the biological activity, if not the specificity, of tRNA. Thus, it is important that we know and understand the secondary and tertiary structure of tRNA molecules.

The sequence of an alanine tRNA from yeast was determined in 1965 by Holley et al.[16] This was the first primary structure of a native RNA to be determined. From the sequence it can be seen that if the polynucleotide chain folds back upon itself several A-U and G-C base pairs can form between the antiparallel chains. These base pairs would be analogous to the Watson-Crick base pairs in DNA. Depending on where the chain is folded, several patterns of base pairs are possible. The one considered to be the closest approximation to reality[17,18] is shown schematically in Figure 1.[19] There are three loops closed by short helical regions. A fourth double-strand region forms from complementary residues near the ends of the molecule. For obvious reasons, this is termed the clover-leaf model of the

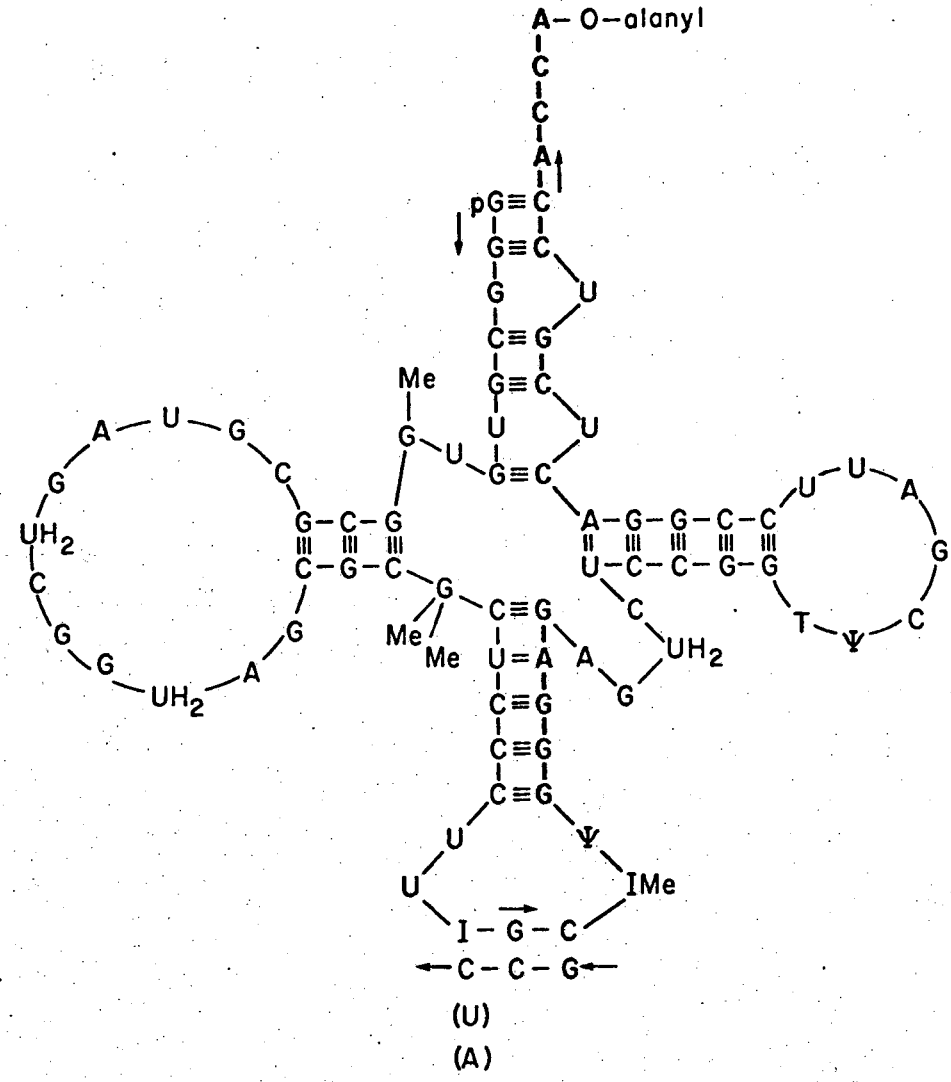

Figure 1. Possible secondary structure of year alanine t-RNA. The proposed anticodon is shown antiparallel and complementary to the messenger coding triplet (from Jukes[19]).

secondary structure of tRNA. An alanine codon is shown antiparallel and complementary to a possible anticodon triplet. A similar pattern of base pairs can be constructed for each of the four other tRNAs from yeast that has been sequenced, serine $tRNA_I$,[20] serine $tRNA_{II}$,[20] phenylalanine tRNA,[21] and tyrosine tRNA.[22]

Our experiments were designed to help us understand RNA secondary structure in general and not the secondary structure of any particular RNA molecule. The three classes of RNA, tRNA, mRNA, and rRNA, differ by definition in their function.[1,23,24] Chemically, they are polymers of mainly the same subunits, A, U, C, and G. No other residues are found in mRNA. Ribosomal RNA from E. coli contains only a few percent methylated or other odd bases.[25] Transfer RNA has the highest composition of odd bases. Even for these RNAs most of the residues are one of the four common bases. Bulk tRNA from yeast contains 9% odd bases.[26] The principles describing the contribution of the four common bases to the secondary structure will presumably be the same for all classes of RNA. Therefore, our experiments, which have been done with mRNA and synthetic oligoribonucleotides of the four common bases, will be relevant to tRNA, rRNA, and mRNA.

We ask, what is the nature of the secondary structure of a polyribonucleotide composed of A, U, C, and G residues? We shall strive to answer this question with a set of rules describing the interaction of the four common residues in RNA.

This is the approach of many physical biochemists who are striving to ascertain and evaluate the various forces that affect the structure of biological macromolecules. The goal is to be able to predict the correct secondary and tertiary structure of such a molecule from its primary structure. If for no other reason, our attention is directed to tRNA because the primary structure of five of these molecules is known. The primary structure is not known for any mRNA or rRNA. The sequences of two 5S RNAs are known[27,28] but their function is still obscure. Thus, whatever we learn from our experiments can be applied directly to making specific predictions about the secondary structure of a particular tRNA molecule. These predictions can be tested since homogeneous preparations of the molecules are available.

Our studies can be divided into three parts. In the first section we examine the nature of the secondary structure of single-strand RNA under conditions where it does not contain any intramolecular base pairs. Many investigators have found evidence for base pairs in RNA. Residues which are not base-paired have been considered to have a random conformation.[29-31] In other words, there is no preferred orientation of the unpaired base with respect to its adjacent neighbors. Our experiments show that bases in RNA which are not hydrogen-bonded to other bases have an average preferred orientation called stacked. In this conformation the planes of neighboring bases are parallel to one another

and the bases are on top of one another. Furthermore, stacking is also important in determining the secondary structure of a single-strand RNA under conditions where base pairs exist.

Our conviction that information like this can be useful in elucidating the nature of the specificity of tRNA molecules was confirmed in a recent communication by Fuller and Hodgson.[8] They present a stereochemical basis for Crick's "wobble" hypothesis[7] concerning the interaction of codon and anticodon. Their explanation of the hypothesis follows principally from the assumption that the number of stacked bases in the anticodon loop of the clover-leaf model should be a maximum. Of course, their proposed conformation of the anticodon loop has not been shown to be correct. Nevertheless, the results are very encouraging.

Our measurements of single-strand RNA under conditions favorable for base pairs are consistent with the presence of A-U and G-C base pairs. But much more specific information is needed. Is it reasonable to expect helical regions as short as those proposed in the clover-leaf model? Even more to the point, is the base-pairing arrangement of the clover-leaf model correct? These questions can conceivably be answered by studying the optical and thermodynamic properties of double-strand RNA as a function of sequence and number of base pairs. One method of doing this is with 1:1 complexes of complementary oligoribonucleotides. The preparation of suitable oligomers is described in the second

section of this dissertation. However, we found that the 1:1 complexes of these oligomers were so unstable that they could not be studied conveniently. A 2:1 complex was observed to form between GpGpC and GpCpC. Estimates of the stability of double-strand regions in tRNA indicate that 3 G-C base pairs is the minimum length. Thus, the helical regions in the clover-leaf model of tRNA are at least reasonable. However, triple-strand regions of 2G:C base triplets are estimated to be just as stable. This suggests that there may be triple-strand regions in tRNA.

In the last section we turn to complexes of synthetic complementary polyribonucleotides as a method of studying the sequential properties of double-strand RNA. Only the preparation of these model compounds is discussed in detail. Preliminary experiments concerning the optical properties of the polyribonucleotides are reported. The actual studies of the double-strand complexes await further experimentation.

PART I

ELEMENTS OF SECONDARY STRUCTURE IN RNA

Introduction

The "clover-leaf" model of the secondary structure of tRNA shown in Figure 1 is a schematic representation of a possible pattern of base pairs. It says nothing about the conformation of the unpaired bases in the loops and between the helical regions. This reflects a general attitude that the stability of the DNA double-strand helix is due to hydrogen-bonded base pairs; therefore, the only important elements of secondary structure in nucleic acids are base pairs.

There have been suggestions that the stability of the DNA helix is due to forces other than hydrogen bonds. The planes of neighboring bases in DNA are parallel, and the bases are as close to each other as van der Waals radii will permit. In other words, the bases are stacked. Theoretical calculations of the free energy in DNA resulting from dipole-dipole, dipole-induced dipole, and London force interactions between the stacked bases have been made by DeVoe and Tinoco.[32] They found that these forces contribute up to -19.8 kcal/base pair to the stability of the helix compared to separated single-strand helices with unstacked bases. The contribution from hydrogen bonds was estimated at 0 ± 1.5 kcal/hydrogen bond. These calculations indicated that the stability of the DNA helix is mainly due to the

electrostatic interaction of stacked bases. Crothers and Zimm[33] have also suggested that DNA is stabilized by stacking. The conclusion is derived from their statistical treatment of the helix-coil transition of helical complexes of synthetic polydeoxyribonucleotides. However, Sinanoglu and Abdulner[34] contend that the DNA helix is stable in water compared to the separated single strands because the surface area between water and the nucleic acid is less.

These studies point out that there are forces other than hydrogen bonds that are important in determining the secondary structure of nucleic acids. There is some question as to the precise molecular origin of these forces. Actually, both van der Waals interactions between aromatic bases and surface tension forces are probably operative. The important thing is that these forces are operative in the presence or absence of hydrogen bonds. The prediction is that the bases of single-strand nucleic acids are confined to geometries in which they are at least partially stacked.

The purpose of the experiments to be presented in Part I is to test whether this prediction is true for RNA. Evidence will be outlined which indicates the bases of single-strand oligoribonucleotides and polyribonucleotides are stacked. With this in mind the evidence for base pairs in single-strand RNA will be reviewed. Although some of the observations could be interpreted as due to base stacking, the preponderance of the experiments can only be explained by base pairs. Cantor's semi-empirical method[35-37] for

calculating the optical rotatory dispersion (ORD) of single-strand helices with stacked bases will be reviewed. It will be used to show that bases in TMV RNA, F2 RNA, R17 RNA, and mixed yeast tRNA are stacked under conditions that are unfavorable for the formation of base pairs. It will be argued that base stacking is also important under conditions where base pairs occur. Finally, the ORD of single strand RNA under these conditions will verify the existence of A-U and G-C base pairs.

Base Stacking in Single-Strand Oligoribonucleotides and Polyribonucleotides

1. Oligoribonucleotides

One method of detecting the existence of stacked bases is with ultraviolet absorption spectroscopy. The molar absorption of an aggregate of stacked chromophores will be less than the average for the constituent monomer chromophores.[38-40] This phenomenon is called hypochromism if we compare the area of the absorption band and hypochromicity if we compare the absorption at a particular wavelength. The hypochromism of DNA was at one time thought to be the result of hydrogen bonding.[42] This view stemmed from the observation that a sharp decrease in the hypochromicity paralells the helix-coil transition. Theories of hypochromism,[38,39] however, show that it results from base stacking and not hydrogen bonding. The theory predicts that stacked bases are hypochromic regardless of whether they

are hydrogen-bonded. Therefore, if base pairing can be ruled out, the existence of hypochromism or hypochromicity is evidence for a single-strand stacked structure.

Hypochromism has been observed for dinucleoside phosphates,[41,43,44,48] trinucleoside diphosphates,[35,45,46,41] and homo-oligonucleotides of adenine[47,49] and cytidine.[50,51] In all cases the solutions that were used to measure the absorption spectra were always dilute in nucleosides, approximately 10^{-4} M. Warshaw and Tinoco[43] showed that there is no aggregation of dinucleoside phosphates at this concentration. They found that the molecular weight of GpC, as measured by sedimentation equilibrium, was that expected for the unaggregated dimer. We expect this dimer to aggregate more readily than most of the other oligomers because G-C base pairs could form. Therefore, we can assume there is no intermolecular aggregation in any of the solutions.

The optical rotatory dispersion[35,43-45,50,52-54] and circular dichromism[51,55,92] of many of these oligomers are also different from the properties of the constituent monomers.[56] Not only is the shape different, but the magnitude of the rotation is usually larger for the oligomer than the monomer. For example, the ORD of ApA[43,52,57] is a double Cotton effect with the long wavelength extremum having a positive rotation. The sum of the ORD of A and pA is a single Cotton curve with the long wavelength extremum having a negative rotation. These two curves are

shown in Figure 2. The magnitude of the peak-to-trough rotation is seven times larger for the dimer than for the monomer. If the oligomers are not aggregated, then this difference is probably the result of intramolecular interaction between the bases.

The shape of the ORD of these oligomers is consistent with what is predicted by ORD theory.[58] A dimer of two identical chromophores in parallel planes is expected to have a double Cotton effect ORD. The central peak or trough will occur at the same wavelength as the absorption maximum. The sign and magnitude of the curve depends on the details of the geometry of the stacked bases. The ORD of ApA has been calculated for the geometry of one strand of a DNA helix.[52,59] The shape of the calculated curve is essentially identical to the experimental ORD. Thus, it was concluded that ApA forms the beginning of a right-handed single-strand helix with stacked bases perpendicular to the helix axis.

The temperature dependence of hypochromism,[60] hypochromicity,[47-49] circular dichromism,[48,51,55] and optical rotation[50,53,54,60] of oligoribonucleotides has provided further insight into the nature of base stacking. The hypochromism, hypochromicity, rotational strength, and magnitude of rotation at the peak and trough decrease gradually as the temperature is increased. The data have frequently been analyzed in terms of a two-state model.[47-49,53,55,60] The oligomer is assumed to be either completely stacked or

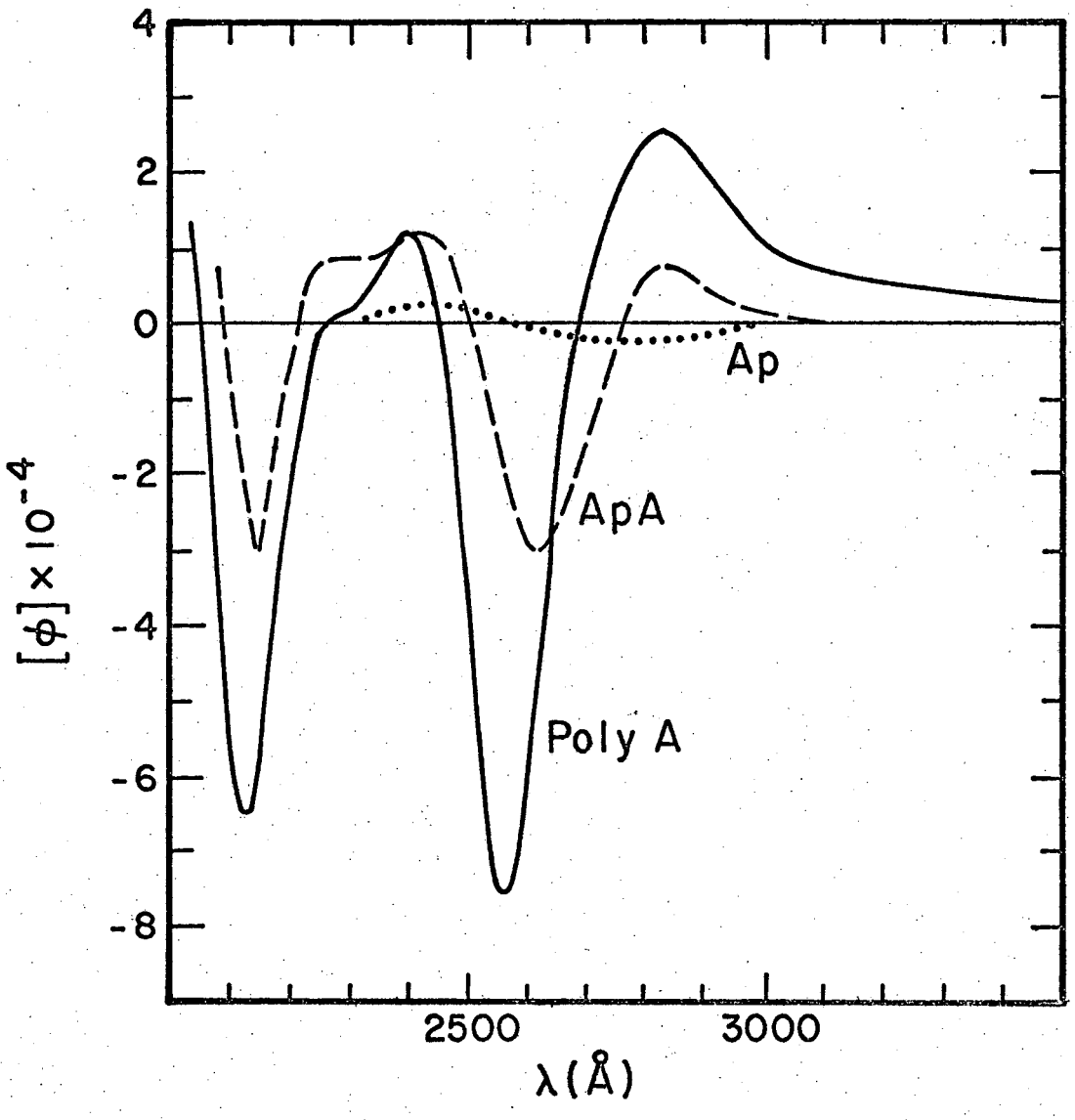

Figure 2. ORD of poly A at 22°C, 0.15 M KCl, pH 7; Ap at 25°C, pH 5.9; and ApA at 25°C, pH 5.9. The molar rotations per residue, [φ], are in units of degrees milliliter/decimeter mole × 10^{-2}. Under these conditions, poly A and ApA are single-strand helices. (Taken from Holcomb and Tinoco.[57])

unstacked. The fully stacked structure is envisioned to be quite rigid. The enthalpy of stacking has been determined by choosing appropriate values for the rotation and hypochromicity of the fully stacked and unstacked structure.

A more realistic interpretation of the temperature dependence is that the average relative orientation of neighboring bases becomes gradually more random as the temperature is increased. From the theory of hypochromism[38] and optical rotatory dispersion we can see what types of changes in base stacking would result in the observed phenomenon. The magnitude of hypochromism depends on the distance between the stacked bases. Therefore, a decrease in hypochromism or hypochromicity may reflect an increase in the average distance between neighboring bases. Optical rotation also depends on this distance. But it also should be affected by relative rotational oscillations about an axis which is perpendicular to the plane of the stacked bases. The greater these oscillations and the less time spent in the preferred orientation the smaller the rotation. Mathematical methods have been developed to analyze the temperature dependence of hypochromicity and optical rotation[61,62] in terms of these molecular mechanisms. Davis and Tinoco[60] have applied them to the data for dinucleoside phosphates.

We shall refer to the conformation of single-strand oligoribonucleotides and polyribonucleotides at all temperatures as stacked. In this context, stacking merely refers

to the existence of a preferred relative orientation of neighboring bases in which, on the average, the planes of the bases are parallel. We realize that the particular nature of the stacking varies with temperature. Nevertheless our convention is realistic since Davis and Tinoco[60] have shown that the bases in ApA are still stacked at 90°C.

Other evidence for stacking has come from the work of Chan, Ts'o, and their colleagues.[63-67] Using nuclear magnetic resonance (NMR) and vapor pressure osmometry, they have shown that nucleic acid bases and nucleosides associate in aqueous solution by stacking. Self-association of purines is greater than the self-association of pyrimidines. The interactions of purines and pyrimidines are intermediate.

NMR techniques have also been used by Chan et al.[68] to show that the bases of the dideoxynucleoside phosphate, TpT, are stacked. Reference is made in the same report to more extensive and unpbulished NMR studies of other dimers which indicate that the bases are stacked in aqueous solution.

2. Poly A

There is good evidence that poly A at room temperature and pH 7 is a single-strand helix with stacked bases. Holcomb and Tinoco[57] have presented ORD data as evidence for this structure. Poly A displays a double Cotton effect under these conditions with a deep trough which occurs at the same wavelength as the absorption maximum. This is the shape which is expected for a single-strand helix with stacked bases

perpendicular to the helix axis.[116] If there are base pairs then the shape of the curve will probably be different. In fact, the shape of the ORD of the double-strand helix of poly A, which forms at low pHs, is different from the ORD of poly A at neutral pH.[57]

Furthermore, the ORD and hypochromism of neutral solutions of poly A at room temperature can essentially be derived from the ORD and hypochromism of ApA under the same conditions. As seen in Figure 2, the shape of the ORD for the two molecules is the same. However, the magnitude of the rotation per mole of residue is larger for the polymer than the dimer. Similarly, the hypochromism of poly A is greater than the hypochromism of ApA. These observations are not surprising, of course. In the first place, each base in the polymer is surrounded by two other bases instead of only one. Additional long-range interactions between bases which are separated by one or more residues along the chain will further increase the magnitude of the rotation and hypochromism of the polymer compared to the dimer. The nearest-neighbor approximation assumes that these additional interactions are negligible. If the average dimer in the polymer has the same geometry as the average dimer which is free in solution and the nearest-neighbor approximation is valid, then the rotation and hypochromism of the polymer will be twice that of the dimer. What is found is that the hypochromism of the polymer is 2.9 times that of the dimer and the rotation at the trough is 2.5 times that of the dimer.

Holcomb and Tinoco[57] point out that if, instead of the nearest-neighbor approximation, we assume that the interaction between bases depends only on the inverse cube of the distance between bases, then the hypochromism and rotation of the polymer will be 2.4 times that of the dimer. Being able to adequately account for the optical properties of the polymer in this manner indicates that the relative orientation of neighboring bases is similar in the polymer and dimer. Since the bases in the dimer are stacked this implies that the bases are stacked in the polymer.

There are three important conclusions from the paper by Holcomb and Tinoco.[57] The first is that poly A at pH 7 is a single-strand helix with stacked bases. Second, the geometry of the polymer and dimer are similar. Poly A may be thought of as a poly – ApA. The bases in the dimer are stacked so as to form the beginning of a right-handed single-strand helix. The polymer is a continuation of this structure. Finally, as a result of this similarity, we can calculate the optical properties of the dimer.

Low angle x-ray scattering experiments on neutral solutions of poly A by Luzzati et al.[69] have also provided important evidence for a single-strand helix with stacked bases. They found that the number of bases per unit length of the molecule is one-half of that for the DNA double-strand helix. They point out that the same observation would be made if the polynucleotide chain is folded over and bases are intercalated. This seems unlikely, however. We

would expect that the ORD of such a structure would have a different shape than the ORD of ApA.

McDonald and Phillips[70] have measured the nuclear magnetic resonance of neutral solutions of poly A as a function of temperature. They conclude that the bases are partially stacked at room temperature.

The structure of poly C is also thought to be a single-strand helix with stacked bases. Fasman et al.[71] have shown that the temperature dependence of the ORD of formylated poly C, which cannot form base pairs, is the same as for unformylated poly C. It has also been shown that the ORD of neutral solutions of poly C can be calculated from the ORD of CpC[36] in the same manner as the ORD of poly A was calculated from the ORD of ApA.[36,57] Once again the results indicate that the relative orientation of adjacent bases in the single-strand helix is similar to the geometry of the dimer.

In summary, there is evidence that the bases in single-strand oligomers and homopolymers are stacked. The ultraviolet absorption and optical rotation properties of these molecules are different from those of their constituent monomers.[43-57] The differences are consistent with the bases being stacked.[38,39,52,58,59,116] The NMR properties of the molecules also indicate that the bases are stacked.[68,70] The strong tendency of nucleic acid bases to stack is also seen in the stacking of nucleosides in aqueous solution.[63-67]

Evidence for Base Pairs in Single-Strand RNA

The significance of base stacking as an element of secondary structure of single-strand RNA and its properties have only recently become known. The basic concepts of the secondary structure of tRNA which are embodied in the clover-leaf model in Figure 1 were originally proposed by Doty, Fresco, and their colleagues[29,42,72] before base stacking was generally accepted. We would like to examine the evidence for base pairs in single-strand RNA in the light of our new information. Are there base pairs in single-strand RNA? Or, does the secondary structure of single-strand RNA only involve base stacking?

1. Hydrodynamic

The radius of gyration of TMV RNA was determined independently from viscosity and light scattering measurements.[73] Light scattering gives the radius of gyration directly and no assumption about the configuration is necessary. However, it is necessary to assume a model of the configuration for the purpose of calculating the radius of gyration from viscosity data. There is good agreement for the radius of gyration determined from each method if the molecule is assumed to have a random-coil configuration. Other evidence that the molecule behaves as a random coil comes from the molecular weight dependence of the light scattering radius of gyration, the sedimentation coefficient, and the intrinsic viscosity.[73]

The existence of intramolecular contacts in the random coil has been inferred[30,73,79] from the temperature and ionic strength dependence of various hydrodynamic properties.[73-76] TMV RNA expands when the temperature is increased as indicated by an increase in the radius of gyration and viscosity. Decreasing the Na^+ concentration from 150 mM to 0.2 mM Na^+ decreases the sedimentation coefficient $S_{20°,w}$ from 28.2 S to 3.3 S.[73] Clearly the configuration of the molecule changes from a compact one to a highly extended one when the ionic strength is decreased just as it does when the temperature is increased. Of course, a flexible polyelectrolyte would be expected to behave similarly. However, Boedtker[73] felt that the changes in sedimentation coefficient with ionic strength were too large and occurred over too narrow a range of ionic strength to be explicable only in terms of electrostatic repulsion. The change in $S_{20°,w}$ parallels the increase in absorption. Thus, it was concluded that the change reflects the occurrence of a helix-coil transition. Cox and Littauer[76] came to a similar conclusion based on the variation of the sedimentation coefficient of E. coli rRNA with ionic strength.

The hydrodynamic properties show that single-strand RNA is a random coil which can assume a very compact configuration at low temperature and high ionic strength. The existence of the compact configuration implies that there are intramolecular contacts. Therefore, under these conditions the

secondary structure involves more than base stacking. However, the intramolecular contacts could be cation bridges or intercalation of the bases instead of hydrogen bonds.

2. Reactivity

The rate of reaction of RMV RNA with formaldehyde is 19 fold greater at 45°C than at 25°C.[42] The rate increases only 6 fold for the mononucleotides over the same temperature range. Similar observations have been made more recently for other mRNAs[77] and mixed yeast tRNA.[77,78]

Furthermore, the rate of digestion of single-strand RNA by pancreatic ribonuclease[42] or polynucleotide phosphorylase[42,80] increases markedly as the temperature is increased. In the latter case,[42] it was shown that there is no enhancement of the rate for poly U, a polynucleotide considered to have no secondary structure.

These observations could all be explained by a secondary structure involving base pairs. As the temperature is increased hydrogen bonds are broken and more residues are available for reaction for formaldehyde or enzymatic digestion. Once again, however, these results could also be explained by intercalation or possibly even base stacking as we shall see.

3. Optical Evidence

The optical density of a neutral solution of TMV-RNA increases 30% in a very gradual fashion as the temperature is increased from 10°C to 90°C.[42] A plot of optical density

versus temperature has an "S-shape" which is similar to the shape of the absorption change for the temperature induced helix-coil transition of DNA. However, for DNA the transition occurs over a temperature range of a few degrees.[41] The transition in TMV RNA occurs over nearly the whole temperature range between 10°C and 90°C.

The helix-coil transition for DNA is obviously very cooperative. The theory of a cooperative phenomena for DNA by Crothers, Kallenback, and Zimm[81] shows that the sharpness of the transition depends on the chain length of the cooperative region. The shorter the chain length the broader the transition and the lower the temperature at the midpoint of the transition (T_m). The T_m of the helix-coil transition of DNA is also known to vary with the base composition of DNA.[82] Thus, the gradual change in the optical density of TMV RNA as a function of temperature was interpreted as the summation of helix-coil transitions of many short helices with varying chain length and base composition.

The temperature dependence of the optical rotation of TMV RNA at the sodium D line (548 mμ) parallels the optical density changes.[42] This was taken as evidence that the base pairs were collected into short helical regions and not randomly scattered throughout the molecule. Once again the decrease in the optical rotation with increasing temperature was interpreted as resulting from a decrease in the number of base pairs.

The fraction of residues that are base paired was estimated from the optical rotation at 548 mμ.[42,83] The specific rotations at this wavelength of poly (A+U), the acid helix of poly A, and the poly U aggregate that forms at low temperatures are all about the same, +300°. At the opposite extreme, poly U at room temperature has a specific rotation of -8°. A yardstick of the percent helix of polyribonucleotides was established from these values. A specific rotation of +300° indicated 100% helix and no rotation indicated the absence of base pairs. The specific rotation of TMV RNA at room temperature is +180°. Thus, it was estimated that the fraction of bases which are in helical regions is 60%.

Urea was found to be as effective as heat in decreasing the hypochromicity of TMV RNA.[42] A solution of 6M urea decreases the T_m of TMV RNA by about 25°. A similar effect has been observed for DNA. Therefore, urea was considered a hydrogen bond-breaking agent. This observation on TMV RNA substantiated the view that hypochromicity and high optical rotation resulted from hydrogen-bonded base pairs.

As we now know, all of these optical properties could result simply from stacked bases rather than stacked base pairs. Both conformations are hypochromic and could have a large optical rotation. The temperature dependence of these optical properties does not distinguish between these two possibilities. The gradual decrease in hypochromism and optical rotation may reflect the denaturation of many short

helical regions or merely the temperature dependence of base stacking. Urea does not help either since it denatures helical structures by virtue of its effect on the structure of water.[84]

In general, we must be cautious in coming to any conclusions about base pairs on the basis of the hydrodynamic, reactivity, and optical properties cited so far because of our experience with poly A.[83,85] Similar observations were made for neutral solutions of poly A. It is 35% hypochromic at room temperature.[86] The absorption increases gradually as the temperature is raised. Nearly the same increase is observed if the room temperature solution is made 7M in urea. The rate of reaction with formaldehyde increases 20-fold over a 20° temperature range. The sedimentation coefficient and intrinsic viscosity depend on molecular weight in the fashion predicted for a random coil. However, it was concluded that the variation was not typical for a polyelectrolyte having such a high charge density. Furthermore, the reduced specific viscosity increases sharply as the salt concentration is reduced. All of these observations suggested that there were helical regions of A-A base pairs similar to those shown in Figure 1 for RNA. The specific rotation of poly A at the sodium D line is 155°. Therefore, it was concluded that 40-60% of the residues of poly A are base-paired.[85]

Nevertheless, we are confident that there are no A-A base pairs in poly A at pH 7. But what about single-strand RNA? It is not possible that it has a secondary structure which only involves base stacking?

Although such a structure can explain some of the optical properties, it cannot account for all of them. The T_m of the helix-coil transition of TMV RNA is dependent on the ionic strength of the solution.[73,74] It decreases with decreasing ionic strength. In other words, the absorption at any temperature increases with decreasing ionic strength. Also, the helical configuration is stabilized better by divalent cations like Mg^{++} than univalent ions like Na^{+}.[73] It is difficult to explain how these changes in the ionic environment of the solution could affect a helix-coil transition involving only the stacking and unstacking of neighboring residues. To the first approximation we expect stacking interactions to be independent of ionic strength. We will verify this assumption later with some experiments. Similar observations have been made for the T_m of DNA[42,82,87] and polynucleotide complexes.[41] The interpretation has always been that increasing the cation concentration decreases the effective charge on the phosphate groups and, thus, decreases the electrostatic intrachain repulsion of the helix.

Fresco measured the absorption of three homogeneous tRNAs from yeast as a function of temperature.[72,88] In each case there is a biphasic transition. The separate transitions

occur over 30°, which is much sharper than the 60° breadth of the single transition of mixed yeast tRNA. Furthermore, the T_m of the separate transitions was different for each of the three tRNAs that were investigated. Vournakis and Scheraga[89] have observed a similar biphasic melting curve for yeast alanine tRNA. These observations support the view that the broad helix-coil transition of single-strand RNA is the supposition of many cooperative transitions of short helical regions with different stabilities. It is difficult to rationalize a biphasic transition if the secondary structure of tRNA consists only of stacked bases.

4. Tritium Exchange

A different sort of measurement has been made by Englander and Englander.[90] They have observed the time dependence of the exchange of normal hydrogen for tritium in tRNA which had been previously equilibrated with THO. An average of 77 hydrogens per tRNA molecule exchange slowly from a sample of mixed yeast tRNA. It had previously been shown that the slowly exchanging hydrogens in DNA are those involved in the hydrogen bonds.[91] Thus, Englander and Englander[90] concluded that the slowly exchanging hydrogens in tRNA were those involved in hydrogen-bonded base pairs. There have been suggestions there are hydrogen bonds between 2'-hydroxyl groups of RNA and either the bases or phosphate groups.[50,51,92,93] If the hydrogen of every 2'-hydroxyl in tRNA exchanges slowly, then that would account

for virtually all the slowly exchanging hydrogens. The evidence for this hydrogen bond is rather circumstantial. In fact, x-ray fiber studies of double-strand RNA do not show any internal hydrogen bond involving the 2'-hydroxyl.[94,95] We are inclined to think that the tritium exchange experiments reflect the existence of hydrogen-bonded base pairs in tRNA.

5. X-ray Diffraction

The most definitive evidence for Watson-Crick base pairs in single-strand RNA is an x-ray diffraction study of semi-crystalline fibers of fragmented yeast ribosomal RNA.[94] Preliminary reports of this work were given several years ago.[96] At that time the RNA was thought to be tRNA. Since then it has been established that the sample is degraded rRNA.[97] The diffraction patterns are consistent with the existence of short double-strand helices of A-U and G-C base pairs. The details of the helical geometry are very similar to those of the totally double-stranded RNAs, reovirus RNA, wound tumor virus RNA, the replicative form of MS2 virus RNA, and rice dwarf virus RNA. (For a review, see Davies.[98]) The overall dimensions of the RNA Watson-Crick double-strand helix are similar to the A-form of DNA.[98] There are 10 or 11 base pairs per turn; they are tilted 10 to 15° from the perpendicular to the helix axis.

The last evidence for base pairs in single-strand RNA that we would like to mention are the results of low angle x-ray scattering experiments. The measurement is made on solutions so the results apply to the structure of RNA in

solution. Witz, Hirth, and Luzzati[99] have determined the mass per unit length of TMV RNA, yeast rRNA and turnip yellow mosaic virus RNA in solution. It is similar for each RNA and also similar to that of DNA. Finally, the radius of gyration of yeast tRNA, as determined by low angle x-ray scattering techniques,[100] eliminates the possibility that tRNA has a completely single-stranded secondary structure.

Calculating Optical Properties of Single-Strand Helices

Most of the evidence that has just been cited supports the view that the secondary structure of single-strand RNA consists of short double-strand regions similar to DNA. What has not been established is the importance and extent of base stacking. It has been suggested that the bases that are not base-paired have a totally random orientation. We expect, however, that the bases in RNA are stacked in regions where there are no base pairs. Furthermore, under conditions where there are no helical regions, we expect the bases are stacked.

If the bases in RNA have a completely random conformation when there are no base pairs, then the optical properties of the polymer should equal the appropriate average of the optical properties of the monomers. This does not appear to be true. The optical rotation at the peak and trough of the Cotton effect is greater for formylated tRNA at 25°C than for the monomers.[78] Formylation presumably prevents

the formation of base pairs. Therefore, this result indicates that bases do not have a random conformation in the absence of base pairs. It has also been observed that RNA is still hypochromic at elevated temperatures where the change of absorption with increasing temperature has become nearly level.[42] Base pairs are probably not stable at these high temperatures. Therefore, whatever residual hypochromism is present must result from base stacking.

These observations are strongly suggestive that the bases do have a preferred orientation even in the absence of base pairs. The nature of the preferred orientation has been suggested by the work of Holcomb and Tinoco on poly A.[57] The ability to calculate the optical properties of poly A from ApA implies that the stacking is similar in the polymer and dimer. We expect that the dimers in RNA also have the same geometry as when they are free in solution. If this is true and if interactions between nearest neighbors are the most important, then we should be able to calculate the optical properties of RNA, under conditions where there are no base pairs, from the optical properties of the dimers. The equations for making these nearest-neighbor calculations and further evidence for the validity of the nearest-neighbor assumption are presented below.

1. Trinucleoside Diphosphates

Cantor and Tinoco[35,37] have developed a formalism for calculating the optical properties of trinucleoside

diphosphates (trimers) from those of the dimers. They showed that if the nearest-neighbor approximation is valid, then the molar rotation of the trimer, IpJpK, per residue, $[\phi_{IJK}(\lambda)]$, can be calculated from the following equation:

$$[\phi_{IJK}(\lambda)] = \frac{2[\phi_{IJ}(\lambda)] + 2[\phi_{JK}(\lambda)] - [\phi_{J}(\lambda)]}{3} \qquad (1)$$

The molar rotations per residue of dimer IpJ, dimer JpK, and monomer J are given by $[\phi_{IJ}(\lambda)]$, $[\phi_{JK}(\lambda)]$, and $[\phi_{J}(\lambda)]$, respectively. Agreement between experiment and calculation can only be expected if the stacked bases in the trimer have a similar geometry as they do in the dimers. Therefore, the optical rotation of the dimers and trimers should be measured under identical conditions of temperature, pH, ionic strength, and at a concentration where there is no intermolecular aggregation.

An analogous equation can be used to calculate the absorption spectrum, $\epsilon_{IJK}(\lambda)$, or the extinction coefficient of trimer IpJpK.

$$\epsilon_{IJK}(\lambda) = \frac{2\epsilon_{IJ}(\lambda) + 2\epsilon_{JK}(\lambda) - \epsilon_{J}(\lambda)}{3} \qquad (2)$$

All variables are defined in an analogous fashion as they are for Eq. (1). There are similar equations for the oscillator strength and hypochromism of the trimer.

The ORD, extinction coefficient at 260 mμ, and the hypochromism of seven trimers were measured at three pHs at room temperature.[35] The optical properties of the dimers have been measured at the same pHs at room temperature by

Warshaw.[43,44] The expected optical properties of the trimers were calculated from the corresponding optical properties of the dimers. The agreements between the semi-empirical calculations and the experiments were excellent for all seven trimers at all three pHs. The ORD of four other trimers have been measured at pH 7.[37] Once again the agreement between experiment and the nearest-neighbor calculation is good.

Experiments which were identical to those done by Cantor and Tinoco[35] have recently been reported for trimers of the form IpJpGp.[45] The letters I and J stand for A, C, or U. The results are similar. The agreement between experiment and calculation, however, is not always as good as found by Cantor and Tinoco.[35]

In general, all of these results indicate that the nearest-neighbor assumption is valid for trimers and that the geometry of the bases in the trimer and dimer are similar.

2. Polyribonucleotides

The optical properties of a polymer can be calculated from the optical properties of the dimers with equations which are analogous to Eqs. (1) and (2). If end effects are ignored, then the molar rotation per residue of a polymer, $[\phi_P(\lambda)]$, is given by:[36]

$$[\phi_P(\lambda)] = \sum_{I=1}^{4} \sum_{J=1}^{4} 2\chi_{IJ}[\phi_{IJ}(\lambda)] - \sum_{I=1}^{4} \chi_I[\phi_I(\lambda)] \quad (3)$$

The equation is given for a polymer which contains only the four common bases. Clearly it can be extended to take into account any number of different residues. The mole fractions of dimer IpJ and nucleoside I in the polymer are χ_{IJ} and χ_I. They are equal to the number of times the dimer IpJ and nucleoside I occur in the polymer divided by the chain length. Of course, the mole fraction of each of the four nucleosides can be found from the base composition. The other variables are defined as they are for Eq. (1).

A knowledge of the sequence of the polymer is required in order to calculate the mole fractions χ_{IJ}. The mole fraction of dimers in an RNA whose sequence is not known can be calculated from the base composition if the nearest-neighbor frequencies are the most probable ones.

$$\chi_{IJ} = \chi_I \chi_J \qquad (4)$$

χ_I and χ_J are defined as they were for Eq. (3). The frequency of the four dimers resulting from the pancreatic ribonuclease hydrolysis of yeast rRNA,[101] MS2 RNA,[101] F2 RNA,[102] T4 mRNA,[102] and E. Coli rRNA[102] is close in each case to what would be calculated from Eq. (4). Thus, it is reasonable to assume that the frequency of nearest neighbors in large RNAs is random. We shall also assume that the frequency of nearest neighbors in a mixture of tRNAs is random.

Substituting Eq. (4) into Eq. (3) we have an equation for calculating the ORD of an RNA from its base composition

and the experimentally measured ORD of the sixteen dimers and the four nucleosides.

$$[\phi_{RNA}(\lambda)] = \sum_{I=1}^{4} \sum_{J=1}^{4} 2\chi_I\chi_J[\phi_{IJ}(\lambda)] - \sum_{I=1}^{4} \chi_I[\phi_I(\lambda)] \tag{5}$$

The absorption spectrum or extinction coefficient of the RNA can be calculated similarly.

$$\epsilon_{RNA}(\lambda) = \sum_{I=1}^{4} \sum_{J=1}^{4} 2\chi_I\chi_J\epsilon_{IJ}(\lambda) - \sum_{I=1}^{4} \chi_I\epsilon_I(\lambda) \tag{6}$$

These equations can be greatly simplified for the case of a homopolymer. The mole fractions of dimer IpJ and nucleoside I are both 1. Thus, the ORD of a polymer, poly N, is merely two times the ORD of dimer NpN minus the ORD of nucleoside N.

$$[\phi_{\text{Poly N}}(\lambda)] = 2[\phi_{NN}(\lambda)] - [\phi_N(\lambda)] \tag{7}$$

The ORD of poly A, poly C, and poly U have been calculated from the appropriate dimer and monomer ORD data at 25°C, pH 7, according to Eq. (7).[36] The calculations are compared with experiment in Figure 3. We have already mentioned the results for poly A and poly C. In general, there is good qualitative agreement between the calculated and experimental curves.

However, for poly A and poly C the quantitative agreement is not as good as for the trimers. Furthermore, the experimental curve is shifted a few mμ to the blue of the

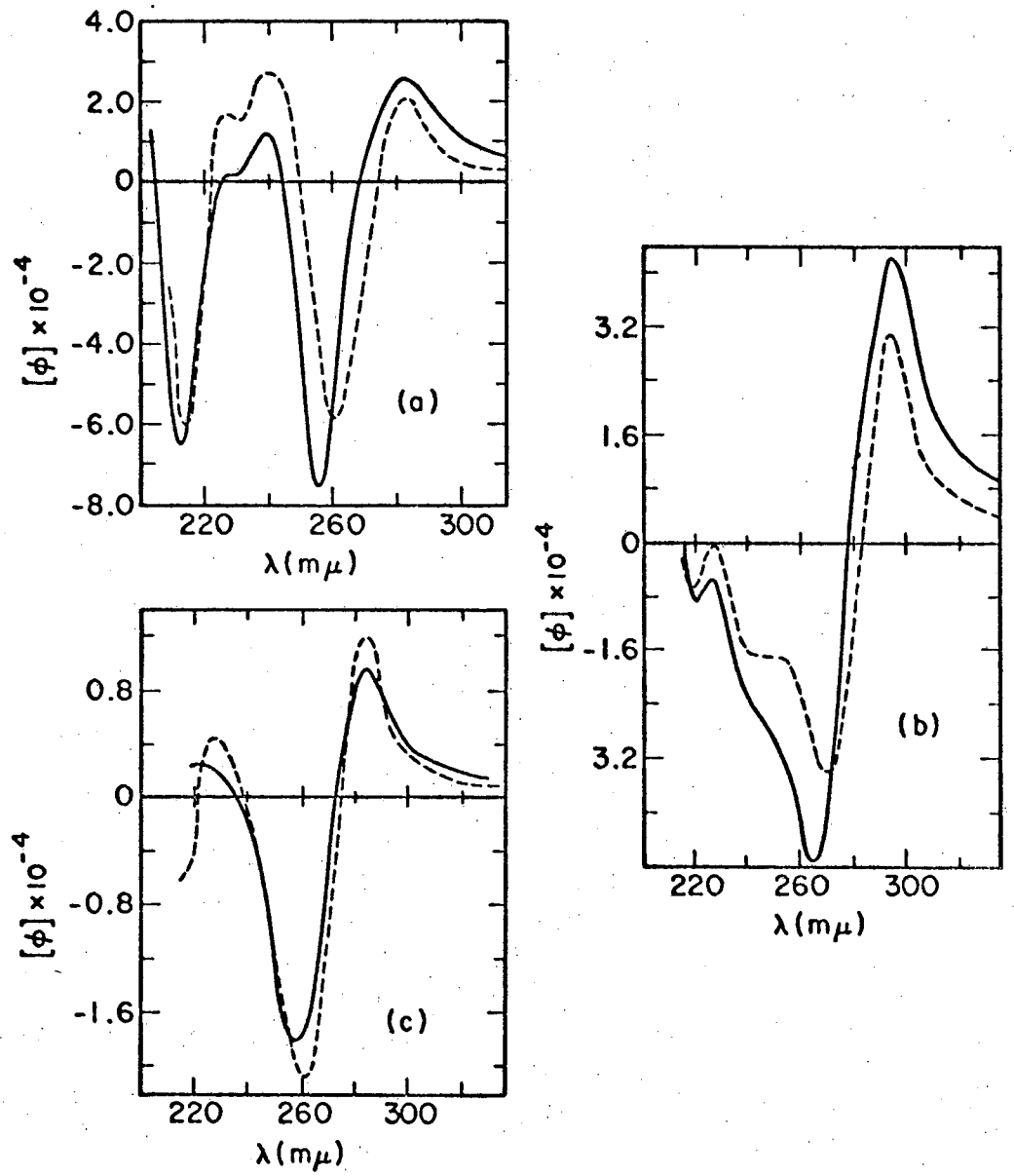

Figure 3. (a) ORD of poly A at neutral pH. ——, Experiment (Holcomb and Tinoco[57]); ---, nearest-neighbor calculation. (b) ORD of poly C at neutral pH. ——, Experiment; ---, nearest-neighbor calculation. (c) ORD of poly U at neutral pH. ——, Experiment (Sarkar and Yang[103]); ---, nearest-neighbor calculation. (Taken from Cantor, Jaskunas, and Tinoco.[36])

calculated curve. Either of these discrepancies could be caused by either next-nearest-neighbor effects or a slightly different geometry in the polymer and dimer.

Neither of these possibilities would be surprising. There are important differences between polymers and dimers that could affect the relative geometry of adjacent bases. For instance, there is electrostatic repulsion between phosphates in a polymer that are absent in a dinucleoside phosphate. This is not likely to result in a major difference between the geometry of the polymer and dimer because the phosphate groups of the polymer will not be much farther apart if the bases are completely unstacked. In addition, because of steric constraints the polymer may be more restricted to a few conformations. In other words, the relative stabilities of different conformations may be greater for a polymer than a dimer. All of these possibilities may be accentuated because of the regularity of the sequence of a homopolymer. The structure is probably very regular. This will make all the next nearest-neighbor effects additive. Thus, the overall effect may be quite large.

The agreement between experiment and calculation is much better for poly U than for poly A or poly C. This may be because the residues in poly U are less rigidly oriented than in the other two polynucleotides. The experiments by Warshaw and Tinoco[43,44] indicated that uracil does not stack

as well as the other three common bases. In this case, the interaction between next nearest neighbors may be less important.

For completeness sake, we have compared, in Figure 4, the ORD of poly G[104] and its nearest-neighbor calculation.[105] The agreement is poor, which is to be expected. The ORD of GpG has not been measured. The dimer ORD needed for the calculation of the ORD of poly G was obtained from the data for GpGpC and GpGpU using Eq. (1).[105] Even more important, however, poly G is probably aggregated under the conditions of the measurement.[106]

Taken together, all of these results on trimers and homopolymers suggest that the ORD of an RNA calculated from Eq. (5) will agree reasonably well with the experimental ORD if there are no base pairs and if it has a conformation of a single-strand helix with stacked bases. The agreement between experiment and calculation will probably be intermediate between what was observed for poly U and what was observed for poly A and poly C. We can expect, however, that the discrepancy will be much greater if there is an extensive amount of base pairing. Formation of the ordered complex poly (A+U) shifts the crossover of the ORD 9 mμ to the blue of the crossover for the calculated single-strand polymers.[36] The average difference between the crossover of the experimental and calculated curves in Figure 3 for poly A, poly C, and poly U is only 4 mμ.

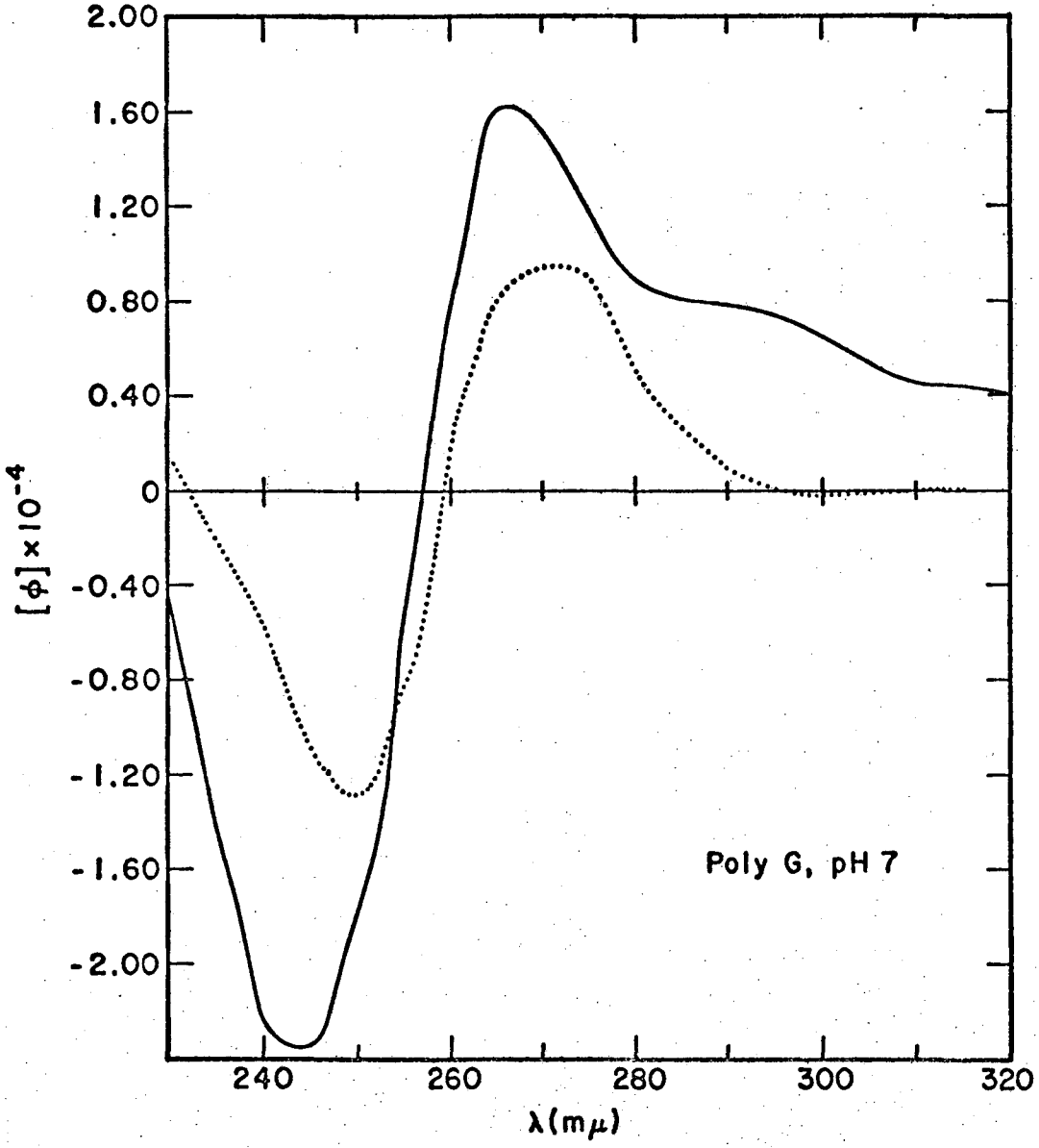

Figure 4. ORD of Poly G.
——, Experimental ORD at pH 7.0, ionic strength = 0.15.
• • •, Nearest-neighbor calculation.

Materials and Methods

1. Materials

Tabacco mosaic virus RNA, F2 RNA, R17 RNA, poly rAU, and RF-MS2-RNA were gifts from Drs. S. Mandeles, M. Takanami, P. Kaesberg, M. Chamberlin, and H. Kamen, respectively. The TMV-RNA preparations were 70 to 80% homogeneous as estimated from the sharpness of the boundary in a sedimentation velocity experiment. Mixed yeast tRNA (lot No. 30449), ApA (lot No. 45564), and CpC (lot No. 45568) were obtained from the California Corporation for Biochemical Research. Poly C (control No. 2938) was obtained from Miles Chemical Corporation.

All buffers were prepared with twice distilled water. Buffers (1), (2), and (3) contained 0.5 M NaCl, 0.01 M EDTA; 0.5 M NaCl, 10^{-4} M EDTA; and 10^{-4} M EDTA, respectively. A 3:1 ratio of tetrasodium and disodium EDTA was used to maintain the pH near 7. Buffer (4) contained 0.5 M NaCl and 10^{-4} M tetrasodium EDTA. Buffer (5) contained 10^{-3} M Tris-HCl, 10^{-4} M tetrasodium EDTA, pH 8.2.

2. Desalting Procedures

Solutions of TMV RNA, R17 RNA, F2 RNA, and mixed yeast tRNA which were used for ORD studies at room temperature were dialized at 4°C for 1 day against buffer (1) and 3 days each against buffers (2) and (3).[107] The volume of the 4 daily changes of buffer was always at least 100 times the

volume of the RNA solution. No bentonite was present during any of these dialyses. As a result, degradation cannot be ruled out. No infectivity tests were made.

"Salt-free" solutions which were used for the optical studies at room temperature were actually equilibrated with buffer (3). For measurements at high salt concentration, KCl was added to bring the salt concentration up to 0.15 M. The ORD of a TMV RNA solution prepared as above is the same, within experimental error, as that of an undialized sample to which salt had been added. This is evidence that extensive degradation of the RNA has not occurred during the dialysis procedure.

A slightly different procedure was used to prepare the TMV RNA sample that was used to measure the ORD as a function of temperature and ionic strength. A solution of TMV RNA was dialyzed at 4°C for 1 day against buffer (1). This was followed by dialysis for 3 days against a buffer containing 0.5 M NaCl, 10^{-5} M EDTA. The pH of this buffer was adjusted to 8.0 with 1 M NaOH. The final dialysis was for three days against twice-distilled water. The volume of the four daily changes of buffer was always at least 100 times the volume of the RNA solution. After dilution with water, solution of TMV RNA had an absorbance at 260 mμ of 2.0. Aliquots of the solution were diluted 1:1 with a buffer of known ionic strength and pH. The four buffers used were: (a) 4×10^{-4} M NaOH plus 1×10^{-4} M Na_4EDTA, adjusted to

pH 8.0 with HCl; (b) 4×10^{-4} M NaOH plus 2×10^{-4} M Na_4EDTA plus 6.8×10^{-3} M NaCl adjusted to pH 8.0 with HCl; (c) 2×10^{-4} M Na_4EDTA plus 6.6×10^{-2} M NaCl plus Perrin's 0.02 ionic strength sodium phosphate buffer, pH 7.7; (d) 2×10^{-4} M Na_4EDTA plus 2.0 M NaCl plus Perrin's 0.02 ionic strength sodium phosphate buffer, pH 7.6. The resultant concentrations of sodium ion after the 1:1 dilution were (a) 4×10^{-4} M Na^+; (b) 4×10^{-3} M Na^+; (c) 4×10^{-2} M Na^+; (d) 1 M Na^+. The pHs of the RNA solutions were measured and found to be between pH 7.5 and pH 8.2.

Poly C was desalted by dialyzing a dilute solution in 10^{-4} M tetrasodium EDTA against buffers (1), (4), and (5) for a total of 3 days. Dry NaCl was added to the desalted solution to make solutions of the desired salt concentration. We did dialyze a sample of poly C at pH 7 against a buffer in which the sodium ion concentration was only 10^{-4} M. The ORD and ultraviolet spectrum of the resulting solution indicated that poly C exists in the double-strand structure under these conditions. This complex forms when one-half the residues are protonated. In order to insure that poly C was single-stranded the final solution was equilibrated against a buffer containing 10^{-3} M cation at pH 8.2. Under these conditions there is no evidence of any double-strand formation.

One-half mg samples of ApA and CpC were desalted separately on a 1 cm x 50 cm Bio-Gel P2 (coarse mesh) column by eluting with twice distilled water. The pH of the eluent

was about 6. A preliminary column was run on a sample of blue dextran which contained KCl. The blue dextran is obtained from Pharmacia (Piscatoway, New Jersey) and has a molecular weight of 2×10^6. The passage of a 1% blue dextran solution through the column can be followed by eye. It comes out at the void volume of the column because of its large size. The salt is retarded by the gel beads and comes out after the blue dextran. The position of the salt peak was determined from the turbidity of the solutions when a few drops of a $AgNO_3$ solution were dropped into each test tube. The dimers appeared almost as soon as the blue dextran but well before the salt peak. Their appearance was followed with a Gilson UV258 flow-through monitor. The patterns of the blue dextran-KCl column and the ApA column are superimposed in Figure 5. We estimate that the concentration of NaCl in the solutions of ApA and CpC is less than 10^{-4} M.

3. Optical Measurements

All ultraviolet spectra were measured at room temperature (25°C) with a Cary 15 spectrophotometer. ORD was measured on a Cary 60 spectropolarimeter.

A standard strain-free cylindrical quartz cell was used for all the measurements discussed in this section. The path length was 1.0 cm and the volume was 3.2 ml. The cell was stoppered with a serum stopper for all measurements above room temperature.

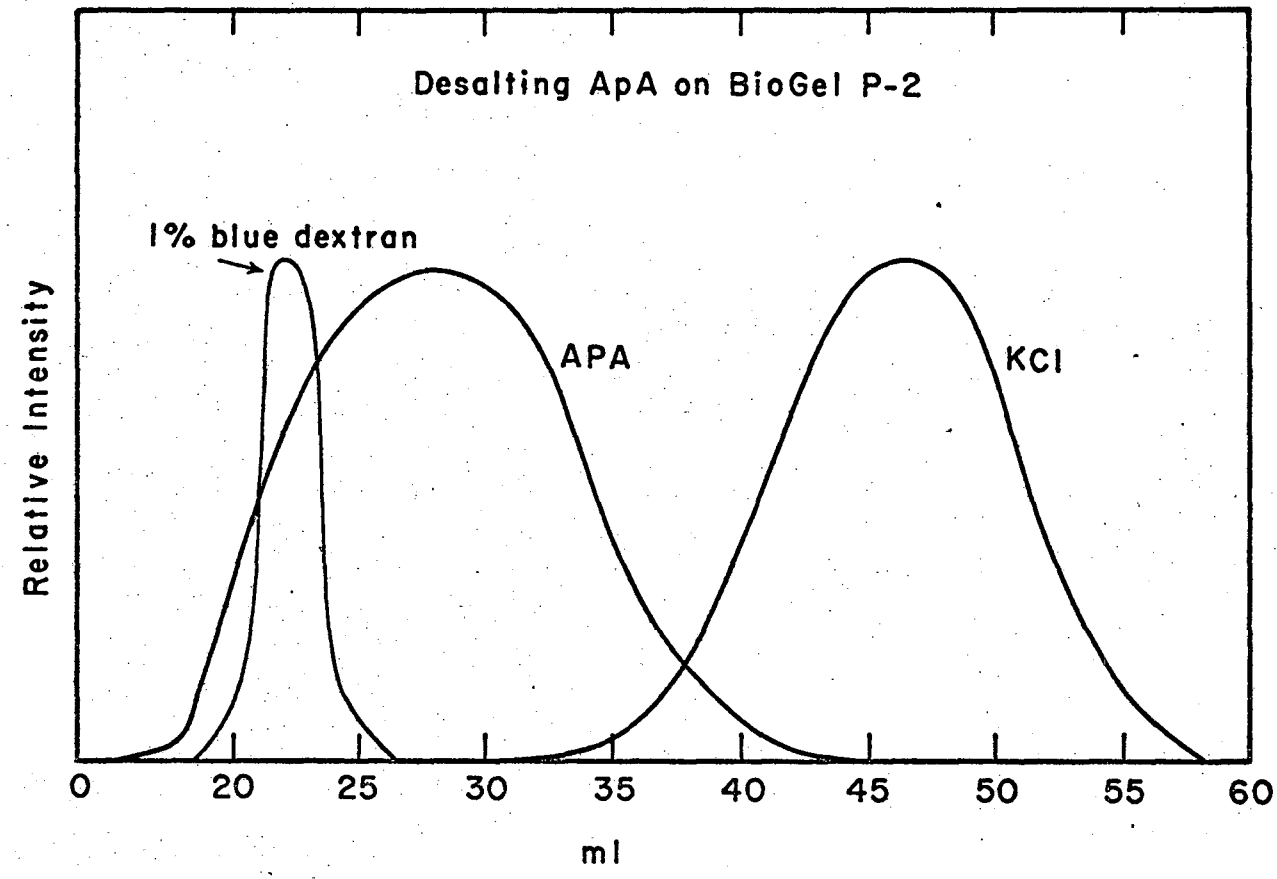

Figure 5. Desalting of ApA on Bio-Gel P-2.

All spectra were recorded on the recorders supplied with the instruments. The optical rotation signals of the baseline and samples were smoothed by drawing a line through the center of the noise as judged by eye. Subsequently, points were picked off every 2.5 mμ between 232.5 and 350 mμ and converted to molar rotation. A more satisfactory method for smoothing the data will be discussed in Part II.

The molar rotation per residue, $[\phi]$, is defined by the following equation:

$$[\phi] = \frac{100\ \theta}{C\ell}$$

where θ is the difference between the rotation in degrees of the cell filled with the sample and the same cell filled with buffer. C is the concentration of residues (mononucleosides) in moles per liter and l is the path length in cm. The uncertainty in the measurement of $[\phi]$ is estimated to be $\pm$ 0.1 x 10^4.

A plot of the rotation of TMV RNA versus pH is shown in Figure 8 (page 64) for 257 and 286 mμ. The reasons for and the conclusions from the experiment will be discussed later. Right now we wish to discuss the precision of the data. Points are shown for two entirely different preparations of TMV RNA. Measurements on each preparation were made on several different days. Thus, the scatter, which is typical, is not only indicative of the noise level but also our ability to reproduce a measurement from sample to sample and from day to day.

Bars indicating the size of the noise at each wavelength are given. The noise level is higher at 257 mμ than because the absorption of the solution is greater at this wavelength. The greater scatter of the points for 257 mμ can be partly accounted for by the higher noise level. However, the scatter is greater than the uncertainty due to the noise. The uncertainty in the measurement is a reflection of our inability to measure a baseline or sample twice and obtain precisely the same thing if the cell is emptied and refilled between runs.

The differences apparently occur because of our inability to precisely reposition the cell in the cell holder. Repetitive measurements of a baseline can be made with the same cell. If the cell is not touched between the measurements, then there is no difference between them. (A small but definite drift can sometimes be detected during the course of a day.) If the cell is taken out of the cell holder between each run and replaced, then there are differences between the various runs. The differences are called baseline shifts because they are nearly independent of wavelength and reflect a change in the position of zero rotation. It should be emphasized that the constancy of the shift with wavelength is not exact.

We attempt to correct for baseline shifts by measuring the rotation of the sample and baseline in the visible region of the spectrum, between 500 and 600 mμ. The actual rotation of nucleic acids in this region, at the concentrations

generally used, is too small to be measured with the spectropolarimeter. Therefore, if there is any difference between the sample and baseline, it must be a baseline shift. The shift is averaged for several wavelengths in the visible region and applied as an additive constant to the rotation in the ultraviolet region. This procedure satisfactorily corrects for most of the shift. Part of the reason for the scatter in Figure 8 is that we assume the shift is independent of wavelength and this is not entirely correct.

These problems might be eliminated if the cell holder were redesigned so that there would be no leeway in positioning the cell. It should be kept in mind, however, that there is no need for more precise measurements of ORD than we are capable of now. We are looking for large differences between ORD curves and not small ones. The conclusions we reach are general ones. Unlike x-ray crystallography, optical rotation experiments cannot yet determine interatomic distances or angles. The problem here is that the theory of optical rotation is not as well refined as the theory of x-ray crystallography. Later we will discuss methods of determining the exact number of base pairs in a tRNA from ORD. Of course, this question requires a precise answer and, therefore, a precise measurement of the ORD. However, at the present time the errors introduced in the form of assumptions are much larger than the scatter of the data in Figure 8.

4. Extinction Coefficients

Extinction coefficients for solutions of RNA in buffer (3) were calculated by using Eq. (6). This equation is strictly true only if the RNA is single-stranded under these conditions. Evidence will be shown that at this low ionic strength RNA is primarily single-stranded. In any case, slight variations in the choice of extinction coefficients will not strongly affect any of the following results. The dinucleoside phosphate and monomer extinction coefficients necessary for the use of Eq. (6) were obtained from the thesis of Dr. M. Warshaw.[108] The calculated extinction per mole of nucleoside at 260 mμ for each of the four RNAs is as follows: TMV RNA, 10,000; R17 RNA, 9770; mixed yeast tRNA, 9650; and F2 RNA, 9700. The calculated extinction of TMV RNA agrees with the value determined experimentally for a salt-free solution.[75] Solutions of RNA in moderate salt concentration were prepared by adding dry salt to a salt-free solution. The volume change is negligible. Thus, it was not necessary to know the extinction coefficient of the RNAs in the presence of salt to determine concentrations. However, an experimental extinction per mole of residue was used for TMV RNA in the presence of 0.15 M NaCl, 7260.[74]

Experimental extinction coefficients for ApA and CpC at 260 mμ were taken from the studies of Warshaw.[108] They are 13,700 and 7,100, respectively.

The extinction coefficient for single-stranded poly C was taken as 6220.[36]

The concentrations of residues as determined from extinction coefficients were corrected for thermal expansion or contraction for ORD measurements at temperatures other than 25°C.

5. Nearest-Neighbor Optical Rotatory Dispersion Calculations

The molar rotation per residue of various RNAs was computed by Dr. C. Cantor using Eq. (5).[36,105] As before, the dinucleoside phosphate and monomer data needed for these calculations came from the studies of Warshaw.[108] These latter measurements were made at pH 7, 25°C. The ionic strength of the solutions was 0.1. Under these conditions none of the bases are protonated. Thus, the calculations should be equivalent to the ORD of unprotonated single-strand RNAs with stacked bases at 25°C.

We have calculated the optical rotation of TMV RNA as a function of temperature using Eq. (5). In this case, the temperature dependent dimer and monomer data at pH 7 were obtained from Dr. R. Davis.[109] The rotation was calculated at a few wavelengths at 10° intervals between 0°C and 100°C. The rotation of each of the dimers and monomers at these particular temperatures and wavelengths was obtained from a plot of rotation at that wavelength as a function of temperature.

Neither Dr. Davis nor Dr. Warshaw measured the ORD of GpG. The room temperature ORD of GpG has been calculated by

Dr. Cantor from the experimental ORD of both GpGpC and GpGpU using Eq. (1).[105] The average has been taken by Dr. Cantor as the room temperature ORD of GpG. This is the curve that has been used for the contribution of GpG in calculating the ORD of RNAs at room temperature with Eq. (5).

Glaubiger[61] has developed a theory to explain the temperature dependence of the rotation of dimers. The theory provides a functional form for the temperature dependence.

$$\ell n[\phi] = \frac{-2\ kT}{\underset{\sim}{k}} + A$$

where k is Boltzmann's constant, $\underset{\sim}{k}$ is a force constant, T is the absolute temperature and A is a constant of integration. The ORD of any dimer can be calculated at any temperature if a force constant is known for the interaction of the two bases and the ORD of the dimer is known at any one temperature. The latter information is needed to determine the constant of integration. Dr. Glaubiger[61] has used the experimental temperature dependence of several dimers to determine the force constants for each of them. The results are given in Table 1.

We have taken the average of these force constants as the force constant for GpG. Thus, the ORD of GpG was calculated at temperatures between 0° and 100°C using the average force constant and the calculated ORD of GpG at room temperature. We realize that these estimates of the optical rotatory properties of GpG are very rough. However, they are probably a better estimate of these properties than zero rotation.

Table 1

Force Constants for Temperature Dependence of Rotation of Dinucleoside Phosphates.[a]

Dinucleoside Phosphate	Force Constant k (erg/mole)
ApA	1.37×10^{-14}
ApG	1.60
ApC	1.98
CpC	2.08
ApU	2.50
UpU	2.93
Average	2.08×10^{-14}

a. Taken from Ph.D. thesis of Glaubiger.[61]

Initially the lines through the experimental points for the rotation of the other dimers and monomers at the wavelengths of interest were drawn by hand. Subsequently a computer program written by Dr. T. Mahan of the Lawrence Radiation Laboratory was used to draw the line through the experimental points. Lines were similarly drawn through the calculated points for GpG. The program was set up to first try to fit the experimental points with a cubic function. The best cubic function was determined by the methods of least squares. The resulting equation was checked to see if any maximum or minimum occurred between 0°C and 100°C. The theoretical treatments of the temperature dependence of the optical rotation of stacked dimers indicate that any such extrema are not real. Therefore, if extrema occurred in the best cubic function, then the experimental points were refit to the best quadratic function. If this equation had extrema, then the experimental points were fit to the best straight line.

The result was a set of equations describing the temperature dependence of all 16 dimers and 4 monomers at every 2.5 mμ between 230 and 330 mμ. The coefficients for the 820 polynomial equations are given in Appendix D. For the dimers, 70% of the polynomials are cubic, 20% are quadratic and 10% are linear. For the monomers, 53% are cubic, 21% are quadratic and 26% are linear. We have calculated a standard deviation, σ, for each equation.

$$\sigma = \sqrt{\frac{\sum_{i}^{N} ([\phi]_{Expt}(T_i) - [\phi]_{Calc}(T_i))^2}{N}}$$

The experimental and calculated molar rotations at T_i are $[\phi]_{Expt}(T_i)$ and $[\phi]_{Calc}(T_i)$, respectively. The total number of temperatures at which $[\phi]_{Expt}$ was determined is N. The average standard deviation for the dimers in units of molar rotation is 0.04×10^4. For the monomers it is 0.03×10^4.

These equations have been used in another program written by Dr. Mahan in order to calculate the ORD of TMV RNA from Eq. (5) as a function of temperature. The plots of rotation versus temperature for the few wavelengths which have been calculated by hand agree very well with the computer calculated plots. The deviation is greatest above 75°C. Of course, it is not clear whether the computer calculation or hand calculation is the better approximation of reality in this temperature region. The ORD at 25°C is nearly identical with the ORD of TMV RNA which has been calculated by Dr. Cantor using Eq. (5) and the room temperature ORD data of the monomers and dimers measured by Dr. Warshaw. The two curves are shown in Figure 6.

This program has also been used to calculate the average rotation of the monomers in TMV RNA at several temperatures.

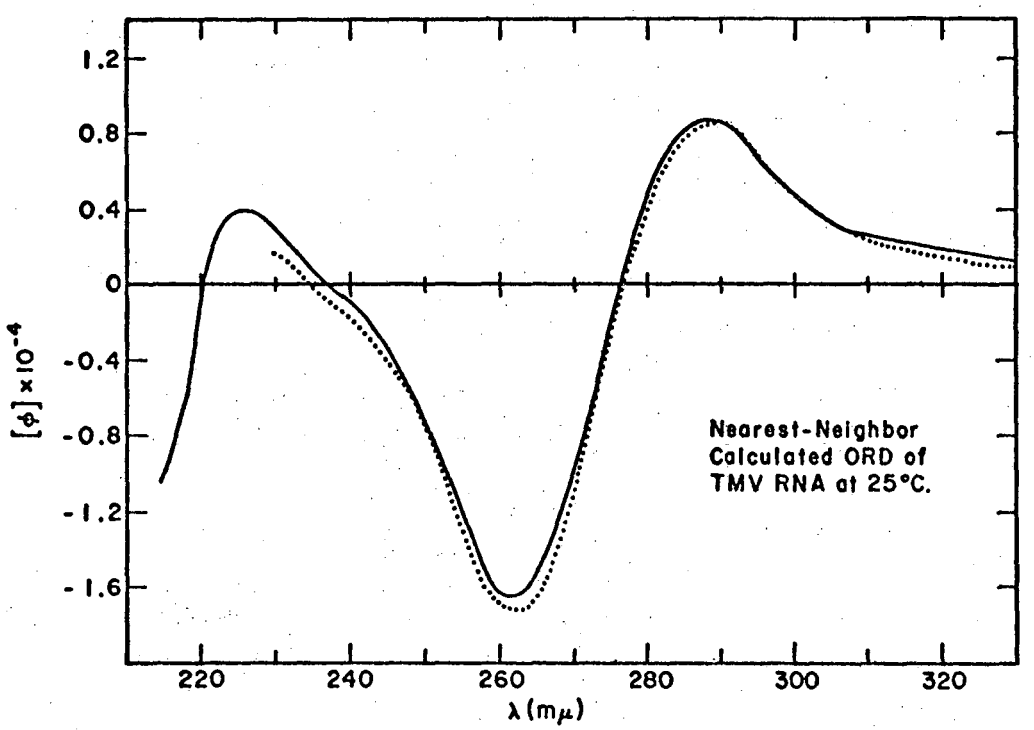

Figure 6. Nearest-neighbor calculated ORD of TMV RNA at 25°C.

--- Calculated from polynomials representing the ORD of dimers and monomers as a function of temperature (see text).

—— Calculated from ORD of dimers and monomers at room temperature (Reference 36).

Base Stacking in Single-Strand RNA

The hypothesis we wish to verify is that under conditions where there are no base pairs in RNA there is still a preferred relative orientation of neighboring bases that is similar to the stacked conformation of bases in dinucleoside phosphates. We will consider the hypothesis verified if the ORD of the RNA under these conditions is similar to the ORD of the RNA that is calculated from the experimental optical rotation spectra of the dimers and monomers using Eq. (5).

One of the conditions under which single-strand RNA probably has few base pairs is low ionic strength. It is well known that the stability of most double-strand nucleic acid complexes decrease with decreasing ionic strength.[41,87] The decreased ionic strength is thought to increase the electrostatic repulsion between phosphate groups on different strands. The only complexes that are stabilized by decreased ionic strength are the double-strand complexes of poly C and poly A.[110] The poly C complex is formed when one-half the residue are protonated[112] and is apparently stabilized by the electrostatic attraction between the positively charged bases and the negatively charged phosphate backbone. The poly A complex is directly stabilized by bonds between the protonated bases and the phosphates.[111]

Experimental observations mentioned earlier confirm the prediction that RNA is primarily single-stranded at low ionic strength. Therefore, we were interested in measuring the ORD of single-strand RNA in the presence and absence of salt and comparing the results with the ORD calculated from the dimers.

1. The Dependence of Stacking on Ionic Strength

The ORD data of the dimers and monomers used for the calculation were obtained from solutions of 0.1 ionic strength.[108] Strictly speaking the ORD calculated from these data should correspond to the ORD of the single-strand helix with stacked bases in a solution of 0.1 ionic strength. The question is, would this hypothetical single-strand polynucleotide have the same ORD at a lower ionic strength? We expect that the answer is yes.

The nature of the stacking probably does not depend on ionic strength. It was noted earlier that stacked structures result because of the van der Waals interactions between the bases and in order to minimize the surface free energy of water. At concentrations of several molar, salt acts as a denaturing agent. At concentrations between 0.1 and 10^{-4} M it does not seem likely that any of these forces are affected. Furthermore, space filling models reveal that the distance between neighboring phosphate groups is not significantly increased if the bases are completely unstacked. Thus, the nature of the stacking should not be affected by variation in the electrostatic potential between neighboring phosphates as a function of ionic strength. Of course, the distances between phosphates separated by one or more residues should be sensitive to the salt concentration. But, these long range interactions should not affect the relative orientation of neighboring bases. These thoughts have received some support from the calculations of Schildkraut and Lifson.[87]

They have been able to explain the ionic strength dependence of the T_m of DNA with a model which ignores changes in the stability of the single strands as a function of ionic strength. With these things in mind, we expect that the ORD of single-strand oligomers and polymers is independent of ionic strength.

The ORD of CpC and ApA have been measured in salt-free solutions at pH 6. The only salt present were the counter-ions and some dissolved CO_2. We have compared the results with the ORD of ApA and CpC measured in a solution of 0.1 ionic strength. In both cases the agreement is well within experimental uncertainty. The results at the peaks and troughs are summarized in Table 2. The magnitude of the rotation of CpC and ApA at their respective peaks and troughs are greater than most other dimers. Thus, the ORD of these dimers should be more sensitive than most others to changes in the nature of the stacking brought on by changes in ionic strength. It seems certain that the ORD of dinucleoside phosphates are independent of ionic strength.

Of course, a dinucleoside phosphate only has one phosphate. If interactions between neighboring phosphates were important then there still might be an effect with longer oligomers and polymers. The ORD of trinucleoside diphosphates, however, are also independent of changes in the ionic strength. The ORD of five trimers measured in the presence and absence of salt by Dr. Cantor[36] are also summarized in Table 2. The pH of these solutions was about 6. Once again

Table 2

Salt Dependence of Optical Rotatory Dispersion of Oligonucleotides

Compound	Wavelength (mμ)	Molar Rotation x 10^{-4} 0.1 Ionic Strength	Molar Rotation x 10^{-4} No Salt Added
ApA	282	0.86	0.80
ApA	260	-2.92	-2.80
CpC	290	1.88	1.85
CpC	267.5	-1.92	-1.84
ApApU	280	1.10	1.09
ApApU	260	-2.92	-2.95
GpGpC	290	0.45	0.55
GpGpC	250	-0.76	-0.72
GpApU	280	0.79	0.88
GpApU	260	-1.14	-1.20
ApGpU	290	0.17	0.21
ApGpU	270	-0.65	-0.67
ApGpU	250	0.13	0.30
GpGpU	275	0.39	0.27
GpGpU	250	-0.55	-0.44

each of the particular wavelengths correspond to a maximum or minimum.

The ORD of single-strand poly C and poly A show a small dependence on ionic strength. The rotation of poly C has been measured at pH 8.2 in a solution containing 10^{-3} M Tris-HCl, 10^{-4} M EDTA and in the same solution to which KCl crystals had been added to a total concentration of 0.15 M. The two curves are shown in Figure 7. The rotation at the trough for the low salt solution is less than for the high salt solution. The opposite effect happens with poly A. Mr. B. Tomlinson[113] has found a 6% increase in the rotation of the trough when the NaCl concentration is decreased from 0.15 M to virtually salt-free. These changes in the rotation of stacked C and A residues with changes in the ionic strength may tend to cancel in an RNA.

Fasman et al.[71] observed a more significant dependence of the ORD of poly C at pH 7 on the added salt concentration. This is probably due to a limited formation of the double-strand complex of poly C at the lower ionic strengths. The ORD and UV spectrum of poly C at pH 7 in a solution containing only 10^{-4} M Na^{+} definitely indicate that it is double-stranded under these conditions.

The conclusion from these experiments is that the ORD of a single-strand RNA helix with stacked bases is insensitive to changes in the added salt concentration between 0.1 M and zero. The rotation of an RNA calculated from Eq. (5) with

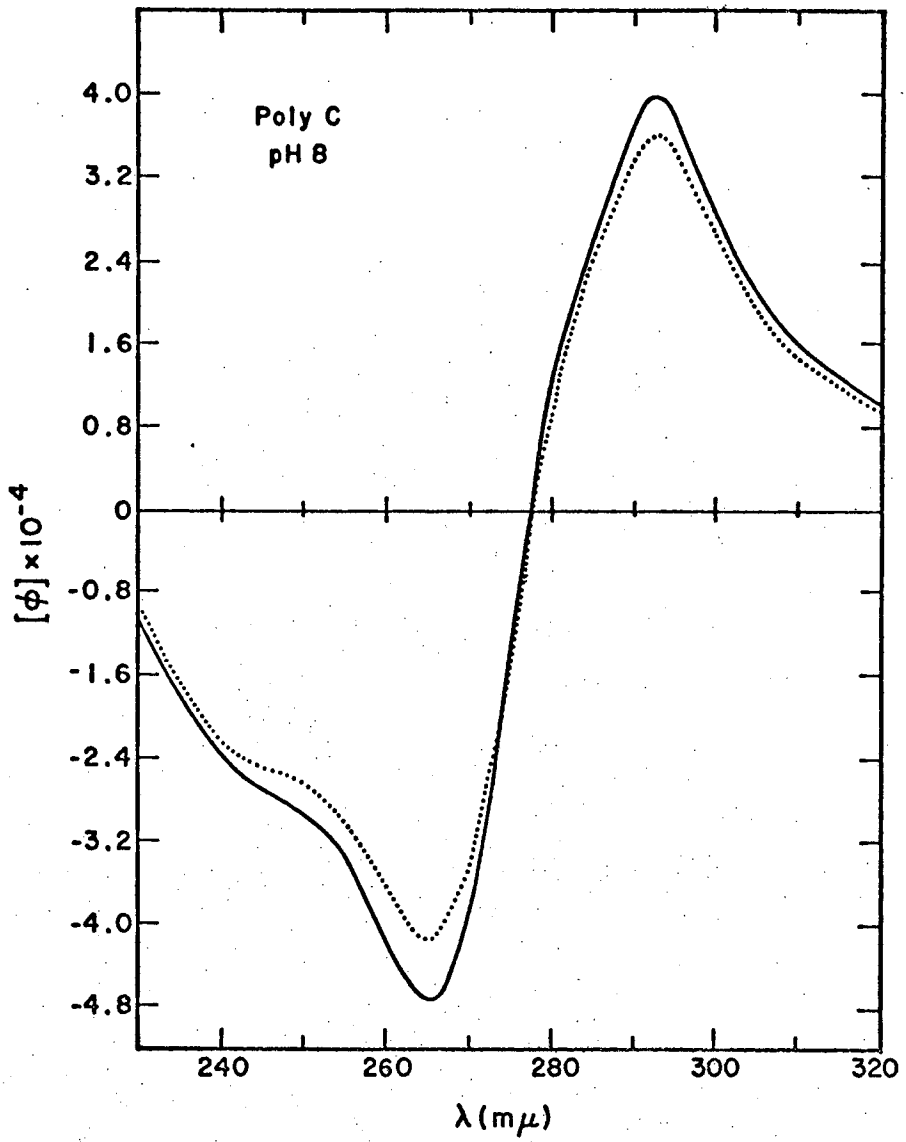

Figure 7. ORD of Poly C.

---, Experiment, 10^{-3} M Trix-HCl, 10^{-4} M EDTA, pH 8.2.

——, Experiment, 0.15 M KCl, 10^{-3} M Tris-HCl, 10^{-4} M EDTA, pH 8.2.

dimer and monomer data obtained from solutions of 0.1 ionic strength will apply to a totally single-strand RNA with stacked bases in a solution containing any amount of added univalnet cation up to a concentration of 0.15 M.

2. pH Dependence of ORD of TMV RNA at Low Ionic Strength

The observations that were made on poly C clearly showed that a significant number of bases are protonated at pH 7 in solutions which contain 10^{-4} M Na^+. The pK of cytidine is 4.3[112] and the pK of one-half the residues of poly C in a solution containing 0.1 M NaCl is 5.7.[112] The large shift in the pK occurs because the electrostatic attraction between the positively charged cytosine bases and the phosphate backbone stabilizes a double-strand helix. Therefore, it is reasonable to expect the pK of cytosine in poly C to be shifted even higher as the ionic strength is lowered. Similar results have been observed by Holcomb for poly A[114] which forms a double-strand helix when all the residues are protonated.

We were concerned that in virtually salt-free solutions a significant number of bases in a single-strand RNA would be protonated. The ORD of such an RNA could not be fairly compared with the calculated ORD from the dimers and monomers. The optical rotation spectra of these latter compounds were all measured in solutions where they were not protonated. Twice-distilled water has enough CO_2 dissolved in it to lower

the pH to at least 6. Of course, an RNA which is only 25% A and 25% C probably does not have many long stretches of A or C. Most of the A and C residues will not be able to form a helix as they do in the homopolymers when they become protonated. Thus, the pKs of A and C in an RNA are probably not as high as they are in poly A and poly C. But they are probably higher than they are for cytidylic acid and adenylic acid because the bases of an RNA are in a negative electrostatic field originating from the cloud of phosphates surrounding them. Therefore, it seemed desirable to determine whether many bases in an RNA would be protonated in a salt-free solution with a pH around 6.

The ORD of TMV RNA has been measured at room temperature in a solution containing 10^{-4} M tetrasodium EDTA as a function of pH. The pH of the solution was adjusted with HCl. The concentration of Na^{+} was 4×10^{-4} M in all solutions. Molar rotation at the peak (286 mμ) and trough (257 mμ) are plotted in Figure 8 as a function of pH. Experimental points are shown for two entirely different preparations of the RNA. The position of the peak and trough remain unchanged throughout the pH range between 5 and 10. However, the rotation at both the peak and trough decrease in magnitude as the pH is lowered below 7. There is essentially no change in the magnitude of the rotation between pH 7 and pH 10.

The interpretation of these observations is that at this ionic strength a significant number of residues are protonated below pH 7. But, none are protonated between pH 7 and pH 10.

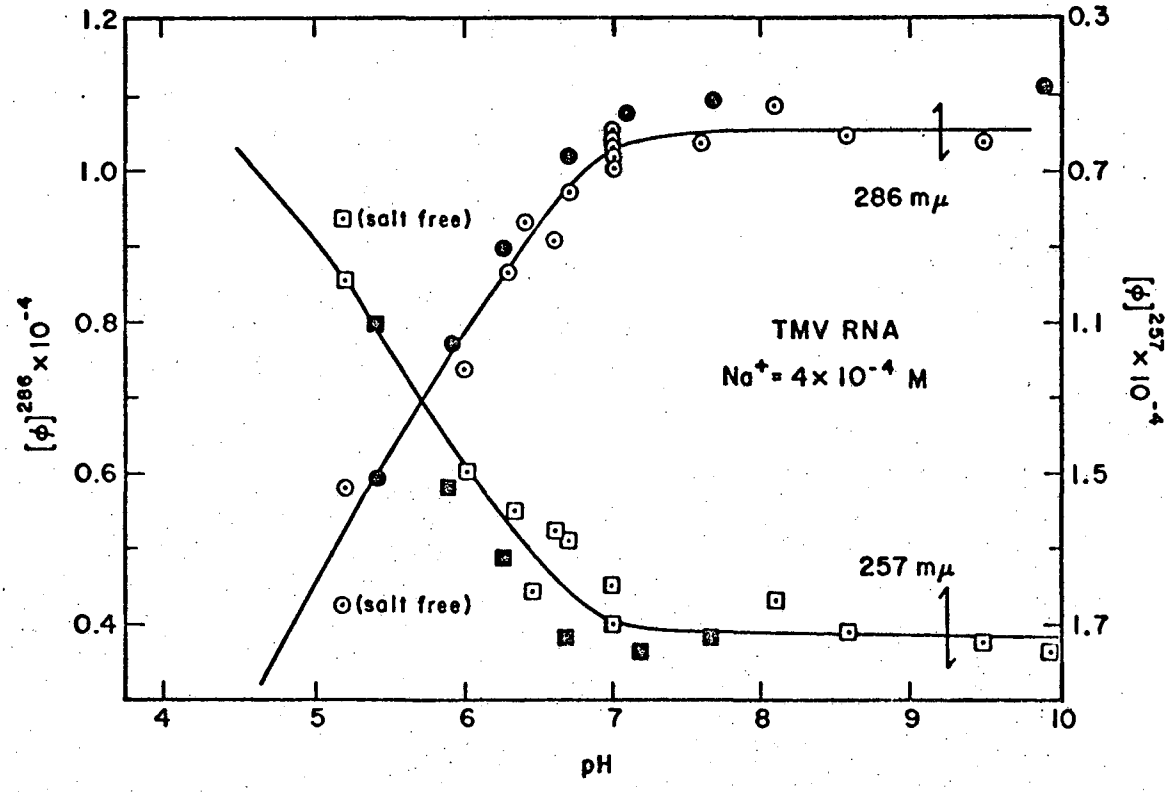

Figure 8. ORD of TMV RNA as a function of pH, $Na^+ = 4 \times 10^{-4}$ M, 25°C.

⊙, 286 mμ; ⊡, 257 mμ. The solid circles and squares refer to a different preparation.

Significant in this context refers to the ability of the ionization to directly or indirectly alter the ORD of the RNA. Clearly the ORD of TMV RNA in a solution containing only 4×10^{-4} M Na^+ must be measured at a pH of 7 or higher if it is to be characteristic of the unprotonated molecule. TMV RNA is probably representative of single-strand RNAs. Therefore, we have assumed the same conclusion for the other RNAs that have been investigated, R17 RNA, F2 RNA, and mixed yeast tRNA.

The rotation at the trough and peak of a completely salt-free sample are included in Figure 8. The pH of the solution is 5.2. The rotation of this solution is not characteristic of an unprotonated molecule. The experimental points fall off the extrapolated line for the solution which contains 4×10^{-4} M Na^+. They fall on the side which indicates that more of the residues are protonated in a salt-free solution at pH 5.2 than in a solution which contains some added Na^+. This may indicate that the pKs are shifted even higher in the complete absence of added cations.

The pronounced dependence of the ORD on pH at this ionic strength is surprising. The acid pHs of A, C, and G nucleosides are 3.5, 4.2, and 1.6, respectively.[115] Uridine only has a basic pK.[115] The principal residues that become protonated between pH 5 and 7 are probably A and C. If we make certain simplifying assumptions, the fraction of these residues which are protonated at pH 5 can be estimated. The rotation at pH 7 is taken as the rotation of the totally

single-stranded unprotonated RNA. Zero rotation can be taken as the rotation of the fully protonated RNA. The absolute value of the rotation at both wavelengths will actually be greater than this. Taking zero as the rotation of the protonated form gives us a conservative estimate of the fraction protonated at pH 5. The result is the same at both wavelengths, more than 75% of the A and C residues are protonated at pH 5. The pKs have been shifted as much as they are in poly A and poly C.

Another interpretation of the data is that the rotation of the RNA at pH 7 is not characteristic of unprotonated single-strand RNA. Rather, it may reflect the existence of some double-strand regions in the RNA. In which case, the rotation could be greater than if there were no double-strand regions. Such regions might become disrupted if only a small fraction of the residues became protonated. Therefore, the plot of rotation versus pH is not equivalent to a plot of hydrogen ions bound versus pH. The change in rotation with pH would reflect protonation and the loss of double-strand character.

The experimental ORD curves that we intend to compare with the calculation from the dimers have been measured in a solution containing 4 x 10^{-4} M Na^{+}, pH 7. The experiment shown in Figure 8 indicates that under these conditions the RNA is unprotonated. If the RNA contains some double strands under these conditions, however, then the ORD at a lower pH may be more characteristic of single-strand unprotonated RNA.

3. The ORD of Single-Strand RNA

The ORD of TMV RNA, R17 RNA, F2 RNA, and mixed yeast tRNA have been measured at 25°C in a solution containing 10^{-4} M EDTA, pH 7. The concentration of added Na^+ in these solutions is 4×10^{-4} M. The spectra are shown in Figures 9-12. The ORD of the same solutions, to which crystalline KCl has been added to a final concentration of 0.15 M, are also shown. These two experimental curves are compared in the figures with the ORD of each of the RNAs calculated from dinucleoside phosphate data using Eq. (5). The calculated curve is consistent with theoretical predictions of the ORD of a single-strand helix with stacked bases perpendicular to the helix axis.[116]

The ORD of the different RNAs under the same conditions are similar. In the presence of 0.15 M KCl the peak, crossover, and trough occur around 280, 265, and 250 mμ, respectively. In the absence of KCl they occur around 286, 272, and 258 mμ. The calculated curves are also very similar in this respect. The magnitude of the rotation at the peak and trough for the different RNAs are similar for each experimental condition and for the calculation. It should also be added that the experimental ORD curves in Figures 9-12 are similar to other measurements of the ORD of single-strand RNA.[78,127-129,89,117] The conclusion is that the four RNAs which have been investigated have nearly identical optical rotation properties and are characteristic of single-strand RNA in general.

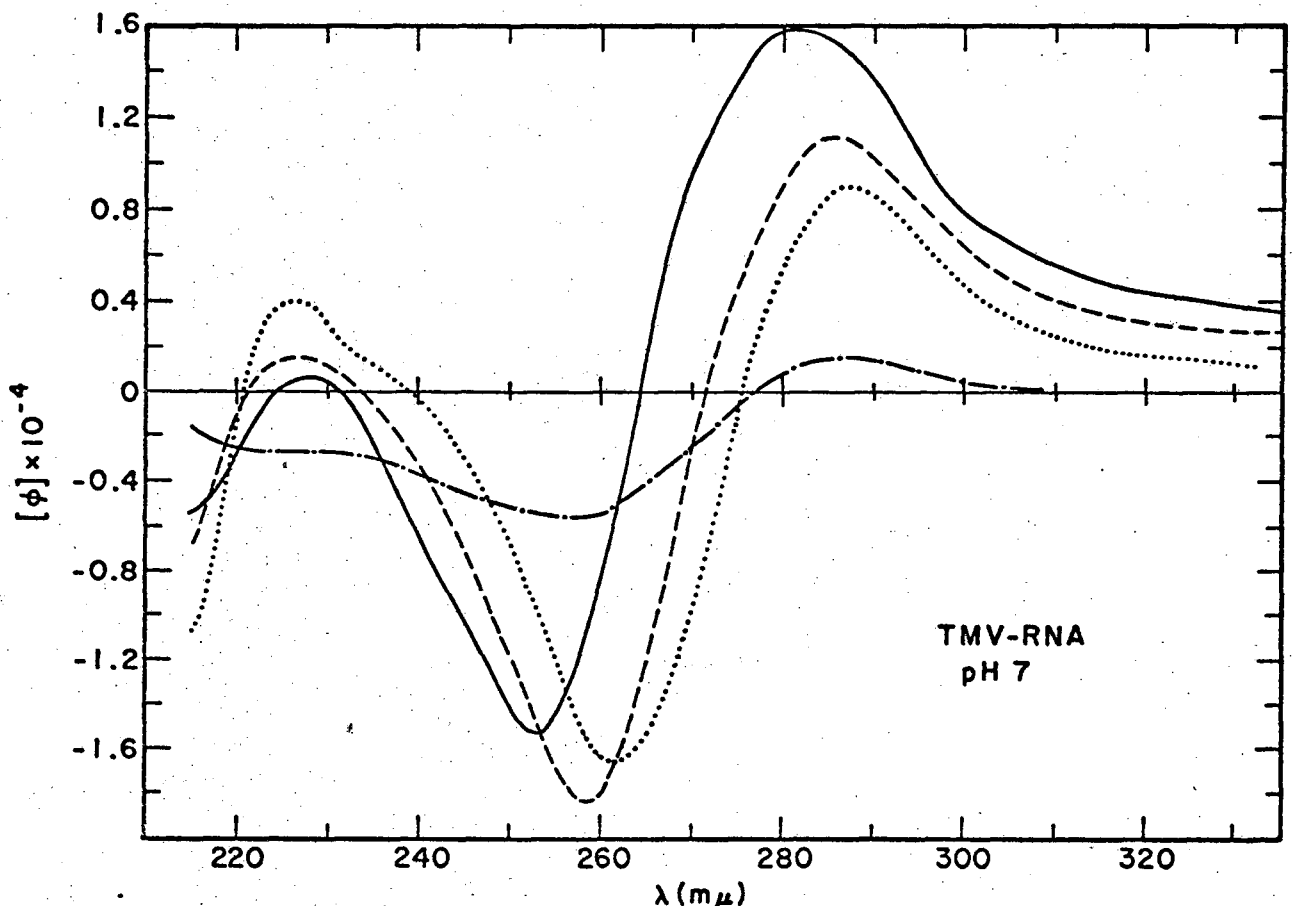

Figure 9. ORD of TMV RNA.

——, Experiment, 0.15 M KCl, 10^{-4} M EDTA, pH 6.5, 26°C.

---, Experiment, 10^{-4} M EDTA, pH 6.9, 26°C.

···, Nearest-neighbor calculation for ORD of single-strand TMV RNA.[36]

-·-, Average of ORD for monomers in TMV RNA.

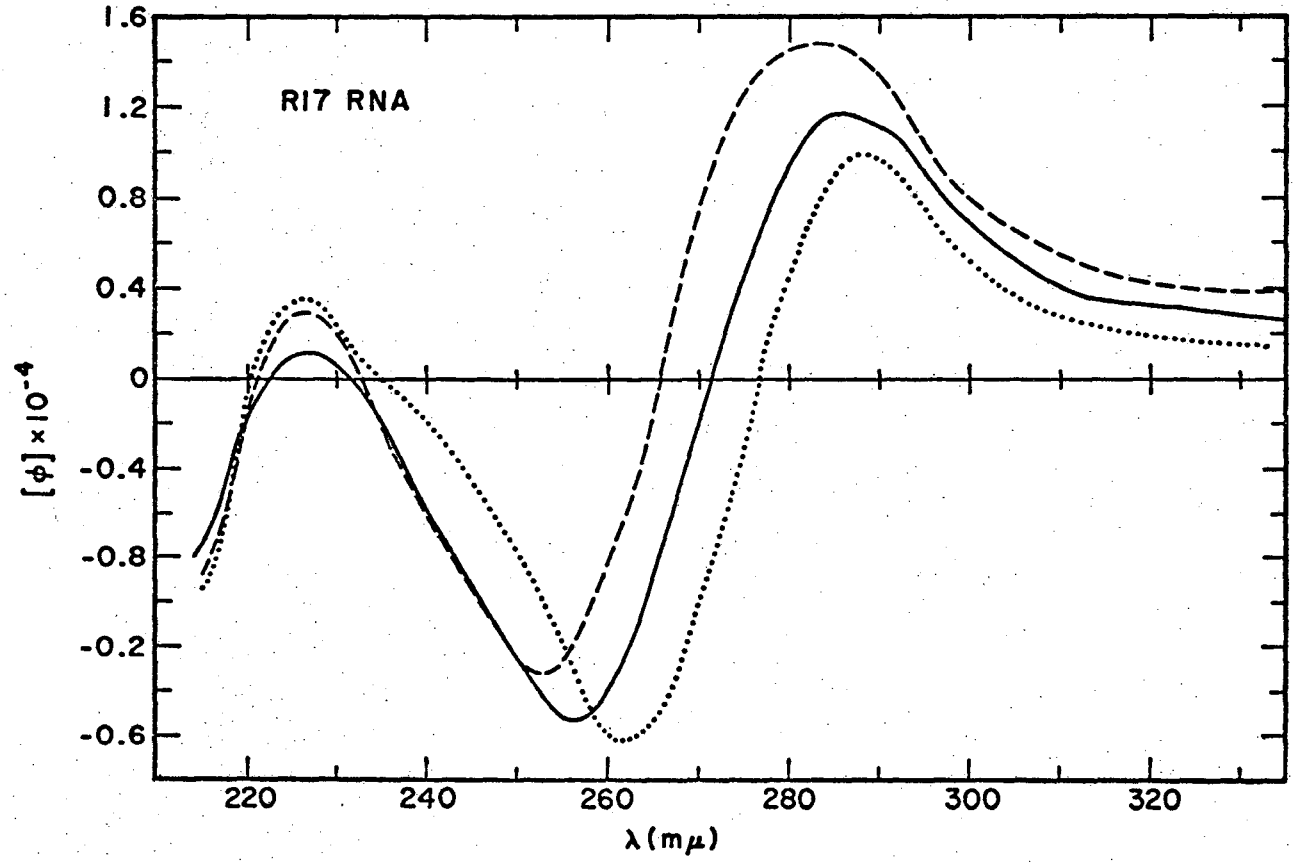

Figure 10. ORD of R17 RNA.

---, Experiment, 0.15 M KCl, 10^{-4} M EDTA, pH 6.5, 26°C.

——, Experiment, 10^{-4} M EDTA, pH 6.9, 26°C.

..., Nearest-neighbor calculation for ORD of single-strand R17 RNA.[36]

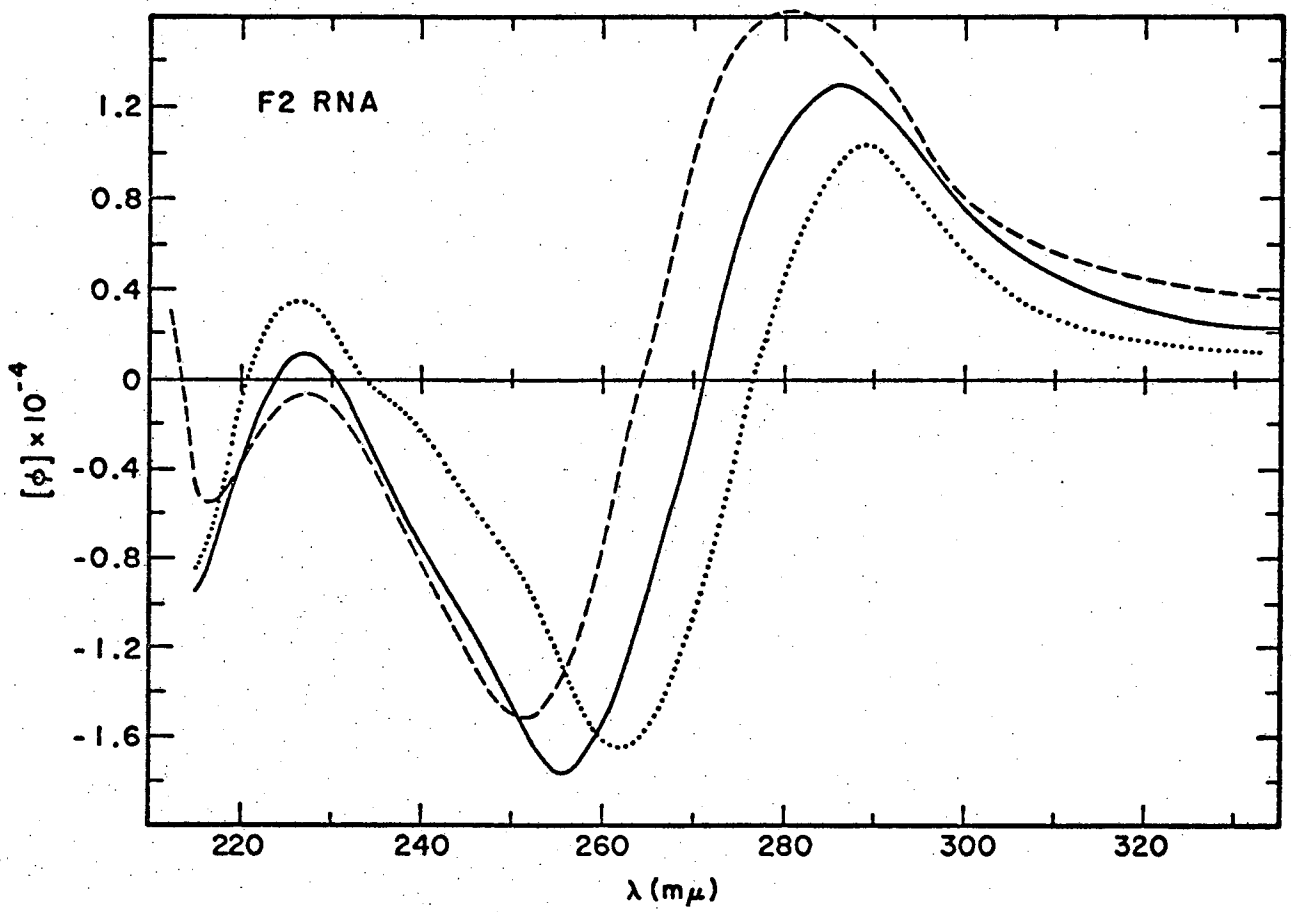

Figure 11. ORD of F2 RNA.

---, Experiment, 0.15 M KCl, 10^{-4} M EDTA, pH 6.5, 26°C.

——, Experiment, 10^{-4} M EDTA, pH 6.9, 26°C.

···, Nearest-neighbor calculation for ORD of single-strand F2 RNA.[36]

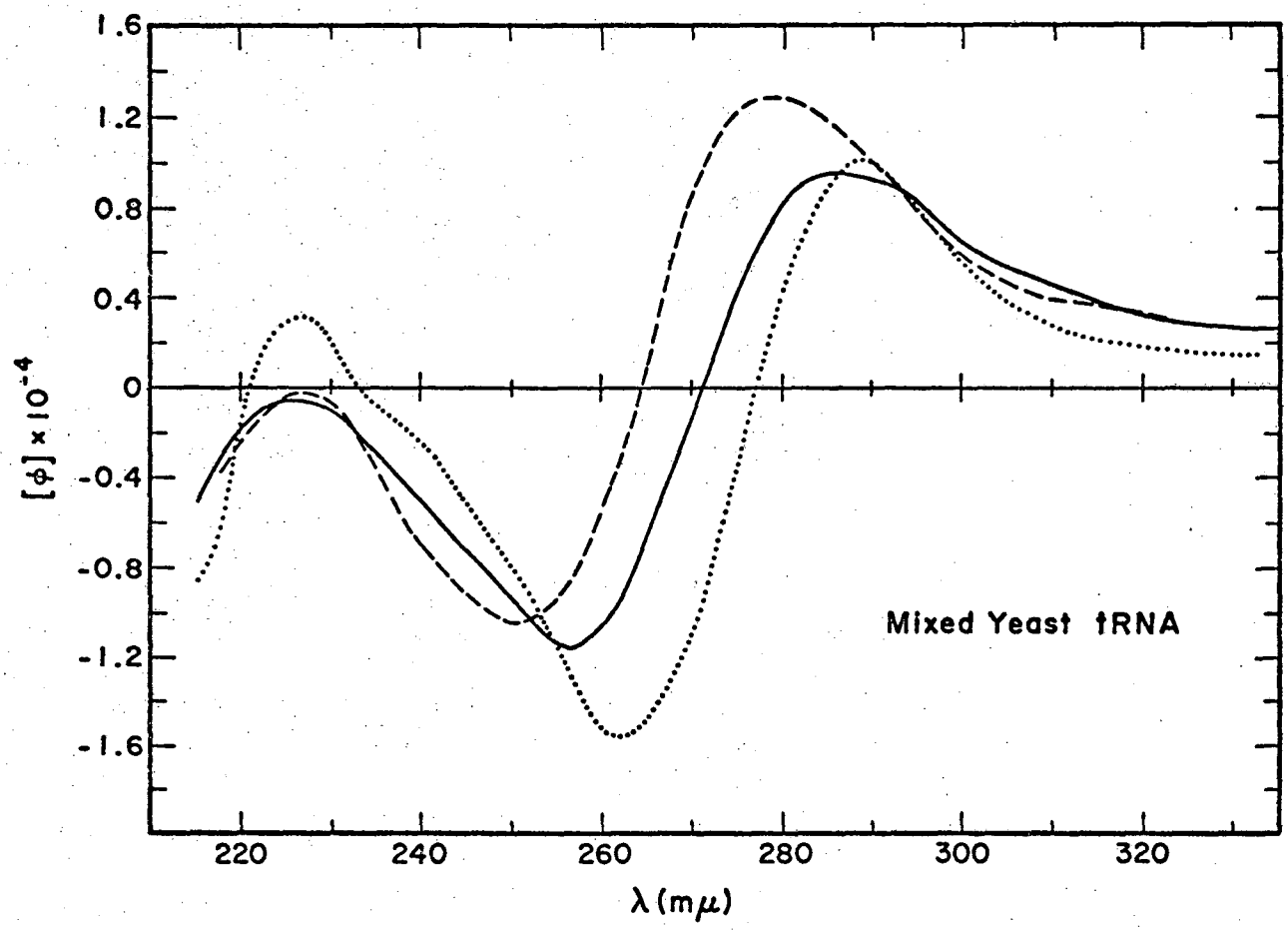

Figure 12. ORD of mixed yeast tRNA.

---, Experiment, 0.15 M KCl, 10^{-4} M EDTA, pH 6.5, 26°C.

——, Experiment, 10^{-4} M EDTA, pH 6.9, 26°C.

···, Nearest-neighbor calculation for ORD of single-strand mixed yeast tRNA.[36]

The result of the comparison between experiment and calculation is also the same for each RNA. The ORD of the RNA in the presence of 10^{-4} M EDTA is more similar to the calculated curve than the ORD of the solution which also contains 0.15 M KCl. Even in the absence of KCl, however, the agreement between the experimental and calculated curves is not perfect. The experimental curve is shifted about 4 mμ to the blue of the calculated curve and the magnitude of the rotation at the peak and trough is greater. The addition of KCl to the solution further shifts the position of the peak, crossover, and trough 6-7 mμ to the blue. The magnitude of the rotation increases at the peak and decreases at the trough.

It has already been shown that the ORD of stacked bases is independent of ionic strength. Thus, the change in the ORD of a single-strand RNA when KCl is added must result from intramolecular aggregation like hydrogen bonding. We eliminate intermolecular aggregation as a possible explanation since the molecular weight of TMV RNA, as determined from hydrodynamic properties of solutions with concentrations equal to or greater than what we have used, indicates that the solutions are monodisperse.[73,74] Our results are consistent with the variation of other physical properties of single-strand RNA with ionic strength.[30,31,73] These experiments have always been interpreted as indicating an increase in base pairing with increasing ionic strength.

The conformation of single-strand RNA in a solution of low ionic strength has been termed a random coil.[29-31] If neighboring bases in a random coil have a completely random orientation relative to one another, then the ORD of the coil should be the same as the average ORD of the constituent monomers. The average ORD of the monomers in TMV RNA is given in Figure 9. The overall shape of the curve is similar to the experimental ORD of TMV RNA in the presence of 10^{-4} M EDTA. The measured magnitude of the rotation at the peak, however, is 6 times the rotation at the peak of the monomer curve. The rotation at the trough is more than 3 times greater. By contrast, the ORD of TMV RNA calculated from the dimers agrees reasonably well with the experimental curve. The sum of the monomers for the other three RNAs would be similar to TMV RNA. The nearest-neighbor calculations for these RNAs also agree much better with the experimental curves obtained in the presence of 10^{-4} M EDTA. Therefore, we conclude that the bases in single-strand RNA are stacked in the absence of base pairing. Furthermore, neighboring bases are stacked similar to the way in which they are stacked in dinucleoside phosphates. The conformation can be visualized as a single-strand helix with stacked bases perpendicular to the helix axis.

Similar results have been recently reported by Bush and Scheraga.[117] They have shown that the ORD of E. coli rRNA in a dilute sal solution is different from the ORD of a salt-

free solution. Furthermore, the ORD of the salt-free solution is almost identical to the curve calculated from the dimers. The agreement is much better than we have found. This is probably because the pH of the salt-free solution was less than 7. At pH 6.5 the experimental ORD of TMV RNA in the presence of 10^{-4} M EDTA is also nearly identical to the calculated curve. The calculated and experimental curves under these conditions are shown in Figure 13. The results of the preceding section clearly indicate that TMV RNA is slightly protonated at pH 6.5. Therefore, it is not entirely correct to compare the experimental curve at pH 6.5 with the curve calculated from the ORD of unprotonated dinucleoside phosphates. Nevertheless, the conclusions are still valid. Single-strand RNA which does not contain any base pairs has an ordered conformation.

But, is stacking an important element in the secondary structure of RNA under conditions where base pairing occurs? It obviously is if it does not prevent the formation of base pairs. If it does then the question cannot be answered unless we know the relative stabilities of base stacking and base pairing.

The enthalpy of formation of an A-U base pair has been measured calorimetrically by Ross and Scruggs[118] and others.[119,120] They found that the ΔH^{o} of formation is -5.95 kcal per base pair. The ΔH^{o} for the formation of a G-C base pair is probably greater, but of the same order or magnitude.[32]

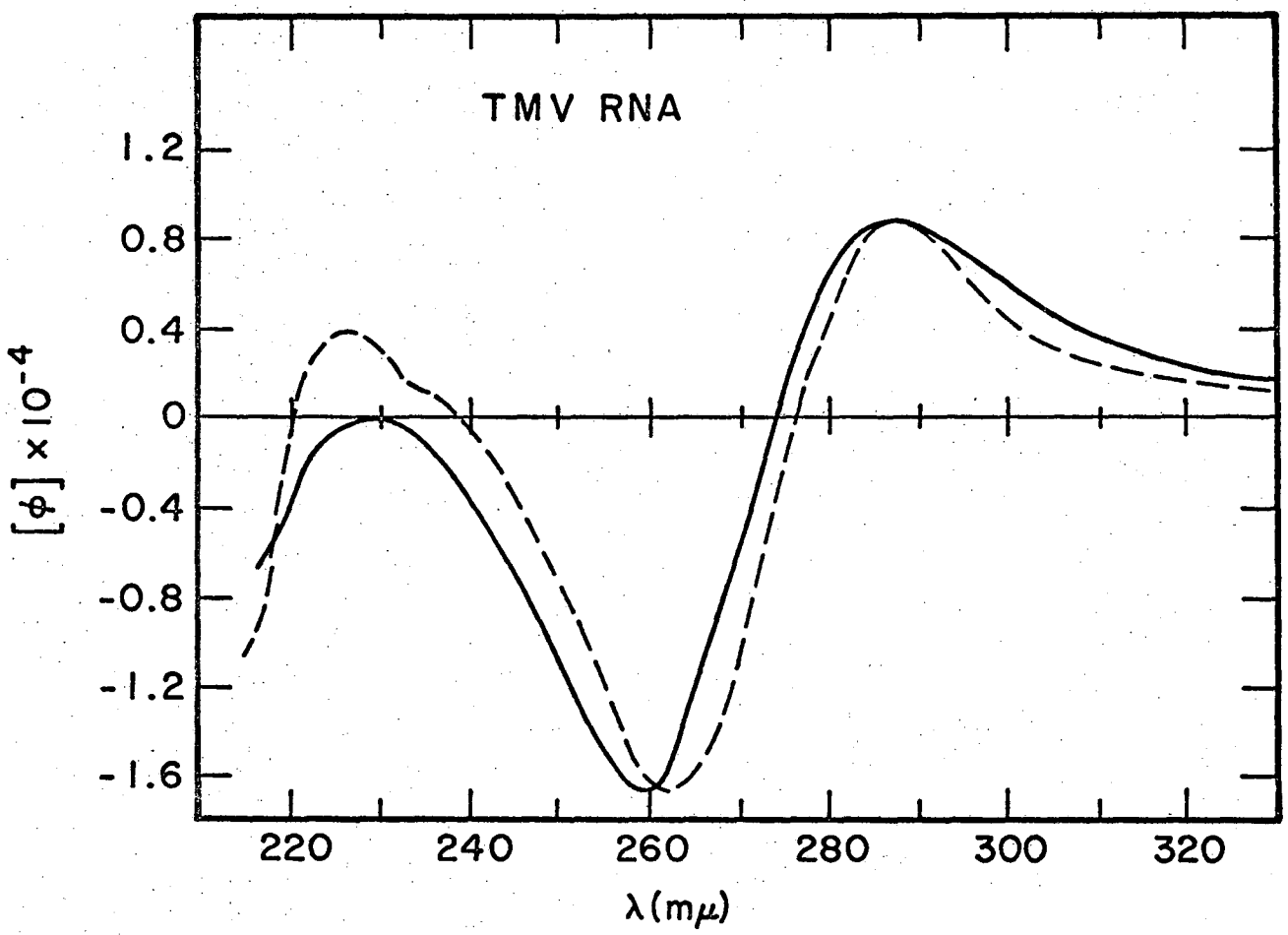

Figure 13. ORD of TMV RNA.
——, Experiment, 10^{-4} M EDTA, pH 6.5, 26°C.
---, Nearest-neighbor calculated ORD of TMV RNA at room temperature.

The enthalpy of stacking has been determined from the temperature dependence of the optical properties of dinucleoside phosphates,[60,92] oligoribonucleotides,[47,51,55,53] and polyribonucleotides.[47,55,51] The values range from -5 to -10 kcal per mole depending on the particular property measured, the bases involved, the model used for the analysis, and the investigator who does the analysis. The important conclusion is that the magnitude of the enthalpy of stacking is the same as for the formation of A-U and G-C base pairs.

The entropy of formation of base pairs is 22 cal./°C per mole of base pair formed.[118,120,122] This number is the same for the average base pair in DNA[122] and the A-U base pair in poly (A+U).[118,120] The estimates of the entropy of stacking are of the same order of magnitude.[47,60]

Therefore, it can be concluded that the free energy of stacking and base pair formation are comparable. In other words, stacking and base-pair formation are equally important elements in the secondary structure of single-strand RNA. The consequence of this is that base-paired helical regions cannot form randomly at the expense of base stacking. Loops which result in an equal number of base pairs and loss of base-base stacking interactions may not be stable.

4. The ORD of TMV RNA as a Function of Temperature and Ionic Strength

The agreement between the experimental ORD of RNA in the

presence of 10^{-4} M EDTA and the ORD that has been calculated for a single-strand helix with stacked bases is not as good as we might hope. There are several possible reasons for this. The nature of stacking might be different in an RNA than the dinucleoside phosphates. Interactions between next nearest neighbors may be important. Any of these explanations are plausible for the same reasons that we rationalized the difference between experiment and calculation for single-strand poly A and poly C. The calculated magnitude of rotation at the peak and trough is closer to the experimental value for RNA than for poly A and poly C. The blue-shift of the experimental curve from the calculated one is larger for RNA, however.

Another possible explanation for the difference between experiment and calculation for RNA is that a small but significant amount of intramolecular aggregation still exists. This explanation can be tested for experimentally. The ORD of the four RNAs have been measured at 25°C. The calculated ORD curves were done with the experimental ORD of the dimers and monomers at 25°C. If the residual intramolecular aggregation is hydrogen bonding then it is probably all "melted-out" at some higher temperature. The ORD of the RNA at that temperature should be closer to the ORD calculated from the dimers measured at that same temperature.

The ORD of TMV RNA has been measured as a function of temperature at four different ionic strengths. The concentrations of Na^+ in the solutions were 4×10^{-4} M, 4×10^{-3} M,

4×10^{-2} M, and 1.0 M. The pH of each solution was between 7.5 and 8.2. An example of the results is shown in Figure 14 for the solution which contains 4×10^{-2} M Na^+.

The molar rotations at 255.0, 287.5, and 267.5 mμ are plotted versus temperature in Figures 15-17, respectively, for all four ionic strengths. The ORD of TMV RNA has been calculated as function of temperature using Eq. (5) and the temperature dependence of the ORD of the dimers and monomers. The calculated rotations at 267.5, 287.5, and 255.0 mμ are also plotted in Figures 15-17.

These three wavelengths have been chosen partly because they represent extremes in the ORD of TMV RNA. Wavelengths 287.5 and 255.0 mμ are near the peak and trough. The cross-over comes near 267.5 mμ. Furthermore, the agreement between experiment and calculation is different at each wavelength.

The rotation at 255.0 mμ decreases in absolute magnitude with increasing temperature for each case shown in Figure 15. The variation with temperature is gradual. There is no indication of a helix-coil transition even for the solution which contains 1.0 M Na^+. The lines for the four ionic strengths and for the calculated rotation parallel one another. There appears to be a small shift in the position of the line with changes in the salt concentration, however. The absolute magnitude of the rotation increases slightly with decreasing salt concentration. Nevertheless, this wavelength is relatively insensitive to the intramolecular aggregation.

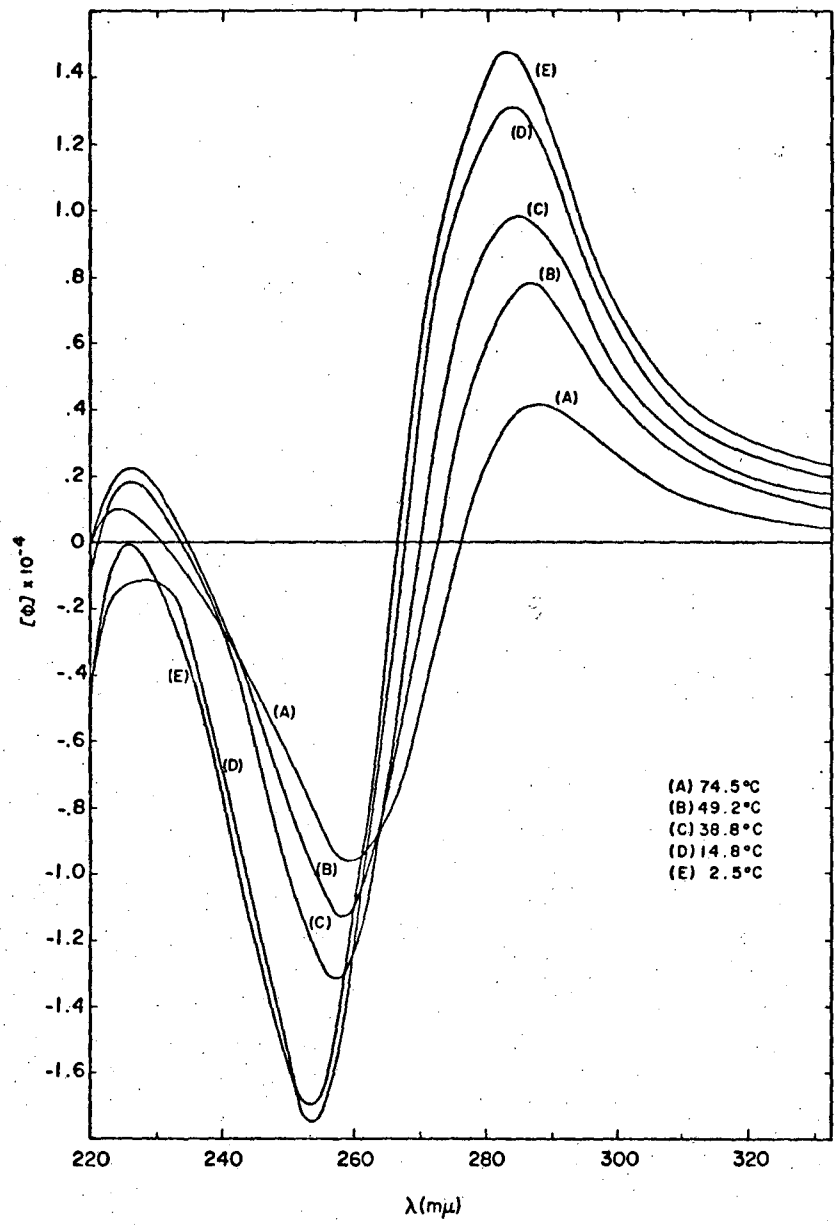

Figure 14. ORD of TMV RNA at a series of temperatures, at pH 7.5, in 0.04 M Na^+. This represents only a selection of the data that were taken at this ionic strength.

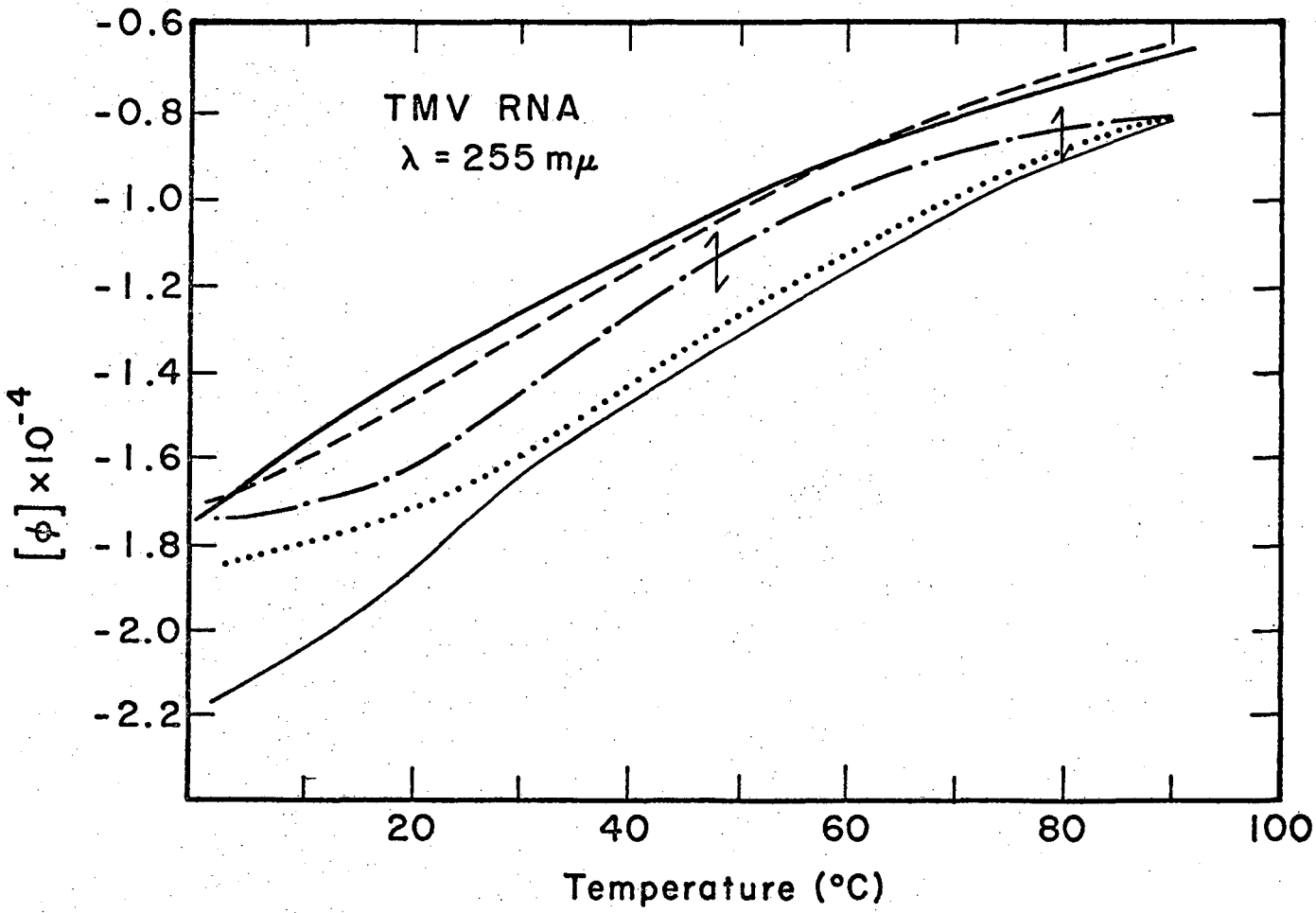

Figure 15. Molar rotation per residue of TMV RNA at 255.0 mμ, pH 7.5-8.2.

---, Na^+ = 1.0 M. -·-·-, $Na^+ = 4 \times 10^{-2}$ M. ···, $Na^+ = 4 \times 10^{-3}$ M.

—— $Na^+ = 4 \times 10^{-4}$ M. ——, Nearest-neighbor calculated rotation

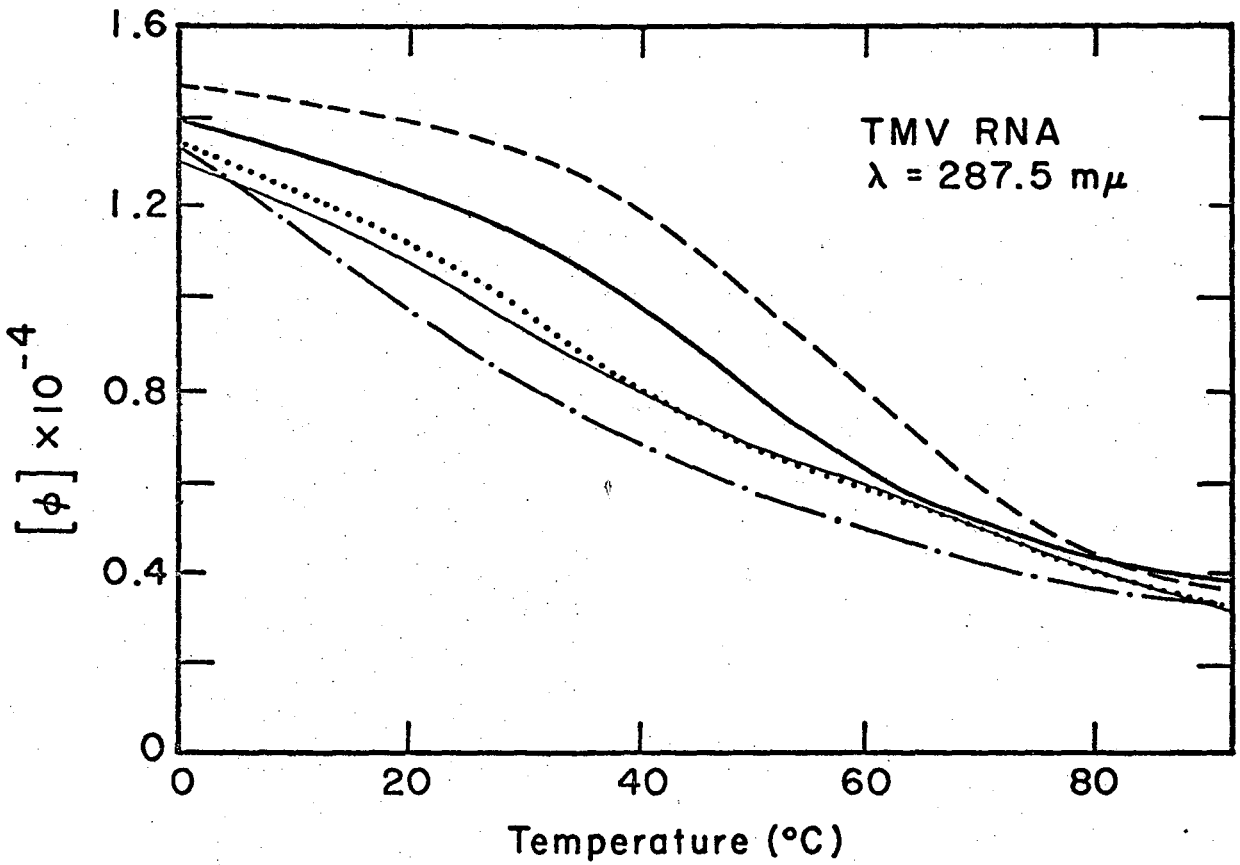

Figure 16. Molar rotation per residue of TMV RNA at 287.5 mμ, pH 7.5-8.2.

---, Na^+ = 1.0 M. ——, $Na^+ = 4 \times 10^{-2}$ M. ···, $Na^+ = 4 \times 10^{-3}$ M. —·—, $Na^+ = 4 \times 10^{-4}$ M. -·-·-, Nearest-neighbor calculated rotation for single-strand helix.

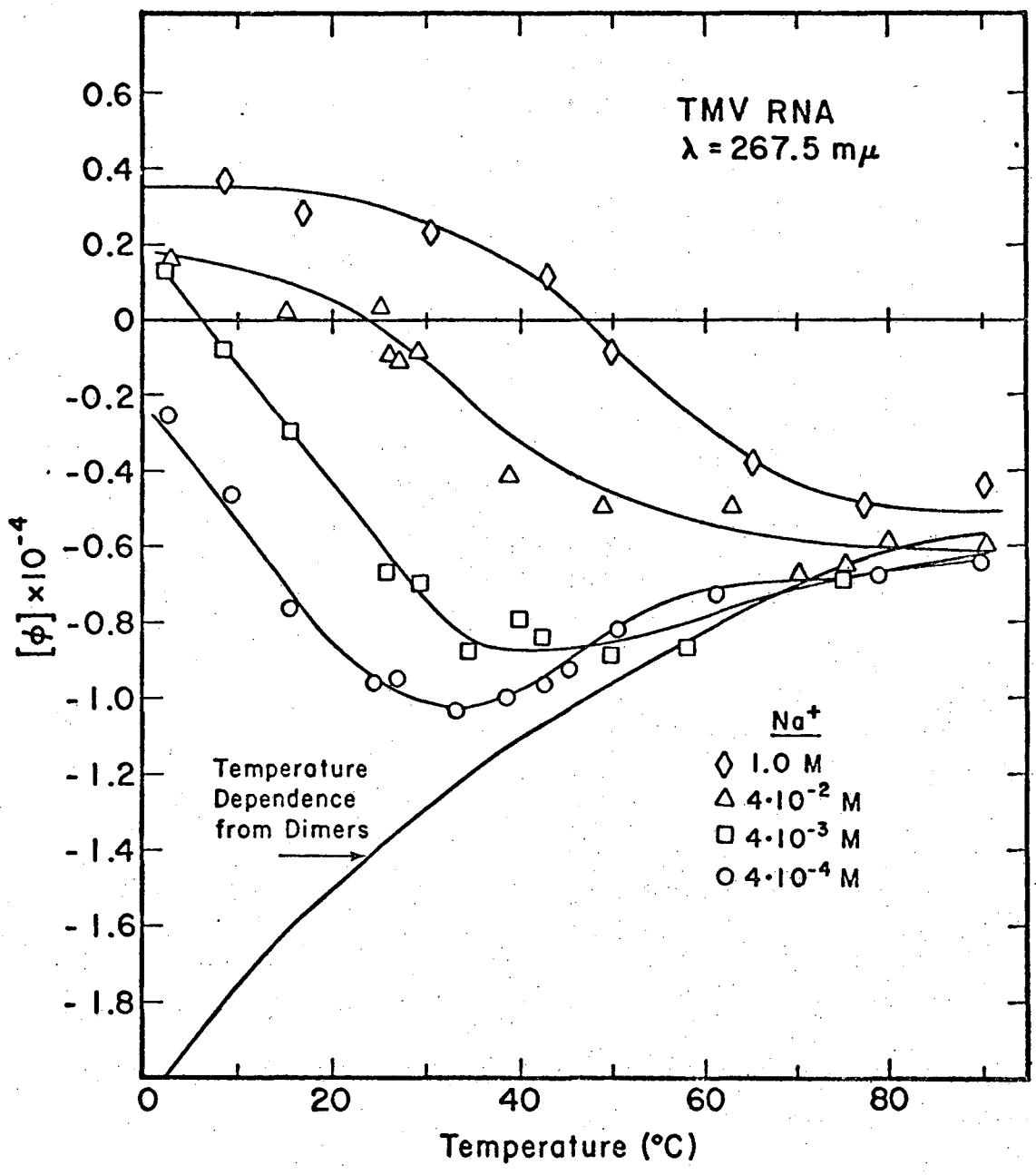

Figure 17. Molar rotation per residue of TMV RNA at 267.5 mμ, pH 7.5-8.2.

The functional dependence of the rotation on temperature is predicted reasonably well by the calculation. Although, the calculated rotation agrees better with the rotation of the solution containing 1.0 M Na^+ even at temperatures above 70°C. There is probably no intramolecular aggregation at these elevated temperatures. Therefore, we cannot expect perfect agreement at this wavelength for the calculated and experimental rotation of a single-strand helix.

The situation is different for 287.5 and 267.5 mμ. The experimental rotation for TMV RNA in the presence of 4 x 10^{-4} M, 4 x 10^{-3} M, and 4 x 10^{-2} M Na^+ follows the calculated rotation only at elevated temperatures. The magnitude of the calculated rotation also agrees with the experimental rotation at these temperatures. At lower temperatures the experimental rotation departs from the calculated rotation and begins to level off. The lowest temperature for which there is good agreement between experiment and calculation increases with increasing salt concentration. Even at the highest temperature the rotation of the solution containing 1.0 M Na^+ is not the same as the calculated rotation.

The interpretation of these observations is that for the temperature regions where there is good qualitative and quantitative agreement between calculation and experiment the RNA is completely single-stranded. By qualitative agreement, we mean that the dependence of the experimental rotation on temperature should have the same functional form as the calculation. According to this criterion, the lowest

temperature for which TMV RNA can be said to be single-stranded are as follows: 35°C for solutions containing 4 x 10^{-4} M Na^+, 50°C for solutions containing 4 x 10^{-3} M Na^+, and 70°C for solutions containing 4 x 10^{-2} M Na^+. In the presence of 1.0 M Na^+ the RNA is not completely single-stranded at 90°C.

For each ionic strength base pairs are present below 25°C. We expect that there is a base-paired structure of TMV RNA which contains as many base pairs as can possibly form. The conformation of the molecules presumably approaches this structure as the temperature is lowered.

The temperature at the midpoint of the transition from the base-paired structure to the stacked structure increases with increasing salt concentration. Thus, at any particular temperature the number of base pairs present increases with increasing ionic strength. The rotation of the base-paired structure is probably relatively independent of temperature. The rotation of the stacked structure depends on temperature in the manner predicted by the calculation; it approaches zero with increasing temperature.

The rotation at 267.5 mμ for TMV RNA in the presence of 4 x 10^{-4} M and 4 x 10^{-3} M Na^+ shown in Figure 17 is particularly illustrative of this picture. The rotation passes through a minimum. It decreases from 0° to 40°C and then increases with further increases in the temperature. Apparently at this wavelength the rotation of the base-paired structure is positive; the rotation of the stacked structure

at low temperatures is negative; the rotation of the stacked structure at 90°C is intermediate. Thus, if the transition from base-paired to stacked structure occurs at a sufficiently low temperature, then the rotation as a function of temperature passes through a minimum. The magnitude and functional form of the calculated and experimental rotation agree remarkably well above the temperature where the minimum occurs. We infer from this that there are no base pairs in this temperature range.

The question that was asked at the beginning of this section was whether the difference between the calculated and experimental ORD of TMV RNA in the presence of 4×10^{-4} M Na^+ at 25°C was due to base pairs or an incorrect calculation. The qualitative and quantitative agreement between experiment and calculation at 267.5 mμ is better at higher temperatures. Therefore, the difference that exists at room temperature is at least partially the result of a residual amount of base pairing.

It is of interest now to compare the entire calculated and experimental ORD curves under conditions where there are presumably no base pairs. The calculated and experimental ORD of TMV RNA, 4×10^{-4} M Na^+, pH 8, at 2.0°, 50.8°, and 79.0° are given in Figures 18-20. The appropriate average of the ORD of the monomers is also given for each temperature.

The experimental curve is shifted to the blue of the calculated curve for all three temperatures. The shift is greater at 2°C. A similar shift had been observed at room

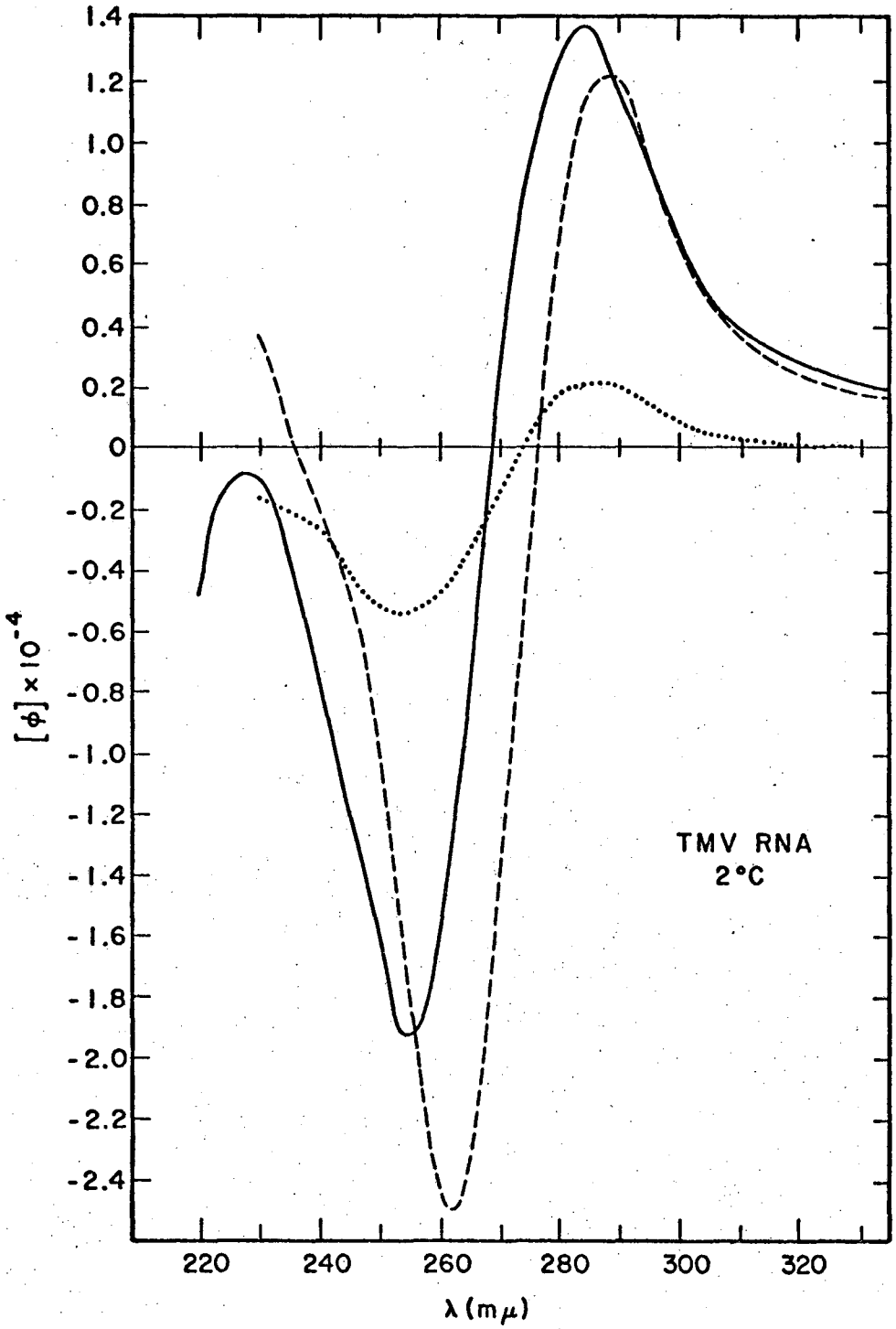

Figure 18. ORD of TMV RNA at 2°C.
——, Experiment, 4×10^{-4} M Na^+, pH 8.2.
---, Nearest-neighbor calculation for 2°C.
···, Average of monomer rotations at 2°C.

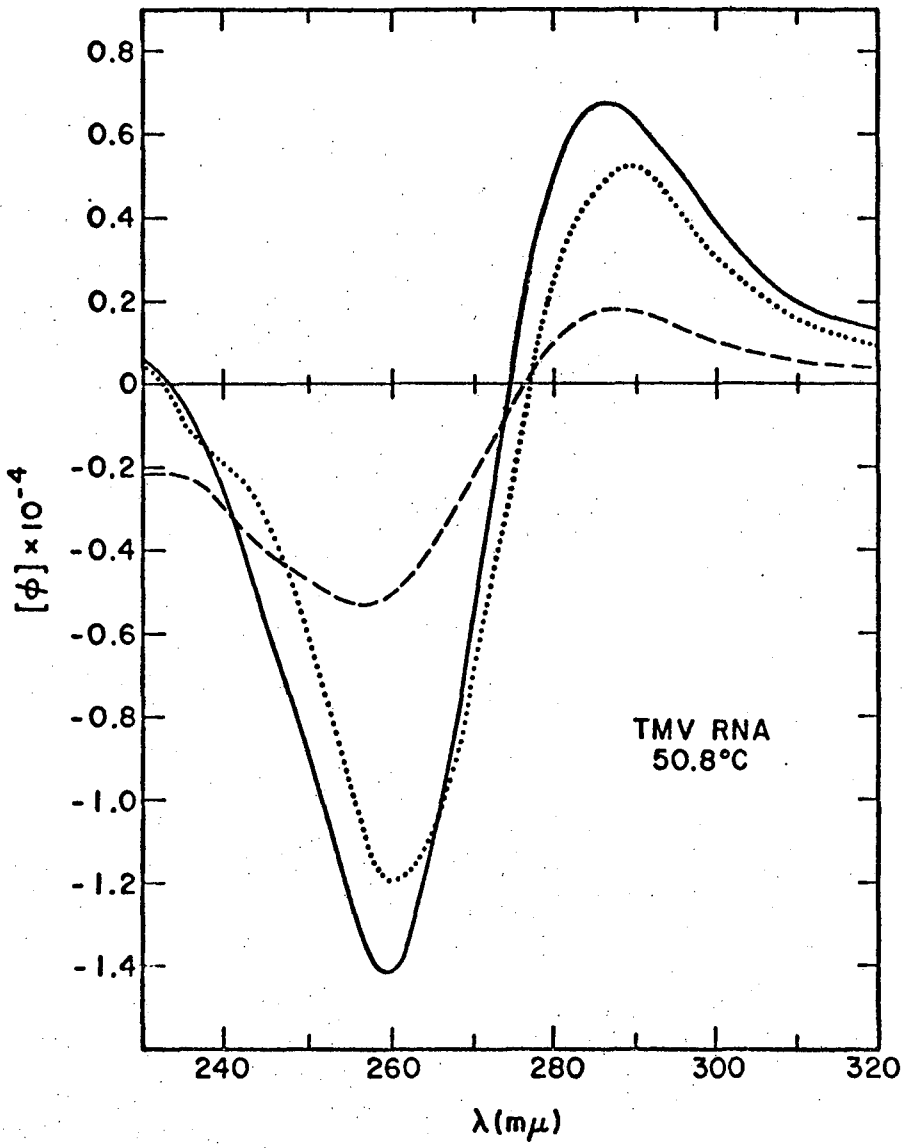

Figure 19. ORD of TMV RNA at 50.8°C.
——, Experiment, 4×10^{-4} M Na^{+}, pH 8.2.
···, Nearest-neighbor calculation for 50.8°C.
---, Average of monomer rotation at 50.8°C.

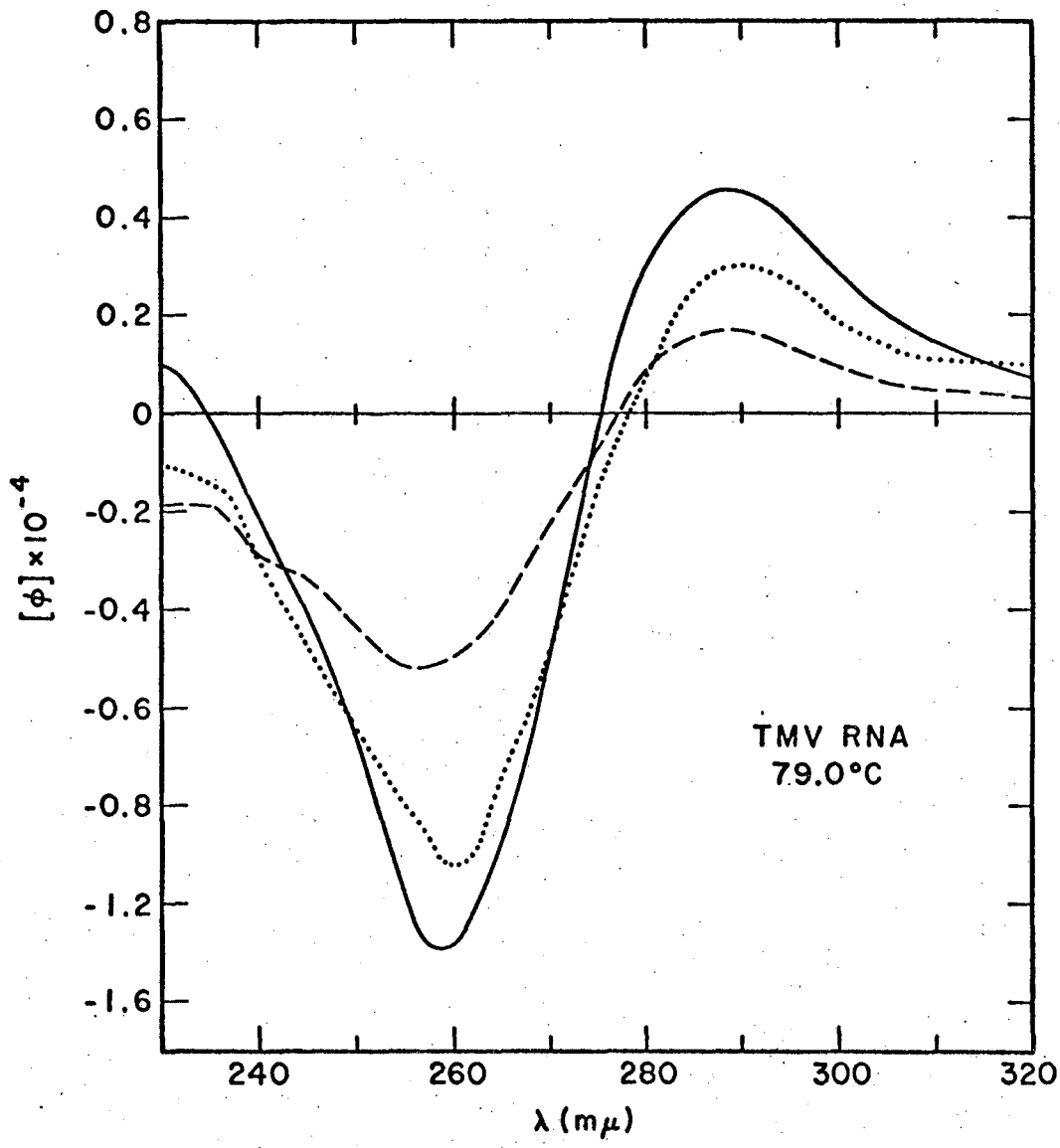

Figure 20. ORD of TMV RNA at 79.0°C.
——, Experiment, 4×10^{-4} M Na^+, pH 8.2.
• • •, Nearest-neighbor calculation for 79.0°C.
---, Average of monomer rotation at 79.0°C.

temperature for TMV RNA, F2 RNA, R17 RNA, and mixed yeast tRNA in the presence of 0.15 M KCl. A blue-shift of the crossover is apparently characteristic of the existence of base pairs. The magnitude of the rotation at the peak and trough of the experimental curve is different from the calculated curve. Once again, the discrepancy is greater at the low temperature.

From the temperature dependence of the rotation at 267.5 mμ we have concluded that there are no base pairs in TMV RNA in the presence of 4×10^{-4} M Na^+ at 50.8° and 79.0°C. The nearest-neighbor calculated ORD is close to the experimental curve at these temperatures. Clearly, the average of the dimers is a better approximation of the experimental curve than the average of the monomers. Even at 79.0°C the magnitude of the experimental rotation and the average of the dimers is larger than the average of the monomers. Thus, base stacking still exists at this high temperature.

In summary, the ORD of single-strand RNA under conditions where it does not contain any base pairs can be calculated from the ORD of dinucleoside phosphates with Eq. (5). Therefore, under these conditions the molecule has the conformation of a single-strand helix with stacked bases. The relative geometry of the stacked bases is similar to that in the dimers at all temperatures. However, the preferred orientation becomes more random with increasing temperature.

Optical Rotation Evidence for Base Pairs in Single-Strand RNA

Up to now we have directed our attention to the conformation of single-strand RNA under conditions where it does not contain base pairs. At low ionic strength and elevated temperatures the ORD of single-strand RNA is equal to the appropriate average of the ORD of the dinucleoside phosphates. At lower temperatures and in the presence of salt the ORD is different from this average. The entire experimental ORD is shifted approximately 5 mμ to the blue of the calculated ORD. The magnitude of the rotation is greater at the peak and smaller at the trough than the calculated rotations.

We have already cited evidence for the existence of base pairs in single-strand RNA. The geometry of stacked bases may be different when they are hydrogen-bonded to other bases. Even if they are not different, there will be cross-chain interactions that will affect the ORD. Therefore, it is not surprising that we cannot calculate the ORD of RNA under conditions where base pairs exist.

We would now like to show that the difference between calculated and experimental ORD of single-strand RNA at low temperature is consistent with the expected contribution of base pairs to the ORD of RNA. Thus, we will have further evidence for the existence of base pairs in single-strand RNA. Then, having shown that optical rotation is sensitive

to the existence of base pairs, we will explore methods for using it to determine the number and nature of the base pairs.

1. Effect of Base Pairs on ORD of RNA

We wish to show that the difference between the ORD of single-strand RNA under conditions where base pairs occur and the nearest-neighbor calculation is the result of base pairs. For this purpose it is useful to think of the ORD of the RNA as the sum of the rotation of the single-strand regions and the double-strand regions. Furthermore, let us equate the ORD of the double-strand regions to the sum of two other ORD curves. The first is the ORD that the residues in the double strand would have if they were part of a single-strand helix, i.e., the average ORD of the dimers. The second is whatever remains of the ORD of double-strand RNA after subtracting off the ORD of the residues if they were in a single-strand helix. This remainder can be thought of as a perturbation on the ORD of the single-strand helix caused by the base pairs. We do not want to imply by this separation that the relative orientation of neighboring bases on the same chain is the same in the single- and double-strand helices. The separation is made for convenience. Now we can see that the observed ORD of RNA under any conditions equals the ORD of the single-strand helix plus a perturbation caused by the base pairs. Of course, the perturbation will depend on the number and nature of base pairs. We shall show that the observed perturbation is that expected

if there are A-U and G-C base pairs present in the RNA. This method of identifying the nature of the intramolecular aggregation in RNA at low temperature was suggested by the work of Cantor that will be discussed at the end of this section.

Some of the base pairs in single-strand RNA are surely A-U and G-C. Fresco[72] has suggested that the base pairs in tRNA and TMV RNA are only A-U and G-C. Therefore, the perturbation on the ORD of single-strand RNA caused by base pairs should be similar to the difference between the ORD of the replicative form of MS2 RNA[123] (RF-MS2 RNA) and the calculated ORD of single-strand MS2 RNA. This completely double-strand molecule contains nearly an equal number of A-U and G-C base pairs. Therefore, the MS2 RNA difference curve is the perturbation for 100% A-U and G-C base pairing.

The ORD of RF-MS2 RNA is shown in Figure 21. The ORD of single-strand MS2 RNA which has been calculated from the dimers and monomers at room temperature with Eq. (5) is also shown. The difference between the two curves is compared in Figure 22 with the difference of the ORD of TMV RNA in the presence of 0.15 M KCl and in the presence of 10^{-4} M Na^{+} at 25°C, pH 7. The calculated rotation for single-strand TMV RNA at room temperature has also been subtracted from the ORD of TMV RNA is a solution of 0.15 M KCl at 25°C. The result is also shown in Figure 22. The shape of each of the three difference curves is similar. The most prominent feature is a positive peak at 267-269 mμ. The magnitude of

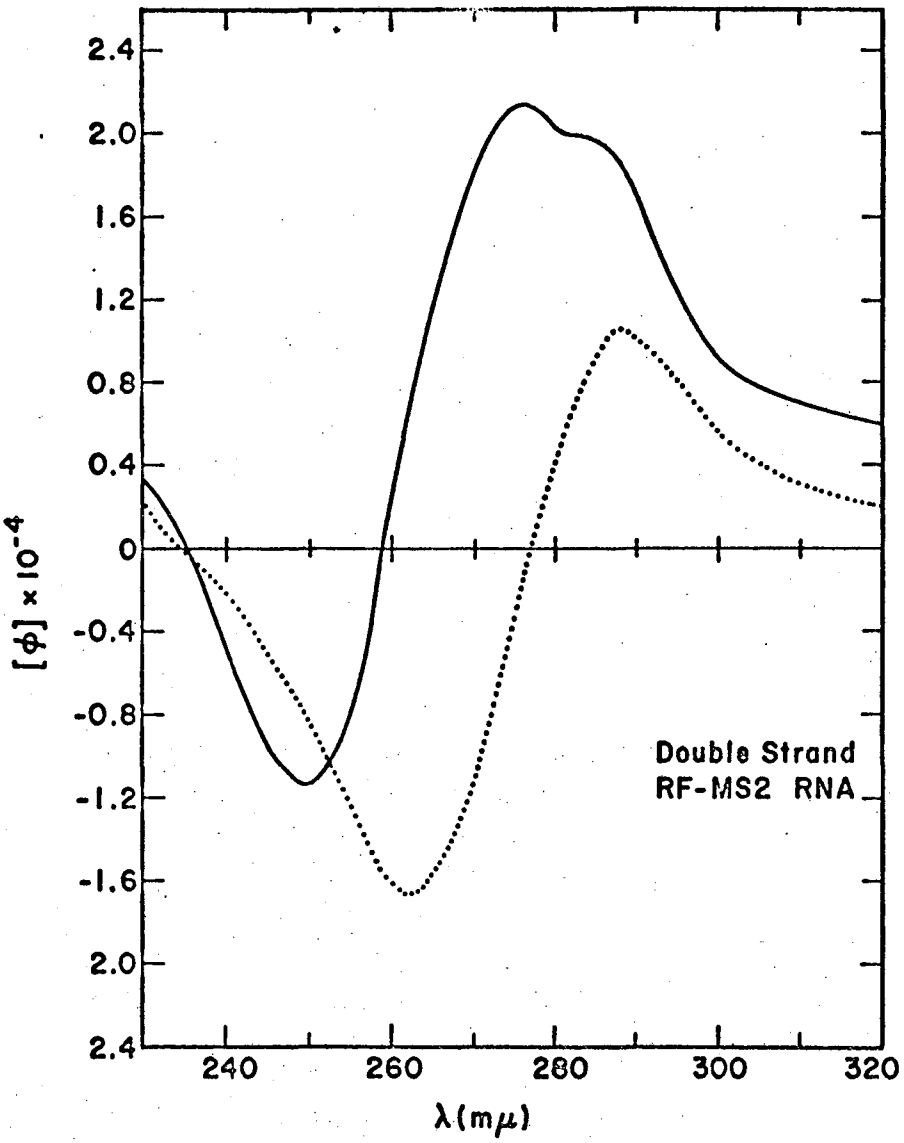

Figure 21. ORD of the replicative form of MS2 RNA:
——, Experiment, 0.15 M KCl, 0.01 M phosphate buffer, pH 6.9, 26°C.
···, Nearest-neighbor calculation for ORD of single-strand MS2 RNA at 26°C.

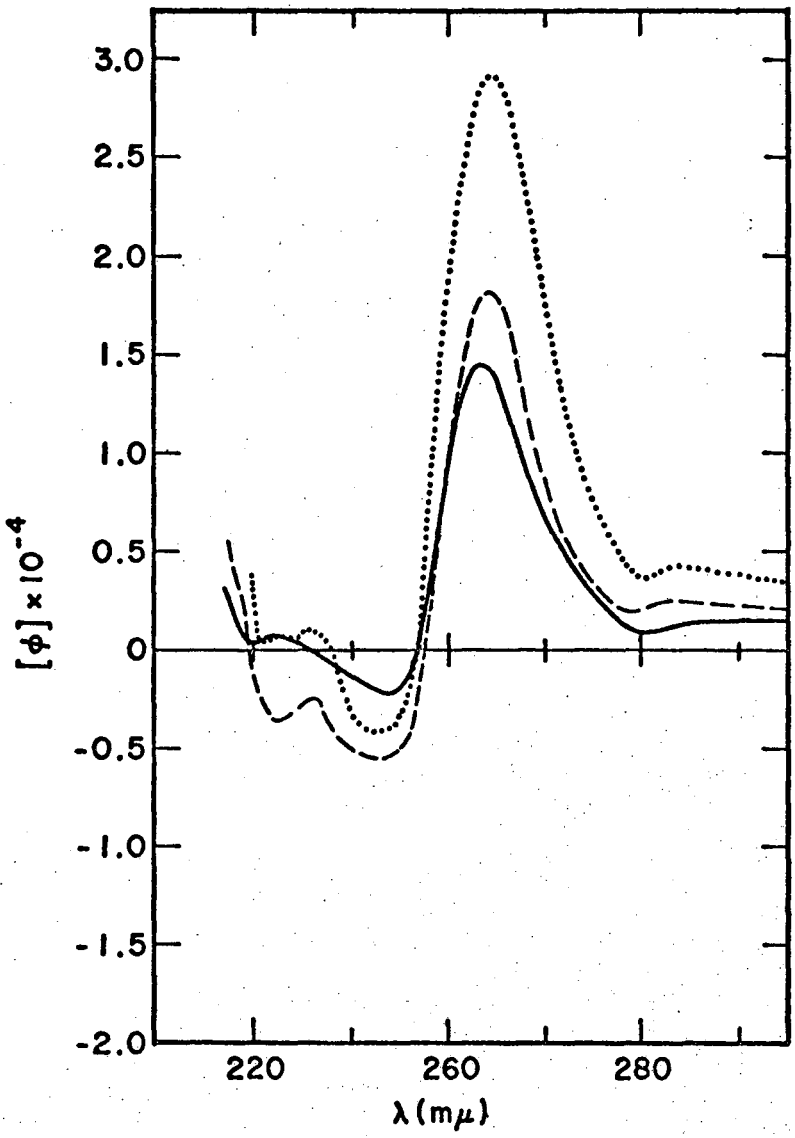

Figure 22. Perturbation on single-strand ORD resulting from base pairs.

——, ORD of TMV RNA, 26°C, 0.15 M KCl, pH 7, minus ORD of TMV RNA, 26°C, $Na^+ = 4 \times 10^{-4}$ M, pH 7.

----, ORD of TMV RNA, 26°C, 0.15 M KCl, pH 7, minus nearest-neighbor calculation for ORD of single-strand TMV RNA.

····, ORD of RF-MS2, 0.15 M KCl, 0.01 M phosphate buffer, pH 6.9, 26°C, minus nearest-neighbor calculation for ORD of single-strand MS2 RNA.

this peak is greater for the MS2 RNA difference curve than for the TMV RNA difference curves. Furthermore, the magnitude of the TMV RNA difference curve is greater when the calculated single-strand rotation is subtracted from the ORD of TMV RNA in the presence of salt than when the ORD in the presence of 10^{-4} M Na^+ is subtracted. We conclude from these observations that the secondary structure of TMV RNA in the presence of 0.15 M KCl, 25°C, pH 7, includes A-U and G-C base pairs. The effect of decreasing the salt concentration from 0.15 M K^+ to 10^{-4} M Na^+ is to decrease the number of base pairs. Taking the magnitude of the peak at 268 mμ as a measure of the number of base pairs, we estimate that TMV RNA at 25°C is 60% double-stranded in the presence of 0.15 M KCl and only 10% double-stranded in the presence of 10^{-4} M Na^+.

The effect of salt is illustrated better in Figure 23. The nearest-neighbor calculated ORD of TMV RNA has been subtracted from the experimental ORD of TMV RNA at four different ionic strengths, all measured at 25°C. The magnitude of the peak increases with increasing salt concentration, indicating a greater number of A-U and G-C base pairs.

A similar set of difference curves is obtained if the calculated ORD of TMV RNA is subtracted from the experimental ORD of TMV RNA at four different temperatures, all measured at the same ionic strength. Changes in temperature appear to have the same effect on the ORD of TMV RNA as changes in ionic strength.

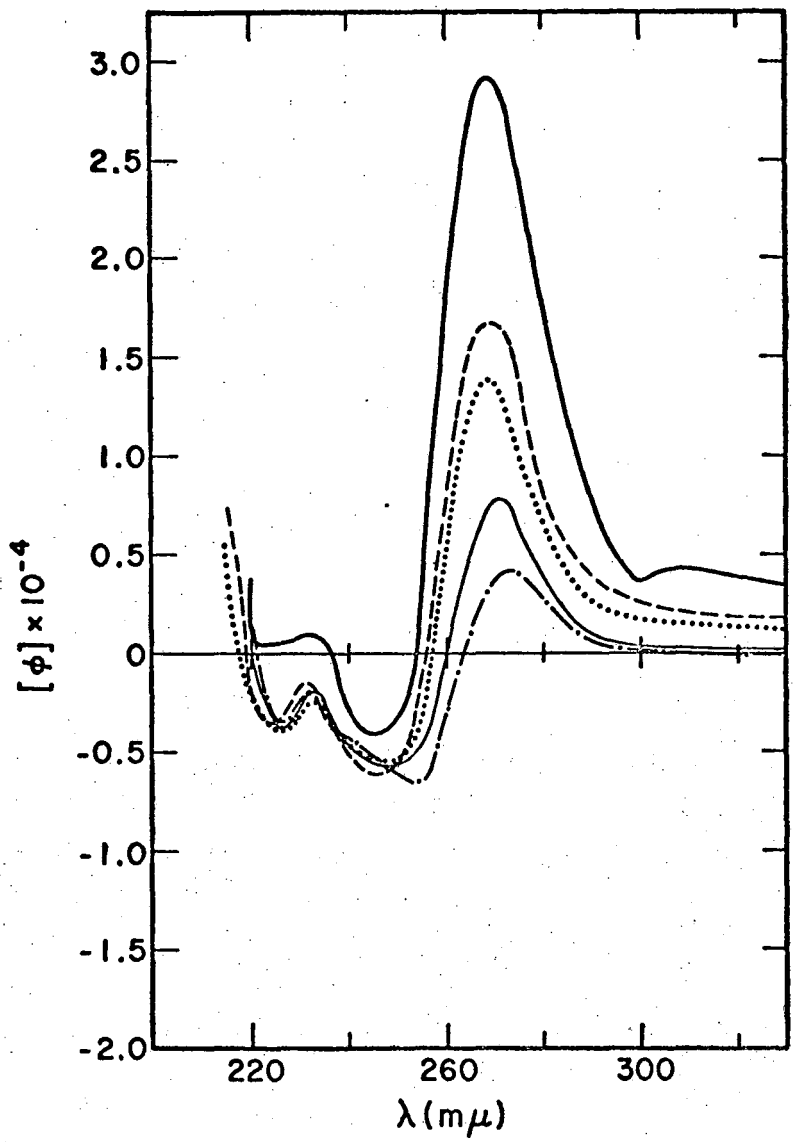

Figure 23. Ionic strength dependence of perturbation on ORD of single-strand TMV RNA resulting from base pairs.

——, ORD of RF-MS2 RNA, 0.15 M KCl, 0.01 M phosphate buffer minus nearest-neighbor calculation for MS2 RNA.

The nearest-neighbor calculated ORD for single-strand TMV RNA has been subtracted from the following ORD curves:

---, ORD of TMV RNA, pH 8, Na^+ = 1.0 M.

···, ORD of TMV RNA, pH 8, $Na^+ = 4 \times 10^{-2}$ M.

— ·, ORD of TMV RNA, pH 8, $Na^+ = 4 \times 10^{-3}$ M.

-··-, ORD of TMV RNA, pH 8, $Na^+ = 4 \times 10^{-4}$ M.

The difference of the experimental ORD at 25°C for mixed yeast tRNA in the presence of 0.15 M KCl and the calculated single-strand ORD is shown in Figure 24 along with the MS2 RNA difference curve. As with TMV RNA, the perturbation on the single-strand ORD is similar to that expected for A-U and G-C pairs. The magnitude of the rotation at the major peak is almost identical to that shown in Figure 22 for TMV RNA. The other two RNAs that we investigated, R17 RNA and F2 RNA, have difference curves which are quantitatively identical to those of TMV RNA and mixed yeast tRNA. Apparently under identical conditions these single-strand RNAs have about the same number of A-U and G-C base pairs. This is not surprising since they have similar base compositions, approximately equimolar in the four common residues.

In summary, the differences between the ORD curves of single-strand RNA and that expected if they have no base pairs are similar to the perturbation that would be introduced by the presence of A-U and G-C base pairs. As expected, the number of base pairs appears to increase with increasing ionic strength and decreasing temperature.

A different method of analysis of the ORD of TMV RNA as a function of temperature and ionic strength has provided further evidence for this interpretation. Matrix rank analysis has been applied by Dr. D. McMullen[124] to the entire body of data, a total of 40 ORD curves of TMV RNA at different temperatures and ionic strength. This method of analysis

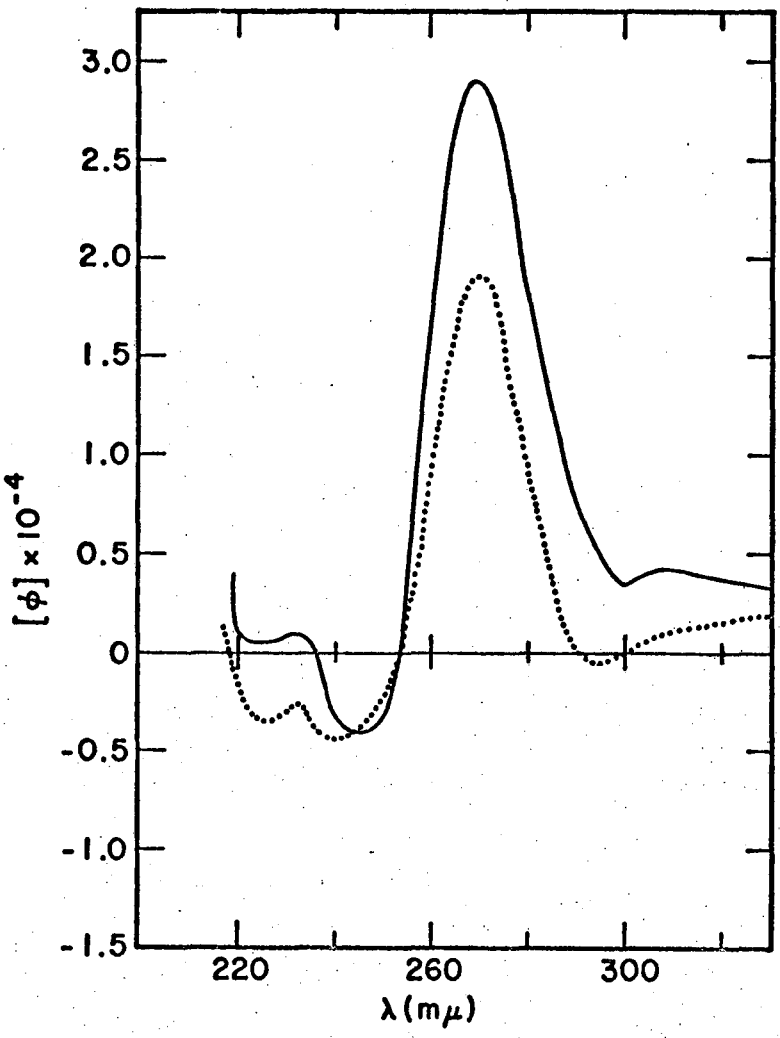

Figure 24. Perturbation on ORD of single-strand mixed yeast tRNA resulting from base pairs.

——, ORD of RF-MS2 RNA, 0.15 M KCl, 0.01 M phosphate buffer, pH 6.9, 26°C, minus nearest-neighbor calculation.

• • •, ORD of mixed yeast tRNA, 0.15 M KCl, 0.01 M phosphate buffer, pH 6.9, 26°C, minus nearest-neighbor calculation.

determines the minimum number of different ORD curves needed to describe the data. Only two curves are needed for the ORD of TMV RNA as a function of temperature and ionic strength. In other words, any of the measured ORD curves can be equated to the weighted sum of the same two ORD shapes. The C's are

$$[\phi]_{\text{TMV RNA}}(\lambda,T,\mu) = C_S(T,\mu)[\phi]_S(\lambda) + C_D(T,\mu)[\phi]_D(\lambda) \qquad (8)$$

the weighting factors which are independent of wavelength. The ORD shapes are denoted by $[\phi]_S(\lambda)$ and $[\phi]_D(\lambda)$.

The fixing of the two shapes is somewhat arbitrary. Any of the experimental curves can be taken as one shape. Then the other shape is determined by matrix rank analysis. The analysis showed that the ratio $C_S(T,\mu)/C_D(T,\mu)$ is independent of temperature for each ionic strength at sufficiently high temperatures. This indicates that the shape of the measured ORD curves is the same in this temperature range. This shape turns out to be similar for each ionic strength and also similar to the shape of the ORD curve calculated from the dinucleoside phosphates at room temperature.

A second shape, D, was calculated from the data taking the common shape observed at high temperature as the first curve, S. This other shape, which has been calculated without any assumptions regarding the nature of the secondary structure, turns out to be nearly identical with the experimental ORD of double-strand MS2 RNA. This latter curve is

shown again in Figure 25. The ORD curve D, which is also shown, has been normalized to the RF-MS2 RNA curve. The agreement is excellent. In fitting the entire body of data with the two curves, S and D, it is found that increasing amounts of the second shape are needed with increasing ionic strength and decreasing temperature.

The interpretation of these observations is that there are two average environments for the bases in TMV RNA that have different optical rotation properties. The first is the environment experienced by a base that is part of a single-strand helix where the bases are stacked as they are in the dimers but not hydrogen-bonded to other bases. The other environment is that experienced by a base that is part of a helical region of A-U and G-C base pairs.

The single-strand helix environment does result in a constant ORD shape. The shape of the ORD for stacked bases is independent of ionic strength and temperature. We have already cited evidence for the former. Evidence for the latter comes from a comparison of the calculated ORD curves for TMV RNA as a function of temperature. The curves differ from each other only by a multiplicative constant. The cross-over shifts 3 mμ between 2° and 90°C. The nearest-neighbor calculated ORD of TMV RNA is shown in Figure 26 for several temperatures.

The optical properties of hydrogen-bonded complexes of nucleic acids are usually independent of ionic strength and temperature below the helix-coil transition region.[41] The

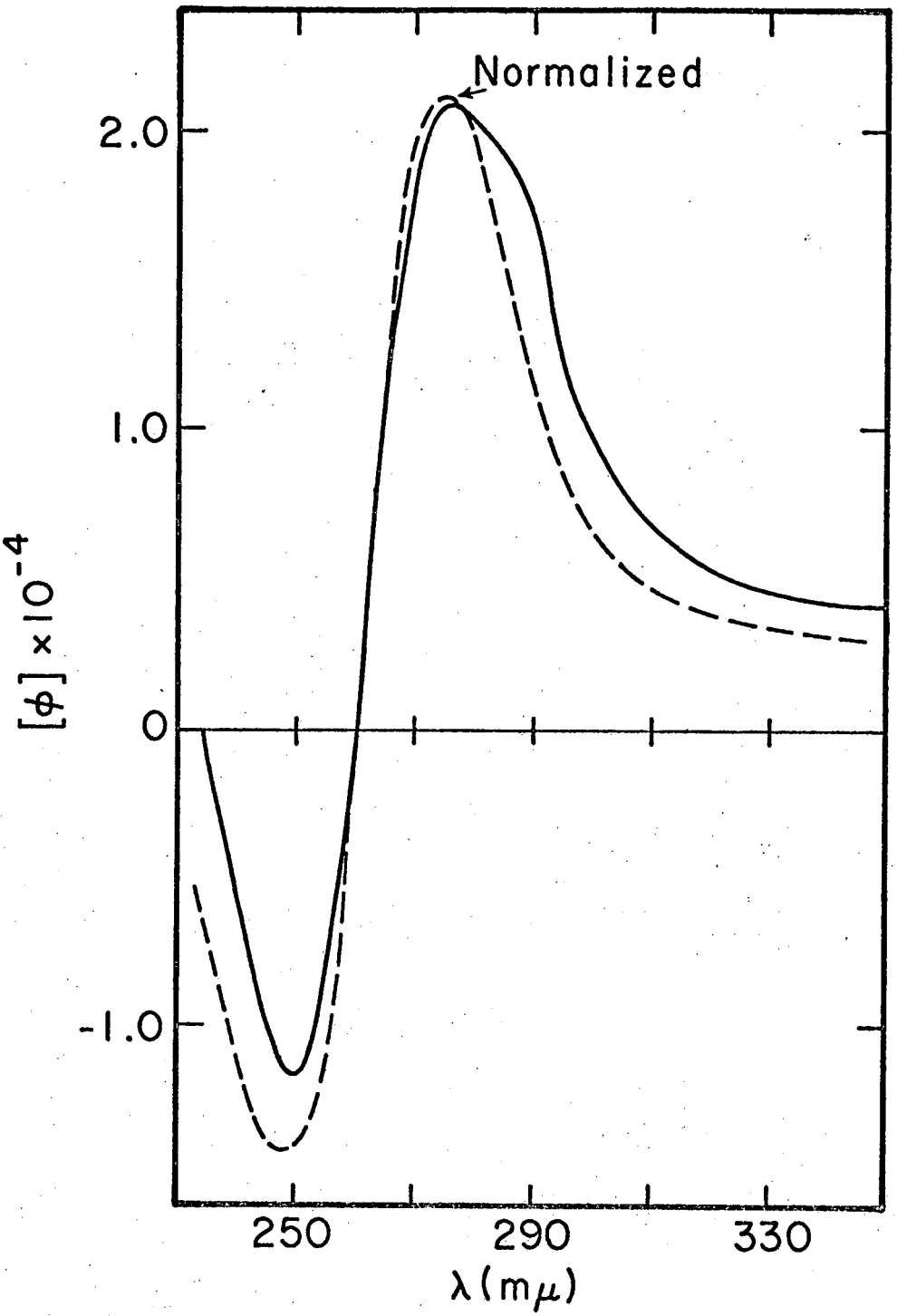

Figure 25. Comparison between component D and the ORD of the replicative form of MS2 RNA. (Taken from McMullen, Jaskunas, and Tinoco.[124])

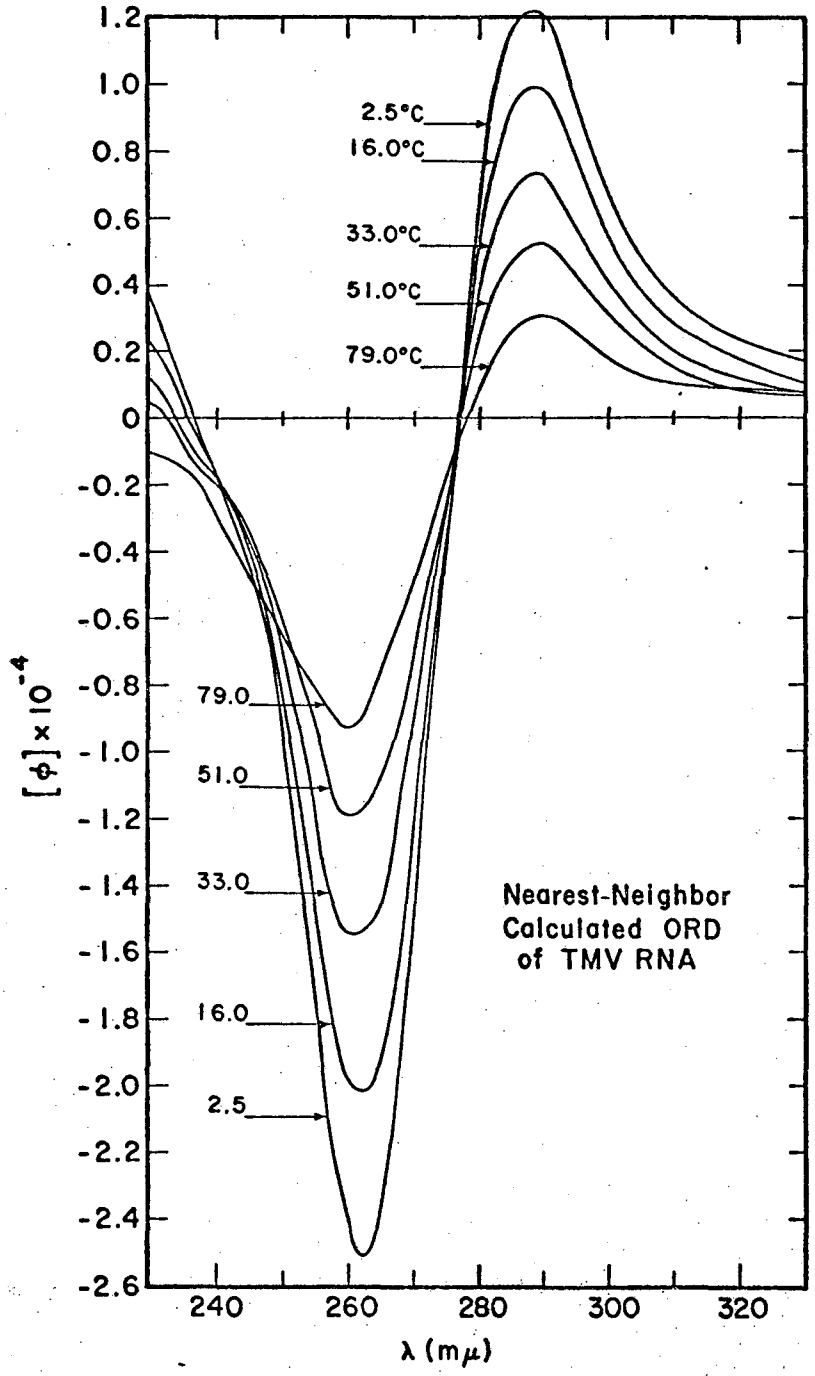

Figure 26. The nearest-neighbor calculated ORD of TMV RNA as a function of temperature.

fact that the optical rotation of this second environment is nearly the same as the ORD of a double-strand RNA is evidence that similar helical regions of A-U and G-C base pairs exist in TMV RNA.

2. Percent Double Strand in TMV RNA

We have just shown that the optical rotation of single-strand RNAs is sensitive to the existence of base pairs. It is of great interest to see if that sensitivity can be used to determine the number and nature of base pairs in single-strand RNA.

Methods have been developed for applying the ultraviolet spectral properties of RNA toward determining the number of base pairs in single-strand RNAs.[72,88,89,125,126] The methods have all involved fitting an experimental spectrum to a sum of two spectra which are representative of A-U and G-C base pairs. The two library spectra are normalized with respect to the number of base pairs that they represent. Thus, the number or fraction of base pairs present in an RNA can be determined. Optical rotation data may be better for this purpose than absorption data because of its greater sensitivity to the existence of base pairs. The major advantage of optical rotation data, however, is its senstivity to sequence. Thus, it might be useful in determining precisely which residues in a tRNA are hydrogen-bonded to which other residues. We shall return to this possibility later.

Dr. D. McMullen[124] has calculated the fraction of double strand in TMV RNA as a function of temperature and ionic strength by fitting the observed ORD to the sum of two appropriately normalized library ORD curves. The two library curves were those which had been found by the methods of matrix rank analysis, S and D. The first curve is representative of the single-strand stacked conformation and the second is proportional to the rotation of an average helical region of A-U and G-C base pairs. He has shown that any of the experimental ORD curves is the appropriate sum of these two curves. The structure of TMV RNA can thus be described as an equilibrium between double-strand and single-strand regions. The position of the equilibrium depends on the temperature and ionic strength and is reflected in the value of the weighting factors.

With this model in mind, Eq. (8) can be rewritten as follows:

$$[\phi]_{\text{TMV RNA}}(\lambda,T,\mu) = f_S(T,\mu)[s(T)\cdot S] + f_D(T,\mu)[d\cdot D] \qquad (9)$$

The functional dependence of S and D on wavelength is understood. The fraction of residues in a single-strand and double-strand region are denoted by $f_S(T,\mu)$ and $f_D(T,\mu)$. The constant d is a normalization factor making the ORD curve, $d\cdot D$, the molar rotation per residue of a 100% helical region of A-U and G-C base pairs. This normalized rotation is independent of temperature and ionic strength. By contrast, the rotation

of the single-strand conformation does depend on temperature. As mentioned before, at sufficiently high temperatures the shape of the ORD of TMV RNA is that expected for a single-strand molecule containing no base pairs. The shape does not change with further increases in the temperature but the magnitude of the rotation decreases. In this temperature region the molecule is probably 100% single-stranded. The decrease in the rotation is merely the temperature dependence of the optical rotation of stacked bases. The function s(T) provides the temperature dependence of the single-strand regions.

The nearest-neighbor calculated ORD of TMV RNA as a function of temperature has been used to determine the function s(T). As indicated in Figures 15-17 the calculated rotation does predict the form of the temperature dependence very well.

The constant d is found by making suitable use of the wavelengths for which the rotation of the single-strand or double-strand regions is zero. As it turns out, the product d·D is an ORD curve which is equivalent to the experimental ORD of double-strand MS2 RNA.

The fraction of residues in the double strand can now be calculated as a function of temperature from Eq. (9) and the fact that the sum of the fractions of double- and single-strand residues is unity. The results are shown in Figure 27 for each of the four ionic strengths that were employed. At 25°C and in a solution containing 4×10^{-2} M Na^+, the fraction

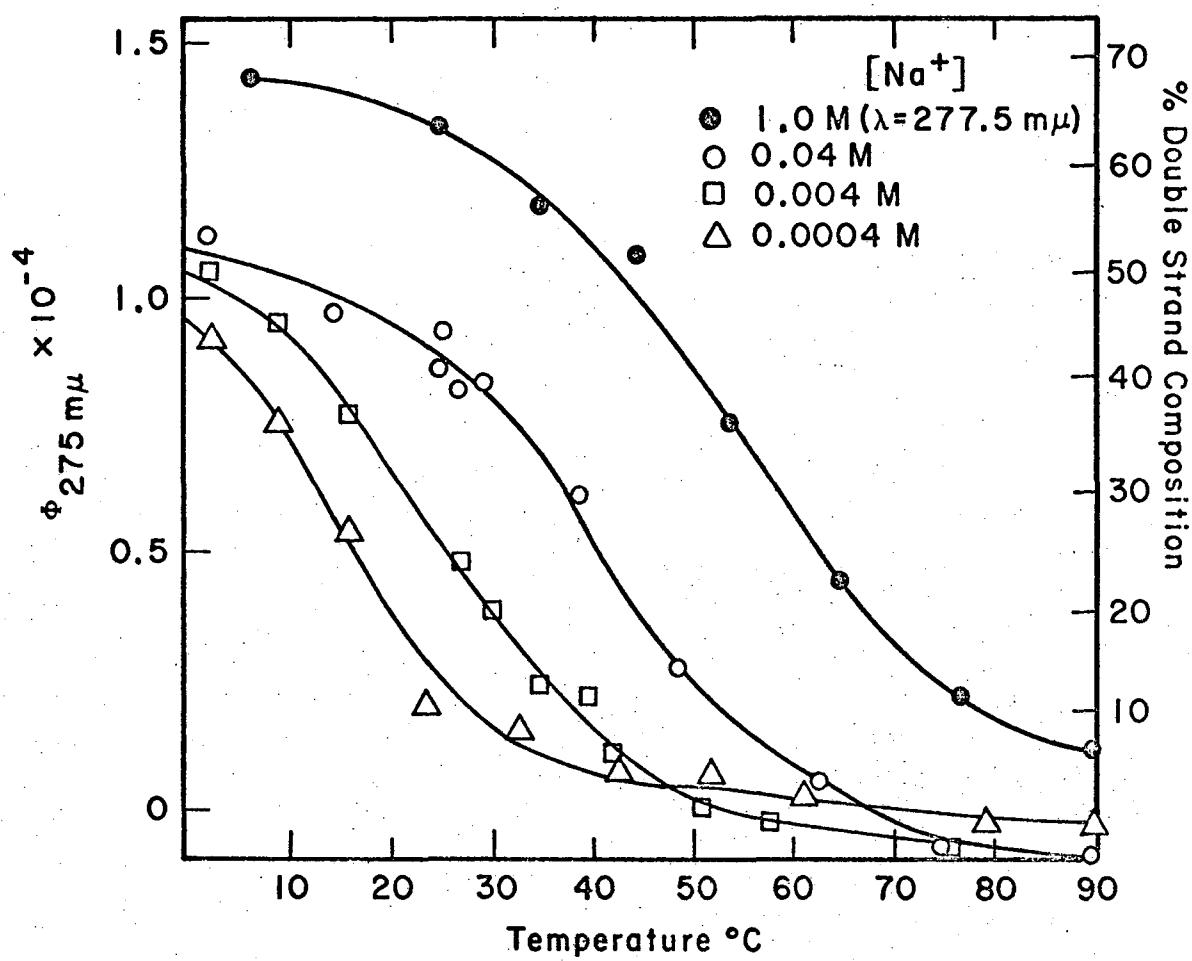

Figure 27. Percent double strand in TMV RNA. The contribution of component D to the observed ORD as a function of temperature and ionic strength is shown as molar rotation of the left. The equivalent percent double strand, $f_D(T,\mu)$, is shown on the right. (Taken from McMullen, Jaskunas, and Tinoco.[124])

of residues in TMV RNA that are base-paired is approximately 50%. This is consistent with other estimates of the percent double strand in TMV RNA.[77]

3. The Number and Nature of Base Pairs in tRNA

Attempts have been made by Cantor[36,105] to employ optical rotation data in determining the base pairing pattern in the alanine tRNA from yeast. The general method is to compare the calculated rotation of possible structures with the measured rotation of the molecule. Ideally the two ORD curves will coincide only when the correct structure is chosen.

A reasonable pattern of base pairing has been constructed from the sequence of bases in the polynucleotide. The criteria of reasonableness is a maximum amount of base stacking and base pairing. Cantor's model of the base pairing in $tRNA_{ala}$[36,105] is similar to that shown in Figure 1. The difference is that Cantor has postulated a few more base pairs and has folded the arms of the clover-leaf together by forming some base pairs between the residues which are in the loops.

The optical rotation of this structure has been calculated using two curves which represent the perturbations of an A-U and G-C base pair on the rotation of a single-strand helix with stacked bases. Thus, the expected ORD is the sum of the curve calculated from the dimers $[\phi]_{SS}$ and the perturbations introduced by the presence of base pairs.

$$[\phi]_{RNA} = [\phi]_{SS} + \chi_{AU}P_{AU} + \chi_{GC}P_{GC} \qquad (10)$$

The perturbations of an A-U and G-C base pairs in units of molar rotation per base pair are P_{AU} and P_{GC}, respectively. The mole fractions of bases in A-U and G-C pairs are χ_{AU} and χ_{GC}, respectively.

The optical rotation curves representating the perturbations have been determined from the ORD of poly (A+U)[103] and poly (G+C).[130]

$$P_{AU} = [\phi]_{poly(A+U)} - \tfrac{1}{2}[\phi]_{poly\ A} - \tfrac{1}{2}[\phi]_{poly\ U} \qquad (11a)$$

$$P_{GC} = [\phi]_{poly(G+C)} - \tfrac{1}{2}[\phi]_{poly\ C} - \tfrac{1}{2}[\phi]_{poly\ G} \qquad (11b)$$

The ORD curves of poly A,[57] poly U,[103] and poly C that were used were measured at 25°C under conditions where the polynucleotides are single-stranded. The ORD of single-strand poly G was calculated with Eq. (7) using the calculated ORD of GpG. The average of the two perturbations is compared in Figure 28 with the difference between the double- and single-strands ORD of MS2 RNA. The difference curve for MS2 RNA is the same one shown in Figures 22-24. It is an average perturbation on single-strand rotation caused by A-U and G-C base pairs. This average perturbation does not have the double peak that is exhibited by the average perturbation calculated from the homopolymers. However, the two curves are otherwise quite similar in shape. Therefore, the perturbation calculated from the homopolymers will give reasonable estimates

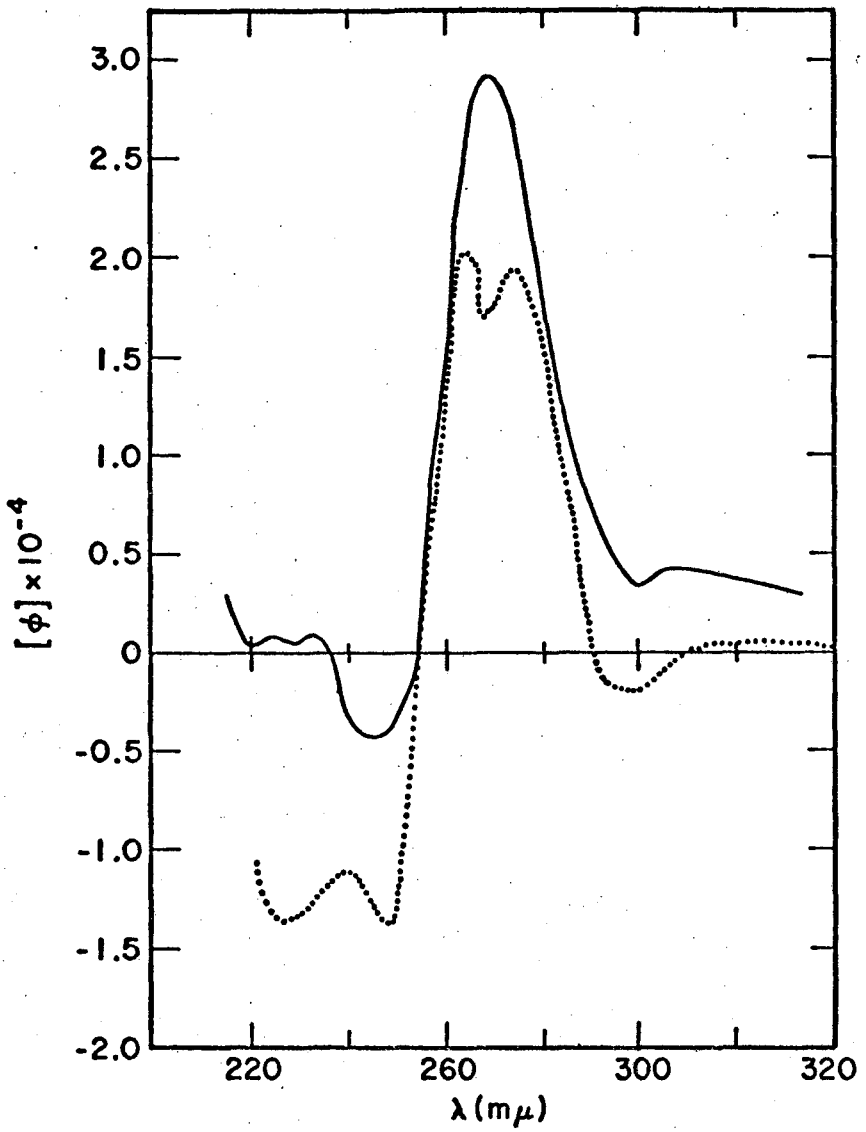

Figure 28. Perturbation on ORD of single-strand RNA due to A-U and G-C base pairs. (Taken from Cantor, Jaskunas, and Tinoco.[36])

——, ORD RF-MS2 RNA, 0.15 M KCl, 0.01 M phosphate buffer minus nearest-neighbor calculation for ORD of single-strand MS2 RNA.

····, ORD of poly $(A+U)^{103}$ minus ORD of poly A^{57} minus ORD of poly U^{103} plus ORD of poly $(G+C)^{130}$ minus ORD of poly C minus calculated ORD of poly G.[105]

of the contribution of A-U and G-C pairs to the rotation of single strands.

To calculate the G-C difference curve, Cantor[36] used the ORD of poly (G+C)[130] as measured by Sarkar and Yang. Recently, another measurement of the ORD of poly (G+C) by Ulbricht, Swan, and Michelson[104] has been reported. The two measurements are different. The two complexes have also been prepared differently which might be the source of their ORD differences. The poly (G+C) used by Sarkar and Yang was prepared by polymerizing GTP onto poly C with RNA polymerase.[131] Ulbrich et al.[106] mixed poly C and poly G to obtain the 1:1 complex. The use of the ORD of the latter poly (G+C) to determine the G-C difference would not affect any of the results, however.

The ORD of alanine tRNA as measured by Scheraga[89] is given in Figure 29. The measurement was made at room temperature in a solution containing 0.15 M KCl, 0.1 M phosphate buffer, pH 6.83. The calculated ORD curves of alanine tRNA are shown for a completely single-strand structure containing no base pairs and for one which has 7 A-U and 19 G-C base pairs.[36] The calculated rotation of a structure containing base pairs compares more favorably with the experimental curve.

This method of calculating the ORD of an RNA containing regions of single- and double-strand would be rigorously valid if the rotation of the stacked bases due to intrachain interactions is the same in the double-strand helix as in the single-strand helix. Furthermore, the only cross-chain

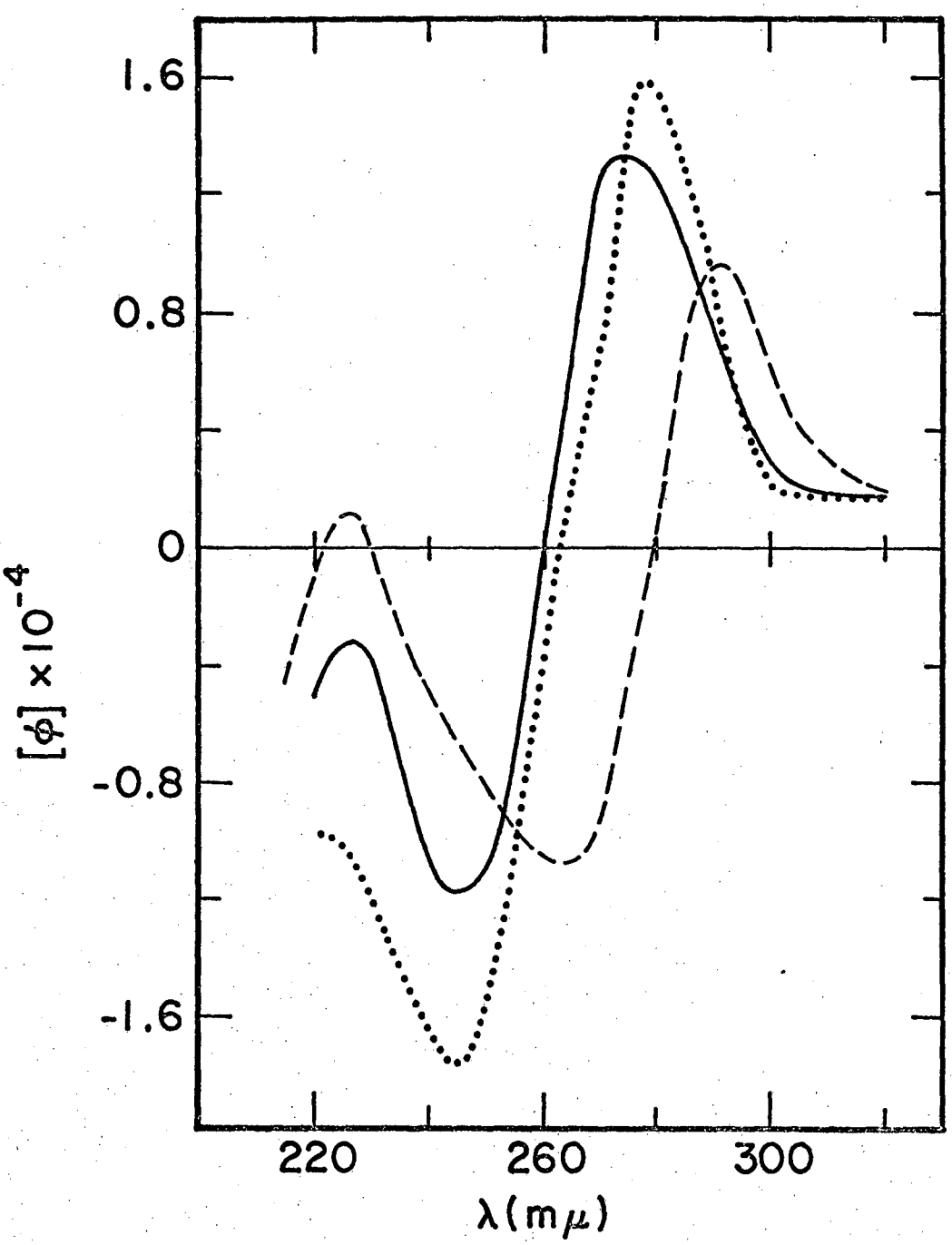

Figure 29. ORD of yeast alanine tRNA. (Taken from Cantor, Jaskunas, and Tinoco.[36])

——, Experimental results of Vournakis and Scherage.[89]

---, Nearest-neighbor calculation.

···, Calculation for structure containing 7 A-U and 19 G-C base pairs.

interactions which are important would have to be between the bases which are actually base-paired.

The geometry of the stacked bases in the double-strand helix may not be the same as for the single-strand helix at 25°C. Even if the average geometries are the same, the time spent in that geometry is surely different. The rotation of a fully stacked single-strand helix is probably a better estimate of the rotation due to intrachain interactions in the double-strand helix. Single-strand helices would only have such a structure at very low temperatures. The dimer ApA is 100% stacked at -70°C in a solution of 7 M LiCl.[60] Unfortunately the ORD of the single-strand helices of poly A, poly U, and poly C have not been measured under such conditions. The perturbation calculation is also not entirely valid because diagonal interactions between the chains are probably important. We shall return to this point later. Even if these arguments were wrong, the G-C perturbation is probably inaccurate because of the questionable validity of the ORD of poly G that was used. Other inaccuracies were obviously introduced into the calculation by approximating the rotation of single-strand dimers involving odd bases with the rotation of one of the 16 common dimers. The error in calculating the rotation of the double-strand regions, however, is probably greater than the error introduced with these approximations.

In conclusion, we cannot say whether the base-paired structure for which the ORD was calculated is correct. However, it seems clear that alanine tRNA under the conditions of the measurement is not completely single-stranded. Its secondary structure involves some A-U and G-C base pairs.

The same calculation of the ORD of yeast alanine tRNA was repeated for other patterns of base pairing.[36,105] The agreement with experiment is not as good as shown in Figure 29. The difference between calculated ORD curves for structures that only differ by a few base pairs is greater than the uncertainty in the measurement. This gives us hope that the secondary structure of tRNA can be determined if we use a better library for the rotation of double strands.

Both intrachain and interchain interactions are important for the optical rotation of double strands. Actually there will be no contribution to the rotation from interactions between the bases that are hydrogen-bonded if the base pair is planar. That is because the rotational strength is proportional to $\vec{R}\cdot(u' \times u'')$.[58] The u's are transition moments that are in the plane of each of the bases. If the base pair is planar, then the cross product of the transition moments is perpendicular to that plane. The vector $\vec{R}$ joins the two transition moments and is in the plane of the base pair. Thus, the dot product is zero for planar base pairs. The x-ray work on double-strand RNA indicate that the base pair is not planar.[98] The bases which are hydrogen-bonded

are rotated a few degrees with respect to one another giving the base pair a propeller-like structure. For such a structure there can be a net rotational strength due to interactions between hydrogen-bonded bases.

Nearest-neighbor effects were found to be the most important for the optical rotation of a single-strand helix with stacked bases. If we think of the double-strand helix as stacks of base pairs, then we might expect that the only important interactions will be between base pairs that are adjacent. For Watson-Crick base pairs between anti-parallel strands, there are 10 distinct arrangements of stacked base pairs.[32] These are illustrated schematically in Figure 30.

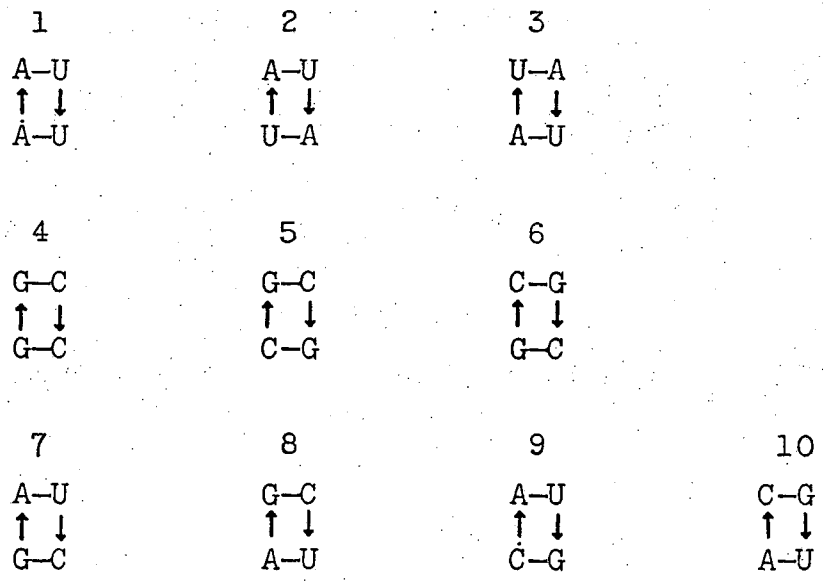

Figure 30. The Ten Distinct Double-Strand Interactions.

The ORD of each of these base-paired dimers may be as different as the ORD of the sixteen dinucleoside phosphates. Some evidence of this is seen in the ORD of poly (A+U)[103] and poly rAU that are shown in Figure 31. The latter compound has an alternating sequence of A and U residues.[132] It exists as a stable ordered complex under the conditions of the measurement. Presumably it is a double-strand helix of A-U base pairs that is similar to the poly (A+U) complex. The optical rotation of poly (A+U) is a measure of the ORD of the first double-strand interaction in Figure 30. The ORD of poly rAU reflects the average of the ORD of double-strand interactions 2 and 3. The ORD of the two complexes of A-U base pairs are strikingly different.

If we knew the ORD of each of the 10 base-paired dimers in Figure 30, then we could calculate the ORD of double-strand RNA in the same way that the ORD of single-strand RNA is calculated.[36]

$$[\phi] = 2 \sum_i \sum_j \chi_{ij}[\phi^D_{ij}] - \sum_i \chi_i[\phi^D_i] \qquad (12)$$

The molar rotation per residue of the base paired dimer IpJ and its antiparallel complement is $[\phi^D_{ij}]$. The molar rotation per residue of a single base pair is $[\phi^D_i]$. For planar base pairs this will be the sum of the ORD of the monomers. χ_{ij} and χ_i are the mole fractions of dimer IpJ and monomer I. The summations are carried out over the sequence of only one of the two strands. Either strand can be used.

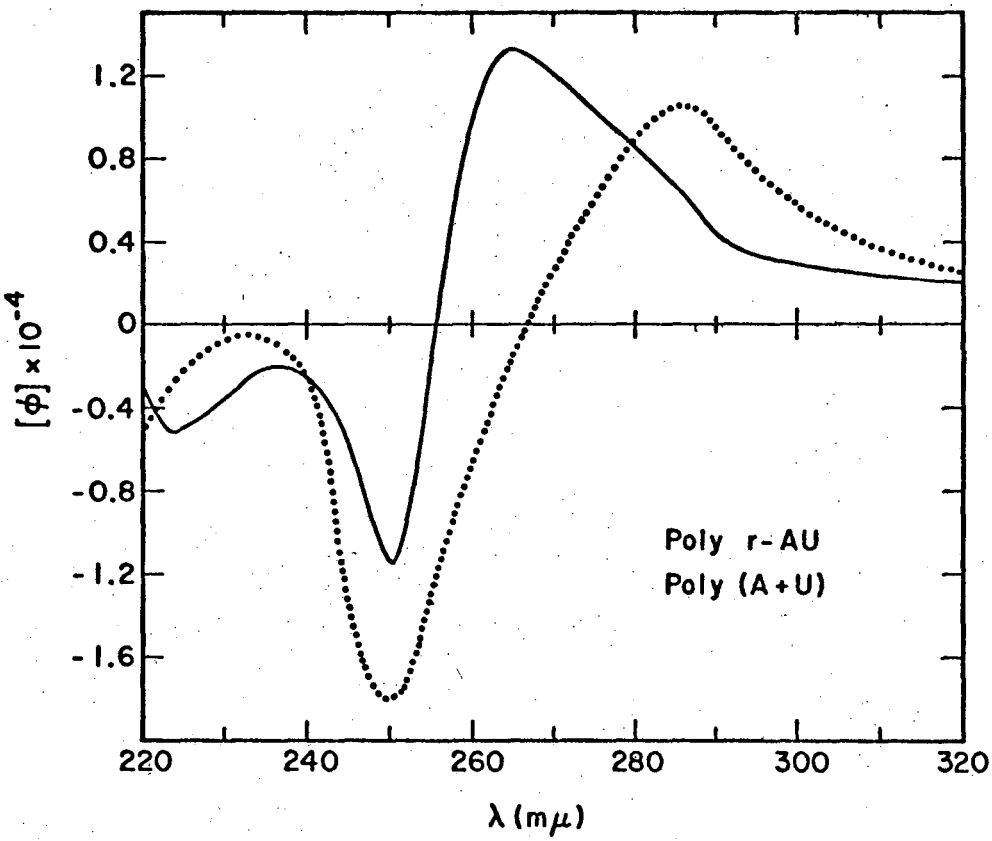

Figure 31. ORD of poly rAU and poly (A+U).

——, ORD of poly rAU, 26°C, 0.01 M phosphate buffer, pH 7.0.

···, ORD of poly (A+U).[103]

Assuming the optical rotation of double- and single-strand regions in tRNA could be calculated accurately, we might expect to be able to determine the base pairing arrangement by comparing the calculated ORD of possible structures with the experimental ORD. At the present time we cannot calculate the rotation of the double-strand regions since the ORD of only a few of the base-paired dimers in Figure 30 is known. The ORD of numbers 1 and 4 can be obtained from the optical rotation of poly (A+U) and poly (G+C), respectively. Furthermore, the ORD of poly rAU is a measure of the average ORD for interactions 2 and 3. The others are not known. In addition there is the problem of calculating the ORD of the single-strand regions in tRNA containing odd bases. The ORD of dinucleoside phosphates containing odd bases have not been reported.

Both of these problems appear to be solvable. In the latter half of this dissertation we shall discuss possible methods of determining the ORD of the base-paired dimers. Mr. C. Formoso in our laboratory is working on the problem of measuring the ORD of dimers containing the odd bases.

However, once this information is available there will still be problems in determining the secondary structure of tRNA. We have tacitly assumed that the only base pairs in tRNA are formed between antiparallel chains and are analogous to those in DNA. Without the rigid constrains of an infinitely long double helix we expect that other base-pairing arrangements are important. Indeed, many non-Watson-Crick

base pairs and base triplets (three-stranded complexes) have been observed with various model compounds.[110] Experiments and calculations will be presented later which will point out the importance of considering the possibility of triple-strand regions. They may be very important in establishing a precise three-dimensional structure for tRNA.

One other possible element of secondary structure in single-strand RNA is intercalation. Chan et al.[68] have shown that purine intercalates between the bases of TpT. They have made similar observations in more extensive studies of the phenomenon.[133] Although it has not been demonstrated that intercalation occurs in structures of RNA, the possibility should not be dismissed.

Summary

The basic conclusion of the experiments that have been described is that base stacking is an important determinant of the secondary structure of single-strand RNA. Under conditions that are unfavorable for intramolecular double strands the ORD of single-strand RNA is that expected for stacked bases. We have concluded from this that the bases in single-strand regions of RNA are stacked. Furthermore, at any temperature the geometry of the stacking is similar to that of the dinucleoside phosphates at the same temperature. The orientation of the bases become more random with increasing temperature. However, even at 90°C the bases do not have a totally random conformation.

Under conditions which are favorable for intramolecular double strands the ORD of single-strand RNA is not that expected for stacked bases. The difference is consistent with the presence of double-strand regions of A-U and G-C base pairs. In particular, the ORD of tRNA is consistent with the presence of A-U and G-C base pairs.

Methods have been discussed for exploiting the sensitivity of optical rotation to base pairs in order to determine the number and nature of base pairs in single-strand RNA. The percent double strand in TMV RNA as a function of temperature and ionic strength was determined by fitting the experimental curves to a sum of two curves representing single-strand and double-strand RNA. The possibility of determining the structure of a tRNA by comparing its ORD with calculated curves for possible structures was discussed. At the present time, we cannot calculate the ORD of double-strand RNA as a function of sequence with the same certainty that we can for single-strand RNA. Therefore, we cannot reliably test possible structures. The minimum information needed to do this includes the ORD of 10 base-paired dimers that are formed by DNA-like double-strand RNA.

PART II

ASSOCIATION OF COMPLEMENTARY OLIGORIBONUCLEOTIDES IN AQUEOUS SOLUTION

Introduction

Base pairing and base stacking are important elements of the secondary structure of tRNA. Evidence was presented in Part I suggesting that the bases in the single-strand regions of tRNA are stacked. The relative geometry of neighboring bases appears to be similar to the geometry of the bases in dinucleoside phosphates. On the average, they are probably stacked perpendicular to the single-strand helix axis.

We would now like to direct our attention to the base pairs in tRNA. Several kinds of evidence point to their existence.[12,90,126] Optical rotation experiments were described in Part I that are consistent with the existence of A-U and G-C base pairs. Other observations indicate the base pairs are organized into several short helical regions.[88,125] More specific information is needed, however, if we are to understand how the biological activity of tRNA molecules is dependent on a correct three-dimensional structure.[12] We must know which bases are hydrogen-bonded to which other bases.

A base-pairing pattern resembling a clover-leaf has been suggested as a possible model of the base pairing in tRNA molecules.[16,20-22] In this model the polynucleotide chain

folds back upon itself forming loops that are held together by A-U and G-C base pairs. Each molecule may contain several loops. An example of this structure is shown in Figure 1 (page 3) for yeast alanine tRNA.

The radius of gyration of mixed yeast tRNA, as determined by low-angle x-ray scattering, is consistent with the clover-leaf model.[100] The relative susceptibility of guanosine residues in tRNA to attack by T_1 ribonucleose is also consistent with the model. Perhaps, the best evidence for the model is that a reasonable clover-leaf pattern of base pairs can be constructed for each of the tRNA molecules whose sequence is known.[16,20-22]

We are interested in finding more direct evidence for the existence of loops that are formed by only a few base pairs. In particular, are these short regions of base pairs sufficiently stable to endow the tRNA molecule with a unique secondary structure? The question can be tentatively answered if we know the equilibrium constant for the association of complementary oligoribonucleotides. The stability of a loop can then be estimated by taking into account the effect of tying the oligomers together.

We are also interested in developing a method to determine precisely which residues are base-paired to which other residues. We have seen that the ORD of molecules containing base pairs is sensitive to the number and sequence of residues that are base-paired. The work described in this part was undertaken with the intention of determining the

ORD of the ten base-paired dimers in Figure 31 (page 116). Using these curves as a library, we expect to be able to calculate quantitatively the ORD of double-strand regions in RNA as a function of chain length and sequence.

Cantor did not observe any specific interaction between ApC and GpU under conditions that were favorable for intermolecular aggregation.[105,134] The highest total concentration of residues that he used was 5×10^{-3} M. We cannot conveniently measure the ORD of nucleotide solutions with a much higher concentration. Therefore, it does not seem possible, at this time, to measure the ORD of base-paired dimers directly.

However, we can still determine the ORD of base-paired dimers by measuring the ORD of complexes of longer molecules of known sequence. Therefore, we have attempted to study complexes that form in aqueous solution between trinucleoside diphosphates (trimers) and tetranucleoside triphosphates (tetramers). Regions of base pairs in tRNA, in general, are presumed to only contain Watson-Crick base pairs, A-U and G-C, that form between antiparallel chains.[88,16,20-22] Thus, at present we have directed our attention to complexes of this type.

Complexes of trimers are especially interesting because of their close analogy to the source of specificity for the interaction of tRNA with the mRNA-ribosome complex. The specificity is presumably the result of base pairs that form between a specific triplet of the tRNA and a complementary

trimer on the mRNA.[7] If the ribosome does not in anyway affect the binding of the tRNA to its codon then the equilibrium constant for a complex of complementary trimers should be the same as for the interaction of tRNA and mRNA. A site for the unspecific binding of tRNA molecules to the ribosome has been suggested.[135] Such binding would increase the equilibrium constant for the interaction of codon and anti-codon as compared to trimers that are free in solution. It would not affect the specificity, however.

ORD has been used to detect the existence of complexes of complementary oligomers. The ORD of each of the oligomers is first measured separately under identical conditions. The oligomers are mixed in a 1:1 mole ratio and the ORD of the mixture is compared with the sum of each measured separately. The change that will accompany base-pair formation can be estimated from the perturbations of A-U and G-C base pairs on the ORD of single strands.[36] In general, the formation of the base pairs will shift the peak, trough, and crossover to shorter wavelengths. For trimers, this shift may be 5-10 mμ. The magnitude of the rotation at the peak should also increase. We, therefore, expect to be able to detect a complex of only 10% of the trimers.

Conditions have been chosen that will favor complex formation. These include low temperature, high concentration of nucleotide, and high ionic strength. Magnesium ions frequently result in the formation of triple strands.[136,137] Double strands are more likely to form in the absence of

magnesium. The experiments to be described have generally been done in both the presence and absence of magnesium ions.

These same conditions are also optimum for self-aggregation. It is important to detect these complexes because they may prevent the formation of the complementary complex. They are also interesting because they may be indicative of non-Watson-Crick base pairs. Self-aggregation can be detected in the usual way by studying the rotation of the oligomers as a function of concentration. More simply, we can compare the measured ORD with the nearest-neighbor calculation for an unaggregated oligomer.[35] Both methods have been employed.

Materials and Methods

Oligomers of known sequence and chain length can be prepared by several different methods.[138,139] The trimers used in this study were prepared by specific enzymatic cleavage of RNA or by synthesis with primer-dependent polynucleotide phosphorylase from Micrococcus lysodeikticus.

Only recently it has become possible to purchase oligoribonucleotides with a chain length greater than two. The tetramers ApApApA and UpUpUpU that were used in our studies were purchased from Miles Laboratories. A two-dimensional map as described below indicated that the compounds were homogeneous, so they were used without further purification.

1. Preparation of Oligomers by Specific Hydrolysis of RNA

This general method has been used previously in this laboratory.[35] We have made modifications in the procedure that have resulted in higher yields and greater convenience. The procedure described here has been used routinely to isolate the trimers and tetramers that can be obtained from RNA by specific enzymatic hydrolysis.

a. Preparation of E. coli RNA

As a source of RNA for specific enzymatic hydrolysis, we have used a high molecular weight RNA from E. coli. The method of preparation, which is described in detail below, was suggested by Dr. S. Mandeles. He credits Tissières et al.[140] as the original source of the basic procedure. The RNA is primarily ribosomal. Dr. Mandeles has informed us that some tRNA is also present, however. Thus, we shall refer to it as E. coli RNA.

i. Materials.-- Frozen E. coli cells, strain W, harvested in the late log phase, were obtained from General Biochemicals (Chagrin Falls, Ohio).

Deoxyribonuclease I (3.1.4.5) was obtained from Worthington Biochemical Corporation (Freehold, New Jersey). We have always used the electrophoretically purified enzyme, code DPFF, which presumably contains no trace of ribonuclease activity.

The standard buffer contained in 1 liter, 10 ml of 1 M magnesium acetate, 10 ml of 1 M Tris-HCl, pH 7-8, 0.39 ml of 1 M 2-mercaptoethanol, and 2.7 g of ammonium chloride.

Mallinckrodt Chromatographic Grade phenol, containing 88% phenol, 12% H_2O, and no preservative, has been used routinely. Generally, the liquid, as supplied by the manufacturer, was colorless. If the liquid had any trace of yellow or brown color it was distilled before use.

We have received generous gifts of bentonite from Dr. Mandeles. It has been prepared according to the procedure of Fraenkel-Conrat et al.[141] The crude bentonite may be obtained from the International Minerals and Chemical Corporation (Skokie, Illinois).

Macaloid has been obtained from the Baroid Division of the National Lead Company (Houston, Texas). It has been prepared as described by Mandeles and Bruening.[142]

ii. Rupture of E. coli Cells.-- The procedure to be described is for 10 g of frozen cells. We generally worked up four 10 g batches at once. This supplied enough RNA for the hydrolysis procedure that will be described later.

Ten grams of frozen E. coli were ruptured by forceful grinding with 25 g of alumina. The grinding was done in the cold room at 4°C until the mixture was pasty, approximately 15 minutes. A precooled mortar and pestle were used. The ultimate yield of RNA was primarily dependent on the vigor of the grinding. In working up 40 g of cells we have found that it is better to do the grinding in four 10 g batches

than in one 40 g batch. In either case, an hour of hard work must be done in the cold room. Because of the distastfulness of this, we suggest that other methods of breaking open the cells be considered. Perhaps it could be done by homogenization in a blendor with glass beads.

Five ml of standard buffer were added to every 10 g of cells. After mixing well, 0.1 mg of deoxyribonuclease was added. A volume of standard buffer that equals the volume of the entire mixture, approximately 35 ml was added. The mixture was allowed to stand at room temperature for 15 minutes and was then centrifuges for 10 minutes at 15,000 RPM. The residue was discarded and the supernatant was taken for the RNA extraction.

iii. RNA Extraction.-- Unless otherwise indicated, the amount of reagents added will be per 50 ml of supernatant.

Step 1. A 2.5 ml volume of 20% sodium dodecyl sulfate (SDS) and 1 teaspoon of the Macaloid preparation was added. The mixture was heated at 30°C for 1 minute and immediately cooled to 4°C in an ice bath while stirring. Cold 2 M Tris-HCl, pH 7.45, was added while the solution was cooling until the final concentration of Tris-HCl in the solution was 0.1 M. When the temperature of the solution reached 4°C, 50 ml of cold 80% phenol was added. The solution was stirred continuously for 10 minutes and then centrifuged for 10 minutes at 1 or 2 thousand rpm. The Macaloid was at the interface.

Step 2. The upper layer (aqueous layer) was withdrawn with a suction pipet and kept cold in an ice bucket. Approximately 1 mg (4 ml) of Bentonite was stirred in. One teaspoon of Macaloid and 50 ml of cold 80% phenol were added. The stirring was continued for 10 minutes in the ice bath and the mixture was centrifuged again at 1 or 2 thousand RPM for 10 minutes. The Bentonite stays in the aqueous layer, which gave the solution a cloudy appearance.

Step 3. The upper layer was withdrawn. One teaspoon of Macaloid and 50 ml of cold 80% phenol were added. Stirring was continued for 10 minutes in the ice bath and the mixture was centrifuged at 1 or 2 thousand RPM for 10 minutes.

Step 4. Dissolved phenol was removed from the aqueous layer by extraction with a volume of cold anhydrous ether equal to the total volume of the solution. The aqueous layer (lower layer) was saved. The extraction was repeated two more times for a total of three extractions. Excess ether was removed by evaporation under the reduced pressure developed by an aspirator until the odor of ether could no longer be detected. The process was speeded up if the solution was stirred. Even so, it took an hour or more.

Step 5. The solution was buffered by adding a volume of 1 M acetate buffer, pH 5, that equaled 1/5 the total volume of the solution. The buffer was prepared by titrating 1 M potassium acetate with glacial acetic acid to pH 5. The RNA was precipitated by adding a volume of cold 95% ethanol

that equaled three times the total volume of the solution. The addition of ethanol was made while the solution was being stirred in an ice bath. The stirring was continued for 30 minutes and the solution was allowed to sit in the ice bath for at least four hours. We usually let the solution sit in the refrigerator overnight.

Step 6. The RNA precipitate was recovered by centrifugation at 12,000 RPM for 30 minutes. The supernatant was discarded. The precipitate was taken up in H_2O or an appropriate buffer and recentrifuged at 12,000 RPM for 30 minutes. The Bentonite remained at the bottom as a fluffy translucent precipitate. The RNA solution was decanted. Since the RNA was subsequently used in an enzymatic hydrolysis, special care was taken to see that no Bentonite got into the RNA solution. More than one centrifugation was frequently necessary. The concentration of RNA was determined using an extinction coefficient of 25 optical density units at 260 mμ per mg of RNA.

The RNA can be prepared ahead of time. However, the Bentonite should not be removed until immediately before use. The solution should be stored frozen until the Bentonite is removed.

b. Isolation of Pancreatic Ribonuclease Trimers and Tetramers from E. coli RNA

i. Hydrolysis.-- In a typical preparation, 300 mg of E. coli RNA (4 mg/ml) was incubated with 30 mg of Worthington pancreatic ribonuclease (2.7.7.6), code R, at 40°C. The pH was adjusted to 7.5 and the reaction was followed to completion by adding 0.5 N KOH in order to keep the pH constant. The titration was done with a Radiometer TTT-1 Titrimeter. At the completion of the reaction, the pH was adjusted to 8 with KOH and 6 mg of Worthington E. coli alkaline phosphatase (3.1.3.1), code BAPC, was added. Incubation was continued for 3 hours at 37°C. The solution was then lyophilized to dryness and redissolved in a small volume of 7 M urea, 0.01 M Tris-HCl, pH 7.5.

A white precipitate usually formed when the phosphatase was added. Incubation of the precipitate with 0.1 N NaOH released nucleotides into the solution. Thus, the precipitate contained some RNA. However, the incubations were repeated until no more nucleotides were released, and a white precipitate still remained. The nature of this precipitate is not known.

ii. Ion-Exchange Column Chromatography.-- The sample was applied to a DEAE Sephadex A-25 column (2.5 x 90 cm). The oligomers were separated according to chain length[143] by elution with a linear gradient from 7 M urea, 0.01 M Tris-Cl,

pH 7.5, to 7 M NaCl, 0.01 M Tris-Cl, pH 7.5, in 15 liters. The flow rate was 100 ml/hr. 20 ml fractions were collected.

The trimer fraction was diluted to 5 times its original volume with distilled water and washed onto a Dowex AG1 x 2 column (1.5 x 80 cm). The column was washed with several volumes of 10^{-3} M HCl. A linear pH gradient was run from 10^{-3} M HCl to 10^{-2} M HCl, in 1 liter. The flow rate was 40 ml/hr, and 10 ml fractions were collected. Trimer ApApC came off at the end of the gradient. The others came off in a subsequent linear salt gradient from 10^{-2} M HCl to 10^{-2} M HCl, 0.4 M NaCl, in 2 liters. The order of appearance was the same as for the chromatography of trinucleotides by Rushizky and Sober [144] on DEAE cellulose. Trimers ApGpC and GpApC were not resolved but ApGpU and GpApU were.

The trinucleotide GpGpCp was prepared by a similar procedure as described above. The alkaline phosphatase treatment was not done. The pH gradient for the Dowex column was eliminated. The salt gradient for this column was from 7 M urea, HCl, pH 3, to 7 M urea, 0.3 M NaCl, HCl, pH 3, in three liters.

We have also prepared dephosphorylated pancreatic tetramers by the same procedure. The Dowex column was run the way it was for GpGpCp. In order to identify the peaks, aliquots were hydrolyzed to completion with 0.1 N KOH. The monomers were separated by electrophoresis on Whatmann 3 mm paper at pH 3.5. Quantitative identification of the spots was made spectrophotometrically. The order of appearance

of the tetramers was the same as observed by Rushizky and Sober.[144] However, our resolution was better. The sequence isomer peaks for (ApGpGp)C, (ApApGp)U, and (ApGpGp)U were cleanly resolved into doublets. The base sequence of the tetramers in these peaks cannot be determined by the alkaline hydrolysis procedure. Since we were interested in the GpGpGpC and GpGpGpU peaks, no further efforts were made to identify these peaks. Since the sequence isomer peaks were resolved into doublets instead of triplets, we know that two of the isomers in each case have the same charge, which is slightly different from the third isomer. This can probably be explained when we know which two in each case have the same charge.

c. Desalting Procedures

The salt has generally been removed from the oligomer fractions by the charcoal method of Mandeles and Kamen.[145] The solution to be desalted was acidified with a few drops of glacial acetic acid. Then 5 mg of acid washed Norit A (100 mg/ml in 0.01 M phosphate, 0.01 M pyrophosphate, pH 6.2) was added per O.D. unit. After standing for 1 minute, the solution was filtered through the 47 mm diameter type A glass fiber filters made by Gelman Instrument Company (Ann Arbor, Michigan). The filter was held with the Millipore (Bedford, Massachusetts) pyrex filter holder. All filtrations were done with the aid of an aspirator. The charcoal was rinsed with five 20 ml fractions of H_2O. The nucleotide material was eluted from the charcoal with 300 ml of cold

60% ethanol: 40% 0.1 M NH_3. In order to keep the charcoal out of the filtrate, it was imperative that the charcoal was not allowed to go to dryness before all 300 ml of the solvent had gone through. If it did, then subsequent addition of the solvent always carried through some charcoal in the first few drops. The volume of the ethanol-ammonium filtrate, containing the nucleotide material, was reduced to 5 ml or less with a rotary evaporator. The temperature in the water bath was kept near 40°C. The resulting solution was nearly always dark. The color was removed by filtering through Millipore HAWP cellulose filters. The solution was then lyophilized to dryness and the salt-free oligomer was stored at -10°C until needed.

We have never been entirely satisfied with the charcoal method of desalting nucleotides. Only 50% of the starting nucleotide material could generally be recovered. The yield would be higher if it was not necessary to remove the charcoal at the end by filtering through the cellulose filters. Clearly, the charcoal which is retained by the filter, adsorbs some of the nucleotide material. We tried adding more of the ethanol-ammonia solvent to the concentrated nucleotide sample and refiltering through the glass filters. But that did not remove all of the charcoal. The ethanol-ammonia solvent cannot be filtered through the cellulose filters because it elutes a UV absorption impurity out of the filter. The charcoal appeared to get into the original ethanol-ammonia filtrate only during the first few drops of the elution.

Mandeles and Kamen[145] did not find it necessary to filter the aqueous nucleotide solution containing charcoal impurity through cellulose filters. Thus, their yields, approximately 75%, are better than ours.

The maximum starting amount of oligomer that should be desalted with the charcoal procedure described above is 50 O.D. units. On one occasion, we desalted 100 O.D. units of GpGpC. Unfortunately, the resulting sample was partially hydrolyzed to monomers. Presumably, this occurred because there was so much charcoal that the ethanol-ammonia filtrate warmed up before the elution was complete. At room temperature, the pH of this solution, approximately 9, may be high enough to catalyze some hydrolysis. If no more than 250 mg of charcoal are filtered, corresponding to 50 O.D. units of nucleotide, then the ethanol-ammonia elution is completed before the filtrate has a chance to warm up. The resulting samples did not show any indication of hydrolysis.

Starting with 350 mg of E. coli RNA, the yield of desalted GpGpC was 70 O.D. units. This is more than twice the yield reported by Cantor when the desalting was done by dialyses.

In order to find more satisfactory desalting methods, on one occasion we used the Amicon (Cambridge, Massachusetts) Diaflo ultrafiltration apparatus with membrane UM-3 to desalt a GpGpC fraction. As judged by the index of refraction (see discussion of ultracentrifugation methods), the final solution was more salt-free and had a lower UV blank than when the charcoal procedure was used. However, the oligomer was partially

hydrolyzed to monomers. The solution used in the ultracentrifugation experiment contained only trimer, however, since the smaller molecules passed through the membrane. Tener[146] has used the Amicon Diaflo apparatus with membrane UM-1 to desalt solutions of tRNA. He apparently has no problem with hydrolysis. One difference between UM-1 and membrane UM-3 is that the latter caries a net negative electrical charge while the former is neutral. It is possible that membrane UM-3 catalyzes the hydrolysis.

2. Preparation of Oligomers with Polynucleotide Phosphorylase

a. Conditions for Synthesis

The trinucleoside diphosphates GpCpC, ApCpU, ApGpC, and GpCpU were synthesized with primer-dependent polynucleotide phosphorylase from Micrococcus lysodeikticus (2.7.7.8). This enzyme catalyzes a reaction between nucleoside diphosphates ppN and dimers LpM to give oligomers of the form $LpM(pN)_n$.[147,148]

The enzyme we used was isolated by Dr. Cantor according to the procedure of Singer and O'Brien[149] through stage VII. Subsequent to the synthesis of these oligomers we have replenished the enzyme supply. Basically, the procedure of Singer and O'Brien[149] was used. However, a new procedure for Step IV, suggested by Thanassi and Singer,[150] was substituted for the previously published procedure. We have also carried the preparation through to stage VIII, the final step in the procedure of Singer and O'Brien.[149] The results for our purification are given in Appendix B.

For the synthesis of trinucleoside diphosphates, we have used incubation conditions similar to those suggested by Thach[138] for the synthesis of tri- and tetra-oligomers. The reaction mixture contained 0.2 M glycine buffer pH 9.3, 0.1 mM $CuSO_4$, 0.4 M NaCl, 10 mM dimer LpM, 10 mM magnesium acetate, 20 mM ribonucleotide diphosphate NDP, 0.02 mg/ml BSA and 120 μg/ml of polynucleotide phosphorylase, stage VII. The incubation was at 34°C or 37°C for 24 hours.

b. Isolation of Oligomers

The trimer LpMpN was first separated from unreacted LpM and ppN and oligomers with chain length greater than 3 by descending paper chromatography on Whatmann 3 mm paper with a solvent containing equal volumes of 95% ethanol and 1 M ammonium acetate.[148] A total reaction volume of 0.400 ml was applied as a band 15 cm long to paper that was serrated at the bottom. The paper was allowed to equilibrate in a pre-equilibrated tank for at least 1 hour. Developing times of 20 hours resulted in excellent resolution of all bands up to about a pentamer. The distances that the various bands in a $GpC(pC)_n$ synthesis moved from the origin are given in Table 3.

Table 3

Compound	Distance Moved from Origin (cm)
GpC	26-28
CDP	21-23
GpCpC	17-18
GpCpCpC	13-14
GpCpCpCpC	8-9

Ammonium acetate was removed from the paper by soaking in absolute ethanol for 1 hour.[148] The paper was then soaked in absolute ether for 10 minutes and dried. After eluting the nucleotide material with twice-distilled water, the volume was reduced to less than 50 µl by lyophilization.

The oligomers were further purified with a two-dimensional map on Whatmann 3 MM paper. The first dimension was electrophoresis, 36 v/cm, in 0.05 M formic acid at a pH between 2.4 and 3.5 for 2.5 hours. The pH was adjusted with concentrated ammonia to a value that will give maximum resolution of oligomers with various chain lengths. If pH 3.5 was used, as it was for $GpC(pC)_n$ syntheses, the concentration of formate was reduced to 0.025 M to decrease the current and the spreading of spots resulting from heating. The paper was first soaked with the electrophoresis buffer and equilibrated in the electrophoresis tank for 1 hour. Excess oil and buffer was removed from the area where the sample was to be applied by blotting with Whatmann 3 MM paper. The sample was then applied as a spot with a capillary pipet. The major advantage of the electrophoresis is that it removes any contamination from diphosphate. For example, CDP moves +34-36 cm from the origin while GpCpC moves +8-10 cm.

The second dimension was descending chromatography with a solvent containing n-propanol, water, and concentrated ammonia in the volume ratio 55:35:10. This chromatography separates the oligomers according to chain length. Developing times of 20 hours resulted in movements from the origin

similar to that given in Table 3 for the ammonium acetate chromatography. The trimer spot was eluted with water, lyophilized to dryness, and stored at -10°C until needed. Frequently the two-dimension map is not necessary except to reassure the investigator that he is working with a pure compound. The yield of GpCpC with respect to the amount of GpC used in the reaction mixture was 22%.

We have made attempts to synthesize CpCpG with polynucleotide phosphorylase by incubating in the presence of CpC, GDP, and T_1 ribonuclease (2.7.7.26).[138] We could not detect any synthesis even using twice as much enzyme as indicated above.

3. Optical Studies

a. Preparation of Solutions

Lyophilized oligomers were dissolved with twice-distilled water and the concentration adjusted so that the absorbance at 260 mμ was 200. To measure the concentration, 5 μl of the stock solution was diluted to 1.00 ml with a 0.1 ionic strength buffer; 5.55×10^{-3} M KH_2PO_4, 4.80×10^{-3} M Na_2HPO_4, 0.080 M $KClO_4$, pH 6.8. The concentration of this solution was determined spectrophotometrically at room temperature from the following molar residue extinction coefficients at 260 mμ: GpGpC, 9.2×10^3;[35] ApGpU, 1.13×10^4;[35] ApCpU, 1.00×10^4; ApApApA, 1.24×10^4; UpUpUpU, 9.75×10^3; GpCpC, 8.10×10^3; ApGpC, 1.03×10^4; GpCpU; 8.80×10^3. Except for those taken from the literature, the extinction coefficients were calculated from the appropriate

dimer data. In the case of ApApApA we used ApApA data[35] instead of dimer data. We assumed that the extinction coefficient of GpGpCp is the same as for GpGpC.

The solution for optical studies were prepared by diluting the oligomer stock solution with an equal volume of the appropriate concentrated buffer. The resulting solutions generally contained either 0.5 M NaCl, 0.2 ionic strength sodium phosphate buffer, pH 7.0, or 0.01 M $MgCl_2$, 0.1 ionic strength sodium phosphate buffer, pH 7.0. These solvents shall be referred to as the NaCl and $MgCl_2$ buffers, respectively. In some instances slightly different buffers have been used. These will be indicated in the text. The pH of a solution containing oligomers is assumed to be that of a solution prepared by diluting the concentrated buffer with an equal volume of twice-distilled water. The buffering capacity of every buffer was sufficiently high to ensure that this is a valid assumption.

The absorbance of each buffered nucleotide solution was about 100 at 260 mμ. The ORD and ultraviolet spectrum of each solution was measured with a 0.125 mm path length quartz cell obtained from Opticell (Brentwood, Maryland) and a specially designed cell holder. The volume of solution needed for each measurement was less than 7 μl. The path length of the cell was determined spectrophotometrically with potassium chromate solution in 0.05 M KOH. Extinction coefficients for dilute solutions were obtained from the

Handbook of Analytical Chemistry[151] and Beer's Law was assumed to hold over a 100-fold range of concentration.

b. Measurements

All UV spectra were measured with a Cary Model 14 or Cary Model 15 spectrophotometer. Optical rotation was measured with a Cary Model 60 spectropolarimeter.

Thermal stability was maintained by circulating an aqueous ethylene glycol solution through a specially designed cell block. Above room temperature, a Haake F bath was used to control the temperature of the circulating solution. A low temperature bath, designed by Dr. M. Warshaw, was used for temperatures below 25°C.

Noise in the optical rotation signal was reduced by applying the smoothing procedures described by Savitzky and Golay.[152] The wavelength and pen position of the spectropolarimeter were recorded every 0.5 mμ on paper tape by a Datex (Monrovia, California) analog-to-digital converter. A least-square fit to a 25 point cubic function was done with the coefficients of Savitzky and Golay.[152] The computer program for the calculation is given in Appendix C.

The smoothing program fits 12.5 mμ intervals of the optical rotation curve to a cubic function. We have also tried smaller intervals. The results for 4.5, 7.5, and 12.5 mμ intervals (9, 15, and 25 point cubic functions) for the same typical ORD are given in Figures 32b, 33, and 34, respectively. The unsmoothed data is given in Figure 32a.

Even the 9 point cubic reduces the noise. Only the 25 point cubic, however, reduces it to a level where a smooth curve can be drawn through the points.

The only disadvantage of fitting 12.5 mμ intervals of an ORD curve to a cubic function is that it flattens the curve more than shorter intervals. The peak-to-trough rotation for the ORD in Figures 32b, 33, and 34 is greatest for the 9 point smooth and smallest for the 25 point smooth. The difference, however, for these two functions is less than 0.1×10^4 molar rotation units. If you compare these results with a hand calculation it is not clear which is actually correct. Therefore, we have mainly used a 25 point function because it does a better job of reducing the noise.

We have also tried taking points every 0.1 mμ and every 0.2 mμ and then smoothing with the 25 point cubic function. The results are similar to those shown in Figure 32 where points were taken every 0.5 mμ and smoothed with a 9 point cubic function.

Recently the Datex has been replaced with a Digital PDP 8/S computer (Digital Equipment Corporation, Maynard, Massachusetts). In this case, the computer finds the arithmetic average of 150 points taken every 0.5 mμ. These data points are subsequently used in a Savitzky and Golay[152] 13 point smoothing program for a cubic function. The latter two computer programs were written by Dr. M. Itzkowitz and Mr. B. Tomlinson, respectively.

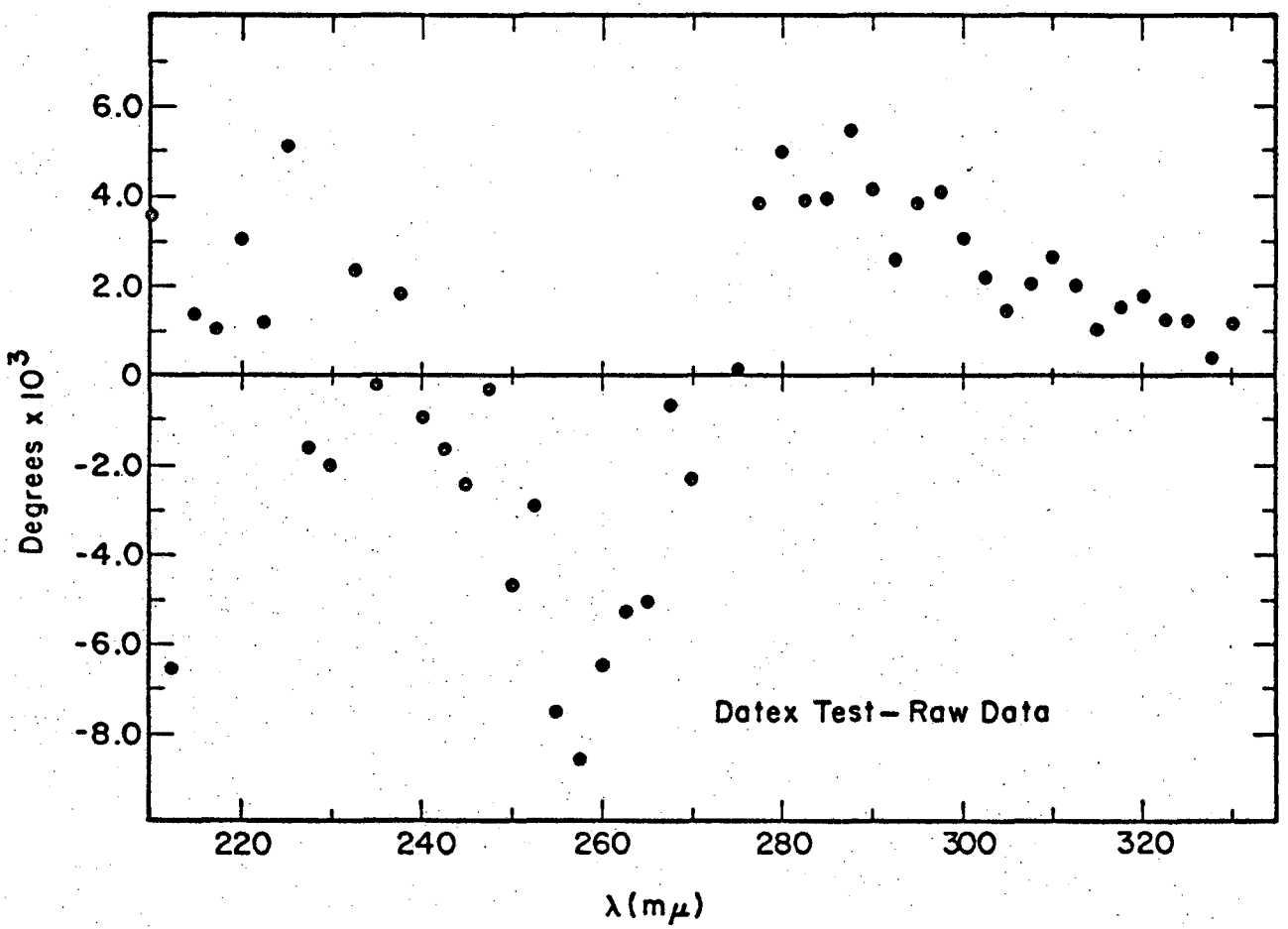

Figure 32a. Unsmoothed data for a typical ORD spectrum. Readings were taken every 0.5 mμ. Every fifth point is shown in the figure. This raw data has been smoothed with 9, 15, and 25-point cubic functions in Figures 32b, 33, and 34, respectively.

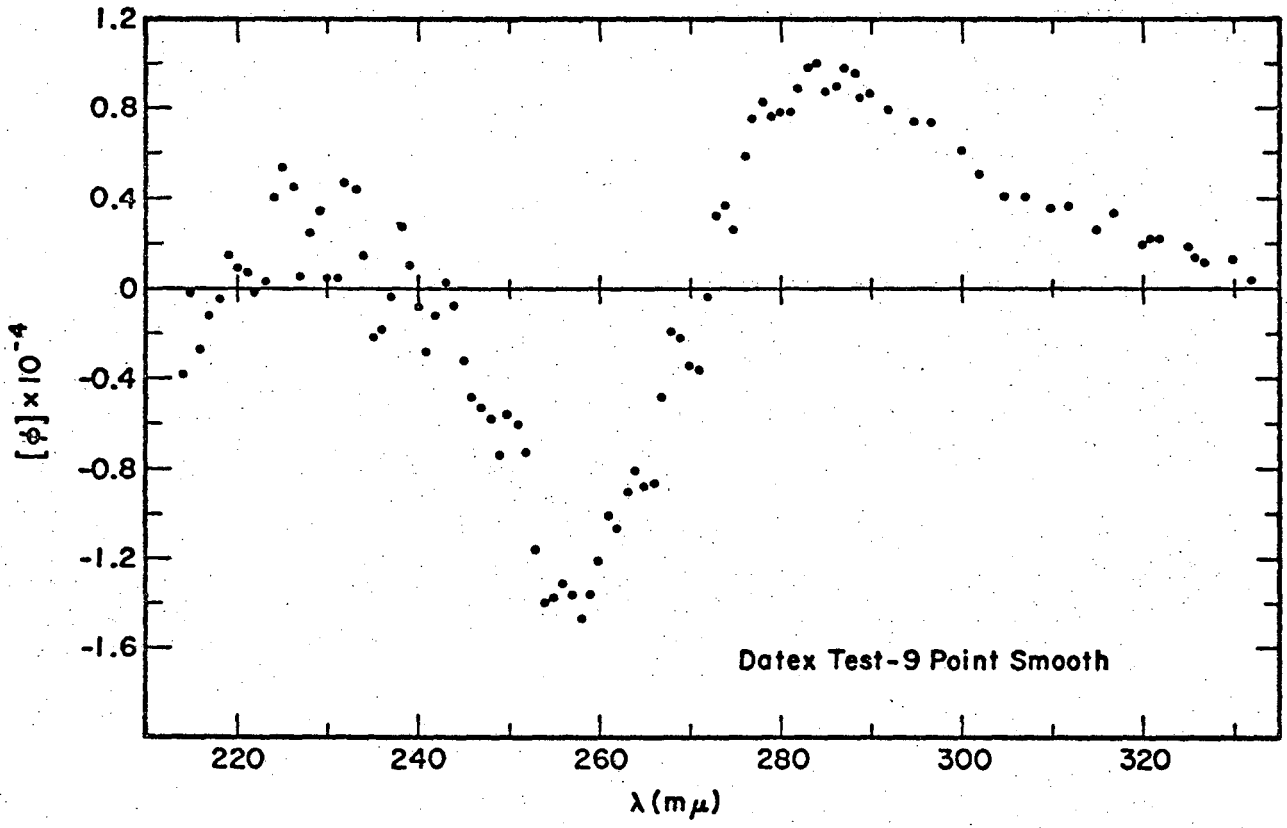

Figure 32b. A typical ORD spectrum was smoothed by taking points every 0.5 mμ and fitting to Savitzky and Golay's 9-point cubic function. The same ORD curve is smoothed with 15 and 25-point cubic functions in Figures 33 and 34. The unsmoothed data is given in Figure 32a.

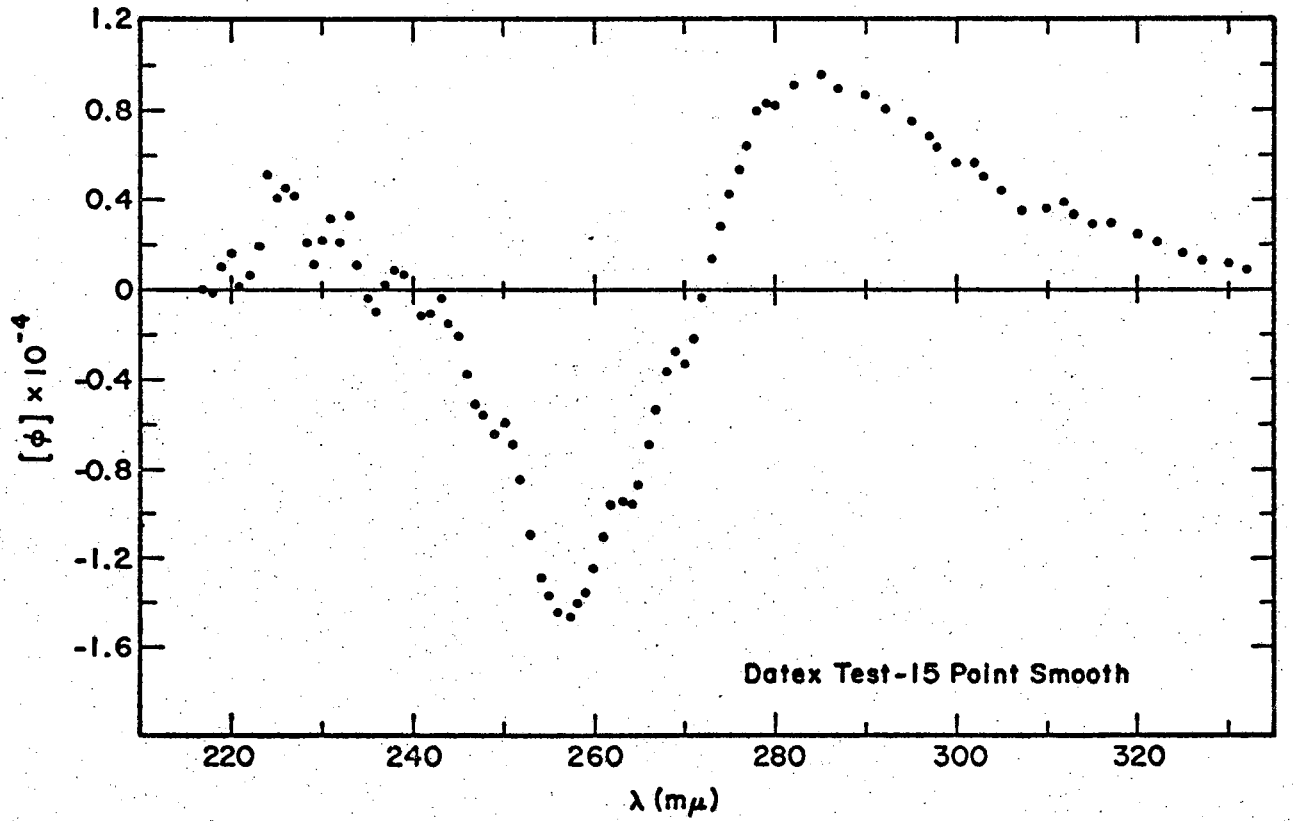

Figure 33. A typical ORD spectrum was smoothed by taking points every 0.5 mμ and fitting to Savitzky and Golay's 15-point cubic function.

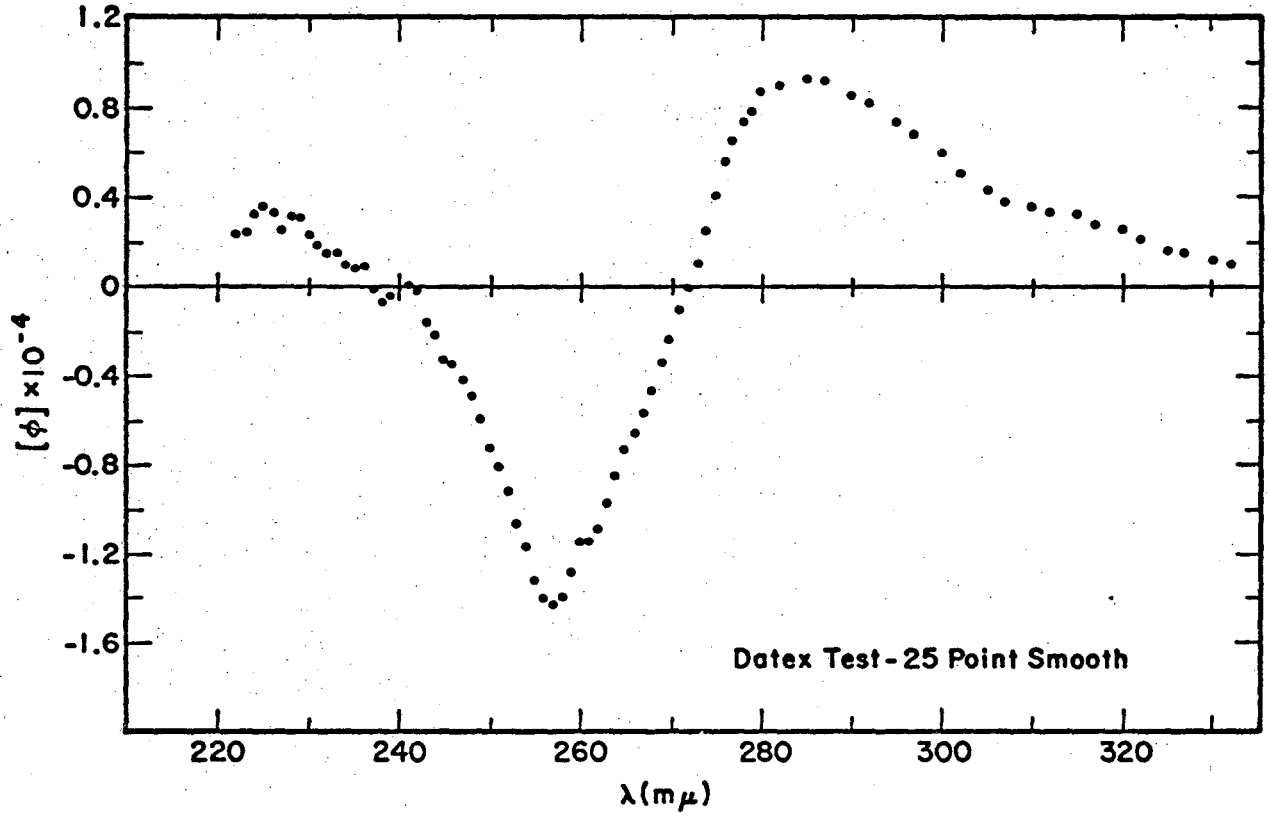

Figure 34. A typical ORD spectrum was smoothed by taking points every 0.5 mμ and fitting to Savitzky and Golay's 25-point cubic function.

Optical rotation data is expressed as molar rotation per residue, $[\phi]$, which was defined in Part I.

c. Nearest-Neighbor Calculations

The nearest-neighbor calculated ORD curves were done according to Eq. (3). The necessary ORD data of the dimers and monomers as a function of temperature were taken from the work of Dr. R. Davis.[109]

4. Ultracentrifugation

All centrifuge experiments were done at 2°C with a Spinco Model E ultracentrifuge equipped with an electronic speed controller designed by Hearst and Gray.[153] Schlieren optics were used. Data for equilibrium experiments, in the form of photographic plates, were taken 24 to 36 hours after the start of the run. There was generally no difference from data taken 12 hours after the start of the run. Measurements on the photographic plates were made with the aid of a Gaertner Toolmaker's Microscope (Gaertner Scientific Corporation, Chicago, Illinois).

Weight-average molecular weights were determined according to Method I of Van Holde and Baldwin.[154] Assuming the derivatives with respect to concentration are zero, the weight-average molecular weight, M_w, can be equated to the refractive index gradient in the cell by the following equation:

$$\frac{2\Delta n_c}{n_c^o(b^2 - a^2)} = \frac{\omega^2 M_w(1 - \bar{v}\rho)}{RT} \qquad (13)$$

where b and a are distances in cm of the bottom of the cell and the meniscus, respectively, from the axis of rotation. These were determined with the help of the known distances of reference holes in the rotor from the axis of rotation. Δn_c is the difference between the refractive index at the bottom of the cell and at the meniscus. Similarly, the refractive increment, n_c^o, is the difference between the refractive index of the starting solution and the solvent. R is the gas constant, 8.314×10^7 ergs/°K/mole, and T is the absolute temperature. The centrifugal speed in radians/sec is ω. The density of the solution is ρ and the partial specific volume of the solute is $\bar{v}$. We have taken $(1 - \bar{v}\rho)$ to be 0.46.[155]

The refractive increment was determined for a solution of poly A in the NaCl buffer from the area of the schlieren pattern that formed at the boundary between buffer and nucleotide solution. A double-sector Kel-F cell was used to establish this artificial boundary. The salt concentration of the poly A solution was adjusted by dialysis against buffer. There was excellent agreement with the refractive increment of one 2:1 mixture of GpGpC and GpCpC in the same buffer. Other solutions of GpGpC and GpCpC had refractive increments that were higher. The GpGpC in the solution with the same refractive increment as poly A had been desalted with

the Amicon Diaflo apparatus. The samples of GpGpC in the other solutions had been desalted with the charcoal procedure. The greater refractive increments for these solutions is probably the result of incomplete desalting. The residual salt in these solutions will not affect the equilibrium experiments, however, since the gradient will be negligible. We have always taken the refractive increment of poly A for the refractive increment of GpCpC, GpGpC, and mixtures of the two oligomers.

The difference between the refractive index at the bottom of the cell and at the meniscus was determined by integrating the schlieren pattern of the equilibrium run, using the Trapezoidal Rule. The refractive increment of poly A was also determined from the area of a schlieren pattern. These areas are proportional to the refractive index. From Eq. (13), it can be seen that the proportionality constants cancel.

The z-average molecular weights were determined from plots of $(1/r)(dn_c/dr)$ versus (n_r-n_a). This is Method II of Van Holde and Baldwin.[154] The distance in cm from the axis of rotation to some point in the cell is r. dn_c/dr at this point was determined directly from the schlieren pattern of the equilibrium run. The difference between the refractive index at that point and the meniscus, (n_r-n_a), was determined by integration using the Trapezoidal Rule. The slope of the line connecting the points for the bottom of the cell and the meniscus is proportional to the z-average molecular weight, M_z.

$$\frac{\left(\frac{1}{r}\frac{dn_c}{dr}\right)_b - \left(\frac{1}{r}\frac{dn_c}{dr}\right)_a}{\Delta n_c} = \frac{\omega^2(1 - \bar{v}\rho)}{RT} M_z \qquad (14)$$

As with Eq. (13) we are assuming the derivatives with respect to concentration are zero.

Results

1. Evidence for Association

The following pairs of complementary oligoribonucleotides were mixed in a 1:1 mole ratio: ApCpU and ApGpU, ApGpC and GpCpU, GpGpC and GpCpC, GpGpCp and GpCpC, and ApApApA and UpUpUpU. The total concentration of mononucleoside residues was between 5 and 10 mM in each case. The solutions were buffered at pH 7 and contained either 0.5 M NaCl or 0.01 M $MgCl_2$. The ORD of the solutions was measured at 1°C and compared with the average ORD of the oligomers measured separately under the same conditions. A significant difference between the two curves was taken as evidence that specific intermolecular association occurs in the mixture. The experiment was also done at 26°C in several instances. The results are summarized in Table 4. Also included is whether any evidence was found for the self-aggregation of each oligomer.

Table 4

Association of Oligoribonucleotides[a] at pH 7

	0.5 M NaCl		0.01 M $MgCl_2$	
	1°C	26°C	1°C	26°C
ApCpU	No	-	No	-
ApGpU	No	-	No	-
ApCpU + ApGpU	No	-	No	-
ApGpC	-	-	Yes	Yes
GpCpU	-	-	No	No
ApGpC + GpCpU	-	-	Slight	No
GpGpC	Yes	Yes	Yes	Yes
GpCpC	No	No	No	No
GpGpC + GpCpC	Yes	Yes	Yes	Yes
GpGpCp	Yes	Yes	-	-
GpGpCp + GpCpC	Yes	Slight	Slight	-
ApApApA	No	No	No	No
UpUpUpU	No	No	No	No
ApApApA + UpUpUpU	No	No	No	No

a. Total concentration of residues between 5 and 10 mM. Yes and No indicate whether any optical rotation evidence for aggregation was found. (-) indicates the ORD of the oligomer(s) under these conditions was not measured.

Specific interaction between GpGpC and GpCpC was observed. There was no evidence of specific interaction between any of the other pairs of complementary oligomers. However, there were indications of self-aggregation in solutions containing GpGpC, GpGpCp, and ApGpC.

The evidence for these qualitative conclusions will be reviewed in greater detail in the following paragraphs. We will then return to the interaction between GpGpC and GpCpC and investigate the nature of the complex.

a. ApCpU + ApGpU

The ORD of ApCpU and ApGpU in the $MgCl_2$ buffer at 2°C are compared in Figures 35 and 36, respectively, with their nearest-neighbor calculated ORD. The calculated curves should correspond to the ORD of the unaggregated oligomer at 2°C. In both cases, the experimental curve is in close agreement with the semi-empirical calculation. We infer from this there is no self-aggregation of either trimer under these conditions. The same experimental curves are obtained at 2°C in the NaCl buffer. The ORD curves in Figures 35 and 36 agree qualitatively with previous measurements of the ORD of ApCpU[35] and ApGpU[37] at room temperature in more dilute solutions. The magnitude of the rotation is greater for our curves, however. This presumably reflects the temperature dependence of the ORD of stacked bases. Our measurements agree as well with the nearest-neighbor calculations for 2°C as the room temperature measurements agree with the nearest-neighbor calculations for 25°C.

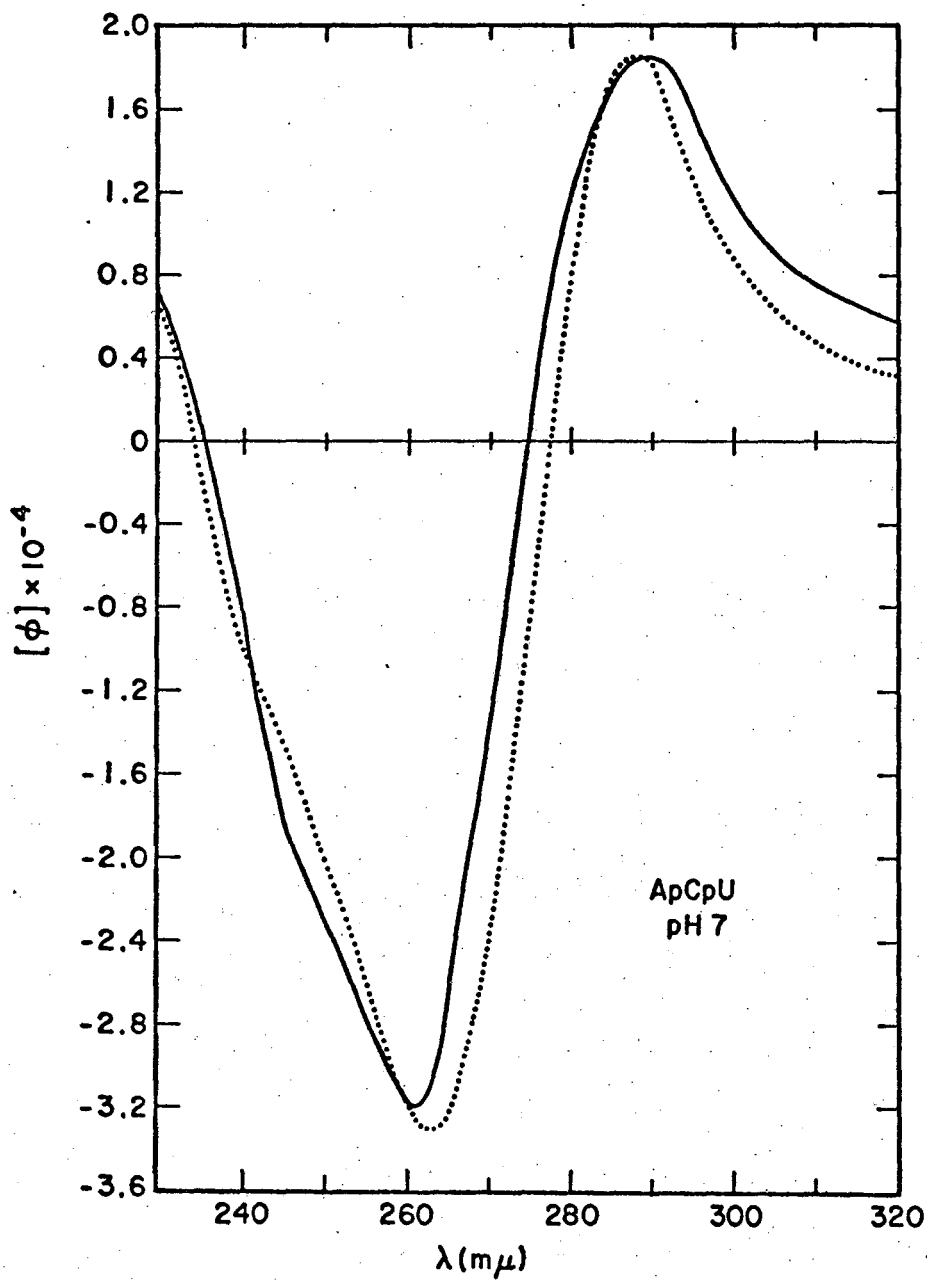

Figure 35. ORD of ApCpU.

—— Experiment, 0.01 M $MgCl_2$, 0.1 ionic strength sodium phosphate buffer, pH 7.0, 2°C, 6.7 x 10^{-3} M mononucleosides.

--- Nearest-neighbor calculated ORD of unaggregated ApCpU at 2°C.

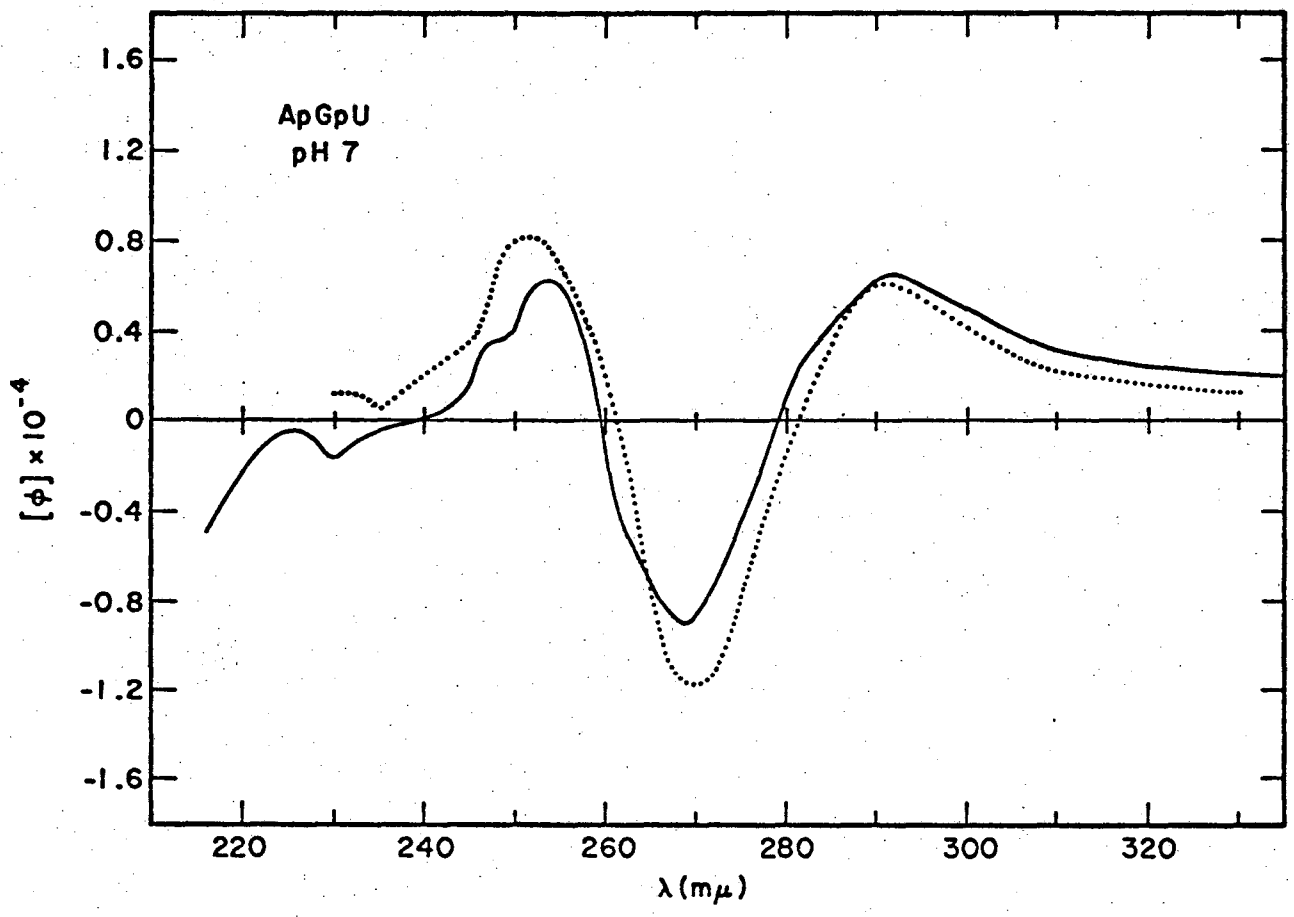

Figure 36. ORD of ApGpU.

—— Experiment, 0.01 M $MgCl_2$, 0.1 ionic strength sodium phosphate buffer, pH 7.0, 2°C, 6.7×10^{-3} M mononucleosides.

--- Nearest-neighbor calculated ORD of unaggregated ApGpU at 2°C.

There is also no indication of any cross interaction in 1:1 mixtures of ApCpU and ApGpU at 2°C in either the NaCl or $MgCl_2$ buffer. The ORD of the mixture is identical, within the experimental uncertainty, to the average of each trimer measured separately. The experimental curve of the mixture in the $MgCl_2$ buffer and that expected for no interaction under these conditions are shown in Figure 37. Also shown is an estimated curve for the ORD of the 100% 1:1 complex. The perturbation of the base pairs on the ORD of the unaggregated trimers was approximated with the A-U and G-C difference curves calculated by Cantor.[36] As indicated in Part I, these difference curves are only rough estimates of the effect of A-U and G-C base pairs. Thus, the calculated ORD of the complex is only a rough estimate. It does give us an idea, however, of the magnitude of the change we expect upon complex formation.

b. ApGpC + GpCpU

Some aggregation probably occurs in equimolar mixtures of ApGpC and GpCpU at 2°C in the presence of magnesium ions. The crossover in the ORD of the mixture occurs 2 mμ to the blue of the crossover that is expected for no interaction. The two ORD curves are shown in Figure 38. This does not happen at 26°C as seen in Figure 39. Although the difference between the calculated and experimental curves at 2°C is small, it is significant and in the expected direction. It is too small to be useful for further studies, however.

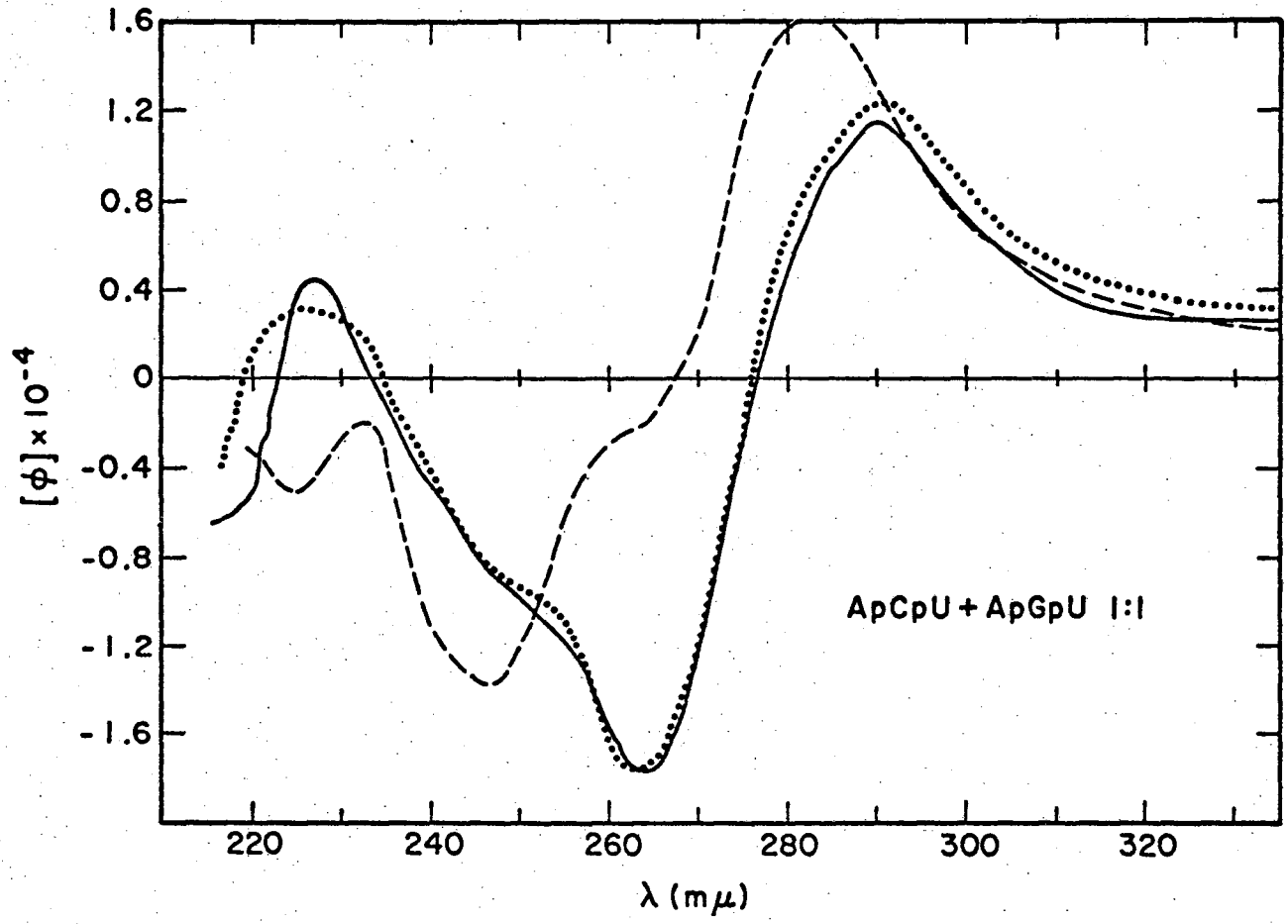

Figure 37. ORD of a 1:1 mixture of ApCpU and ApGpU.

—— Experiment, 0.01 M $MgCl_2$, 0.1 ionic strength sodium phosphate buffer, pH 7.0, 2°C, 7.3 x 10^{-3} M mononucleosides.

... Average of ORDs of ApCpU and ApGpU measured separately under the same conditions.

--- Estimated ORD of 100% 1:1 complex.

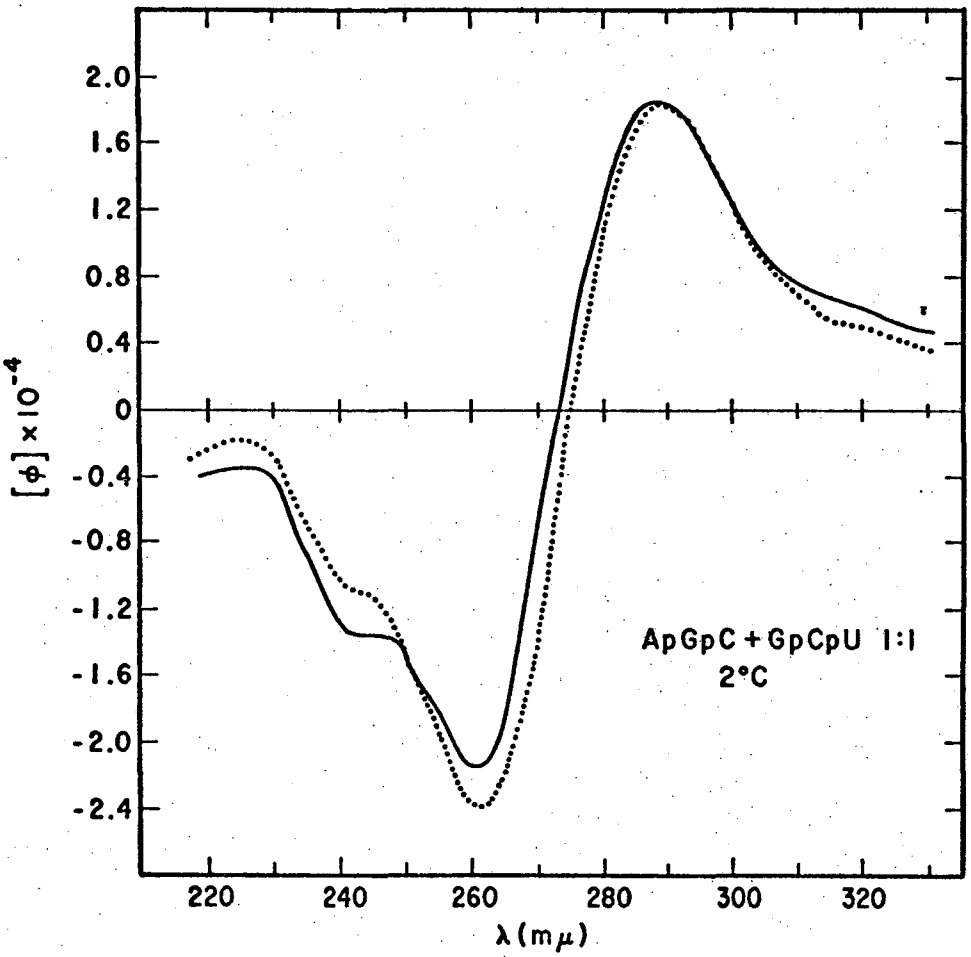

Figure 38. ORD of a 1:1 mixture of ApGpC and GpCpU at 2°C.

—— Experiment, 0.01 M $MgCl_2$, 0.1 ionic strength sodium phosphate buffer, pH 7.0, 2°C, 9.4 x 10^{-3} M mononuclesides.

··· Average of ORDs of ApGpC and GpCpU measured separately under the same conditions.

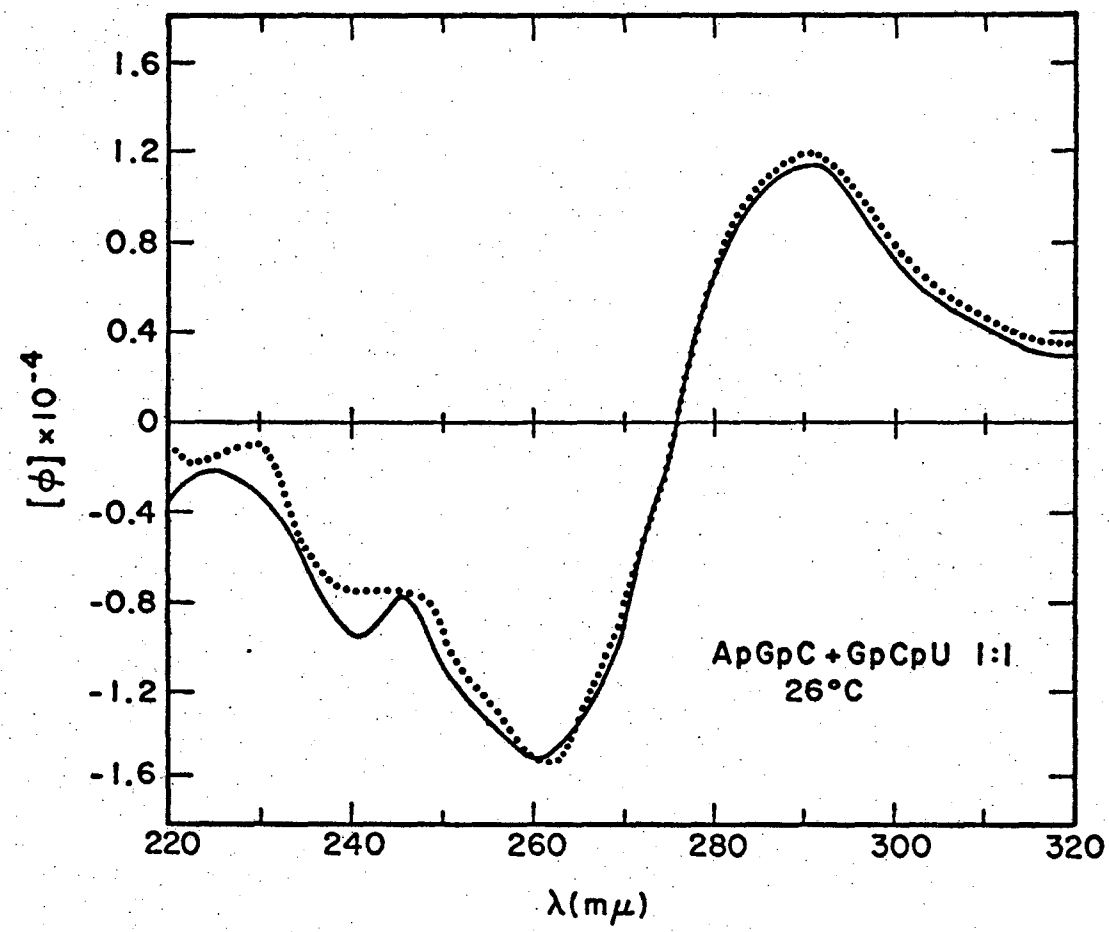

Figure 39. ORD of a 1:1 mixture of ApGpC and GpCpU at 26°C.

—— Experiment, 0.01 M $MgCl_2$, 0.1 ionic strength sodium phosphate buffer, pH 7.0, 26°C, 9.4 x 10^{-3} M mononucleosides.

··· Average of ORDs of ApGpC and GpCpU measured separately under the same conditions.

The situation is further complicated by the self-aggregation of ApGpC under these conditions. The ORD of ApGpC in the $MgCl_2$ buffer at +0.8°C and 26.6°C is compared in Figure 40 with the ORD of a more dilute solution of ApGpCp[37] at 26°C. The concentration of residues in the dilute solution is a factor of 100 smaller than that of the concentrated solution. The peaks, troughs, and crossovers of the three curves occur at nearly the same wavelengths. However, the magnitudes of rotation at the peak and trough for the concentration solution are much larger than that of the dilute solution. The presence of a 3'-terminal phosphate is not expected to affect the ORD of single-strand oligomers. In fact, the ORD of ApGpCp is similar to the nearest-neighbor calculated ORD of ApGpC.[37] Therefore, the ORD of ApGpCp is a fair measure of the ORD of unaggregated ApGpC. The concentrated and dilute solutions also differ in that the concentrated solution contains $MgCl_2$. The presence of this salt should not affect the ORD of unaggregated oligomers. Therefore, the larger magnitudes of rotation for concentrated solutions of ApGpC compared to dilute solutions of ApGpCp must be because of self-aggregation.

In contrast to the case for ApGpC, there is apparently no self-aggregation in solutions of GpCpU under similar conditions. The experimental and nearest-neighbor calculated ORD of GpCpU for our conditions are compared in Figure 41. There is good agreement.

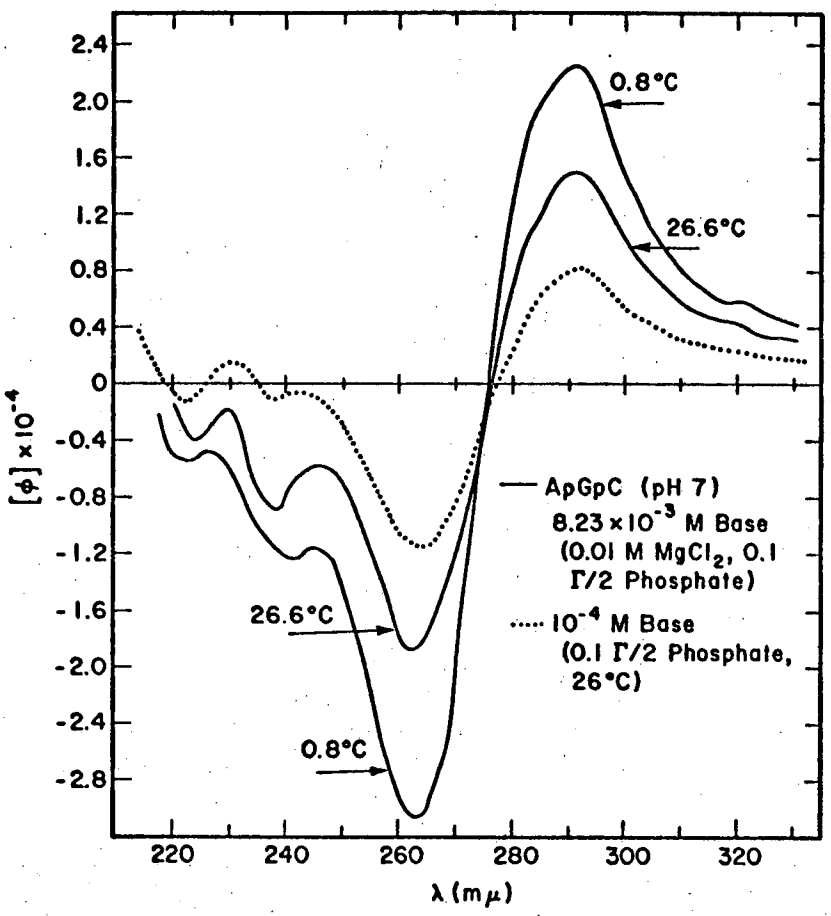

Figure 40. ORD of ApGpC and ApGpCp.

—— Experimental ORD of ApGpC.

... Experimental ORD of ApGpCp. (Γ/2 is a symbol for ionic strength.)

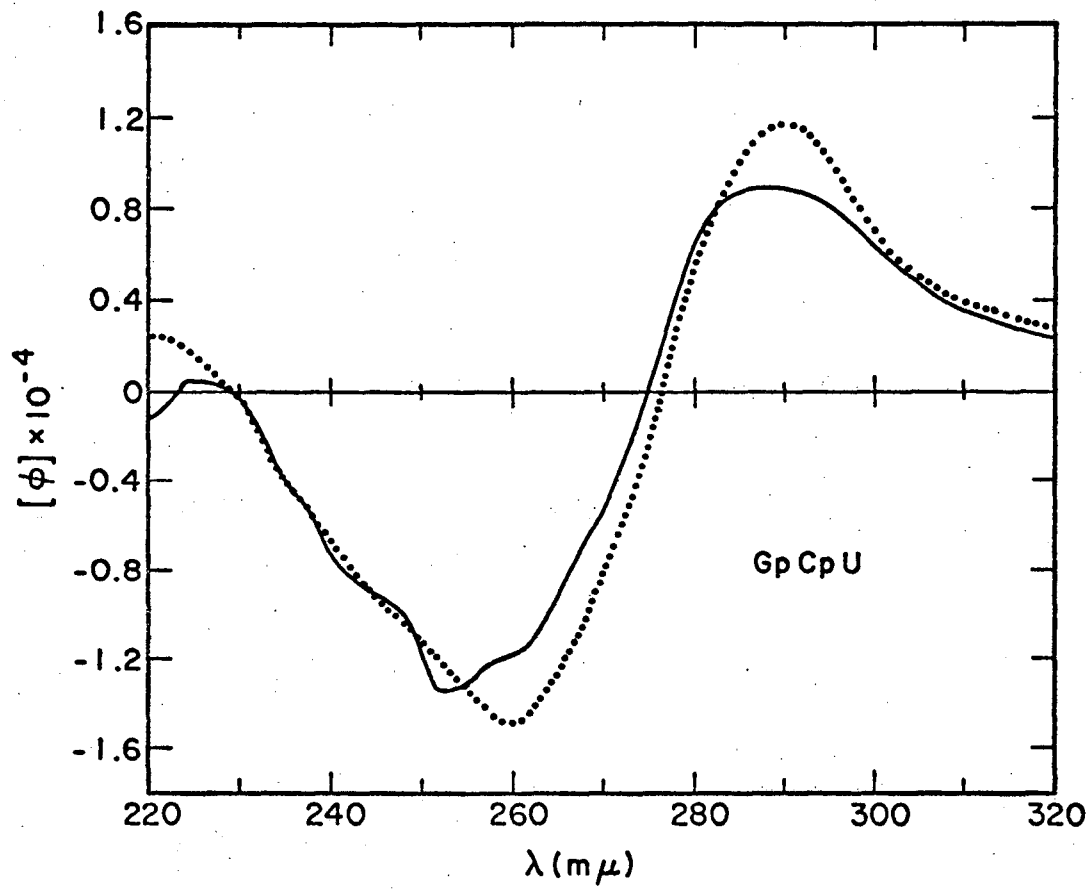

Figure 41. ORD of GpCpU.

—— Experiment, 0.01 M $MgCl_2$, 0.1 ionic strength sodium phosphate buffer, pH 7.0, 0.8°C, 1.11 x 10^{-2} M mononucleosides.

... Nearest-neighbor calculated ORD of unaggregated GpCpU at 1°C.

The extent of specific association in solutions containing both ApGpC and GpCpU may not be accurately reflected in the difference between the experimental and calculated ORD of the mixture. The difference will be small if the ORD of the 1:1 complex is similar to the ORD of the ApGpC aggregate. Furthermore, the concentration of ApGpC in the mixture is one-half the concentration in the solutions used to measure its ORD. Thus, there may be less aggregation of ApGpC in the mixture.

c. GpGpC + GpCpC

A complex between GpGpC and GpCpC is formed in either the NaCl or $MgCl_2$ buffer at 1°C. The ORD of a 1:1 mixture is compared in Figure 42 with the average ORD of the two oligomers measured separately in the same buffer. A second long wavelength peak occurs for the mixture and the crossover is blue-shifted 3 mμ. A similar but smaller difference between experiment and calculation is obtained at 26°C in each buffer.

The complex between GpGpC and GpCpC forms despite the self-aggregation of GpGpC. ORD curves for dilute and concentrated solutions of GpGpC alone are shown in Figure 43. The magnitude of the rotation at the peak and trough is greater for the more concentrated solution. This is clearly indicative of some sort of association of GpGpC with itself. The aggregation also has a hypochromic effect on the absorption spectrum of GpGpC. The extinction coefficient at 260 mμ

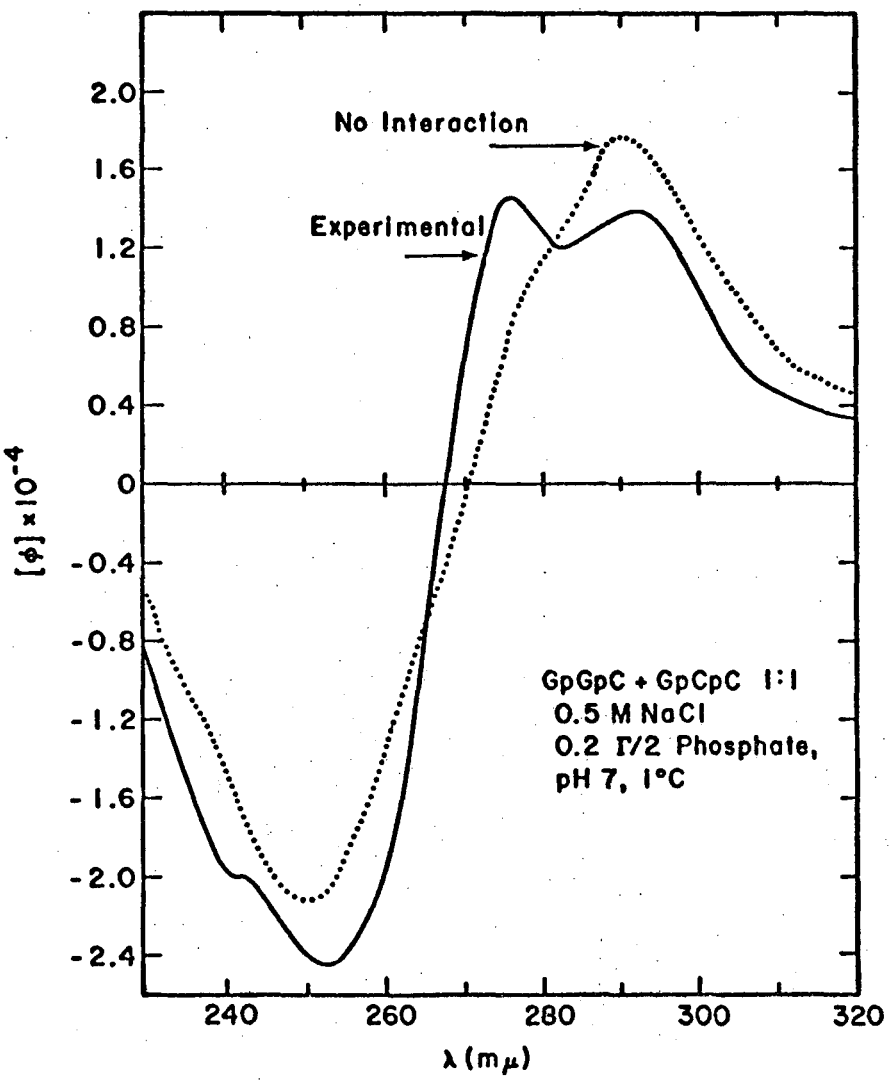

Figure 42. ORD of a 1:1 mixture of GpGpC and GpCpC.

—— Experiment, 0.5 M NaCl, 0.2 ionic strength sodium phosphate buffer, pH 7.0, 1°C, 8.1×10^{-3} M mononucleosides.

··· Average of ORDs of GpGpC and GpCpC measured separately under the same conditions.

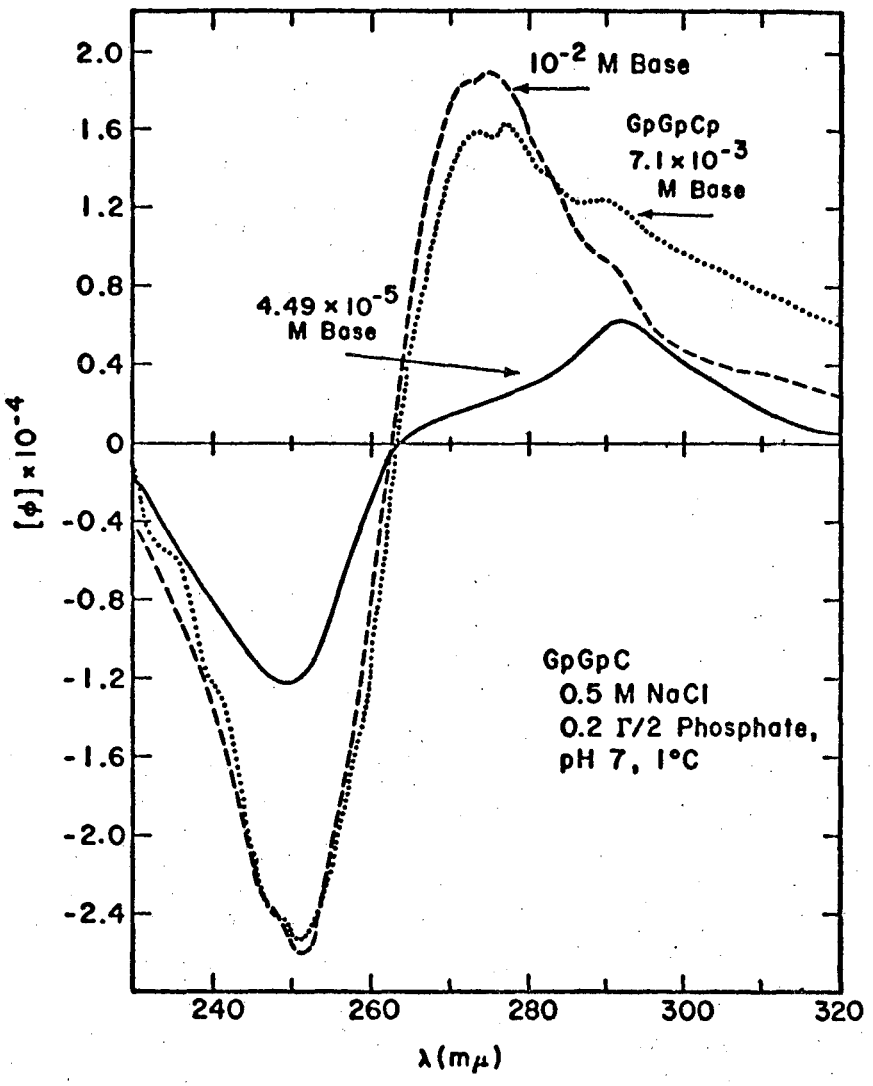

Figure 43. ORD of GpGpC aggregate.

—— 4.49×10^{-5} M mononucleosides, 0.5 M NaCl, 0.2 ionic strength sodium phosphate buffer, pH 7.0, 1°C.

--- 1.00×10^{-2} M mononucleosides, 0.5 M NaCl, 0.2 ionic strength sodium phosphate buffer, pH 7.0, 1°C.

... ORD of GpGpCp, 7.1×10^{-3} M mononucleosides, 0.5 M NaCl, 0.2 ionic strength sodium phosphate buffer, pH 7.0, 1°C.

increases from 7950 to 9200 at 1°C in the $MgCl_2$ buffer as the concentration is decreased from 10^{-2} M to 10^{-4} M.

Equilibrium in concentrated GpGpC solutions is reached in an hour after the temperature is changed by as much as 25°. This association and disassociation is faster than found for G oligomers by Lipsett[156,157] and for GpGpGpU and GpGpU by Dr. S. Podder[158] in this laboratory.

The ORD of GpCpC under our conditions does not agree as well with the nearest-neighbor calculated curve as other trimers. The two curves for 2°C are shown in Figure 44. However, the experimental curve in either buffer at 1°C or 26°C is not concentration dependent between 10^{-2} M and 10^{-4} M total residue concentration. The absorption spectrum also does not depend on concentration in this range. We conclude, therefore, there is no self-aggregation of GpCpC under conditions where specific interaction is observed between GpGpC and GpCpC.

d. ApApApA + UpUpUpU

There is no evidence that a complex forms between ApApApA and UpUpUpU in either buffer at 1°C or 26°C. For all four cases, the ORD of a 1:1 mixture is identical to the average of each measured separately. An example is shown in Figure 45.

Poly U is known to aggregate below 4°C.[159] The ORD of this complex, as measured by Sarkar and Yang,[103] is shown in Figure 46. The ORD of UpUpUpU that we obtained under similar

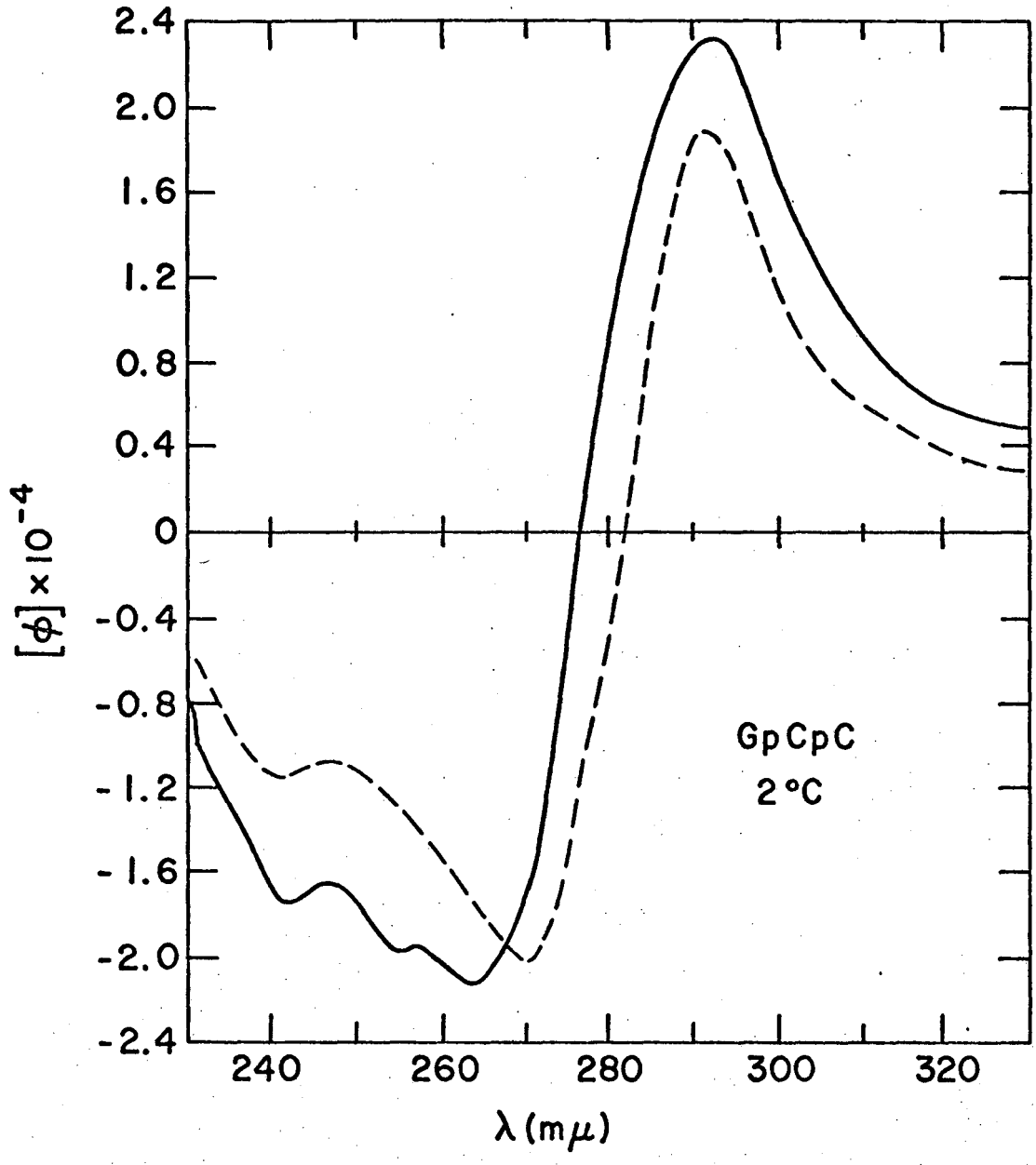

Figure 44. ORD of GpCpC.

—— Experiment, 0.01 M $MgCl_2$, 0.1 ionic strength sodium phosphate buffer, pH 7.0, 2°C, 1.23 x 10^{-2} M mononucleosides.

--- Nearest-neighbor calculated ORD of unaggregated GpCpC at 2°C.

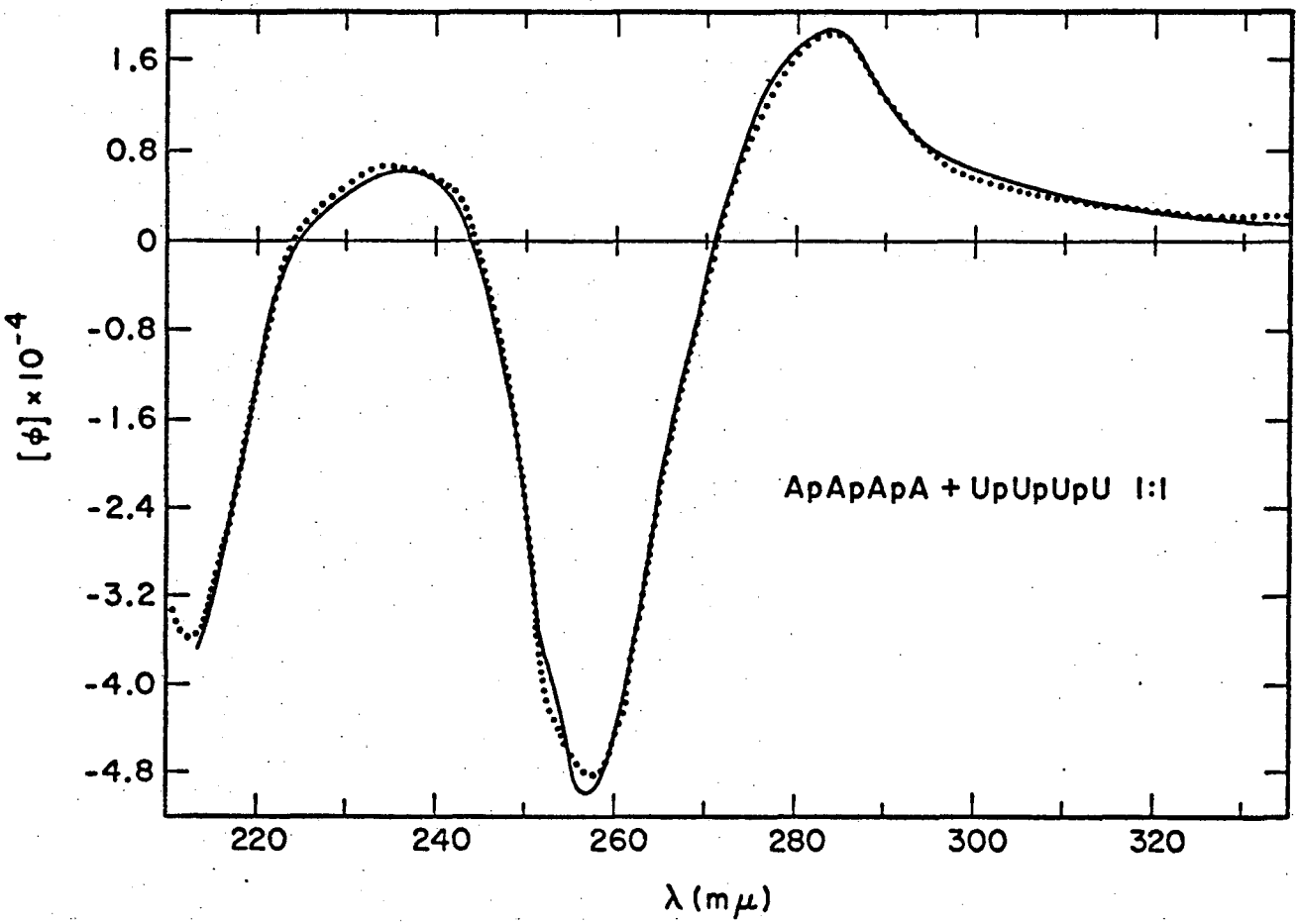

Figure 45. ORD of a 1:1 mixture of ApApApA and UpUpUpU.

—— Experiment, 0.01 M $MgCl_2$, 0.1 ionic strength sodium phosphate buffer, pH 7.0, 1°C, 7.4 x 10^{-3} M mononucleosides.

... Average of ORDs of ApApApA and UpUpUpU measured separately under the same conditions.

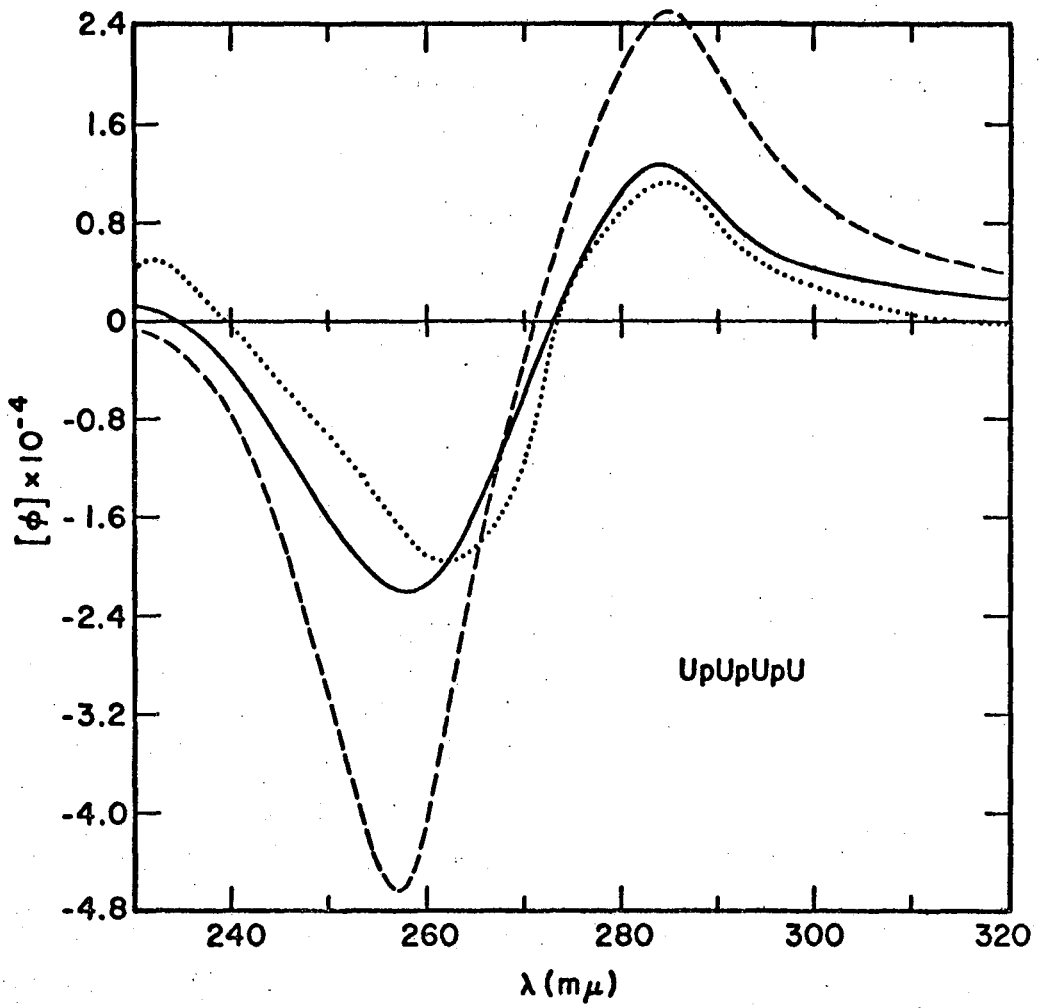

Figure 46. ORD of UpUpUpU.

—— Experiment, 0.01 M $MgCl_2$, 0.1 ionic strength phosphate buffer, pH 7.0, 1°C, 8.5 x 10^{-3} M mononucleosides.

··· Nearest-neighbor calculated ORD of unaggregated UpUpUpU at 1°C.

--- ORD of poly U aggregate (Reference 103).

conditions of temperature and ionic strength but at a 100-fold higher residue concentration is also shown. The magnitude of the rotation of the poly U complex is much larger. In fact, the ORD of UpUpUpU is almost identical to its nearest-neighbor calculated ORD, which is also shown in Figure 46.

The ORD of ApApApA also agrees very well with the nearest-neighbor calculation. The measurement in the presence of the NaCl buffer at room temperature is shown in Figure 47 along with the curve calculated from the dimers.

These are the first cases where the ORD of tetramers have been compared with their nearest-neighbor calculated ORD. The agreement is as good as reported for trimers. The agreement with calculation is much better for ApApApA than for poly A.[36]

Miles et al.[160] have obtained infrared evidence for a complex between UpUpUpU and ApApApA and between UpUpU and ApApA. The stoichiometry in both cases is 2U:1A. Their experiments were done at a 10-fold higher concentration of mononucleosides than we used. They also used a higher concentration of $MgCl_2$. These differences presumably account for our inability to detect a complex between UpUpUpU and ApApApA.

2. The Nature of the Complex Between GpGpC and GpCpC

a. Stoichiometry

The stoichiometry of the complex between GpGpC and

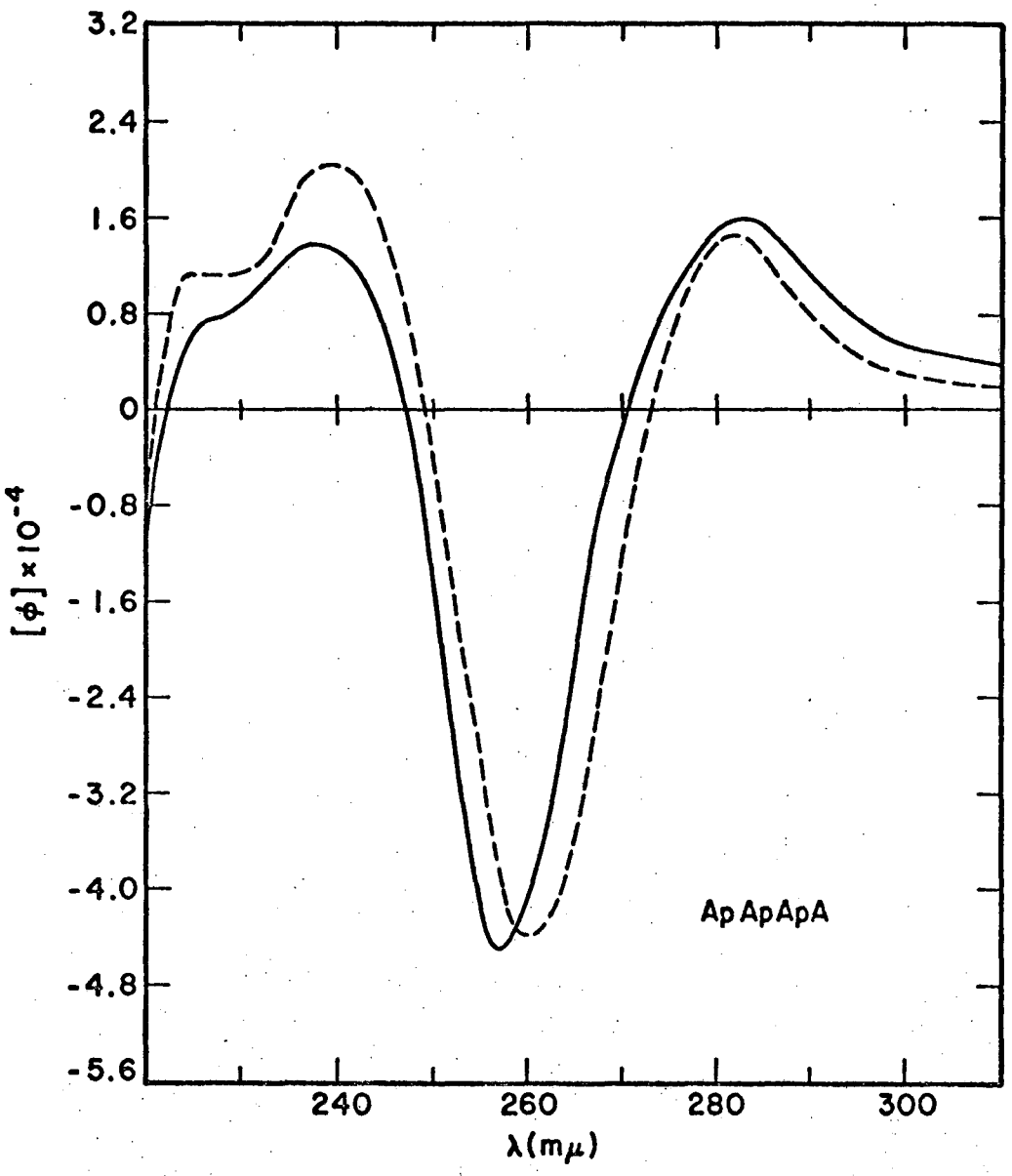

Figure 47. ORD of ApApApA.

—— Experiment, 0.5 M NaCl, 0.2 ionic strength sodium phosphate buffer, pH 7.0, 26°C, 6.6×10^{-3} M mononucleosides.

--- Nearest-neighbor calculated ORD of unaggregated ApApApA at 26°C.

GpCpC was determined by the continuous variation method of Job.[161,162] We measured the ORD of mixtures at 1°C containing equal total concentration of nucleoside by varying ratios of GpGpC and GpCpC. Molar rotations for two wavelengths are plotted as a function of mole fraction of GpGpC for each buffer in Figures 48 and 49. Separate lines are drawn through points for solutions containing an excess of each of the components. For each wavelength and both buffers, the two lines intersect near 66% mole fraction GpGpC. Similar results are obtained at other wavelengths. Taking into account the uncertainty of the data, we can say that the complex contains 66% ± 5% GpGpC. This indicates that the complex probably contains 2 moles of GpGpC for every mole of GpCpC. It does not necessarily indicate, however, that the complex contains only three trimers.

The lines in Figures 48 and 49 intersect at points that should correspond to the rotation of the pure complex at that wavelength. The actual rotation of a solution containing a 2:1 ratio of GpGpC to GpCpC is different. This means that the fraction of trimers in the 2:1 complex is less than one. The difference between the rotation at the intercept and the experimental rotation can be used to determine the percent complex formation. The scatter in the data is such that it cannot be determined accurately. We estimate that 75% ± 20% of the trimers are in the 2:1 complex for either buffer at 1°C.

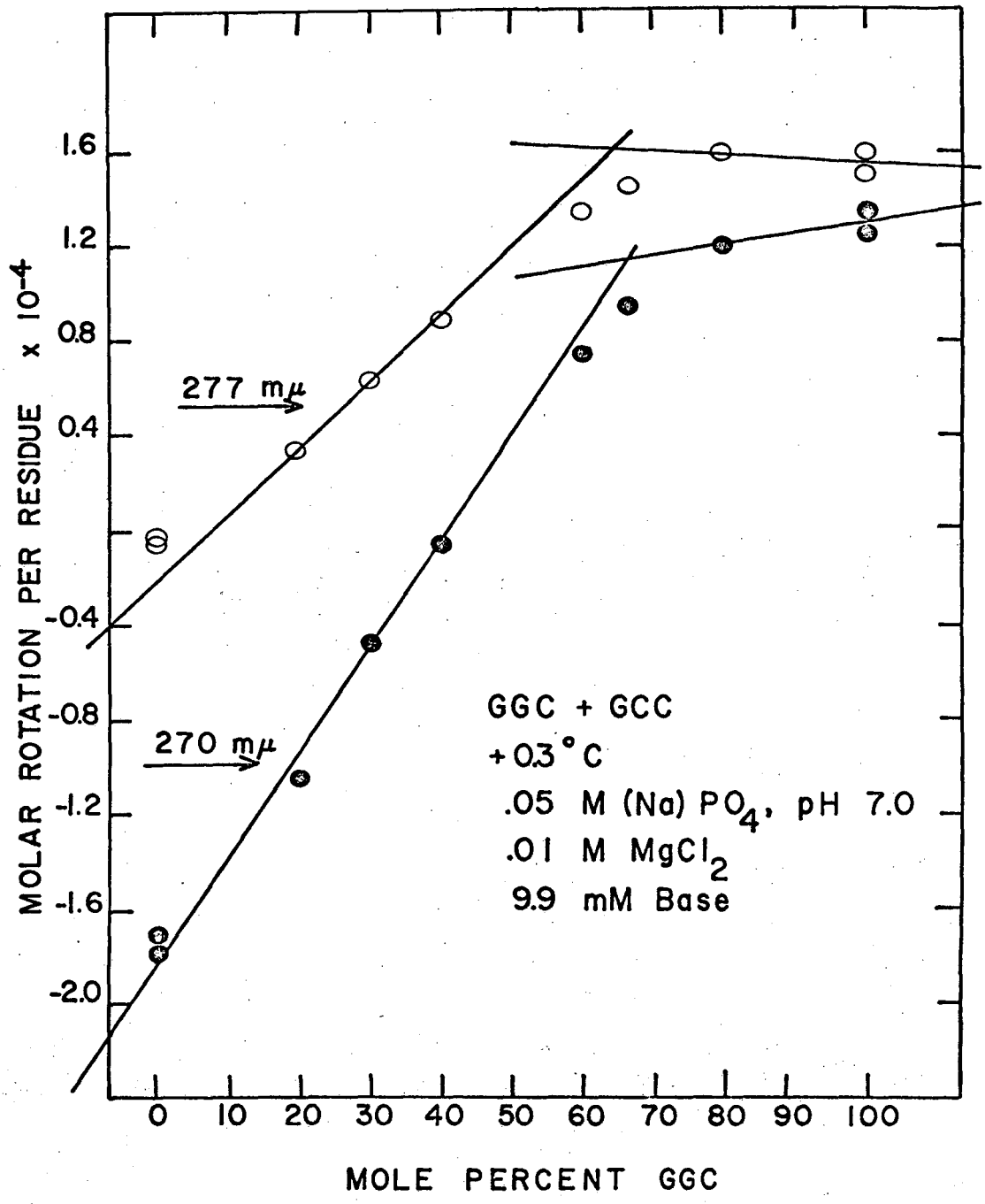

Figure 48. Continuous variation experiment for mixtures of GpGpC and GpCpC in the $MgCl_2$ buffer.

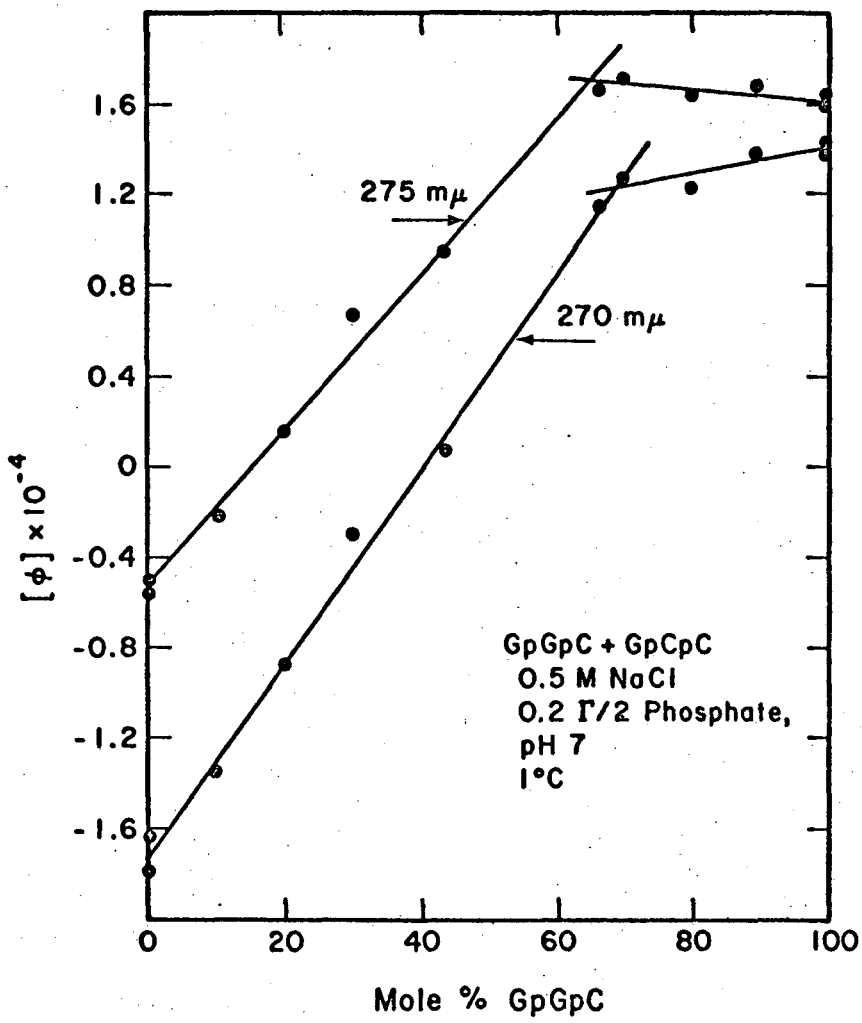

Figure 49. Continuous variation experiment for mixtures of GpGpC and GpCpC in the NaCl buffer. The concentration or mononucleosides was 8.9 x 10^{-3} M for each mixture.

b. Molecular Weight

The number of trimers in the complex of GpGpC and GpCpC can be determined from its molecular weight. The weight-average and z-average molecular weights of the species present in a 2:1 mixture of GpGpC and GpCpC in both the NaCl and $MgCl_2$ buffers at 2°C have been determined by equilibrium sedimentation. The same molecular weight averages have been determined for the GpGpC aggregate in both buffers and for GpCpC in the NaCl buffer. The results are given in Table 5.

A plot of $(1/r)(dn_c/dr)$ versus (n_r-n_a) is shown in Figure 50 for a 2:1 mixture of GpGpC and GpCpC. The plot has a constant slope except near the bottom of the cell. The same was true for each of the other solutions. Some of the curvature at the bottom of the cell is probably because of the concentration dependence of the aggregation. Even for a homogeneous solution we expect some curvature, however, because concentration terms have been neglected in writing down Eq. (14). We do not know the relative importance of these two contributions to the curvature. Furthermore, points near the bottom of the cell cannot be determined accurately. Therefore, we have neglected the curvature introduced by these points. We have calculated the z-average molecular weight of the solution from the constant slope. The z-average molecular weights for the species in the other solutions have been determined similarly. By not using the slope

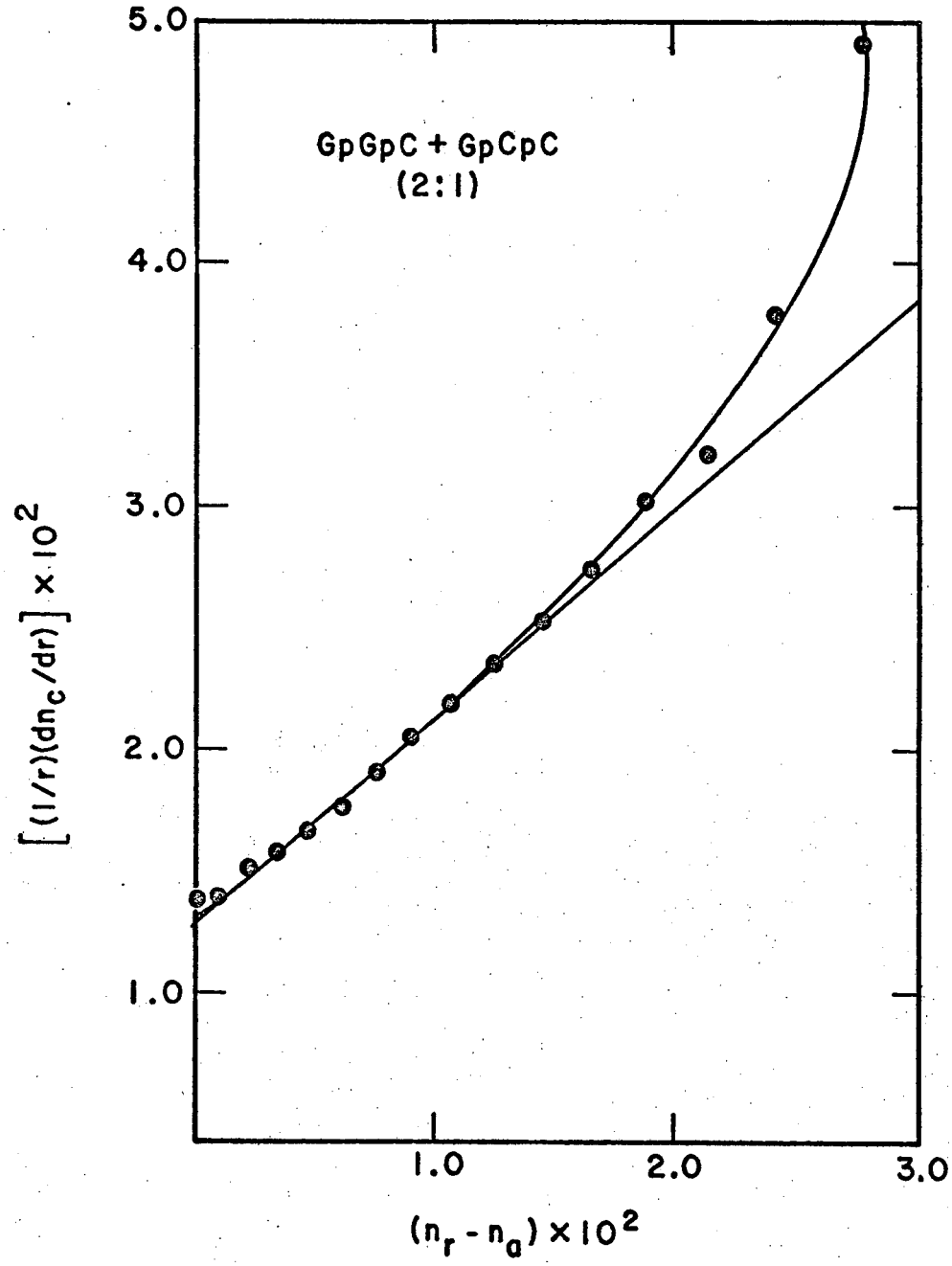

Figure 50. Equilibrium sedimentation of 2:1 mixture of GpGpC and GpCpC, 0.01 M $MgCl_2$, 0.1 ionic strength sodium phosphate buffer, pH 7.0, 2°C, 0.85 x 10^{-2} M mononucleosides. A z-average molecular weight, 16,700, was calculated from Eq. (14) and the slope of the line drawn tangent to the curve.

Table 5

Molecular Weights[a] by Sedimentation Equilibrium.

	Sum of Atomic Weights	0.5 M NaCl			0.01 M $MgCl_2$		
		0.2 Ionic Strength Phosphate Buffer, pH 7.0			0.1 Ionic Strength Phosphate Buffer, pH 7.0		
		Bulk Residue Concentration	M_z	M_w	Bulk Residue Concentration	M_z	M_w
GpCpC	891	0.96×10^{-2} M	2,400	1,200	-	-	-
GpGpC	931	1.27×10^{-2} M	14,200	10,200	0.93×10^{-2} M	40,000	15,000
GpGpC+GpCpC(2:1)	2753	1.09×10^{-2} M	9,500	6,500	0.85×10^{-2} M	16,700	8,700

a. The estimated uncertainty is ±5%.

of the line connecting the points for the bottom of the cell and the meniscus we are probably underestimating the z-average molecular weight.

The z-average and weight-average molecular weights of unaggregated GpCpC should be 891. For the pure GpCpC solution, they are close to this. Some aggregation does occur, however. Neither the absorption spectrum nor the ORD showed any evidence of aggregation. Thus, the aggregation is probably nonspecific.

Solutions of GpGpC in the two buffers are optically quite similar. Magnesium ions more effectively stabilize the aggregation, however, as seen by the higher molecular weights in the $MgCl_2$ buffer. The z-average molecular weight is 40,000 for the $MgCl_2$ buffer and 14,200 for the NaCl buffer. The molecular weight of the trimer is 931, so there are aggregates of more than 40 trimers in the solution containing magnesium ions.

The molecular weights of the aggregates in the solutions containing 2:1 mixtures of GpGpC and GpCpC are less than those for the pure GpGpC solutions. They are greater than 2750, however, which is the molecular weight of a complex containing 2 molecules of GpGpC and 1 molecule of GpCpC. This is not surprising since the continuous variation experiments indicated that the fraction of trimers in the 2:1 complex is less than 1. The species present in these solutions include a 2:1 complex between GpGpC and GpCpC, GpGpC

aggregate, and GpCpC aggregate. The molecular weight of the mixture is the average of these different species.

From the known weight-average molecular weight of GpCpC, GpGpC, and the mixture of all three species, we can calculate the molecular weight of the 2:1 complex. We shall use the weight-average molecular weights in Table 5. The weight-average molecular weight of GpCpC was only determined for the NaCl buffer. There is no optical evidence for more aggregation in the $MgCl_2$, so we shall assume the same weight-average molecular weight for this buffer.

The weight fraction, $W_f(A)$, of a particular species, A, can be calculated from the mole fraction, f(A), of trimer in that species.

$$W_f(A) = f(A) \frac{M_A}{M}$$

The molecular weight of A per trimer is M_A, and the average molecular weight of a trimer in the solution is M. The molecular weight of the average trimer in solution and in the 2:1 complex is 918. The fraction of molecules in the 2:1 complex was estimated from the continuous variation experiment to be 0.75. The weight fractions of the 2:1 complex, GpGpC and GpCpC are 0.75, 0.17, and 0.08, respectively.

The molecular weight of the 2:1 complex has been calculated with these values of the weight fractions for both buffers. The results are shown in Table 6. From these

molecular weights and the molecular weight of the average trimer in the 2:1 complex, 918, we can calculate the number of trimers in the complex. These numbers are also given in Table 6. There are more than three trimers per complex in either buffer. The numbers are not a multiple of three, however. Therefore, the complex is not a discrete entity.

The calculations have also been done for other values of f. For the N-Cl buffer, the number of trimers in the complex varies from 5.4 to 7.1 for f between 0.33 and 0.95. For the $MgCl_2$ buffer, the number of trimers in the complex varies from 5.6 to 9.4 for the same range of f. This range of f is greater than the uncertainty in the determination of f. Thus, there does not seem to be any doubt that the complex contains more than two molecules of GpGpC and one molecule of GpCpC.

The number of trimers in the complex as calculated above is acually a lower limit. The weight-average molecular weight of the GpGpC aggregate will be lower in the mixture than in the pure GpGpC solution because of the dilution of molecules capable of aggregating. We have calculated the molecular weight of the 2:1 complex taking this dilution into account through the use of an approximate equilibrium constant for the self-aggregation of GpGpC. The determination of the equilibrium constant will be described in the Discussion. As expected, the molecular weight of the complex is greater than when the dilution is not considered. The results are given in Table 6.

Table 6

Molecular Weight of the Complex 2GpGpC:1GpCpC

Fraction of oligomers in complex (f)	0.5 M NaCl, 0.1 M $PO_4^{\equiv}$ pH 7.0		0.01 M $MgCl_2$, 0.05 M $PO_4^{\equiv}$ pH 7.0	
	Molecular Weight of Complex	n (number of trimers in complex)	Molecular Weight of Complex	n (number of trimers in complex)
3/4	6200	6.8	8100	8.8
3/4[a]	7100	7.7	--	--
0.33-0.95	500-6500	5.4-7.1	5100-8700	5.6-9.4

a. Taking dilution of GpGpC into account (see text).

c. Temperature Dependence

The extent of aggregation in solutions of GpGpC decreases with increasing temperature. The ORD of GpGpC corresponds to that found in dilute solutions only above 40°C. The rotation of GpGpC in the NaCl buffer is plotted in Figure 51 as a function of temperature for 250, 275, and 292 mμ.

In contrast to these results, the ORD of GpCpC is insensitive to changes in temperature. Molar rotation at 275, 292, and 265 mμ is plotted in Figure 52 as a function of temperature. The curvature at low temperatures may reflect the small amount of aggregation that was observed in the sedimentation equilibrium experiments.

The molar rotation at 275 mμ of the 2:1 complex in the NaCl buffer is shown in Figure 53 as a function of temperature. Also shown is the temperature dependence of the appropriate average of the molar rotation of GpGpC and GpCpC measured separately in the same buffer. The complex is completely "melted-out" above 40°C. Similar curves are obtained at 270 mμ. There is no evidence of a biphasic transition in the 2:1 mixture of GpGpC and GpCpC at either 275 or 270 mμ. Taking 0.75 as a fraction of complex formation and assuming the rotation of the 100% complex is independent of temperature, the T_m of the complex determined from Figure 53 is 13°C.

The temperature-induced disassociation of the 2:1 complex appears to be more biphasic in the $MgCl_2$ buffer. The molar rotation of a 2:1 mixture at 292 mμ and 275 mμ is shown in Figure 54 as a function of temperature. The sedimentation

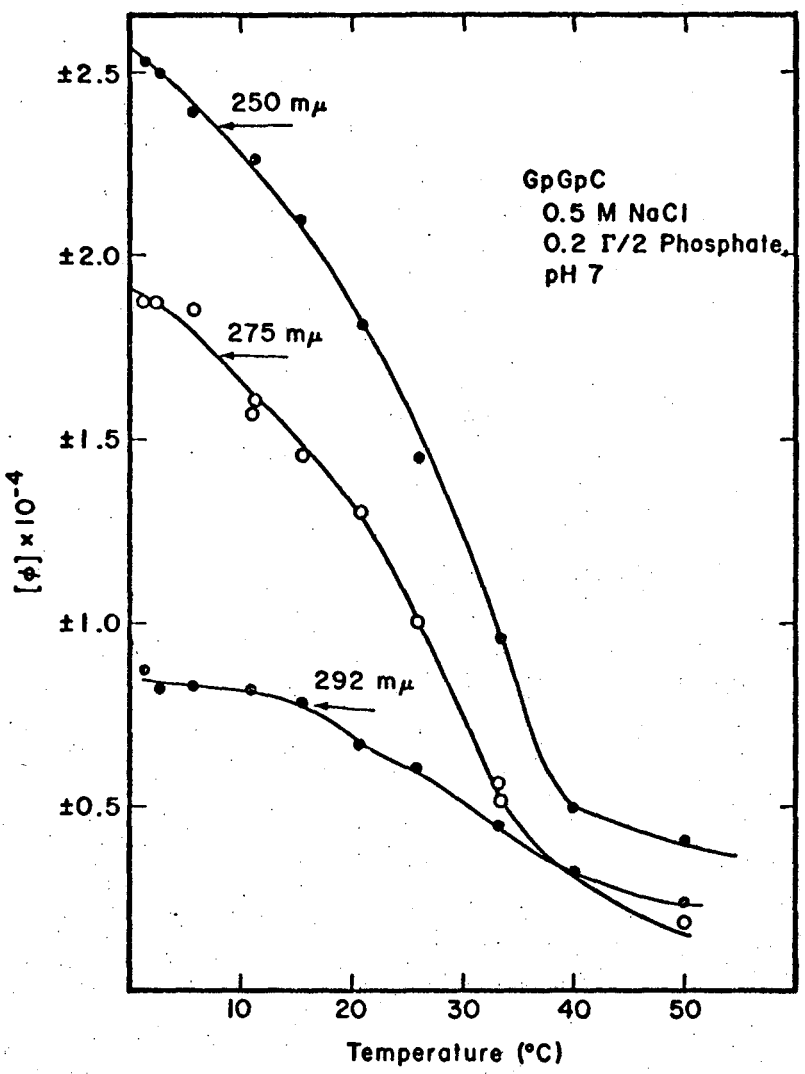

Figure 51. Molar rotation of GpGpC at 250, 275, and 292 mμ as a function of temperature.

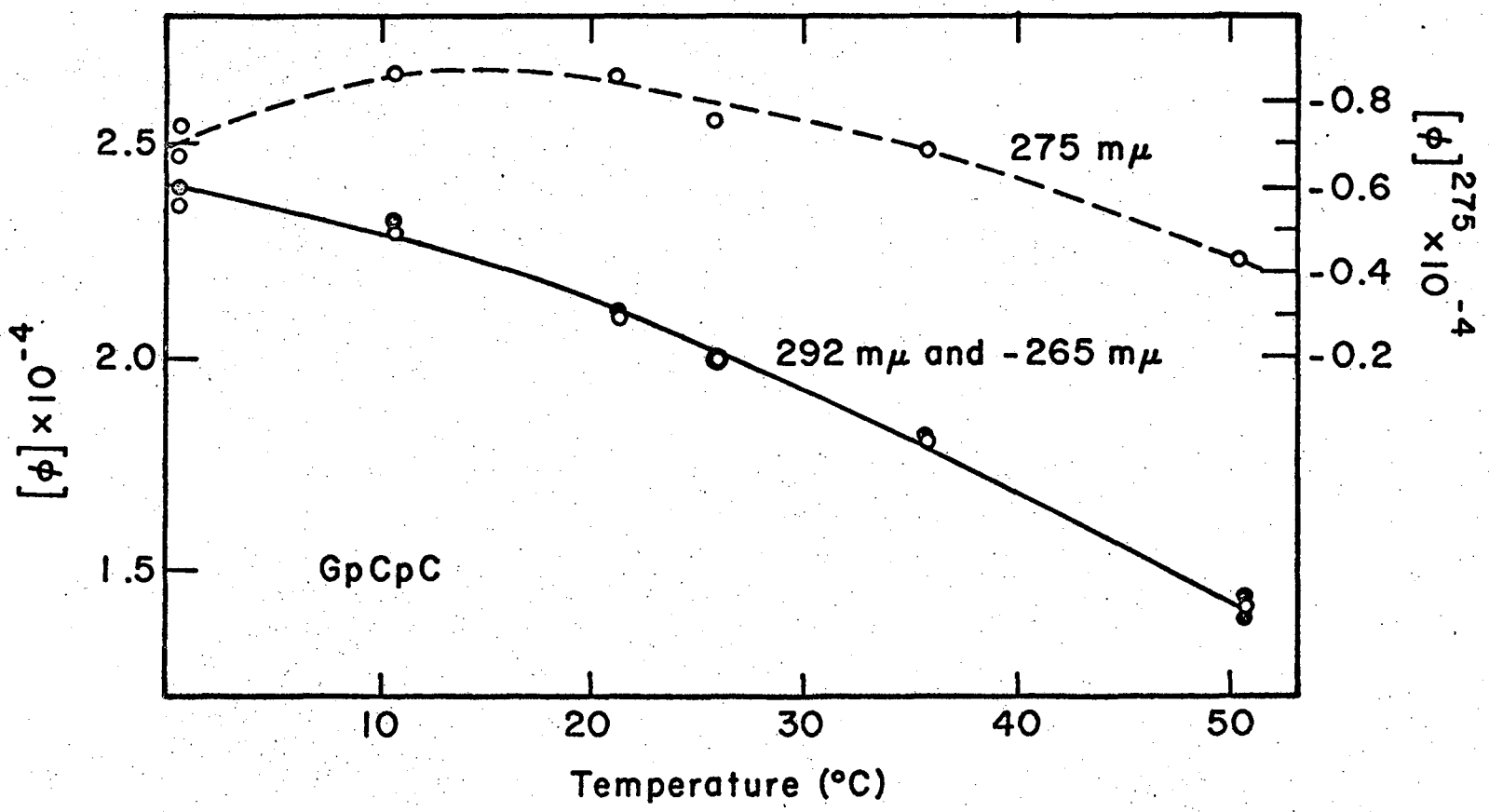

Figure 52. Molar rotation of GpCpC, 1.04 x 10^{-2} M mononucleosides, at 265, 275, and 292 mμ as a function of temperature, 0.5 M NaCl, 0.2 ionic strength sodium phosphate buffer, pH 7.0.

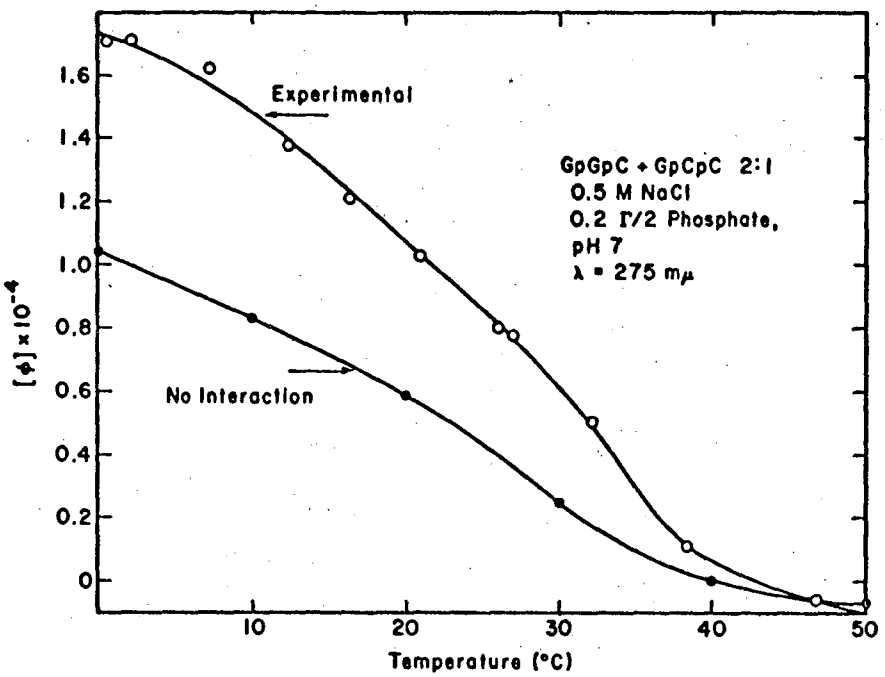

Figure 53. Molar rotation of 2:1 mixture of GpGpC and GpCpC, 1.14 x 10^{-2} M, at 275 mμ as function of temperature and (2:1) average molar rotation at 275 mμ of GpGpC and GpCpC measured separately as a function of temperature under the same conditions.

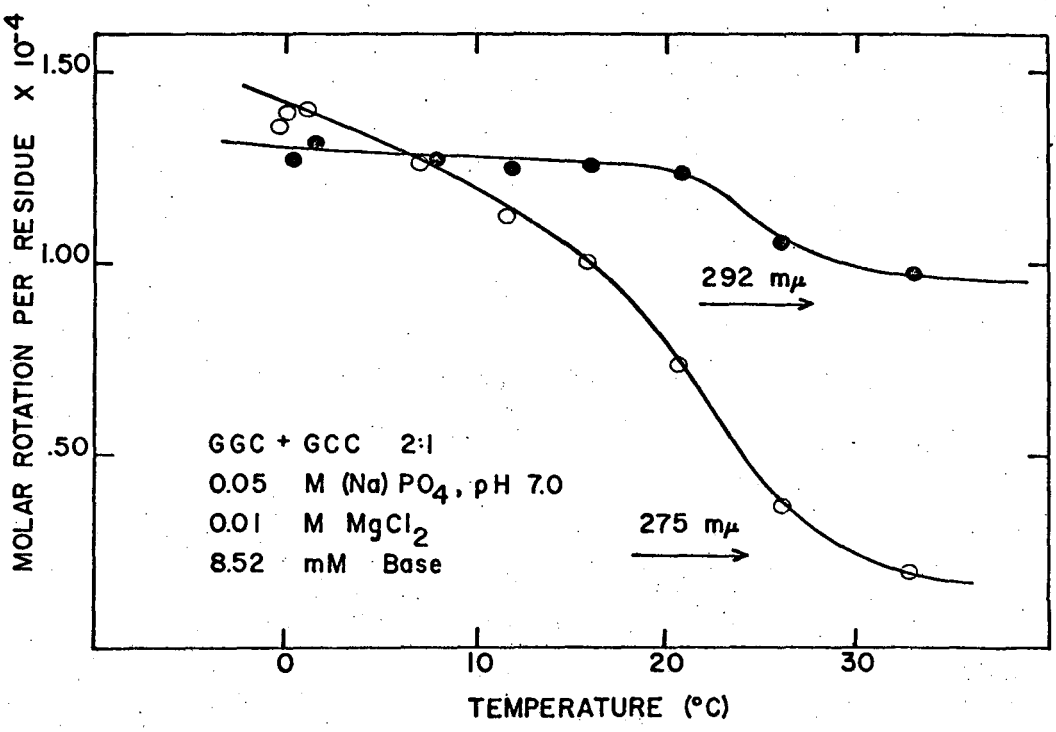

Figure 54. Molar rotation of 2:1 mixture of GpGpC and GpCpC, 8.2 x 10^{-3} M mononucleosides, at 275 and 292 mμ as a function of temperature.

equilibrium experiments indicated that the molecular weight of the 2:1 complex is greater in the $MgCl_2$ buffer. The T_m of the complex also seems to be higher in this buffer than in the NaCl buffer.

d. pH Dependence

The rotation of GpGpC, GpCpC, and the 2:1 mixture in the NaCl buffer at 1°C have been followed as a function of pH between 5.8 and 8.0. The results for GpCpC and the 2:1 mixture are shown in Figures 55 and 56. For all three, no change occurs between 7.0 and 8.0. Below 7.0, the rotation of the 2:1 mixture at 275 and 270 mμ decreases. The ORD curves of GpGpC and especially GpCpC are sensitive to pH changes in this region. The change in the calculated ORD for no interaction, also shown in Figure 56, partially parallels the changes for the 2:1 complex. However, the fraction of trimers in the complex decreases from 0.75 at pH 7.0 to 0.31 at pH 5.8.

The cytosine residues are probably titrating in this pH region. The pK_a of Cp is 4.2.[115] This pK_a is shifted up to 5.7 in poly C because of the stable double-strand helix that forms when one-half the residues are protonated.[112] A similar phenomenon might occur for GpCpC. However, there is no indication that a complex is formed between pH 5.8 and 8.0. The fraction of Cp protonated at pH 5.8 is only 5%. The fraction protonated in GpCpC solutions appears to be greater. The pK_a of C in GpCpC is apparently intermediate between that for Cp and poly C. The important observation

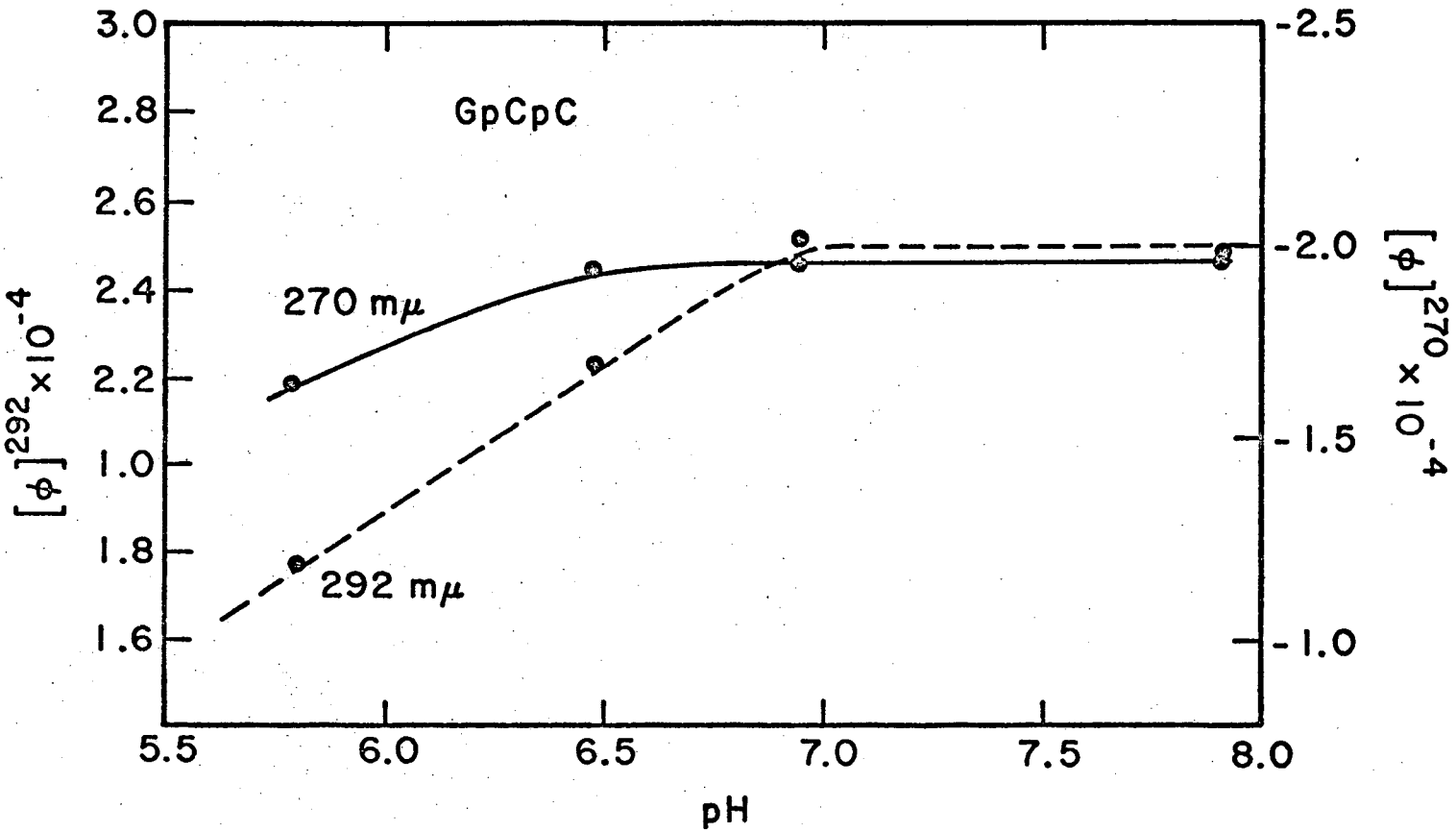

Figure 55. Molar rotation of GpCpC, 1.03 x 10^{-2} M mononucleosides, 1°C, at 270 and 292 mμ as a function of pH.

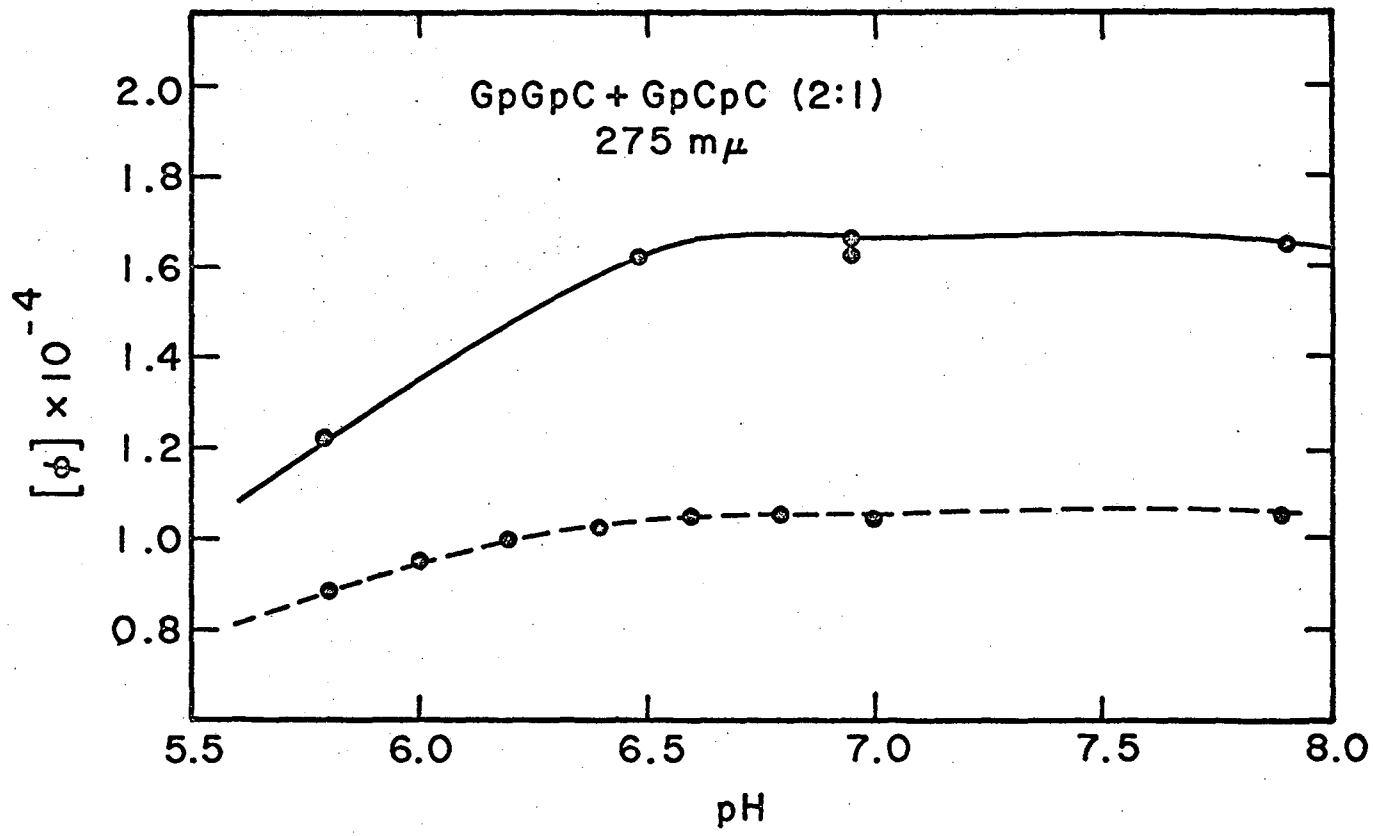

Figure 56. Molar rotation of 2:1 mixture of GpGpC and GpCpC, (——), 1.08 x 10^{-2} M mononucleosides, 1°C, 0.5 M NaCl, 0.2 ionic strength sodium phosphate buffer, at 275 mμ as a function of pH and the (2:1) average molar rotation at 275 mμ of GpGpC and GpCpC measured separately, (---), as a function of pH under the same conditions.

from the pH studies is that the 2:1 complex is destabilized by decreasing the pH.

e. Ionic Strength Dependence

The ORD of a 2:1 mixture of GpGpC and GpCpC has been measured at 1°C in a buffer that contains only a 0.1 M phosphate buffer, pH 7.0, and no additional salt. As measured by the magnitude of the rotation at the peak, the aggregation of GpGpC is less in this buffer than in a solution containing 0.5 M NaCl or 0.01 M $MgCl_2$. The fraction of trimers in the GpGpC:GpCpC complex is also less than for a solution that contains salt. However, the position of the peaks, troughs, and crossover in the ORD curve is the same. Thus, we infer that the 2:1 complex is present at this lower ionic strength, but the fraction of oligomer in the complex is less.

f. Effect of Substituting GpGpCp for GpGpC

The presence of a 3' phosphate on GpGpC decreases the fraction of trimers in the 2:1 complex to less than one-half of what it is with the dephosphorylated compound. The ORD of a 2:1 mixture of GpGpCp and GpCpC is compared in Figure 57 with the calculated curve for no interaction. The shoulder at 275 mμ for the mixture implies that some complex is present. The fraction of trimers in the complex is 30% if the same rotation for the 100% complex applies here. The complex might contain a 1:1 ratio of GpGpCp to GpCpC, however.

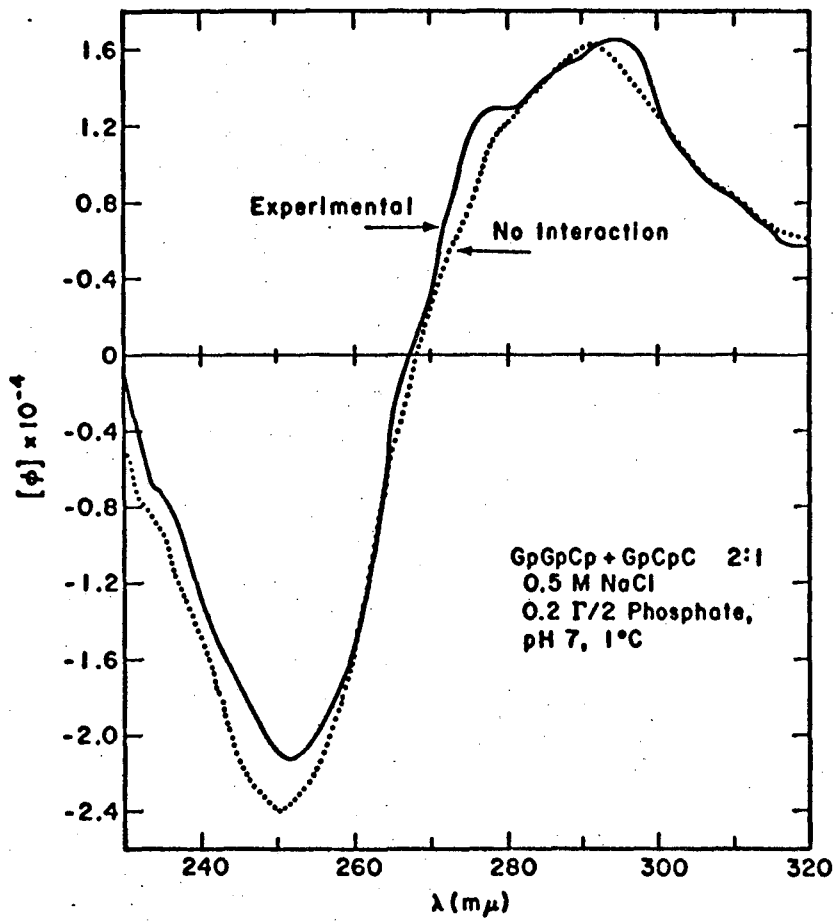

Figure 57. ORD of 2:1 mixture of GpGpCp and GpCpC.

—— Experiment, 0.5 M NaCl, 0.2 ionic strength sodium phosphate buffer, pH 7.0, 1°C, 7.5 x 10^{-3} M mononucleosides.

• • • Average of ORDs of GpGpCp and GpCpC measured separately under the same conditions.

Unfortunately the difference between the two curves at any wavelengths in Figure 57 is too small to be useful in a mixing experiment.

The rotation of GpGpCp is slightly less than GpGpC. An ORD curve for GpGpCp in the NaCl buffer is included on Figure 43 (page 163). The mononucleoside concentration of the GpGpCp solution is less than the more concentrated GpGpC solution whose ORD is shown in the figure. The ORD of GpGpC for the conditions shown, however, is essentially invariant down to the nucleoside concentration used in the GpGpCp solution. The magnitude of the rotation of GpGpC in the absence of added salt is still smaller than for GpGpCp in the presence of 0.5 M NaCl.

g. ORD of the 2:1 Complex

We might examine the ORD of the 2:1 complex between GpGpC and GpCpC to see if it could reveal the nature of the aggregation. If 75% of the trimers are in the 2:1 complex than the measured rotation $[\phi]_M$ is:

$$[\phi]_M = 3/4\ [\phi]_C + 1/4\ [\phi] \qquad (15)$$

The molar rotation of the complex is $[\phi]_C$ and the rotation of the trimers not in the complex is $[\phi]$. The rotation of the 2:1 mixture calculated for no interaction will be equivalent to $[\phi]$. As in Part I, let us say the rotation of the complex is the sum of the rotation of the single strands, $[\phi]_S$, and a perturbation, P.

The rotation of the single strands is the average ORD of dilute solutions of GpGpC and GpCpC. Solving the original equation for the perturbation we have:

$$P = 4/3\ [\phi]_M - 1/3\ [\phi] - [\phi]_S \qquad (17)$$

The perturbation calculated from the ORD of the various substances at 2°C is plotted in Figure 58 along with the change in the ORD when poly G and poly C form a 1:1 complex.[36] The two curves are qualitatively similar. This indicates there are G-C base pairs stacked on top of each other in the 2:1 complex as in the poly G:poly C structure.

Discussion

Several pairs of antiparallel complementary oligomers have been mixed under conditions favorable for intermolecular association. Interaction between GpGpC and GpCpC has been observed at pH 7 in the presence of 0.5 M NaCl or 0.01 M $MgCl_2$ between 1°C and 50°C. The total concentration of residues was 0.01 M. Other pairs of complementary oligomers were mixed under similar conditions but no interaction was observed. These included ApCpU and ApGpU, ApGpC and GpCpU, and ApApApA and UpUpUpU. Self-aggregation has been observed with GpGpC and ApGpC.

We shall first discuss the nature of the complexes that have been observed. Then we shall consider what the results reveal about the structure of tRNA and the specificity of the interaction of tRNA with the mRNA-ribosome complex.

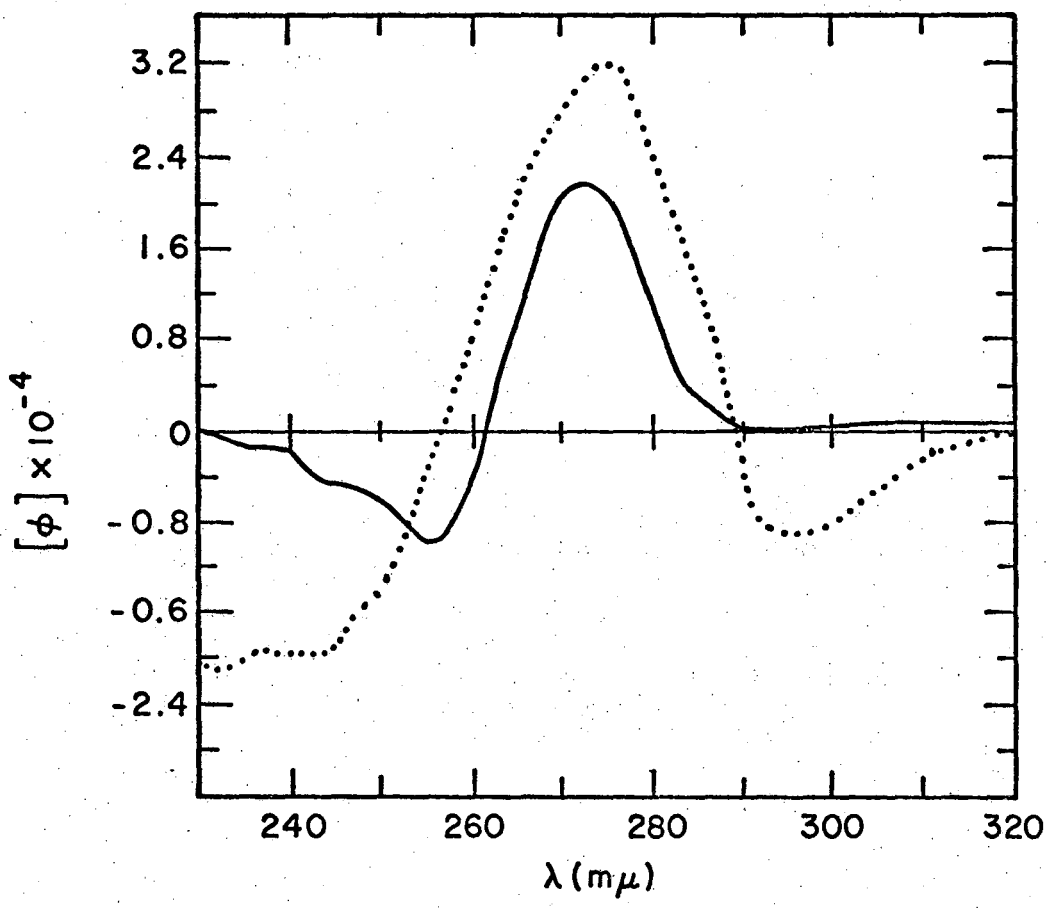

Figure 58.

—— Perturbation of association of GpGpC and GpCpC into a 2:1 complex on the ORD of the unaggregated trimers.

··· Change of ORD upon formation of a 1:1 helix by poly C and poly G (see Reference 36).

1. The Complex of GpGpC and GpCpC

The structure of the complex between GpGpC and GpCpC is not known. The following experimental observations should be kept in mind in considering possible structures: (1) The ratio of GpGpC to GpCpC in the complex is approximately 2:1. (2) There are more than three trimers per complex. (3) The complex becomes less stable in the absence of salt, at pH's less than 7, and if GpGpC carries a 3'-terminal phosphate.

The nature of the complex may be similar to the 2-G:1-C[72,106,156] aggregate that forms between G oligomers and poly C. In which case, the complex might consist of GpGpC and GpCpC hydrogen-bonded to each other as they are in the RNA double-strand helix.[94,95] The second GpGpC molecule could be parallel to the first GpGpC molecule and bonded to it by hydrogen bonds between the guanine bases. This possible 2:1 complex is shown as Structure I in Figure 59.

There would be two G_2:C base triplets of the type proposed by Lipsett[156] for the 2:1 complex of G oligomers and poly C. It is not obvious how the C residue of the second GpGpC molecule would fit into such a complex. Of course, it may be excess baggage. The observation there are more than three trimers per complex can be understood if the triple strand complexes aggregate end-to-end. This is reasonable since they have large hydrophobic areas on either end.

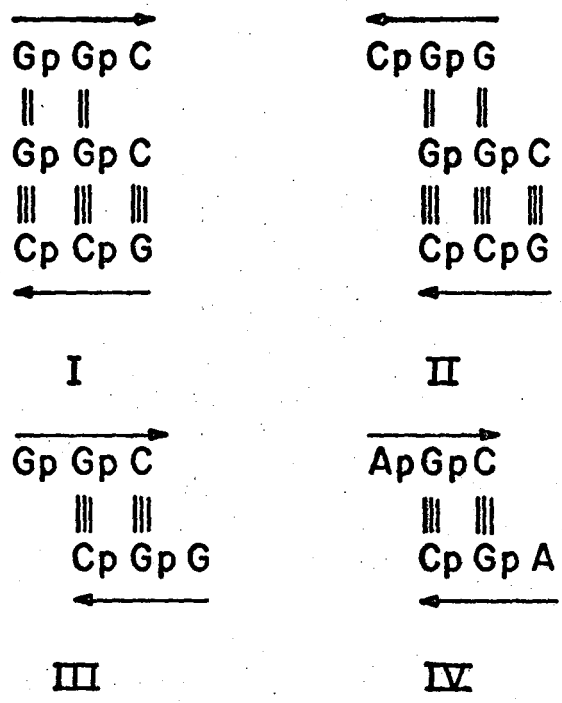

Figure 59. Possible base-pairing pattern in: I and II, 2:1 complex of GpGpC and GpCpC; III, GpGpC aggregate; IV, ApGpC aggregate.

A second possible structure would have the second GpGpC molecule anti-parallel to the first GpGpC molecule. The G-G base pairs could bond these trimers together. This base pairing arrangement is shown in Figure 59 as Structure II. It could also aggregate end-to-end.

All of the experimental observations can be explained by the structures that have just been outlined. There are probably other structures that are consistent with the experiments, however.

In particular, the conformation about the glycosidic bonds for all of the residues in the above structures is anti. This is the conformation in most crystal structures. The conformation is syn for deoxyguanosine in a crystalline complex with 5-bromodeoxycytidine,[163] however. There are other examples where the conformation is syn.[164,165] Recent calculations by Haschemeyer and Rich[164] and by Davis and Tinoco[60] indicate there may only be a small energy difference between the syn and anti-conformations of guanosine. Therefore, structures of the complex might be considered in which all or some of the G residues have a syn conformation.

2. The GpGpC Aggregate

The nature of the self-association product of GpGpC is quite obscure. Oligomers[157] and polymers[106] rich in G residues are known to readily aggregate. Poly G forms multistranded complexes that can only be disassociated with the most extreme conditions.[106] Guanylic acid forms gels at sufficiently high concentration. X-ray studies[166,167]

of these gels indicate that the 5'-nucleotide forms a super helix with 3.75 bases per helix turn. The 3'-nucleotides form stacks of planar structures.[167] Each layer contains 4 guanylic acid residues hydrogen-bonded to each other.

The GpGpC aggregate probably involves some vertical stacking as well as intermolecular hydrogen bonding. If the aggregate is only vertical stacks of trimer molecules we might expect them to have the same conformation as they would in a single-strand polynucleotide of alternating triplet sequence. We have calculated the ORD of the infinite polymer $(GpGpCp)_n$ from the experimental ORD of GpGpC at 1°C in dilute nucleoside solutions and the ORD of CpG at 1°C. This is a possible model for the structure of the end-to-end aggregate of GpGpC. The result is compared in Figure 60 with the experimental ORD of the GpGpC aggregate. The peak and trough of the calculated curve occur about 20 mμ to the red of those for the aggregate. In general, we can say that the ORD of the GpGpC aggregate does not resemble at all what would be expected if the aggregate were only vertical stacks of GpGpC molecules.

It is more likely that the aggregate involves some hydrogen bonds between G residues and between G and C residues. The ORD of poly (G:C)[130] and the ORD of poly G[104] are also shown in Figure 60. Poly G is aggregated under the conditions used for the measurement.[106] Either of these curves is qualitatively a better approximation of the ORD of GpGpC

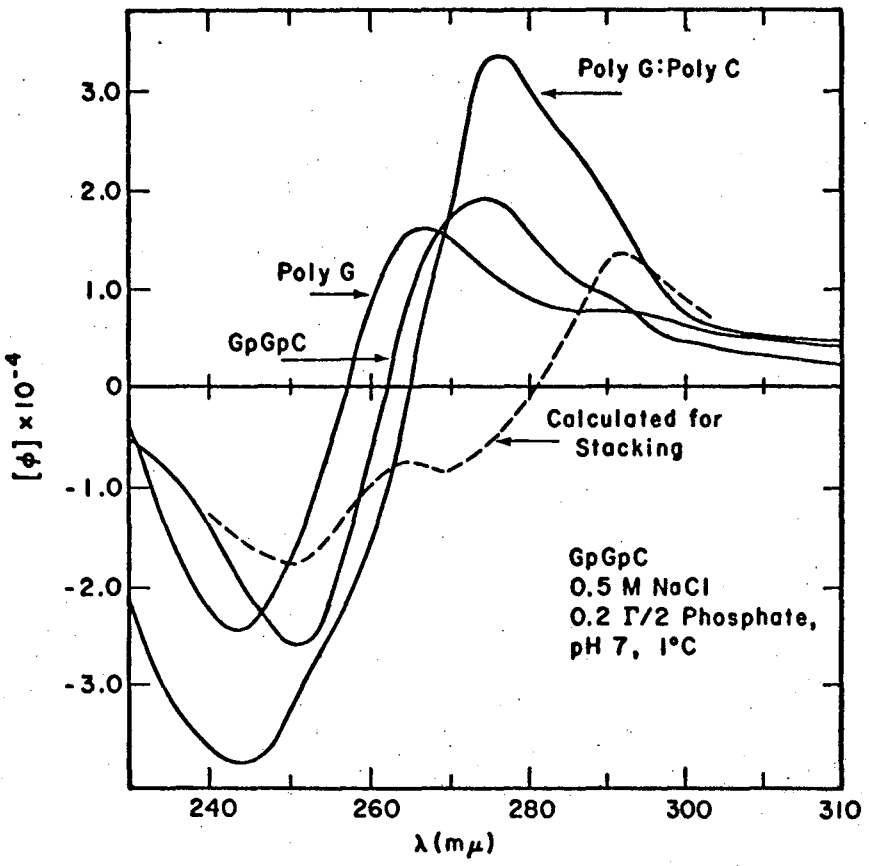

Figure 60. ORD of GpGpC, 1.0 x 10^{-2} M mononucleosides, poly G (Reference 104), Poly (G:C) (Reference 130), and nearest-neighbor calculated ORD of poly (GpGpCp).

aggregate than the ORD of single-strand stacks. Thus, we feel the aggregation in concentrated solutions of GpGpC involves hydrogen-bonded base pairs.

A possible hydrogen-bonding scheme for the GpGpC aggregate is Structure III in Figure 59. The two GpGpC molecules are anti-parallel and translated one residue so that two Watson-Crick G-C base pairs can form. A similar structure can be envisioned for the ApGpC aggregate. This is Structure IV in Figure 59. End-to-end aggregation of these structures might be stabilized by G-G and A-A base pairs. Additional stacking interactions would also aid end-to-end aggregation.

A structure like III or IV in Figure 59 can be drawn for any trimer containing the sequence (GpC) or (CpG). We did not observe any aggregation for GpCpU and only a small amount for GpCpC, however. The additional stacking interaction may not be great enough for these trimers, or the non-Watson-Crick base pairs may not be able to form.

The aggregation of GpGpC may be envisioned to occur by the following steps:

$$M_1 + M_1 \overset{k_2}{\rightleftharpoons} M_2$$

$$M_2 + M_1 \overset{k_3}{\rightleftharpoons} M_3 \qquad (18)$$

$$M_1 + M_{n-1} \overset{k_n}{\rightleftharpoons} M_n$$

For the purpose of calculating an overall equilibrium constant K we assume $K_2 = K_n = K$. Furthermore, we assume the aggregation is similar to the polymerization of bifunctional

monomer units. That is, each monomer unit GpGpC has two functional parts capable of reacting with another monomer unit. The fraction of functional parts p that has reacted can be calculated from the weight-average and z-average molecular weights of the heterogeneous solution.[168] For the NaCl buffer p is 0.83 ± 0.01.

Let [M] be the concentration of all species.

$$[M] = [M_1] + [M_2] + [M_3] + \cdots [M_n] + \cdots \qquad (19)$$

An expression for the mole fraction of M_1, X_1, in terms of K can be derived directly from this equation. If there is no limit on the size of the aggregate

$$X_1 = \frac{[M_1]}{[M]} = 1 - K\,[M_1] \qquad (20)$$

In addition we have the following equalities:[168]

$$X_1 = \frac{M_1}{M_0(1-p)} = (1-p) \qquad (21)$$

where M_0 is the initial total concentration of M_1. By appropriate substitution of Eq. (21) into Eq. (20) we have

$$K = \frac{P}{(1-p)^2 M_0}$$

The concentration of GpGpC in the solution for which p is known was 4.2×10^{-3} M. Therefore, the equilibrium constant for aggregation of GpGpC in the NaCl buffer is 6.8×10^3 $(\text{moles/liter})^{-1}$. This number was used to calculate the weight-average molecular weight of GpGpC in a solution

containing the complex of GpGpC and GpCpC. The molecular weight of the complex that is obtained when this M_w for GpGpC is used is given in Table 6 (page 179).

3. Stability of Codon-Anticodon Complex

The mechanism for the translation of the genetic code is centered on the association of two complementary triplets, the codon and anticodon.[7] Yet the equilibrium constant for the association of two complementary triplets that are divorced from the rest of the translation apparatus is so low that we were unable to observe the complex. It is not clear how large the equilibrium constants must be to account for the translation mechanism. Nevertheless, it seems likely that the equilibrium constant for the interaction of codon and anticodon is greater than for two complementary trimers that are free in solution.

The greater stability of the codon-anticodon complex can be easily rationalized. Part of it is surely the result of unspecific binding of tRNA to the ribosome. There are probably other reasons, however, since the stability of the complex of complementary triplets must be sufficiently great to provide specificity. The environment for the interaction of the two complementary triplets on the ribosome is probably different from what is experienced in solution. The interaction may take place in a pocket on the ribosome similar to the cleft found in the crystal structures of lysozyme.[169] The effective water activity and dielectric

constant may be lower in such a pocket than in the bulk solution. The phosphate charges of the codon and anticodon may be partially neutralized by positively charged amino acid side chains.

Fuller and Hodgson[8] have shown that it is possible to construct models of the anticodon loop in yeast alanine tRNA so that the codon-anticodon complex is part of an almost continuous double-strand helix. This should increase the stability of the complex between codon and anticodon and may be responsible for some of the specificity as well.

4. Stability of Loops in tRNA

Specific 1:1 complexes of complementary trimers are not stable under the conditions we have employed. It is of interest to see whether they could still stabilize loops in tRNA. Let us assume that a 1:1 complex of three G-C base pairs is as stable as the 2:1 complex of GpGpC and GpCpC. Similarly, we assume a 1:1 complex of 3 A-U base pairs is as stable as the 2:1 complex between ApApA and UpUpU as found by Miles et al.[160] Clearly these are upper limits for the stability of the actual 1:1 complexes. We want to calculate what fraction of loops would be closed by complexes with these stabilities if the complementary oligomers were tied together with a polynucleotide chain.

One effect of the chain will be to increase the effective concentration of the complementary oligomers. This is equivalent to saying there will be less translational entropy

loss for loop closure than for association of oligomers that are not connected with a polynucleotide chain. If this is the main effect then the fraction of oligomers complexed will be greater when they are connected with a chain. However, there will also be enthalpy effects that will tend to decrease the fraction of oligomers complexed. For shorter chains, loop closure probably results in the unstacking of some of the bases in the loop. Loops in the clover-leaf models for the tRNAs whose sequence is known contain many uridine residues.[16,20-22] This base does not stack as well as the other.[43,44] Therefore, we shall assume, for the time being, that enthalpy effects are small by comparison to the entropy effects. For this approximation, the equilibrium constant for loop closure by two complementary oligomers is directly proportional to the equilibrium constant for association of the same oligomers unconnected by the chain. The proportionality constant is the ratio of the probability of finding the oligomers near each other in the two cases.[171]

Jacobson and Stockmayer[170] have derived an equation for calculating this ratio which is designated j. If the end-to-end distance of the loop has a Gaussian distribution as a function of chain length and the contour length is long compared to the mean end-to-end distance then they find

$$j = \left(\frac{3}{2\pi m b^2}\right)^{3/2} \qquad (22)$$

where n is the number of units of length b in the loop. In the absence of information to the contrary we shall assume that j can be calculated with this equation for chain lengths of 10 or greater. Therefore, the fraction of oligomers bound in the loop, f_1, can be related to the fraction, f_2, bound in solution by the following equation:

$$\frac{f_1}{1-f_1} = \frac{548}{n^{3/2}b^3} \frac{f_2}{(1-f_2)^2 m} \qquad (23)$$

where m is the initial concentration of each oligomer (moles of oligomer/liter) which leads to a fraction f_2 bound in solution. The unit length b is measured in angstroms.

For a solution of GpGpC and GpCpC with a concentration of 0.003 M trimer/liter the fraction of trimers in the 2:1 complex is 75% at 1°C and 9% at 37°C. At a 10 fold higher concentration of oligomers Miles et al.[160] found that the fraction of ApApA and UpUpU in a U_2:A complex is also 75% at 1°C. In analogy with the results for GpGpC and GpCpC of ApApA and UpUpU we shall assume that the fraction complexed at 37°C is 9%. Now we shall take these fractions as an upper limit of the fraction of oligomers bound in a double-strand complex at the same concentration of oligomer. The fraction of loops closed by double-strand complexes with these hypothetical stabilities has been calculated at 37°C for n equal to 10, 20, and 100. The length of a monomer, 7 Å, has been chosen for b. The results are given in Table 7. They indicate that a loop can only be closed by 3 base pairs

at 37°C if they are all G-C base pairs. More than 3 A-U base pairs are needed to close the loop at this temperature.

These calculations have been for loops closed by double-strand complexes. However, it appears that triple-strand complexes of oligomers are more stable than the double-strand ones. We have been unable to find conditions for a 1:1 complex of GpGpC and GpCpC. Similarly, Pochon and Michelson[106] were unable to find conditions for a 1:1 complex between oligo G and poly C, although Lipsett[156] has succeeded. Aparently Miles et al.[160] have only observed a 2:1 complex between oligo A and oligo U. On the other hand, conditions have been found where the stoichiometry of the complex between poly G and poly C and between poly A and poly U is 1:1.[110] The one other relevant observation here was given in a recent communication of Cassani and Bollum.[172] They have reported the T_m of complexes between poly d(pA) and oligo d(pT) and between poly d(pT) and oligo d(pA) as a function of the chain length of the oligomer. The stoichiometry of the complex between poly d(pT) and oligo d(pA) is 2T:1A for oligomer chain lengths less than 16 and 1T:1A for chain lengths greater than 16. The complex between poly d(pA) and oligo d(pT) was 1:1 for chain lengths of d(pT) greater than seven. It is possible that the shorter oligomers will give a 2T:1A stoichiometry. In summary, what is common to these observations is there is a pronounced tendency for short oligomers to form triple-strand complexes in preference to double-strand ones.

Conversely, longer oligomers are more likely to form double-strand complexes.

Complementary regions in tRNA are probably rather short. Therefore, we should consider the possibility that loops in tRNA are closed by triple-strand complexes even at the expense of short double-strand regions. There are regions in each of the five tRNAs whose sequence is known[16,20-22] that can form triple strands instead of some of the double-strand helical regions that have been proposed. Such triple-strand helical regions may be important in giving tRNA molecules precise three-dimensional structures.

As in the case of double-strand loop closure, we must determine what effect the polynucleotide chain has on the equilibrium constant of the triple-strand complexes. Let f_4 be the fraction of oligomer in the triple-strand complex that forms in a solution of m moles of one oligomer and 2 m moles of its complement. Proceeding as before, we can relate the fraction f_3 of double loop closed by a triple-strand complex to f_4 and m by the following equation:

$$\frac{f_3}{1-f_3} = \frac{7.49 \times 10^{+4}}{(nn')^{3/2}(bb')^3}\left[\frac{f_4}{(1-f_4)^3 m^2}\right] \qquad (24)$$

The number of units in the different loops are designated by n and n'. The lengths of these units are b and b'.

The fraction f_3 has been calculated at 37°C for n = n' = 10, 20, and 100. The results are included in Table 7. The

calculations indicate that double loops can be closed by a triple-strand complex like 2 GpGpC:GpCpC but not by 2 UpUpU:ApApA.

Table 7

Formation of Double and Triple-Strand Loops

No. of monomers in loops (n)	Fraction of loops closed (f_1) for b = 7 Å	
	m = 0.003 M (G-C)	m = 0.03 M (A-U)
	Double Strand	
10	0.65	0.16
20	0.39	0.06
100	0.06	0.01
No. of monomers in each loop (n=n')	Fraction of double loops closed (f_3) for b = b' = 7 Å	
	m = 0.003 M (G-C)	m = 0.03 M (A-U)
	Triple-Strand Loops	
10	0.89	0.08
20	0.51	0.01
100	0.01	0.00

PART III

SYNTHESIS OF POLYRIBONUCLEOTIDES OF ALTERNATING SEQUENCE

Introduction

In the previous section we explored methods of studying the optical and thermodynamic properties of double-strand RNA as a function of sequence and chain length with complexes of complementary oligoribonucleotides. The results indicate that this may not be a very useful method of studying double-strand RNA. A complex was observed to form between GpGpC and GpCpC. However, it is multi-stranded. Other complexes of complementary trimers are so unstable that they could not be studied conveniently. In general, our results with GpGpC and GpCpC and the results of others[106,160,172] indicate that short oligomers are more likely to form multi-stranded complexes than double-strand ones.

The problems of multi-strandedness and instability would probably be eliminated if we could study complexes of longer oligomers. Unfortunately, suitable compounds are not readily available. The preparation of oligomers of known sequence with a chain length greater than three or four is much more difficult.

Another method of studying double-strand RNA is with the polyribonucleotides of repeating sequence that have been synthesized by Khorana and his colleagues.[2] They have prepared several complementary pairs of polymers with repeating dinucleotide, trinucleotide, and tetranucleotide sequences.

Two pertinent examples are poly rAC and poly rUC. These compounds contain alternating A and C residues and alternating U and G residues, respectively.[174]

The origin of these polymers are short polydeoxyribonucleotides that have been chemically synthesized, $d(AC)_{2-6}$ and $d(TG)_{2-6}$.[175] The subscripts refer to different chain lengths. Mixtures of these complementary oligomers serve as templates for the DNA polymerase from Escherichia coli.[176] In the presence of the oligomers and the four triphosphates, TTP, dATP, dGTP, dCTP, the enzyme catalyzes the formation of a high molecular weight DNA-like polymer, polydAC:dTG. This polymer has been characterized as having alternating A and C residues in one chain and alternating G and T residues in the other.[176] Poly rAC and poly rUG are made by RNA polymerase transcription of poly dAC:dTG, one strand at a time.

Khorana and his colleagues[2] have synthesized several complementary pairs of short polydeoxyribonucleotides with repeating di-, tri-, and tetranucleotide sequences. A list of them is given in Table 8. Most of these pairs have been shown to serve as templates for DNA polymerase. Specific 1:1 complexes of the complementary polyribonucleotides made from the DNAs would be an excellent system for studying the sequential properties of double-strand RNA. Complexes of complementary polymers will be more stable than oligomer complexes. Thus, they can be

Table 8

Repeating Dinucleotide Sequences	
$d(AC)_{2-6}$	$d(AG)_5$
$d(TG)_{2-6}$	$d(TC)_5$

Repeating Trinucleotide Sequences		
$d(TTC)_4$	$d(CCT)_{3-5}$	$d(TAC)_{4-6}$
$d(AAG)_4$	$d(GGA)_{3-5}$	$d(TAG)_{4-6}$
$d(TTG)_{4-6}$	$d(CGA)_{3-5}$	$d(ATC)_{3-5}$
$d(CAA)_{4-6}$	$d(CGT)_{3-5}$	$d(ATG)_{3-5}$
		$d(GGA)_{3-5}$
		$d(GGT)_{3-5}$

Repeating Tetranucleotide Sequences		
$d(TTTC)_3$	$d(TATC)_3$	$d(TTAC)_4$
$d(AAAG)_{3-4}$	$d(TAGA)_2$	$d(TAAG)_2$

Taken from Khorana et al.,[2] Wells et al.,[176] and Byrd et al.[177]

studied at nucleotide concentrations where multi-strandedness and random aggregation will not be a problem. By contrast to homopolymers, many of these repeating polymers may not be able to form triple-strand complexes. In any case, it appears that polymers are less likely to form multi-stranded complexes than oligomers.

The ORDs of the complexes will reflect various combinations of the ORDs of the ten base-paired dimers shown in Figure 30. Of course, these complexes would be an excellent system for testing our ability for calculating the optical and thermodynamic properties of double-strand RNA.

With these thoughts in mind, we have collaborated with Dr. Michael Chamberlin in developing a procedure for the preparation of polyribonucleotides of repeating sequence, suitable for optical studies, starting with a seed of the repeating DNA-like polymer. All of the experiments to be described were carried out in Dr. Chamberlin's laboratory. He supplied us with a few optical density units of poly dAC:dTG and poly dAG:dTC and a generous supply of DNA polymerase and RNA polymerase. The conditions and methods that have been employed were his suggestions.

The general scheme for preparing the RNAs from a small amount of DNA is essentially identical to that used by Khorana and his colleagues.[2] The first step is to prepare more of the DNA using DNA polymerase. The second is to use the product as a template for RNA polymerase. The method

is outlined schematically for poly rAC and poly rUG in Figure 61.

We will describe in detail the procedure for preparing these two complementary alternating polyribonucleotides. Preliminary measurements of the ORD of poly rAC, poly rUG, poly dTG, and poly dAC will be reported. The results for poly rUG indicate that it may be aggregated. This is a particularly interesting result in view of the fact that U-G base pairs have been postulated to occur between codon and anticodon and in tRNA.

We have also attempted to prepare poly rAG and poly rUC starting with poly dAG:dTC. However, the seed DNA was contaminated with poly dAT. In the absence of an effective way of separating poly dAT from poly dAG:dTC, the method outlined in Figure 61 cannot be used to prepare the desired polymers.[176]

Replication of Poly dAC:dTG with DNA Polymerase

1. DNA Polymerase Assay

DNA polymerase activity is defined in terms of the amount of a C^{14} label in ATP that is incorporated into acid precipitable poly dAT. The conditions we have used for the assay are similar to those used by others.[176,178] The procedure for recovering the incorporated radioactivity is basically the same as used by Josse and Kornberg[179] for the assay of DNA glucosyltransferase. However, many of the details of both the conditions and the procedure are different.

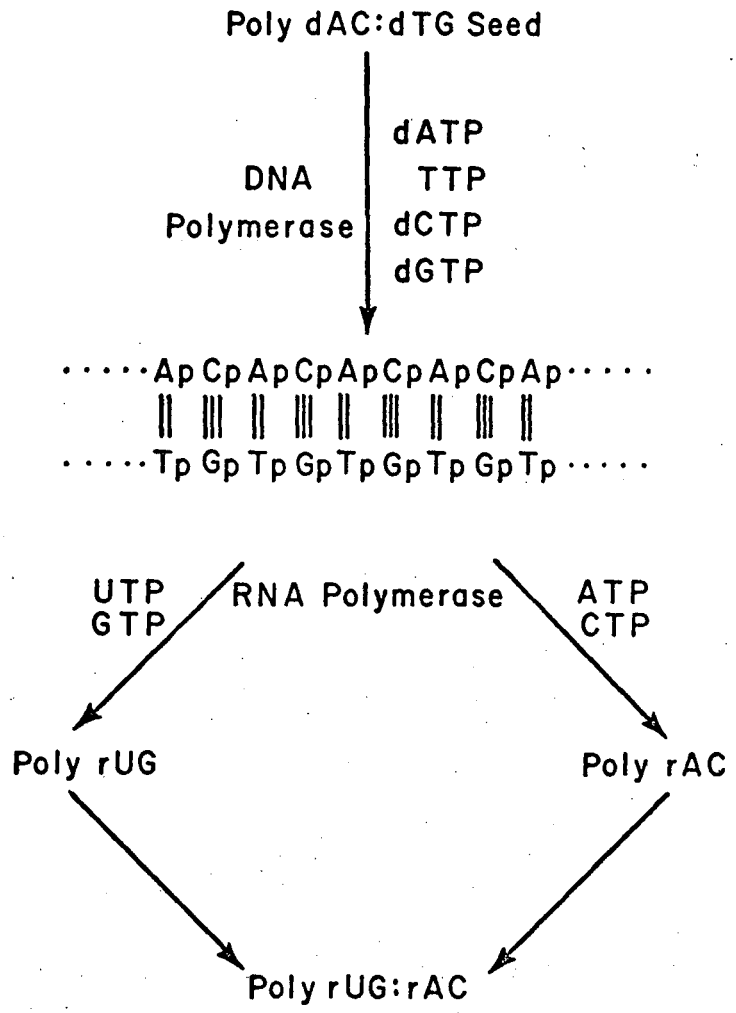

Figure 61. Schematic outline for preparation of poly rUG:rAC from a poly dAC:dTG seed.

Thus, we have included a detailed descriptions of the entire assay procedure.

The assay reaction mixture contained in 0.3 ml: 20 μmoles of potassium phosphate buffer, pH 7.4, 300 mμmoles of 2-mercaptoethanol, 2 μmoles of $MgCl_2$, 10 mμmoles of dATP-C^{14} (2000 cpm/mμmole), 10 mμmoles of TTP, 10 mμmoles of poly dAT and 0.5 to 1.0 unit of DNA polymerase. The mixture was incubated at 37°C for 30 minutes. Synthesis was stopped by plunging that test tube into ice and adding 3 ml of ice cold 3.5% perchloric acid (PCA). After standing for 15 minutes, the solution was filtered on a Whatman GF/C glass filter, 2.4 cm diameter. Both the tube and filter were rinsed with three 3-ml volumes of cold 1 M HCl, 0.1 M pyrophosphate. The filter was dried under an IR lamp and placed in a vial. Ten mls of scintillation fluid were added and the C^{14} radioactivity was counted in a scintillation counter. The scintillation fluid was prepared by mixing in a total volume of two liters, 8 gm of scintillation grade 2,5-diphenyloxazole (PPO), 6.2 gm of scintillation grade 1,4-bis-2-(5-phenyloxazolyl)-benzene (POPOP) and tolune.

2. Conditions for Synthesis of Poly dAC:dTG with DNA Polymerase

Nearly 100 optical density units of poly dAC:dTC were synthesized from a few optical density units of the DNA by using the seed as a template for DNA polymerase in the presence of the four deoxytriphosphates. The reaction

mixture contained in 1 ml: 100 μmoles of potassium phosphate buffer, pH 7.42, 12 μmoles of $MgCl_2$, 1 μmole of 2-mercaptoethanol, 500 mμmoles of each of the four deoxytriphosphates, 0.6 optical density units of poly dAC:dTG and 25 units of Stage VII E. coli DNA polymerase.[178] The primer polydAC:dTG was first heated at 90°C for 10 minutes and then cooled in an ice bath before being added to the synthesis mixture. The synthesis mixture was incubated at 37°C.

The optical density of the solution at 260 mμ is a sensitive measure of the progress of the synthesis.[180] As the synthesis progresses the $O.D._{260}$ decreases because of the hypochromism of the DNA that is synthesized. A small aliquot of the reaction mixture was incubated at 37°C in a 1 mm path length absorption cell that was kept in the thermostated cell compartment of a Zeiss PMQ II spectrophotometer. The reading was usually blanked against an ATP solution that had an $O.D._{260}$ of approximately 1.2. After a period of time, the $O.D._{260}$ levelled off and began to increase. The length of time until this occurred depended on the amount of primer and enzyme that had been used. For the amount of primer indicated above, the progress of three syntheses, with varying amounts of enzyme, is shown in Figure 62. As expected, the $O.D._{260}$ levelled off sooner when greater amounts of enzyme were used. The synthesis using the smallest amount of enzyme in Figure 62 corresponds to the amount that was

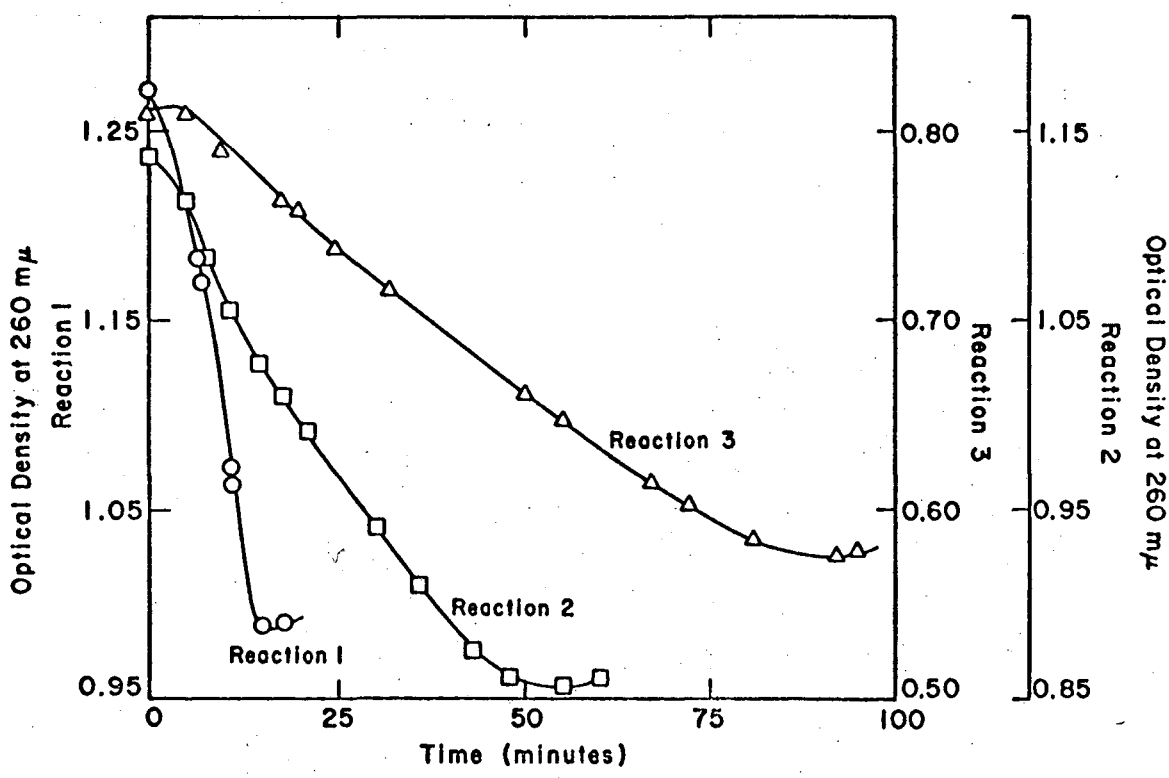

Figure 62. DNA polymerase replication of poly dAC:dTG. See text for concentration of all reactants except enzyme. The concentration of DNA polymerase was as follows: Reaction 1, 340 units/ml; Reaction 2, 56 units/ml; Reaction 3, 22 units/ml.

generally used for large scale syntheses of poly dAC:dTG. As indicated, maximum synthesis was reached in 80-100 minutes. The exact time was variable. Thus, we found it necessary to monitor the progress of every synthesis. As soon as the O.D.^{260} levelled off, the reaction was stopped by adding an equal volume of 0.1 M EDTA, pH 8.

The DNA polymerase was removed from the solution by phenol extraction. We used Mallinckrodt Chromatographic Grade phenol. This reagent contains no preservatives and is 88% phenol, 12% water. The phenol is first neutralized by shaking with 0.1 M phosphate buffer, pH 7. Equal volumes of phenol and the reaction mixture are shaken together at room temperature for 2 minutes in a test tube stoppered with a silicone rubber stopper. The aqueous and phenol layers are separated by centrifugation for 5 minutes at 2000 rpm at room temperature. The lower layer, which is the phenol layer, is removed with a capillary pipet and the extraction is repeated. After removal of the reaction mixture, the second phenol aliquot is extracted with phosphate buffer and the aqueous layer added to the reaction mixture.

After the phenol extraction, excess triphosphates were removed by dialysis. The apparatus described by Englander and Crowe [181] was used for dialysis. Buffer 1 contained 1 M NaCl, 0.01 M Tris-HCl, pH 8, and 10^{-3} M EDTA, pH 8. Buffer 2 contained 0.01 M phosphate buffer, pH 7, and 10^{-4} M EDTA. The reaction mixture was dialyzed against three or four changes of buffer 1, with at least two hours between changes.

It was then dialyzed similarly against three changes of buffer 2. The volume ratio of buffer to reaction mixture was always at least 100. The purpose of the high salt in the first buffer is to aid in the removal of the triphosphates. Apparently the dialysis membrane is negatively charged when in contact with aqueous solutions. If the buffer does not contain a large amount of salt, then it is very difficult to remove the triphosphates.

The yield of poly dAC:dTG per ml of reaction mixture was approximately 4 $O.D._{260}$ units. This included the 0.6 $O.D._{260}$ units of primer. Thus, the synthesis was 7 fold. Large scale syntheses were done with 5 ml reaction mixtures.

3. Characterization of the DNA Polymerase Product

We were naturally interested in assuring ourselves that the product of the DNA polymerase synthesis was actually poly dAC:dTG. From a poly dAC:dTG primer, the enzyme has been shown to synthesize more of the DNA-like polymer accurately.[176] Thus, we were not concerned that the alternating sequence had been replicated faithfully. Rather, we were concerned about possible contamination from poly dAT.

DNA polymerase shows a remarkable propensity for the synthesis for poly dAT. In the absence of any added primer, the enzyme will synthesize this perfectly alternating polymer from dATP and TTP.[180] Under conditions similar to those we used for the replication of poly dAC:dTG, this de novo

synthesis proceeds after a two-hour lag period.[180] Thus, it seems unlikely that any de novo synthesis had taken place during the 90 minute primed synthsis of poly dAC:dTG. However, if our seed of poly dAC:dTG had been contaminated with even a small amount of poly dAT, then we might expect that the enzyme would replicate poly dAT in preference to poly dAC:dTG. The last possibility is that we had contaminated the synthesis in some way with poly dAT. Since DNA polymerase is assayed with poly dAT, nearly all the glassware we used had at one time or another been in contact with this polymer. If contamination occurs during the first stages of our replication of the poly dAC:dTG seed, then successive generations of the product will be primarily poly dAT.

We shall see that the product of the poly dAC:dTG replication does not contain any poly dAT. Nevertheless, our concern for this problem was justified with our experiences with poly dAG:dTC. We shall return to this matter later.

a. Base Composition

The base composition of the product was determined by degrading the DNA to nucleoside 5'-monophosphates by sequential treatment with pancreatic DNase[182] and snake venom phosphodiesterase.[183] The four nucleotides were separated by paper chromatography. The number of moles of each nucleotide was determined spectrophotometrically.

To 3.5 O.D. units of the poly dAC:dTG product in 2.5 ml was added 1.0 ml of 7% ice cold PCA. After standing in ice for 10 minutes, the mixture was centrifuged for 5 minutes at 10,000 RPM. The $O.D._{260}$ of the supernatant was 0.20. The precipitate was washed twice with ice cold water and centrifuged each time. Finally, the precipitate was taken up in 0.15 ml of water and 0.03 ml of 0.10 M Tris-HCl, pH 8.0. The pH of the solution was estimated with pH paper and adjusted to 7.5 with drops of 0.10 M NH_4OH. The solution was incubated for 3 hours at 37°C after adding 0.02 ml of 0.05 M $MgCl_2$ and 0.03 ml of pancreatic DNase (0.5 mg/ml).

After the completion of the DNase digestion, the pH was adjusted to 8.5 with 0.1 M NH_4OH. Approximately 0.01 ml is needed. Then, 20 units of snake venom phosphodiesterase were added and the solution was incubated for another three hours at 37°C. By definition, one unit of snake venom phosphodiesterase is the amount catalyzing the hydrolysis of one μmole of p-nitrophenyl-thymidine-5'-monophosphate per hour at pH 8.9 and 37°C in 0.01 M Tris-HCl buffer.[183]

The 5'-nucleotides were separated from one another by paper chromatography on Schliecher and Scheull 589 Orange Ribbon C paper. The solution was first evaporated to dryness and then taken up in 0.05 ml of water. It was applied to the paper as a strip 2 or 3 cm long with a capillary. The chromatography solvent was prepared by mixing 80 ml of

saturated aqueous ammonium sulfate, 18 ml of 1.0 M sodium acetate and 2 ml of isopropanol. Developing times of 15 hours resolved the four nucleotides nicely. Each spot was cut out and soaked overnight in 2.0 ml of 0.01 M potassium phosphate buffer, pH 7.0. Four blank spots were also cut from the paper chromatogram at an equal distance from the origin as the four nucleotide spots. They were treated in the same way as the nucleotide spots.

The identity of each nucleotide spot was established from the absorption spectrum.[184] The order of the nucleotides, in increasing mobility, was A, G, T, and C. The number of μmoles of each nucleotide was also established spectrophotometrically from the appropriate extinction coefficients at 260 mμ.[184] The results are as follows:

5'-Nucleotide	μmoles
A	0.021
G	0.020
T	0.020
C	0.019

They indicate that the product of the poly dAC:dTG synthesis contained an equimolar mixture of the four residues, as expected.

b. Optical Properties

The absorption spectrum of the poly dAC:dTG product showed a maximum at 258 mμ and a minimum at 236 mμ. Wells et al.[176] found the maximum at 257 mμ and the minimum at 231 mμ. It is not clear why there was a 5 mμ difference in

the position of the minimum. Nevertheless, in every other respect that we tested, our product had similar characteristics to theirs. Thus, we have discounted this observation.

The T_m of the poly dAC:dTG product in a solution containing 0.01 M phosphate buffer, pH 7, 10^{-4} M EDTA, was 70.5°C. The change in the optical density at 260 mμ with temperature is shown in Figure 63. The helix-coil transition occurred over a very narrow temperature range, 1° or less. The absorption increased 26%. Most important, there was no indication of an increase in the absorption at 41°C, which is the temperature at which poly dAT would melt in this solvent.[185] Wells et al.[176] found the T_m of poly dAC:dTG to be 74°C in a buffer that had a slightly higher ionic strength than ours. They also observed that the absorption increased 26%.

c. Strand Separation

Doerfler and Hogness[186] observed two bands when poly dAC:dTG is banded in a CsCl gradient at pH 13. It has also been shown that this DNA is denatured at pH 13.[176] Thus, the two bands are presumably poly dAC and poly dTG. The heavier one is probably poly dTG since this strand is ionized and will bind more cesium ions. We have repeated Doerfler and Hogness's experiment[186] with the product of our poly dAC:dTG primed DNA polymerase synthesis. We also observed two equally intense UV absorbing bands.

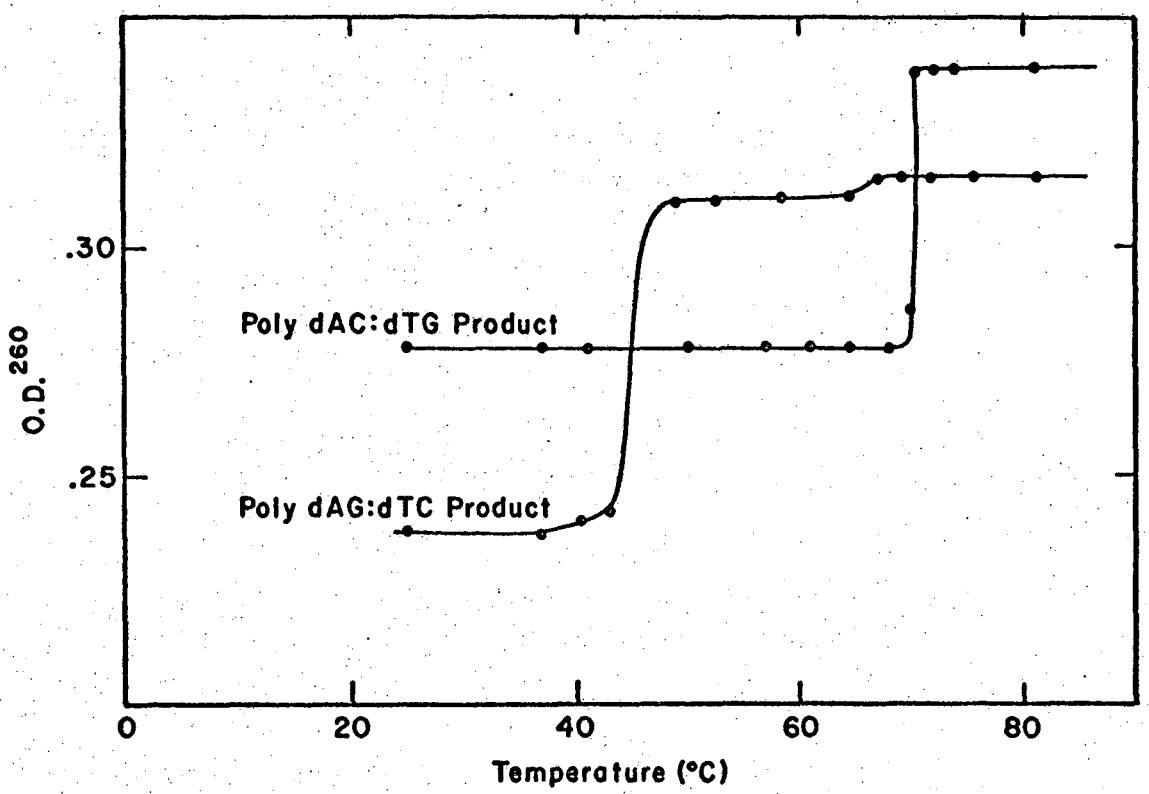

Figure 63. The absorbance at 260 mμ of the poly dAC:dTC and poly dAG:dTC products as a function of temperature. The poly dAC:dTG solution contained 0.01 M sodium phosphate buffer, pH 7. The solution of the poly dAG:dTC contained 0.01 M NaCl and 0.01 M Tris-HCl, pH 8. Both solutions contained 10^{-4} M EDTA.

We have used this phenomenon as a method of separating the two strands. A solution containing 11 O.D. units of poly dAC:dTG was made pH 13 with NaOH. The density was adjusted to 1.71 with CsCl in a total volume of 3.0 ml. The solution was centrifuged in a cellulose acetate tube at 35,000 RPM for three days in a Spinco Model L preparative centrifuge using the swinging bucket rotor No. 39. At the end of that period, the rotor was brought down without the brake, and fractions were collected from a hole that was punched in the bottom of the tube. The O.D. profile of the fractions is shown in Figure 64. There were two bands of UV absorbing material. The heavier band, which came out of the tube first, was tentatively identified as poly dTG. The other was presumably poly dAC.

The fractions containing the two polymers were dialyzed separately against several changes of a 0.01 M phosphate buffer, pH 7. The absorption spectrum of the poly dAC showed a maximum at 261 mμ and a minimum at 232 mμ. By contrast, the spectrum of poly dTG had a maximum at 255 mμ, a shoulder at 270-280 mμ, and a minimum at 230 mμ. These spectra confirm the identity of the two polymers. We expect that compounds containing G and T will exhibit a shoulder around 280 mμ and a maximum to the blue of 260 mμ. We also expect the maximum for a compound containing A and C to be to the red of 260 mμ.

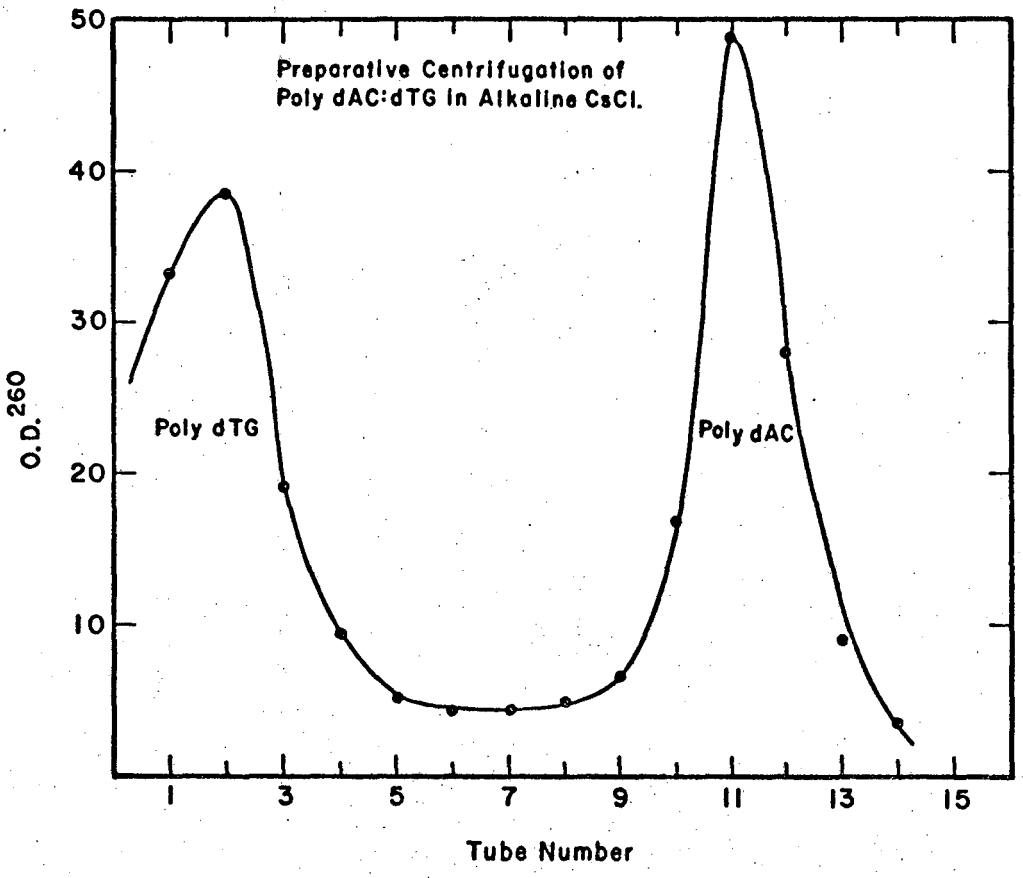

Figure 64. Preparative centrifugation of poly dAC:dTC in alkaline CsCl. The absorbance at 260 mμ of fractions collected from the bottom of the tube is plotted.

Replication of Poly dAG:dTC With DNA Polymerase

By contrast to the results with poly dAC:dTG, all our observations on the replication of poly dAG:dTC with DNA polymerase indicated that the seed sample was contaminated with poly dAT. These two DNA-like polymers must be separated before we can proceed toward the synthesis of poly rAG and poly rUC. In the presence of poly dAT, the enzyme will synthesize mainly poly dAT.

There were several observations that revealed the presence of poly dAT in the seed sample. As seen in Figure 63, the product of the replication of the sample with DNA polymerase had a T_m near 45°C. For the ionic strength of the buffer that was used, this is the temperature at which we expect poly dAT to melt. We expect the T_m of poly dAG:dTC in our buffer to be about 66°C. A small increase in the optical density did occur at that temperature.

In addition, the absorption spectrum of the product had a maximum at 261 mμ, which is closer to the 260 mμ maximum of poly dAT than the 257 mμ maximum of poly dAC:dTG. (No spectrum of poly dAG:dTC has been reported.)

These tests have been confirmed by tests of the incorporation of radioactive nucleotides into the product. The results for C^{14}-AMP are given in Table 9. These experiments were performed in the same way as the assay for DNA polymerase. The concentrations of the various reagents, except where indicated, were the same as for the synthesis of poly dAC:dTG.

Table 9

Reaction No.	mμmoles of C^{14}-AMP Incorporated per ml of Reaction	
	Poly dAC:dTG primer	Poly dAG:dTG primer
1. Complete, all four triphosphates plus enzyme and primer.	3.3	13.0
2. Complete, except twice as much enzyme as for Reaction No. 1.	4.1	17.7
3. Complete, except NO GTP. Same amount of enzyme as for Reaction No. 2.	0.4	16.3

The first two reactions contained all four triphosphates, primer, and enzyme. The second contained twice as much enzyme as the first. For the third reaction, GTP was left out, and the same amount of enzyme was used as for Reaction 2. In the absence of one of the triphosphates there should be much less synthesis. The enzyme does not seem to be capable of synthesizing only one strand.[176] There will be some synthesis, however, because the enzyme will repair the ends of the DNA molecules with the available triphosphates. These expectations were confirmed when poly dAC:dTG was used as the primer. One-tenth as much C^{14}-AMP was incorporated when GTP was left out as when it was included. Similar results were found when we followed a H^3 label in CTP. However, when the poly dAG:dTC seed was used as the primer, there was almost no effect on the incorporation of C^{14}-AMP when GTP was left out.

RNA Polymerase Synthesis of Poly rAC and Poly rUG from Poly dAC:dTG

1. RNA Polymerase Assay

The assay for RNA polymerase that we used was similar to the one described for DNA polymerase. The assay measured the amount of radioactivity in ATP that became incorporated into an acid precipitable polymer.[187] The incubation was generally done in the presence of poly dAT. Other DNAs can be used. However, the specific activity depends on the primer.

We found that 10 poly dAT units equals 1 salmon sperm DNA unit.

It was usually necessary to dilute the stock enzyme solution. The dilutions were done with a solution containing 0.01 M Tris-HCl, pH 8, 0.01 M $MgCl_2$, 0.01 M 2-mercaptoethanol and 5 x 10^{-5} M EDTA. This buffer is referred to later as the RNA polymerase diluting buffer.

The assay mixture contained in 0.25 ml: 10 μmoles of Tris-HCl, pH 8, 1 μmole of $MgCl_2$, 0.25 μmoles of $MnCl_2$, 3 μmoles of 2-mercaptoethanol, 100 mμmoles of ATP-C^{14}, 2000 cpm/mμmole, 100 mμmoles of UTP, 0.1 optical density units of poly dAT and 3 to 5 units of enzyme. The incubation was for 10 minutes at 37°C. The reaction was terminated by plunging the tube into ice and adding 4 ml of ice cold 3.5% PCA. The radioactivity was recovered and counted in a manner identical to that described for the DNA polymerase assay. The solution was filtered. The tube and filter were rinsed with cold 1 M HCl, 0.1 M pyrophosphate. The filter was dried, and the radioactivity was counted in a liquid scintillation counter. One unit of activity is the incorporation of one mμmole of AMP per hour.

2. Optimum Conditions for Synthesis

The conditions used for the synthesis of poly rAC and poly rUG were similar to those used in the assay. There are three variables that we have juggled in an attempt to to find optimum conditions for the synthesis. These are the

amount of primer, poly dAC:dTG, the amount of enzyme, and the length of time of the incubation. Variations in all three are shown in Figure 65. The mμmoles/ml of reaction mixture of C^{14} incorporated into an acid precipitable product are shown as a function of time for three different synthesis conditions for both poly rAC and poly rUG. Each reaction mixture contained in 0.25 ml: 10 μmoles of Tris-HCl, pH 8, 1 μmole of $MgCl_2$, 0.25 μmole of $MnCl_2$, 3 μmoles of 2-mercaptoethanol, poly dAC:dTG and RNA polymerase. The syntheses of poly rAC contained 200 mμmoles of ATP-C^{14}, 2000 cpm/mμmole, and 200 mμmoles of CTP. The syntheses of poly rUG contained 200 mμmoles of UTP-C^{14}, 2000 cpm/mμmole, and 200 mμmoles of GTP. The first reaction in both cases contained 300 units of Stage IV enzyme[187] and 0.03 O.D. units of poly dAC:dTG. The second reaction in both cases contained the same amount of DNA but twice as much enzyme. The third reaction in both cases contained 0.06 O.D. units of DNA and 600 units of enzyme. The incubation was at 37°C. The incorporation as a function of time was determined by taking out 0.05 ml aliquots at various times. The incorporated radioactivity was determined in the same fashion as for the assay.

The results indicate that the incorporation as a function of time reaches a maximum in 60 minutes. Other assays of the incorporation of C^{14}-AMP into poly rAC and C^{14}-UMP into poly rUG have confirmed this observation. Thus, all the

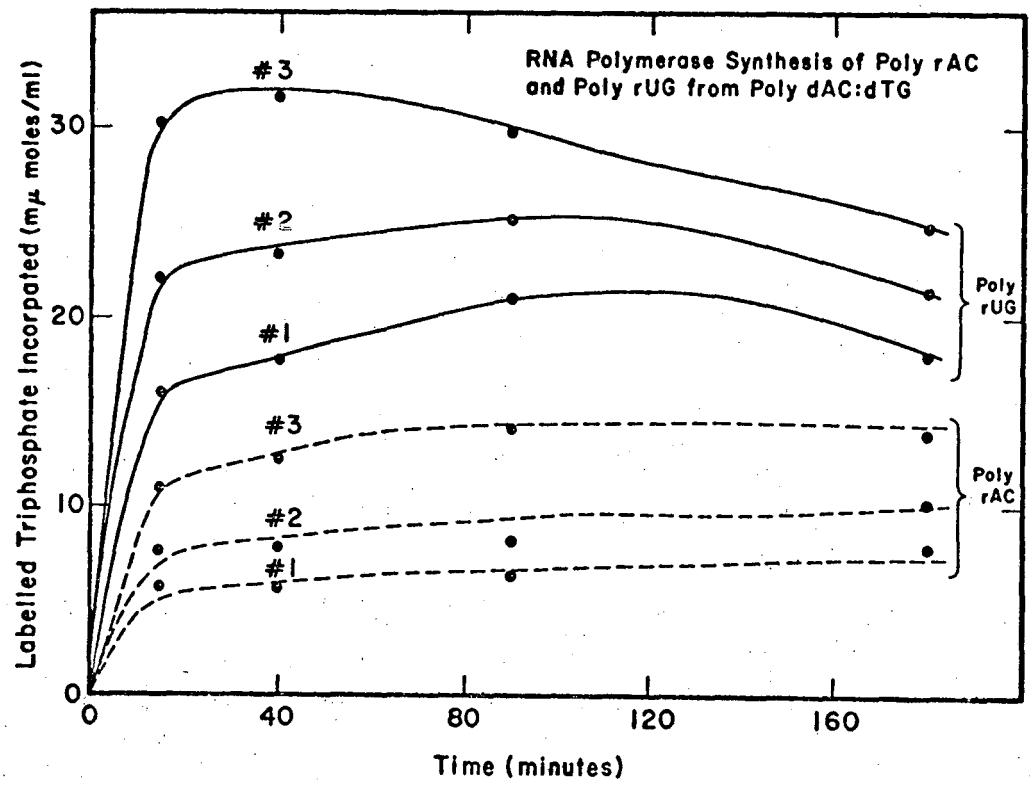

Figure 65. The incorporation of C^{14}-UMP and C^{14}-AMP into poly rUG and poly rAC, respectively, by RNA polymerase transcription of poly dAC:dTC. For both the synthesis of poly rUG and the synthesis of poly rAC: Reaction 1 contained 300 units of enzyme and 0.03 O.D. units of poly dAC:dTC; Reaction 2 contained 600 units of enzyme and 0.03 O.D. units of poly dAC:dTG; Reaction 3 contained 600 units of enzyme and 0.06 O.D. units of poly dAC:dTG. Total volume in all cases was 0.25 ml. See text for concentration of other reagents.

syntheses of poly rAC and poly rUG have been terminated after 60 minutes.

As expected, the data in Figure 65 indicates that increasing the DNA and enzyme concentration increases the yield of acid precipitable material. Of course the goal is to optimize the O.D. units of poly rAC and poly rUG synthesized per O.D. unit of DNA, per unit of enzyme, and per unit of time spent by the investigator. Thus, it is not always clear what the optimum conditions are. Note in Figure 65 that Reaction 3 for both poly rAC and poly rUG used twice as much DNA as Reaction 2. The yield was greater for Reaction 3. However, it was not twice as great. We had a fair amount of success in synthesizing poly dAC:dTG. Thus, in large scale syntheses of poly rAC and poly rUG we have used higher concentrations of DNA than even those used in Reaction 3.

The dependence of the yield on enzyme concentration is shown more explicitly in Figure 66. Except for the DNA and enzyme concentrations, the reaction conditions were identical to those for Figure 65. The concentration of poly dAC:dTG was 0.57 O.D. units/ml. The concentration of RNA polymerase was as indicated in the figure. The incubation was at 37°C for 60 minutes.

Note that more poly rAC was synthesized than poly rUG for each of the reactions of Figure 66. The reverse was true in the previous figure. The discrepancy is definitely real

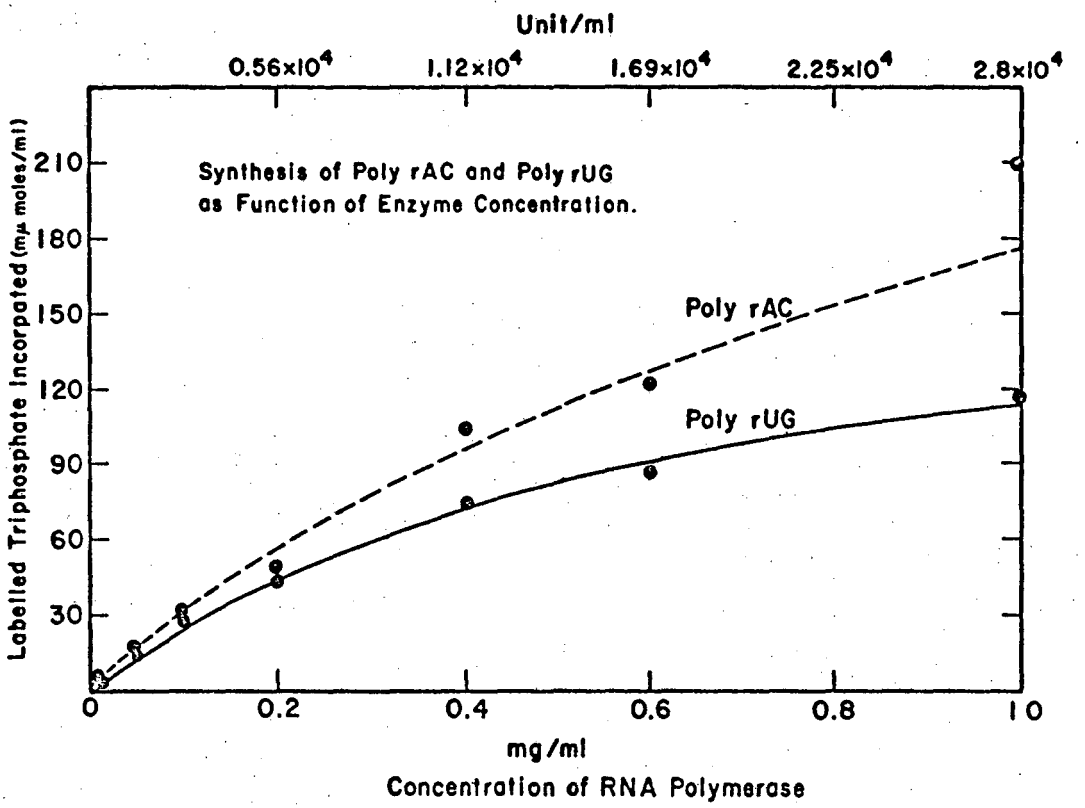

Figure 66. Synthesis of poly rAC and poly rUG by RNA polymerase transcription of poly dAC:dTG as function of enzyme concentration. See text for concentrations of other reactants.

and the result of using different enzyme preparations. The results for poly rUG were identical for the two enzyme preparations. However, for unknown reasons, the enzyme that was used for the reactions in Figure 66 synthesized poly rAC much better than the other enzyme preparation. Naturally, we used this second enzyme preparation most frequently because of the enhanced yield of poly rAC.

The increasing yield with increasing enzyme concentration levelled off at 0.40 mg/ml. For large scale syntheses we used enzyme concentrations around 0.5 mg/ml. Using more enzyme than this would increase the yield further, but the cost in terms of units of enzyme per O.D. unit of polymer synthesized would increase rapidly.

We have varied some of the other conditions in an attempt to increase the yields. Compared to the results in Figure 66, increasing or decreasing the $MgCl_2$ concentration by a factor of 2 did not significantly alter the yields. However, using one-fifth the concentration of triphosphates or incubating at 45°C instead of 37°C decreased the net synthesis.

The one trick we tried that did enhance the yields a small amount was to precipitate the RNA polymerase and redissolve it before adding it to the synthesis mixture. The enzyme was precipitated with an equal volume of room temperature saturated ammonium sulfate. After standing 15 minutes in ice the mixture was centrifuged at 4°C. The supernatant was removed with a pipet and the precipitate was taken up in the RNA polymerase diluting buffer (see description of assay).

In fact, all the experiments shown in Figure 66 were done with enzyme that had been treated in this way. This treatment does not alter the differences between the two enzyme preparations that are mentioned above.

In summary, for large scale syntheses of poly rAC and poly rUG the concentration of Tris-HCl buffer, pH 8, $MgCl_2$, $MnCl_2$, and 2-mercaptoethanol were the same as used in the assay and as indicated for the reactions in Figures 65 and 66. In addition, the reaction mixture contained the two appropriate ribotriphosphates, 800 mμmoles of each/ml, poly dAC:dTG, 0.57 O.D. units/ml, and Stage IV RNA polymerase,[187] 0.5 mg/ml (1.4×10^4 units/ml). The enzyme was precipitated and redissolved as described. The incubation was at 37°C. The synthesis was stopped after 60 minutes by adding an equal volume of cold 0.1 M EDTA, pH 8. The protein was removed by one phenol extraction. The phenol layer was washed with 0.1 M phosphate buffer, pH 7. Then, the combined aqueous layers were dialyzed as indicated for poly dAC:dTG.

For these conditions, 5 ml reactions yielded 7-10 O.D. units of poly rAC and 3-4 O.D. units of poly rUG. A total of 2.8 O.D. units of poly dAC:dTG were used per 5 ml reaction. Thus, there was a 2.5 to 3.5-fold synthesis of poly rAC and barely more than a 1-fold synthesis of poly rUG.

3. Separation of RNA from DNA

The solutions of poly rAC and poly rUG, as prepared above, still contained the primer DNA, poly dAC:dTG. The RNA

was separated from the DNA by preparative equilibrium centrifugation in Cs_2SO_4. The method is basically similar to that described for the separation of the DNA strands. However, Cs_2SO_4 was used instead of CsCl because RNA is too dense to be banded in solutions of CsCl. The other major difference is that the banding was done at neutral pH instead of alkaline pH.

The solutions were made up to a density of 1.553 in 3 ml. Previous work by Chamberlin[188] indicated that this density would effect a good separation of RNA and DNA. The weight percent of Cs_2SO_4 in the solution, 44.5%, was determined from the report of Wake and Baldwin.[189]

The results for poly rUG and poly rAC are shown in Figures 67 and 68, respectively. The poly rAC solution contained a total of 14 O.D. units, including 2.8 O.D. units of poly dAC:dTG. The poly rUG solution contained a total of 4.7 O.D. units, including the same amount of DNA. In both cases, after centrifugation for three days, there was a visible band of precipitated material. The band was closer to the bottom of the tube for the solution containing poly rUG than for the solution containing poly rAC. We followed the progress of the bands during the collecting procedure. They came out in the fractions labelled poly rAC and poly rUG in the figures. The precipitates immediately disappeared upon the dilution of the fractions.

There were three other bands of UV absorbing material in the poly rUG tube. The lightest one, on the right in the

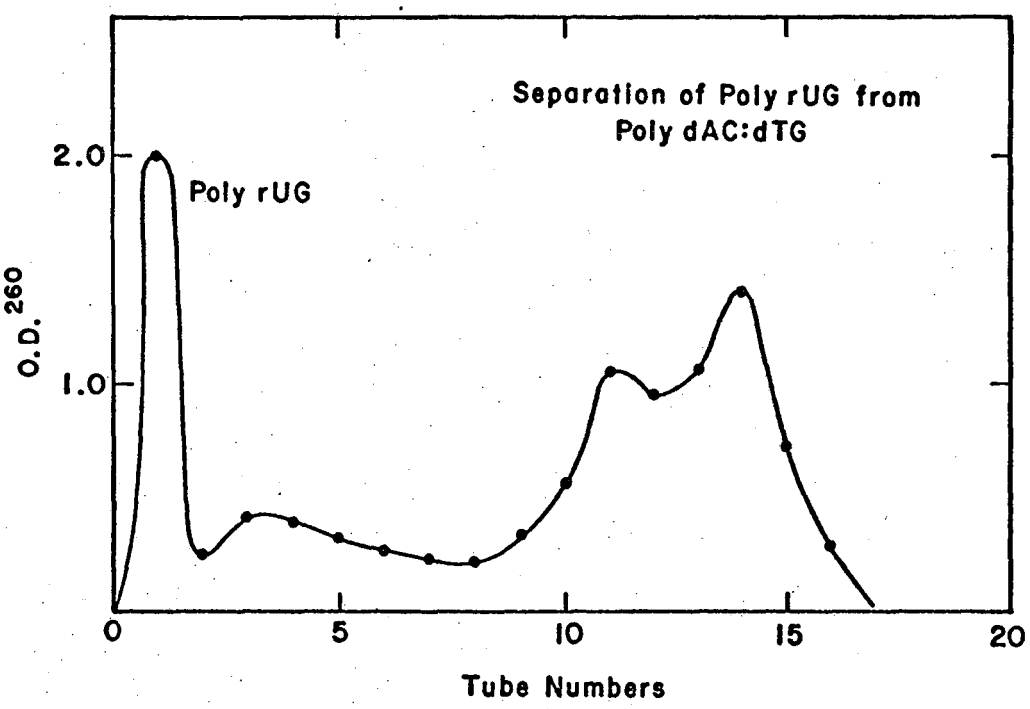

Figure 67. Separation of poly rUG from poly dAC:dTG by preparative centrifugation. The absorbance at 260 mμ is plotted for fractions collected from bottom of a test tube after centrifugation for three days. The solution contained 4.7 O.D. units of nucleic acid in a Cs_2SO_4 solution, density = 1.553.

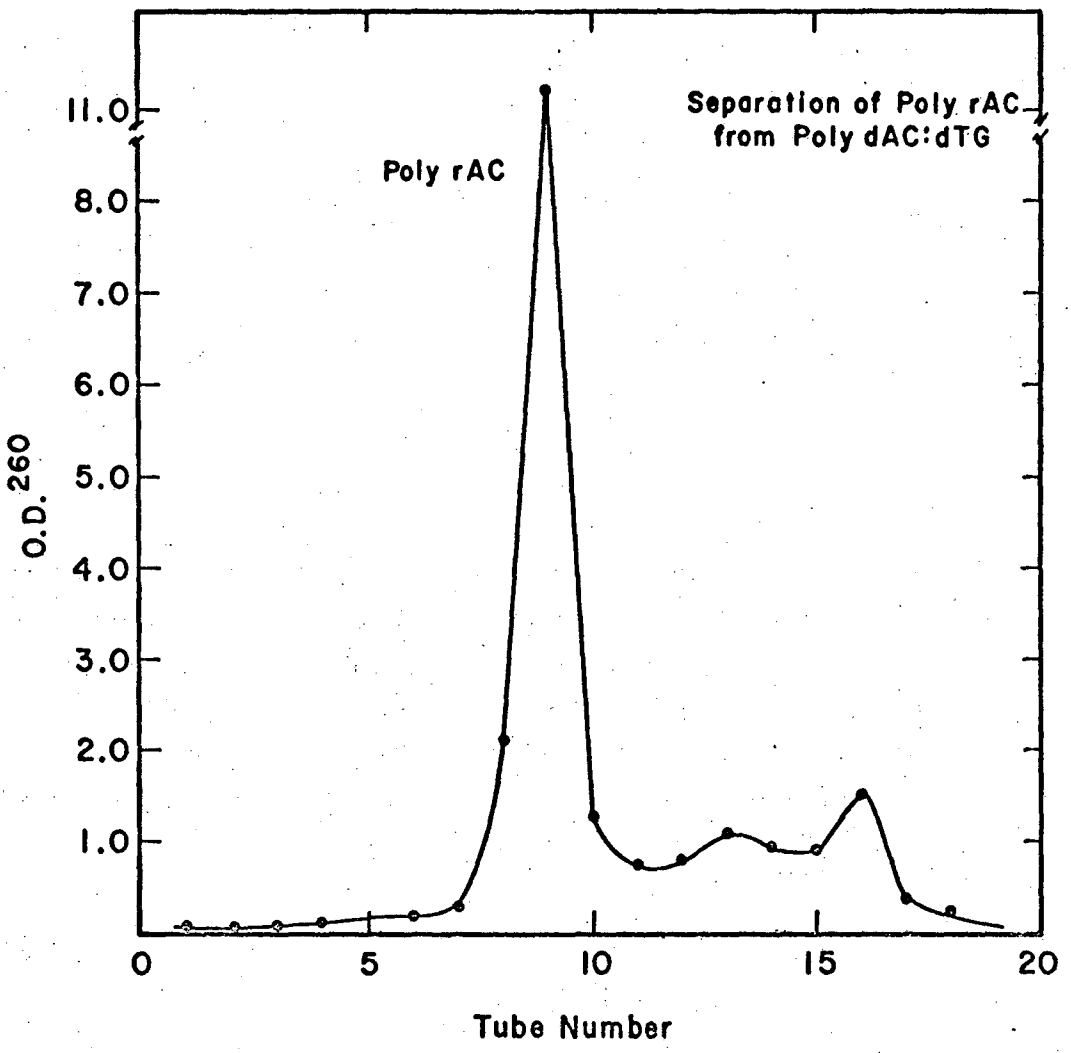

Figure 68. Separation of poly rAC from poly dAC:dTG by preparative centrifugation. The absorbance at 260 mμ is plotted for fractions collected from bottom of a test tube after centrifugation for three days. The solution contained 14 O.D. units of nucleic acid in a Cs_2SO_4 solution, density = 1.553.

figure, was presumably poly dAC:dTG. The next heaviest band was probably a DNA:RNA hybrid. In which case, the third unidentified band was poly dTG.

There were only two extra bands in the poly rAC tube. The same species were probably present in this system as in the poly rUG system. If our identification of the bands in the poly rUG tube was probably single-strand DNA. It might have been buried under the poly rAC peak.

The fractions containing poly rAC and poly rUG were pooled and dialyzed against 0.01 M phosphate buffer, pH 7.5, 10^{-4} M EDTA. If there was a single-strand DNA contamination in the poly rAC sample, it probably amounted to less than 10% of the UV absorbing material. A total of 8.4 optical density units of poly rAC and 1.0 optical density units of poly rUG were recovered. Approximately 1.5 optical density units were recovered from each of the lightest bands.

Preliminary Optical Properties of Poly rAC and Poly rUG

The wavelengths of the extrema in the optical rotation and absorption spectra of poly rAC, poly rUG, poly dAC, and poly dTG are given in Table 10. The analogous absorption properties of poly dAC:dTG are also shown.

1. Poly rAC

The absorption spectrum of neutral solutions of poly rAC at 25°C is given in Figure 69. It is similar to the

Table 10

	UV Spectrum			ORD		
	λ_{max} [a]	λ_{min} [a]	280/260	λ_o [b]	λ_o [b]	λ_t [b]
poly rAC	258	233	0.41	285	272	258
poly rAC[c] (calc)	-	-	-	286	276	261
poly dAC	261	232	0.48	290	279	259
poly rUG	256	228	0.49	284	270	250
poly rUG[c] (calc)	-	-	-	290	282	272
poly dTG	255	230	0.63	292	286	270
poly dAC:dTG	258	236	0.56	-	-	-

a. λ_{max} and λ_{min}, refer to the wavelengths of maximum and minimum absorption in the UV spectrum.

b. λ_p, λ_o, and λ_t refer to the wavelengths of the peak, crossover, and trough, respectively, in the ORD.

c. Nearest-neighbor calculated ORD.

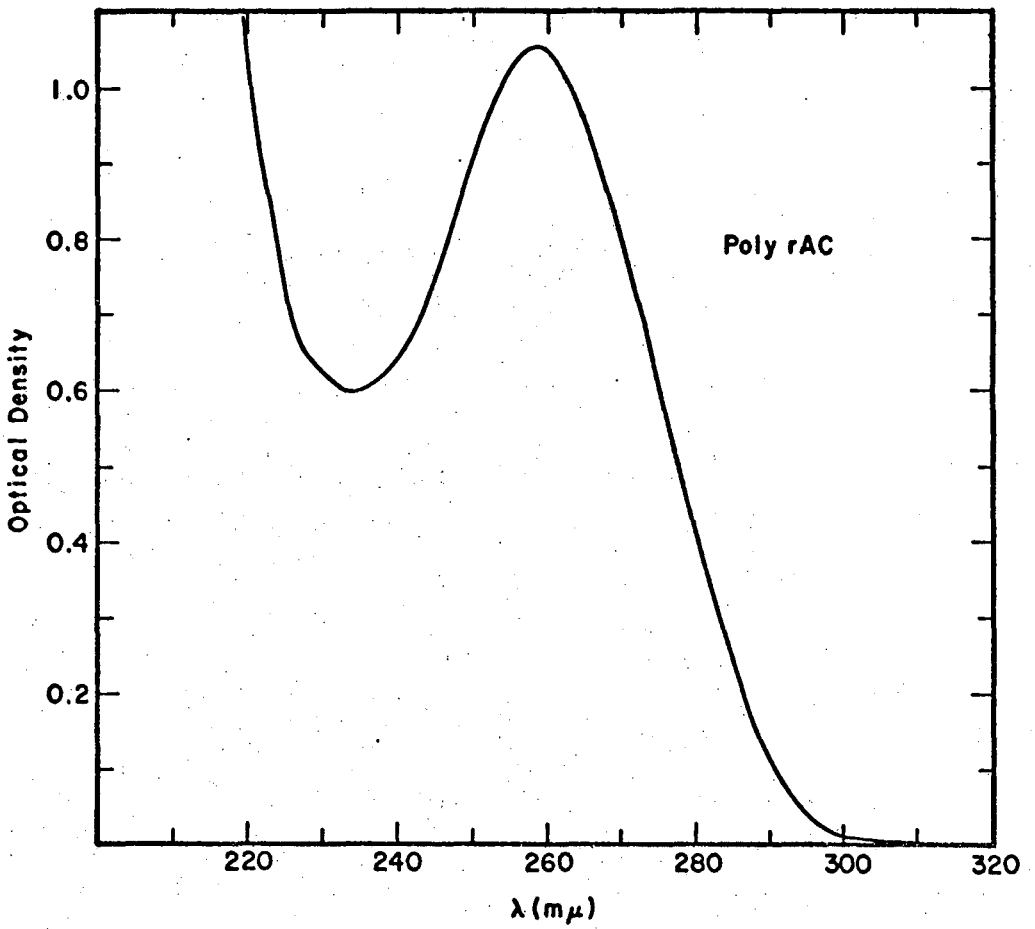

Figure 69. Ultraviolet absorption spectrum of poly rAC, 0.01 M sodium phosphate buffer, pH 7.6, 10^{-4} M EDTA, 25°C.

spectrum of poly dAC. The maximum and minimum of the poly rAC spectrum are at 258 mμ and 233 mμ, respectively. The 280/260 ratio is 0.41.

The optical density of poly rAC at the wavelength of maximum absorption is shown in Figure 70 as a function of temperature. There is a gradual increase in absorption with increasing temperature. There is no indication of any helix-coil transition. In this respect, the absorption-temperature profile resembles that found for poly A[85] and poly C[71] at pH 7. At this pH, these homopolymers have been characterized as single-strand helices with stacked bases.[57,71] We expect that poly rAC has a similar structure at pH 7. The gradual increase in optical density with increasing temperature presumably reflects a gradual change in the base stacking.

The ORDs of poly rAC and poly dAC are shown in Figure 71. The extinction coefficient of poly rAC was calculated with Eq. (6) and the known extinctions of ApC and CpA.[108] At 260 mμ it is 9600. We assumed the same extinction coefficient for poly dAC. The difference between the ORDs of poly rAC and poly dAC is similar to that found for other pairs of ribo- and deoxyribo- polymers with analogous sequences.[190] The magnitude of the rotation at the extrema of the ORD is generally larger for the polyribonucleotide.

The nearest-neighbor calculated ORD of poly rAC is also shown in Figure 71. The three curves are qualitatively similar.

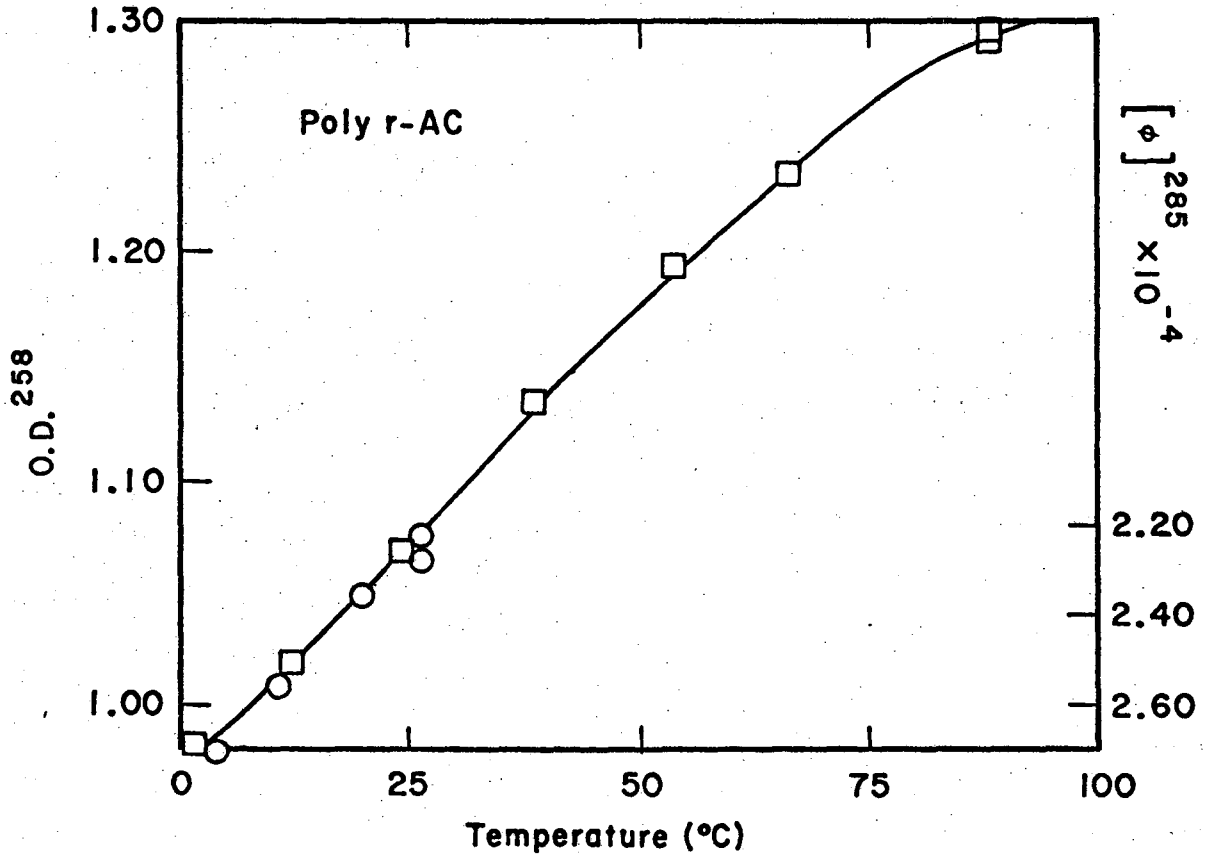

Figure 70. Temperature-dependence of absorption and molar rotation of poly rAC, 0.01 M sodium phosphate buffer, pH 7.6, 10^{-4} M EDTA. □, absorbance at 258 mμ. ○, molar rotation per residue at 285 mμ.

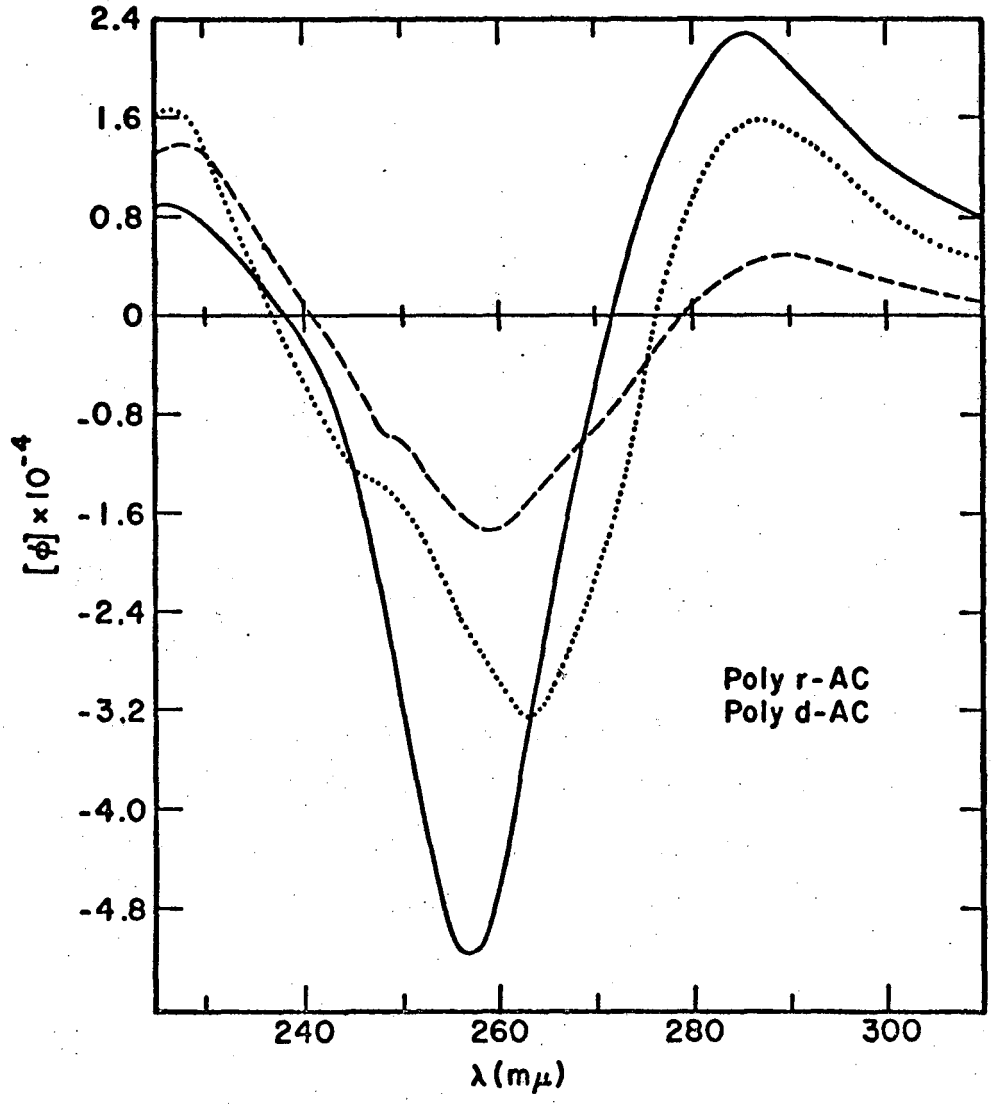

Figure 71. ORD of poly rAC and poly dAC, 0.01 M sodium phosphate buffer, pH 7.6, 10^{-4} M EDTA, 25°C.

—— Experiment for poly rAC.

--- Experiment for poly dAC.

··· Nearest-neighbor calculated ORD for poly rAC at 25°C.

They each have a peak between 285 and 290 mμ, a trough between 257 and 263 mμ, a second peak near 225 mμ, and a second trough (not shown) at 213 mμ. From this standpoint, the ORD of poly rAC compares as well with the nearest-neighbor calculation as do the ORDs of poly A, poly C, and poly U, shown in Figure 3 (page 37). The magnitudes of the rotation are not as close for poly rAC, however. This is probably partially due to the use of a calculated extinction coefficient. They are generally too high for the homopolymers by 10 or 20%. They may also be too high for repeating polymers.

The ORD of poly rAC at pH 7 has been measured at a few temperatures between 0 and 25°C. By suitable juggling of the ordinate, the rotation at 285 mμ can be made to fall on the line for the absorption of poly rAC as a function of temperature.

These few measurements strongly suggest that poly rAC at pH 7 has the conformation of a single-strand helix with stacked bases. Poly dAC probably has a similar conformation.

It will be interesting to see what kind of structures form at lower pHs. The constraints of a helix may prevent the formation of a structure in which C-H^+-C base pairs alternate with A-H^+-A base pairs. The problem would be to fit both purine-purine base pairs and pyrimidine-pyrimidine base pairs into the same helix. Perhaps A-H^+-C base pairs will occur. Such base pairs have been postulated to occur in 1:1 mixtures of poly A and poly C at pH 5.[192]

2. Poly rUG

The absorption spectrum of poly rUG is shown in Figure 72. The maximum is at 256 mμ and the minimum is at 228 mμ. There is no shoulder on the red side of the absorption peak for poly rUG. However, there is a pronounced shoulder near 275 mμ for poly dTG. The 280/260 ratio is 0.49 for poly rUG and 0.63 for poly dTG. These differences probably reflect the dissimilarities of the optical properties of thymidine and uracil. The absorption maximum is at 267 mμ for thymidine and 262 for uridine.

The most interesting result for poly rUG is its ORD, which is shown in Figure 73. The ORD of poly dTG and the nearest-neighbor calculated ORD of poly rUG are also shown. Once again, a calculated extinction coefficient at 260 mμ, 9900, has been used for both polymers. The ORD of poly dTG is qualitatively similar to the nearest-neighbor calculated ORD of poly rUG. However, the ORD of poly rUG is quite different from the calculated curve. In particular, the trough of the experimental curve occurs 22 mμ to the blue of the trough of the calculated curve. The calculated curve actually has a peak near the wavelength where the experimental curve has a trough.

The difference between experiment and calculation may be indicative of base pairs in poly rUG. This is a particularly intriguing possibility since U-G base pairs may occur in the secondary structure of tRNA[16,20-22] and in the interaction

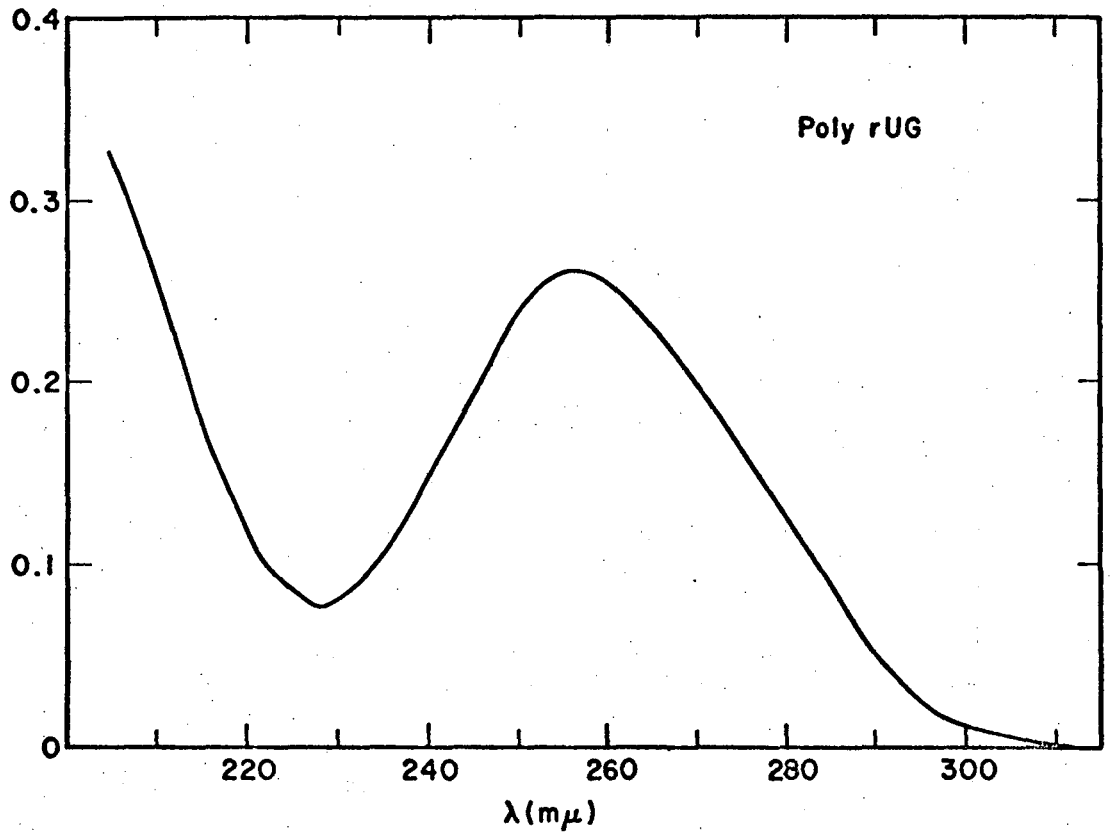

Figure 72. Ultraviolet absorption spectrum of poly rUG, 0.01 M sodium phosphate buffer, pH 7.6, 10^{-4} M EDTA, 25°C.

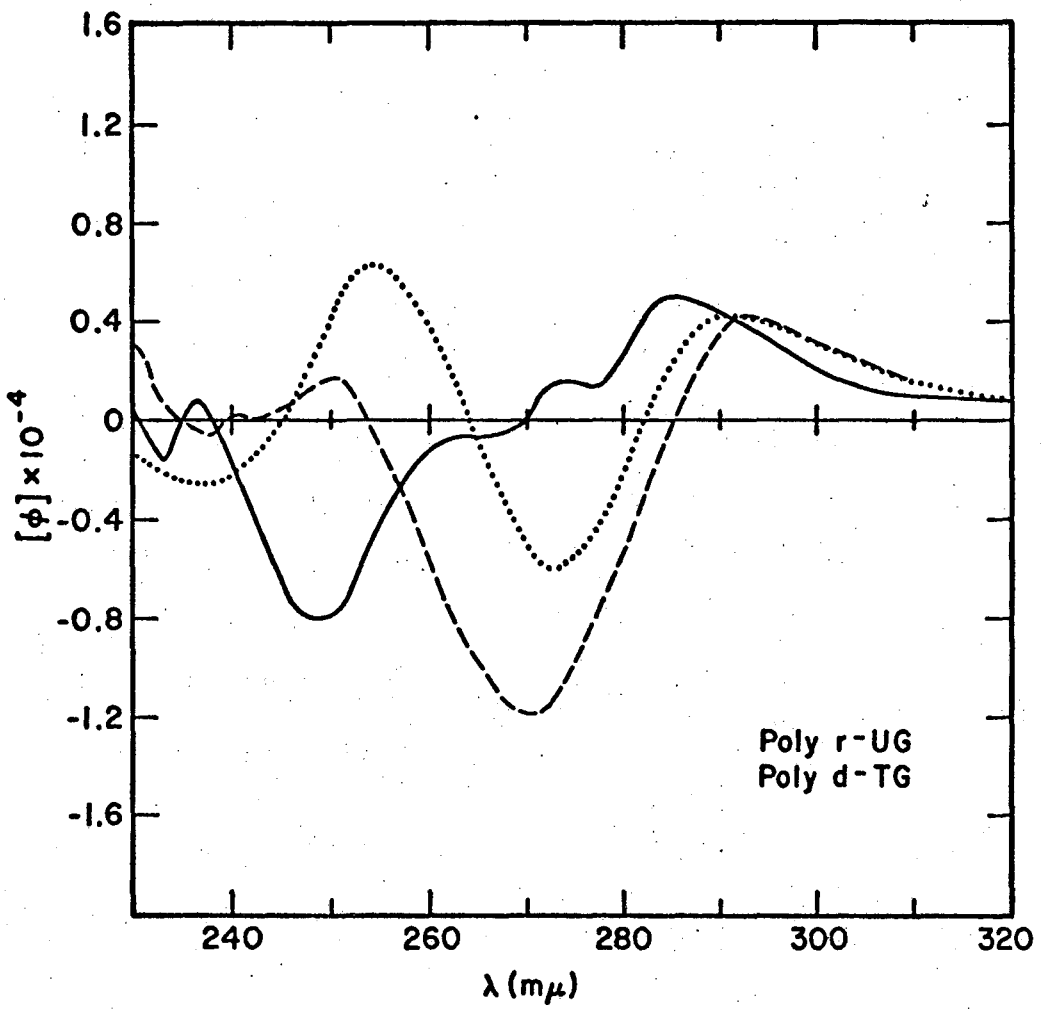

Figure 73. ORD of poly rUG and poly dTG, 0.01 M sodium phosphate buffer, pH 7.6, 10^{-4} M EDTA, 25°C.

—— Experiment for poly rUG.

--- Experiment for poly dTG.

··· Nearest-neighbor calculated ORD of poly rUG for 25°C.

of codon and anticodon.[7] There are no known examples of U-G base pairs, however.

Summary

Procedures have been worked out for the preparation of poly rAC and poly rUG starting with a few optical density units of poly dAC:dTG and a generous supply of DNA polymerase and RNA polymerase. The first step involves the synthesis of more of the DNA-like polymer with DNA polymerase. Poly rAC and poly rUG have been synthesized independently by RNA polymerase transcription of poly dAC:dTG one strand at a time. A few optical density units of each of these polymers have been separated from the DNA. Preliminary reports of their optical properties indicate that poly rAC at pH 7 is a single-strand helix with stacked bases, but under the same conditions, poly rUG may contain some base pairs.

APPENDIX A

Abbreviations

Following is a list of some of the abbreviations and terms frequently used in this dissertation:

A	Adenosine
U	Uridine
C	Cytidine
G	Guanosine
T	Thymidine
N	A general nucleoside
dN	A general deoxynucleoside. In all terms referring to thymidine, the sugar is assumed to be deoxyribose and the small d is left off.
Np	3' (2') nucleotide
NMP	5' nucleoside monophosphate
NDP	5' nucleoside diphosphate
NTP	5' nucleoside triphosphate
NpN	3'-5' dinucleoside phosphate. Longer oligomers are abbreviated similarly.
poly N	Homopolymer of nucleoside N, the nucleosides are connected by 3'-5' phosphate bridges
poly dN	Homopolymer of deoxynucleoside dN.
poly rAC	Polyribonucleotide of alternating A and C residues.
poly rUG	Polyribonucleotide of alternating U and G residues.
poly rAU	Polyribonucleotide of alternating A and U residues.

poly dAC	Polydeoxyribonucleotide of alternating A and C residues.
poly dTG	Polydeoxyribonucleotide of alternating T and G residues.
poly dAC:dTG	1:1 complex of poly dAC and poly dTG
poly (A+U)	1:1 complex of poly A and poly U
poly (G+C)	1:1 complex of poly G and poly C
RNA	Ribonucleic acid
DNA	Deoxyribonucleic acid
TMV	Tobacco mosaic virus
tRNA	Amino acyl transfer RNA
mRNA	Messenger RNA
rRNA	Ribosomal RNA
ORD	Optical rotatory dispersion
CD	Circular dichroism
O.D.	Optical density
O.D. unit	An amount which when dissolved in 1 ml, has an optical density at 260 mμ of 1 in a 1 cm path length cell.
λ	Wavelength
$[\phi]$	Molar rotation per residue
$\Gamma/2$	Ionic strength where concentration is expressed in moles per liter.

APPENDIX B

Prepration of Polynucleotide Phosphorylase from Micrococcus lysodeikticus

Polynucleotide phosphorylase has been purified from Micrococcus lysodeikticus according to the procedure of Singer and O'Brien[149] as modified by Thanassi and Singer.[150] Some of the details for all steps except IV and VIII are given by Cantor.[105] Our results are summarized in Table 11. The level of purification at all stages is similar to that reported by Thanassi and Singer.[150]

The modification introduced by Thanassi and Singer[150] was to replace the protamine Steps IV and V with a DEAE-cellulose column. This new step is called IV in the modified procedure and there is no Step V. The purpose of the protamine steps was to separate protein from nucleic acid, a must for a primer dependent enzyme. We, as well as others,[138,150] have found the reported results of these steps[149] extremely difficult to reproduce. Furthermore, the results have seemed to vary from one lot of protamine sulfate to another. By contrast, the DEAE-cellulose column in our hands has worked very well. The large jump in the 280/260 ratio from Step III to Step IV is evidence of the removal of nucleic acid from the enzyme solution. We have also found the results reproducible.

The only problem we encountered during the purification was with the concentration step after stage VIII. The stage

Table 11

Fraction[a]	Protein (mg/ml)	Specific Activity[b] (u/ml)	Total Units[b]	$\frac{A^{280}}{A^{260}}$
I. Crude extract	--	--	--	--
II. $(NH_4)_2SO_4$ (30 to 65%)	21	0.15	299	1.07
III. $(NH_4)_2SO_4$ (43 to 57%)	21	0.17	157	1.16
IV. DEAE-cellulose pooled tubes	10	0.24	194	1.60
VI. $(NH_4)_2SO_4$ (40 to 60%) pH 6.3	26	0.33	147	1.78
VII. Zinc-Sephadex G-75 Zinc supernatant	4.3	0.61	116	--
Pooled tubes from columns[d]	0.64	2.3	129	1.25
VIII. DEAE-cellulose pooled tubes from columns[d]	0.11	7.5	116	--
Final concentrated enzyme	0.6 to 1.0	5.3	70[e]	--

a. Fractions refer to steps in the purification procedure of Singer and O'Brien[149] as modified by Thanassi and Singer.[150]

b. The units refer to assays by the phosphorolysis of poly A. This assay is Assay A of Singer and O'Brien.[149] It is also described by Cantor.[105]

c. The results are for the lysis of three 20 gm batches of cells. Two of the lyses were pooled after Stage I.. The third lysis was pooled with the first two after Stage IV.

d. The enzyme solution was divided into three equal portions and each portion was carried though Stages VII and VIII separately.

e. This is the estimated recovery if the concentrating is done with Sephadex G-200 as described in the text.

VIII enzyme is too dilute for normal synthesis conditions. Singer and O'Brien[149] have concentrated the enzyme by adsorbing it on a small DEAE-cellulose column and eluting it off in a small volume. They were able to concentrate the enzyme solution more than 10 fold and still recover 80% of the activity. However, on several attempts we were never able to recover more than 50% of the activity. An alternative procedure suggested by Mr. D. Lloyd has proved to be satisfactory. Up to 15 ml of the stage VIII enzyme was placed in dialysis tubing that had been heated for at least an hour in 7 M urea and thoroughly rinsed with twice-distilled H_2O. The water was removed from the dialysis bag by packing it in dry Sephadex G-200 resin (Pharmacia, Piscataway, New Jersey). After 30 to 60 minutes the wet Sephadex was stripped away and replaced with dry Sephadex. After four changes the volume of the solution was one-fifth to one-tenth of the original volume. The solution was kept cold during the entire procedure by placing the shallow trough containing the dialysis bag and resin in ice. We were able to recover 70% of the activity.

Thanassi and Singer[150] have shown that both the stage VII and stage VIII enzyme when purified according to the modified procedure is primer dependent. We have not tested our preparation. However, our results so closely parallel theirs that it seems reasonable to presume that our concentrated stage VIII enzyme is also primer dependent. However,

there have been reports[191] that this procedure results in a primer independent enzyme for certain lots of the bacterial cells purchased from Miles Laboratory.

A recent report by Klee[191] shows that primer dependency can be induced by treatment with trypsin. The use of this method should make the preparation of large quantities of primer dependent enzyme much easier than with the procedure that has been used until now.

APPENDIX C

Fortran Program for Converting Raw Data of a Spectropolarimeter to an ORD Curve

The Fortran computer program presented in this Appendix, program DORD25S, was designed to convert the raw data generated by the Cary Model 60 spectropolarimeter into ORD curves. The smoothing procedures of Savitzky and Golay[152] were used to reduce the noise in the signal. As indicated in the text, we found that the best procedure for reducing the noise without altering the signal was to take points every 0.5 mμ and fit them to Savitzky and Golay's 25-point cubic function.[152]

The program was written in Chippewa Fortran for use with the Control Data 6600 Computer. The subroutine for the smoothing, subroutine SMOOTH, was taken from the paper by Savitzky and Golay.[152]

The raw data were recorded on punched paper tape in a Scientific Data System (SDS) code by a Datex analog-to-digital converter. An IBM 1401 Computer was used to convert the data to IBM code and transfer it to magnetic tape that was used for input.

The pen position and wavelength of the spectropolarimeter were recorded in 10 character records. The first character was always a space. As indicated below, we have used this feature in developing a procedure for signaling the end of a spectrum and for changes of the pen center control on the

machine. The second, third and fourth characters recorded the pen position from 0 to 999. If the pen position was greater than 1000, then a + was recorded in the second character and the other digits were recorded in the third and fourth character positions. The maximum value of the pen position was 1035. An analogous system was used for pen positions less than zero. In this case, a - was recorded in the second position. The minimum value of the pen position was -35. The wavelength in angstroms was recorded in characters 5 through 10.

Besides the data recorded directly from the machine, a 10 character record could be entered on the paper tape manually through a control panel on the Datex. Any digit could be entered in any of the 10 character positions. We shall refer to these manual entries as parameter entries.

For purposes of explaining the input data required by the program we shall outline the instructions for recording an optical rotation spectrum with the Datex. The input data consists of a series of parameter records entered manually and data records taken directly from the machine. Each record would correspond to one card if the input was with cards. The first record was a parameter entry recording the date and a four digit identification number for the spectrum or baseline. The second record was the same as the first. We found it necessary to enter it twice since there were occasional mispunches in the first record. The absorption

of the solution in the cell being used for the optical rotation measurement was recorded in the third record. The molar extinction coefficient per residue at the same wavelength was also recorded in the third record. For a baseline the absorption was set to zero. The scale and pen center were entered in the next record. The baseline shift and specific rotation options, described below, were also made in this record. The pen positions and wavelength from the spectropolarimeter were recorded in the succeeding records while scanning from long wavelength to short wavelength. If during the scan it was necessary to change the pen center, then the scan was stopped and a 1 was entered in character one of a parameter entry. The new pen center and scale, although the scale was never changed during a scan, were then entered manually. After the entry of this record the scan was continued while recording the data. At the end of the scan, a 1 was entered in character one of a parameter entry as before. The next record contained zeros in the first three characters.

The program was designed so that up to five baselines and eight sample scans could be run in any order. Each scan was stored in memory. After the last scan and the ending parameter entries, zeros were recorded in characters 6 through 10. This record was entered twice. Each succeeding record contained the identifications of a baseline and a sample scan that were to be used for calculating an ORD curve. The same

baseline could be used with more than one sample. Similarly, more than one baseline could be subtracted from the same sample spectra. After recording all the desired pairs, a new group of baselines and samples could be run or the tape could be ended.

The operator was given the option of checking for a baseline shift. The option was entered with the first recording of the pen position and scale for a sample spectrum. If this option was chosen then any difference between the baseline and sample for the first 100 points (50 mμ) was assumed to be due to a baseline shift. The arithmetic average of the differences for the 100 points, after the difference curve had been smoothed, was taken as the magnitude of the baseline shift. This shift was then applied as an additive constant to the entire remainder of the spectrum.

The resulting ORD curves were printed-out in units of molar rotation per residue. An option was provided for the calculation of specific rotation. This option was made in the same record as the baseline shift option.

In addition to printed output, the final results were recorded on magnetic tape. This tape was used for storage of all smoothed spectra. Control cards were used to space the tape forward to the end of the last spectrum recorded on the tape. Similarly, the raw data was stored on another magnetic tape.

Another Fortran program was written to convert the raw data generated by the Cary Model 15 Spectrophotometer into absorption spectra. The program was very similar to the DORD25S program presented here.

```
      PROGRAM DORD25S (INPUT,OUTPUT,TAPE1,TAPE2,TAPE3)
      DIMENSION DEG(800,8),WAVEL(800,8),PEN(10,9),BDEG(800,5),
     1  BWAVEL(800,5),ROT(800),SCALE(10,9),MARK(10,9),PATH(10,9),
     2  JEND(10,9),PHI(800),SHIFT(100),CORR(100),JMARK(10,9),
     3  MO(9),MDAY(9),MYEAR(9),IDENT(9),ABS(9),EMP(9),
     4  BSCALE(10,5),BPEN(10,5),JFIN(9),JBEND(10,5),JBFIN(9),
     5  B(3),III(3),BIDENT(5),KWAVEL(800,8)
      INTEGER WAVEL, BWAVEL, BIDENT
      FSCALE=0.0
C
C     STATEMENTS 1000 UP TO 660 BEGIN INPUT FOR SERIES OF BASELINE
C     (MAXIMUM OF 5) AND SAMPLE SPECTRA (MAXIMUM OF 8).  THE IDENT
C     RECORD IS RECORDED TWICE.  ABSORPTION = 0 FOR A BASELINE.
C     IDENT = 0 SIGNALS THE END OF THE SERIES OF SPECTRA.
C     A MOLAR EXTINCTION COEFFICIENT IS RECORDED EVEN IF
C     SPECIFIC ROTATION IS DESIRED.
C
 1000 NL=1
      N=1
   50 READ INPUT TAPE1,2000
 2000 FORMAT (2X,I2)
 2002 READ INPUT TAPE1,2222,MO(N),MDAY(N),MYEAR(N),IDENT(N)
 2222 FORMAT (3I2, I4)
      IF (IDENT(N)) 99,100,10
   10 J=1
      I=1
      WRITE OUTPUT TAPE3,3,MO(N),MDAY(N),MYEAR(N),IDENT(N)
    3 FORMAT (3I4,I6)
      READ INPUT TAPE1,51,ABS(N),EMP(N)
   51 FORMAT (F4.3, F6.0)
      WRITE OUTPUT TAPE3,4,ABS(N),EMP(N)
    4 FORMAT (F6.3,F8.0)
      IF (ABS(N)) 99,660,70
C
C     STATEMENTS 660 UP TO 70 READ IN RAW DATA FOR BASELINE SPECTRA,
C     PRINT THEM, AND RECORD THEM ON THE RAW DATA MAG TAPE.  A CHANGE
C     IN PEN CENTER, JUMP IN THE WAVELENGTH, OR END OF SPECTRUM IS
C     SIGNALLED BY A 1 IN COLUMN ONE.  SCALE = 0 FOR END OF SPECTRUM.
C
  660 BIDENT(NL)=IDENT(N)
   60 READ INPUT TAPE1,61,BSCALE(J,NL),BPEN(J,NL)
   61 FORMAT(F3.2, F3.0)
      IF (BSCALE(J,NL)) 99,450,62
   62 READ INPUT TAPE1,63,NZ,B(1),B(2),B(3),BWAVEL(I,NL)
   63 FORMAT (I1,A1,A1,A1,I6)
      DECODE (11,540,B(2)) III(2),III(3)
  540 FORMAT (I1,9X,I1)
      IF (B(1)-1H+ ) 500,510,500
  500 IF (B(1)-1H- ) 520,530,520
  510 BDEG(I,NL)=1000+10*III(2)+III(3)
      GO TO 560
  530 BDEG(I,NL)=-(10*III(2)+III(3))
      GO TO 560
  520 DECODE (1,550,B(1)) III(1)
  550 FORMAT (I1)
```

```
      BDEG(I,NL)=100*III(1)+10*III(2)+III(3)
  560 CONTINUE
      IF (NZ) 99,64,80
   64 I=I+1
      GO TO 62
   80 JBEND(J,NL) = I-1
      J=J+1
      GO TO 60
  450 NBN=I-1
      JBFIN(NL)=J-1
      PRINT 81, MO(N),MDAY(N),MYEAR(N)
   81 FORMAT (1H1,50X, 10H DATE=     , I3,I3,I3,///)
   82 PRINT 83, IDENT(N)
   83 FORMAT (31H THE RAW DATA FOR BASELINE NO.      ,I4,2X,
     1 10H FOLLOWS.      ,//)
      K=J-1
      DO 470 J=1,K
      JK=J-1
      M=JBEND(J,NL)
      IF (J-1) 471,471,472
  471 L=1
      GO TO 473
  472 L=JBEND(JK,NL)+1
  473 PRINT 84, BSCALE(J,NL),BPEN(J,NL)
   84 FORMAT (15X, 14H FULL RANGE=     , F3.2, 50X, 13H PEN CENTER=    ,
     1  F3.0,//)
      PRINT 85, ((BWAVEL(I,NL),BDEG(I,NL)), I=L,M)
   85 FORMAT (10(I7, F5.0))
      WRITE OUTPUT TAPE3, 5,BSCALE(J,NL),BPEN(J,NL)
    5 FORMAT (F4.2,F4.0)
      WRITE OUTPUT TAPE3,6, ((BWAVEL(I,NL),BDEG(I,NL)),I=L,M)
    6 FORMAT (10(1X,I6,F4.0))
      WRITE OUTPUT TAPE3,7,NZ
    7 FORMAT (I1)
  470 CONTINUE
      WRITE OUTPUT TAPE3,12,FSCALE
   12 FORMAT (F3.2)
      ENDFILE 3
      NL=NL+1
      GO TO 50
C
C     STATEMENTS 70 TO 78 READ IN RAW DATA FOR SAMPLE SPECTRA,
C     PRINT THEM, AND RECORD THEM ON THE RAW DATA MAG TAPE.  CHANGES
C     IN PEN CENTER, JUMPS IN WAVELENGTH, AND ENDS OF SPECTRA ARE
C     SIGNALLED AS THEY ARE FOR BASELINE SPECTRA.  MARK = 5 FOR THE
C     BASELINE SHIFT OPTION, AND JMARK = 4 FOR THE SPECIFIC ROTATION
C     OPTION.
C
   70 READ INPUT TAPE1, 71, SCALE(J,N), PEN(J,N),MARK(J,N),
     1  JMARK(J,N),PATH(J,N)
   71 FORMAT (F3.2, F3.0, I1, I1, F2.1)
      IF (SCALE(J,N)) 99,76,72
   72 READ INPUT TAPE1,73,NZ,B(1),B(2),B(3),WAVEL(I,N)
   73 FORMAT (I1,A1,A1,A1,I6)
      DECODE (11,5540,B(2)) III(2),III(3)
```

```
 5540 FORMAT (I1,9X,I1)
      IF (B(1)-1H+ ) 5500,5510,5500
 5500 IF (B(1)-1H- ) 5520,5530,5520
 5510 DEG(I,N)=1000+10*III(2)+III(3)
      GO TO 5560
 5530 DEG(I,N)=-(10*III(2)+III(3))
      GO TO 5560
 5520 DECODE (1,5550,B(1)) III(1)
 5550 FORMAT (I1)
      DEG(I,N)=100*III(1)+10*III(2)+III(3)
 5560 CONTINUE
      IF (NZ) 99,74,75
   74 I=I+1
      GO TO 72
   75 JEND(J,N)=I-1
      J=J+1
      GO TO 70
   76 NN=I-1
      JFIN(N)=J-1
      PRINT 142, MO(N),MDAY(N),MYEAR(N)
  142 FORMAT (1H1, 50X,10H DATE=       ,I3,I3,I3,///)
      PRINT 77, IDENT(N)
   77 FORMAT (27H THE RAW DATA FOR ORD NO.          ,I4,2X,
     1 10HFOLLOWS.      ,//)
      K=J-1
      DO 778 J=1,K
      JK=J-1
      M=JEND(J,N)
      IF(J-1)  65,65,66
   65 L=1
      GO TO 69
   66 L=JEND(JK,N)+1
   69 PRINT 79, SCALE(J,N),PEN(J,N)
   79 FORMAT (1H0,15X,14H FULL RANGE=     ,F3.2,50X,13H PEN CENTER=    ,
     1   F3.0,//)
      PRINT 90, ((WAVEL(I,N), DEG(I,N)), I=L,M)
   90 FORMAT (10(I7,F5.0))
      WRITE OUTPUT TAPE3,8,SCALE(J,N),PEN(J,N),MARK(J,N),
     1  JMARK(J,N),PATH(J,N)
    8 FORMAT (F5.2,F5.0,I3,I3,F5.2)
      WRITE OUTPUT TAPE3,9, ((WAVEL(I,N),DEG(I,N)),I=L,M)
    9 FORMAT (10(1X,I6,F4.0))
      WRITE OUTPUT TAPE3,11,NZ
   11 FORMAT (I1)
  778 CONTINUE
      WRITE OUTPUT TAPE3,13,FSCALE
   13 FORMAT (F3.2)
      ENDFILE 3
      N=N+1
      GO TO 50
   78 CONTINUE
C
C     FROM A BASELINE SPECTRUM AND SAMPLE SPECTRUM, STATEMENTS 78 UP TO
C     199 CORRECT FOR A BASELINE SHIFT (IF DESIRED) , COMPUTE MOLAR OR
C     SPECIFIC ROTATION, SMOOTH THE RESULTING CURVE, PRINT THE DATA
```

```
C      FOR THE SMOOTHED CURVE, AND RECORD THEM ON THE SMOOTH SPECTRA
C      MAG TAPE.
C
       DO 143 N=1,8
       IF (IDENT(N)-NS) 143,144,143
  143  CONTINUE
       PRINT 147
  147  FORMAT (95H1NO SPECTRUM HAS THE IDENT NUMBER YOU PUNCHED AT THE
      1 END.  CHECK YOUR TAPE LISTING.                    )
       GO TO 99
  144  NS=N
       DO 145 NL=1,5
       IF (BIDENT(NL)-NB) 145,146,145
  145  CONTINUE
       PRINT 148
  148  FORMAT (95H1NO SPECTRUM HAS THE IDENT NUMBER YOU PUNCHED AT THE
      1 END.  CHECK YOUR TAPE LISTING.                    )
       GO TO 99
  146  NB=NL
       BSHIFT=0.
       L=1
       N=1
       J=1
       K=1
       I=1
   95  IF (BWAVEL(I,NB)-WAVEL(K,NS)) 200,101,300
  300  I=I+1
       GO TO 95
  200  K=K+1
       GO TO 95
  101  NST =K
       IST=I
       IF(J-1) 99,102,131
  102  ADDN=10.*(PEN(J,NS)-BPEN(L,NB))
       IF (MARK(1,NS)-5) 186,108,186
  108  M=1
       KB=K+88
       DO 130 K=NST,KB
       I=IST+(K-NST)
       M=1+(K-NST)
       CORR(M)=(DEG(K,NS)-ADDN)-BDEG(I,NB)
  130  CONTINUE
       NBB=100
       NC=NBB-24
       CALL SMOOTH (NBB,CORR,NC,SHIFT)
       DO 140 I=1,76
       BSHIFT=SHIFT(I)+BSHIFT
  140  CONTINUE
       BSHIFT=BSHIFT/76.
  186  CONTINUE
       IF (JFIN(NS)-1) 141,6000,141
  141  JJ=JFIN(NS)-1
       DO 600 J=1,JJ
       JK=JEND(J,NS)
       IF ((WAVEL(JK,NS)-WAVEL(JK+1,NS))-25) 600,600,172
```

```
  600 CONTINUE
 6000 CONTINUE
      J=1
      K=NST
      I=IST
      GO TO 131
  179 J=J+1
      K=JK+1
      GO TO 95
  131 ADDN=10.*(PEN(J,NS)-BPEN(L,NB))+BSHIFT
  120 ROT(N)=((((DEG(K,NS)-ADDN)-BDEG(I,NB))*SCALE(J,NS))
     1  /(100000.*ABS(NS)))*(EMP(NS))
      WAVEL(N,NS)=WAVEL(K,NS)
      IF (JFIN(NS)-J) 114,114,109
  114 IF (JBFIN(NB)-L) 115,115,105
  109 IF (JBFIN(NB)-L) 117,117,103
  103 IF (JEND(J,NS)-K) 104,104,111
  111 IF(JBEND(L,NB)-I) 106,106,110
  110 I=I+1
      N=N+1
      K=K+1
      GO TO 120
  106 L=L+1
      N=N+1
      I=I+1
      K=K+1
      GO TO 131
  104 IF (JBEND(L,NB)-I) 107,107,112
  112 K=K+1
      N=N+1
      J=J+1
      I=I+1
      GO TO 131
  107 L=L+1
      J=J+1
      K=K+1
      N=N+1
      I=I+1
      GO TO 131
  105 IF (JBEND(L,NB)-I) 116,116,113
  113 IF (JEND(J,NS)-K) 150,150,118
  116 IF (JEND(J,NS)-K) 150,150,106
  115 IF (JEND(J,NS)-K) 150,150,118
  118 IF (JBEND(L,NB)-I) 150,150,110
  117 IF (JBEND(L,NB)-I) 150,150,119
  119 IF (JEND(J,NS)-K) 112,112,110
  150 NN=N
      N=N-24
  160 CALL SMOOTH (NN,ROT,N,PHI)
      IF (JMARK(1,NS)-4) 185,200,185
  800 DO 850 N=1,N
C
C     SPECIFIC ROTATION/1000 IS CALCULATED FROM MOLAR ROTATION/10000
C     BY AN EQUATION OF THE FORM
C     PHI(N) = 1000*PHI(N)/
```

```
C      WHERE M IS THE MOLECULAR WEIGHT OF THE MATERIAL.
C
  850 CONTINUE
  185 WRITE OUTPUT TAPE2,161,MO(NS),MDAY(NS),MYEAR(NS),IDENT(NS)
  161 FORMAT(3I2, I4)
      WRITE OUTPUT TAPE2,261,BIDENT(NB),IDENT(NS)
  261 FORMAT (I4,I4)
      WRITE OUTPUT TAPE2, 170,ABS(NS),EMP(NS)
  170 FORMAT (F6.3,F6.0)
      WRITE OUTPUT TAPE2, 162, ((KWAVEL(I+12),PHI(I)), I=1,M)
  162 FORMAT (10(I6,F6.3))
  180 CONTINUE
  163 PRINT 164, MO(NS),MDAY(NS),MYEAR(NS),IDENT(NS)
  164 FORMAT (10H1DATE=        , I3, I3, I3, 50X, 12HEXPT. NO.        ,
     1    I4,//)
      PRINT 264, BIDENT(NB)
  264 FORMAT (45H0THE BASELINE FOR THIS SPECTRUM HAS IDENT NO.        ,
     1   I8,//)
      PRINT 460, EMP(NS),ABS(NS)
  460 FORMAT (25H0EXTINCTION COEFFICIENT=      ,F6.0,50X,
     1    13H ABSORPTION=      ,F6.3,//)
      IF (MARK(1,NS)-5) 862,865,862
  865 BSHIFT=BSHIFT/1000.
      PRINT 863, BSHIFT
  863 FORMAT (50X,25H THE BASELINE SHIFT IS       ,F8.3,//)
  862 IF (JMARK(1,NS)-4) 440,860,440
  860 CONTINUE
      PRINT 864
  864 FORMAT (50X,6HLAMBDA     ,3X,
     1    36H SPECIFIC ROTATION PER GRAM / 1000      ,///)
      GO TO 168
  440 PRINT 165
  165 FORMAT (50X,6HLAMBDA    ,3X,12HPHI / 10,000      ,///)
  168 NWAVEL=KWAVEL(5,NS)/2
      IF (NWAVEL-(KWAVEL(6,NS)/2)-2) 99,166,167
  166 LBG=14
      GO TO 169
  167 LBG=13
  169 M=M+12
      NCOL=M/5
      IF ((NCOL+1)/2-NCOL/2) 99,188,187
  187 NCOL = NCOL-1
  188 CONTINUE
      NSTOP = LBG+ NCOL
  183 PRINT 181, ((KWAVEL(L,NS),PHI(L-12)), L=LBG,M,NCOL)
  181 FORMAT (5(I15, F10.3))
      LBG=LBG+2
      IF (LBG-NSTOP) 183,183,184
  184 CONTINUE
      ENDFILE 2
C
C     STATEMENT 199 READS IN IDENTS OF BASELINE AND SAMPLE SPECTRA
C     FROM WHICH AN ORD CURVE IS TO BE CALCULATED.  THESE NUMBERS ARE
C     RECORDED AT THE END OF A SERIES OF SPECTRA AND AFTER THE TWO
C     RECORDS IN WHICH IDENT = 0.  FOR BEGINNING NEW SERIES OF SPECTRA
```

```
C     NB = 0 AND NS IS NOT EQUAL TO 0.  TO EXIT FINALLY NB = 0 AND
C     NS = 0.
C
  199 READ INPUT TAPE1, 201, NB,NS
  201 FORMAT (1X,I4,1X,I4)
      IF (NB) 78,299,78
  299 IF (NS) 1000,99,1000
   99 ENDFILE 2
      ENDFILE 3
      STOP
      END
C
C
      SUBROUTINE SMOOTH (N,ODATA,M,DATA)
      DIMENSION ODATA(800),DATA(800),P(25)
C
C     THIS SUBROUTINE SMOOTHES THE RAW DATA BY FITTING IT TO A 25
C     POINT CUBIC EQUATION.  THE COEFFICIENTS AND FORTRAN PROGRAM ARE
C     FROM SAVITZKY AND GOLAY, ANALYTICAL CHEM VOL 36, 1627 (1964).
C
      M=N-24
      DO 10  I=2,25
      J=I-1
   10 P(I)=ODATA(J)
      DO 200  I=1,M
      J=I+24
      DO 11 K=1,24
      KA= K+1
   11 P(K)=P(KA)
      P(25)=ODATA(J)
      SUM=467.*P(13)+462.*(P(12)+P(14))
     1  +447.*(P(11)+P(15))+422.*(P(10)+P(16))+387.*(P(9)+P(17))
     2   +322.*(P(8)+P(18))+287.*(P(7)+P(19))+222.*(P(6)+P(20))
     3.   +147.*(P(5)+P(21))+62.*(P(4)+P(22))-33.*(P(3)+P(23))
     4.  -138.*(P(2)+P(24))-253.*(P(1)+P(25))
      DATA(I)=SUM/5175.
  200 CONTINUE
      RETURN
      END
```

APPENDIX D

Coefficients for Calculating ORD of Dinucleoside Phosphates and Nucleotides as a Function of Temperature.

For several wavelengths the temperature dependence of the molar rotation per residue of each of the 16 dinucleoside phosphates and 4 monomers of A, U, C, and G has been fit to a polynomial of the highest power up to a cubic that would not give any maxima or minima between 0°C and 100°C. The experimental data of Dr. R. Davis[109] have been used for all compounds except GpG, where a calculated temperature dependence of the ORD has been used. See text for details of this calculation. The polynomial has the following form:

$$[\phi] \times 10^{-4} = A + BT + CT^2 + DT^3$$

where T is the temperature in °C. The coefficients A, B, C, and D for a least-squares fit are given in the following pages for every 2.5 mμ between 230 and 330 mμ for all 20 compounds. The average standard deviation as defined in the text for all wavelengths of all 16 dimers in units of molar rotation is 0.04×10^4. For the monomers it is 0.03×10^4.

		A	B	C	D
330.0	AA	1.1041313E-01	-4.3034480E-03	8.1684324E-05	-5.2875662E-07
327.5	AA	1.2831304E-01	-3.3505268E-03	4.5111331E-05	-2.4359572E-07
325.0	AA	1.3325639E-01	-2.6292880E-03	2.7004974E-05	-1.4043785E-07
322.5	AA	1.3863625E-01	-2.5034613E-03	2.3696586E-05	-1.3157850E-07
320.0	AA	1.4502591E-01	-2.7903780E-03	2.7559396E-05	-1.5513167E-07
317.5	AA	1.5732990E-01	-2.4291746E-03	1.3427609E-05	-4.9258833E-08
315.0	AA	1.6854865E-01	-2.7893665E-03	1.7160514E-05	-6.1725207E-08
312.5	AA	1.8356031E-01	-3.1182260E-03	1.9816014E-05	-7.2474930E-08
310.0	AA	2.0023332E-01	-3.7501854E-03	3.4381103E-05	-1.8519013E-07
307.5	AA	2.2266578E-01	-4.5464766E-03	4.7434558E-05	-2.6531497E-07
305.0	AA	2.5658582E-01	-5.9963158E-03	7.2316582E-05	-4.1287551E-07
302.5	AA	3.0128334E-01	-6.0049402E-03	4.2037916E-05	-1.2575928E-07
300.0	AA	3.6318591E-01	-4.6907454E-03	-3.0852227E-05	4.5027800E-07
297.5	AA	4.3960854E-01	-7.6032921E-03	3.2089882E-05	0.
295.0	AA	5.4166749E-01	-9.7301059E-03	4.0080276E-05	0.
292.5	AA	6.6375828E-01	-1.2635755E-02	5.7120481E-05	0.
290.0	AA	8.2677856E-01	-1.5967418E-02	7.2979413E-05	0.
287.5	AA	1.0486284E+00	-2.0280158E-02	9.3436322E-05	0.
285.0	AA	1.4135778E+00	-3.0637742E-02	2.4141321E-04	-8.9364578E-07
282.5	AA	1.5843726E+00	-3.3925124E-02	3.0769231E-04	-1.5237275E-06
280.0	AA	1.4286723E+00	-3.3124864E-02	2.9502609E-04	-1.2946143E-06
277.5	AA	1.0278311E+00	-2.9231873E-02	3.3540595E-04	-1.7760157E-06
275.0	AA	3.0912933E-01	-1.3792126E-02	1.8738722E-04	-1.1279138E-06
272.5	AA	-7.1801880E-01	7.8103601E-03	-3.8923425E-05	0.
270.0	AA	-1.7703085E+00	2.5065302E-02	-8.4209809E-05	-4.5642923E-07
267.5	AA	-2.7364146E+00	5.0533944E-02	-4.3098167E-04	1.4638075E-06
265.0	AA	-3.7663058E+00	6.4986954E-02	-3.5775535E-04	3.0214982E-08
262.5	AA	-4.5677565E+00	8.7102051E-02	-6.7825453E-04	1.9124374E-06

		A	B	C	D
260.0	AA	-4.713752EE+0C	8.0973258E-02	-4.1050906E-04	-8.1950279E-08
257.5	AA	-4.3853381E+CC	7.4115417E-02	-3.2565760E-04	-2.5202071E-07
255.C	AA	-2.8428376E+CC	3.6243731E-02	1.2666235E-C4	-2.5011855E-06
252.5	AA	-1.6238556E+CC	2.8446225E-02	-9.6379530E-05	-4.0803793E-07
250.0	AA	-3.7052671E-C1	1.C869140E-02	-9.7151098E-05	2.7926772E-07
247.5	AA	7.4751359E-C1	-1.441446CE-02	2.C092988E-04	-1.3984952E-06
245.0	AA	1.3273927E+CC	-1.4715517E-02	-9.9554211E-05	1.3935248E-06
242.5	AA	1.621C756E+C0	-1.64168C5E-02	-2.6232706E-C5	4.2317608E-07
240.C	AA	1.6883411E+CC	-1.3596995E-02	-1.1899133E-04	1.0826794E-06
237.5	AA	1.5450471E+CC	-3.6875352E-03	-3.7661635E-04	3.0615128E-06
235.0	AA	1.1113565E+0C	-1.6C179C8E-03	-9.4489160E-05	0.
232.5	AA	5.8888510E-01	-4.E618155E-03	-4.1316012E-C5	C.
230.0	AA	9.9930534E-01	-5.8516318E-03	-9.3541208E-05	5.1895568E-07
330.C	AU	-5.8773113E-C3	1.2849365E-03	-1.2914555E-C5	-3.1320874E-C8
327.5	AU	-6.C412052E-C3	1.380C263E-03	-1.1666255E-C5	-6.8863931E-08
325.0	AU	-7.26C4947E-03	1.6767822E-03	-1.2C8610CE-05	-1.1094767E-07
322.5	AU	-3.85C8701E-03	1.7152534E-03	-9.6143425E-06	-1.5365809E-07
32C.0	AU	-1.6541345E-04	1.6323257E-03	-2.5169701E-06	-2.2868020E-07
317.5	AU	1.0135902E-C2	1.5123751E-03	4.5440127E-07	-2.7833504E-07
315.0	AU	2.2989058E-C2	1.2556251E-03	4.5643599E-06	-3.0895928E-07
312.5	AU	4.0240728E-02	4.58C03C3E-04	2.1235300E-C5	-4.1898166E-07
31C.0	AU	5.9791881E-02	-1.26433C0E-04	3.C028790E-05	-4.7C94605E-07
3C7.5	AU	7.3362840E-C2	2.6575821E-04	1.5937533E-05	-3.8151917E-07
3C5.0	AU	1.0025112E-01	-1.4404871E-04	1.6860110E-05	-3.7518950E-07
3C2.5	AU	1.2611776E-C1	-1.1334694E-04	4.2182909E-06	-2.7134248E-07
3CC.0	AU	1.5643946E-01	-2.627S1C1E-04	-1.C480973E-05	-1.2545789E-07
297.5	AU	1.8426C49E-01	7.45367C4E-04	-5.4754322E-05	2.1388959E-07
295.0	AU	2.1546607E-C1	1.2191844E-C3	-8.5117962E-05	4.5440285E-07
292.5	AU	2.6579214E-01	2.14661C0E-03	-1.3896770E-04	8.8551567E-07
290.0	AU	3.68C4772E-C1	-4.1015858E-03	-2.8483057E-C6	C.
287.5	AU	4.6640666E-01	-6.5705592E-03	1.5077099E-05	0.
285.C	AU	6.3806880E-C1	-1.0925717E-02	4.2322700E-C5	0.
282.5	AU	8.1203492E-C1	-1.3991264E-02	5.0257466E-C5	0.

		A	B	C	D
280.0	AU	9.8826093E-01	-1.8415226E-02	7.0357257E-05	0.
277.5	AU	9.6779126E-01	-1.9432963E-02	7.7142279E-05	0.
275.0	AU	7.7710425E-01	-1.6461053E-02	5.4263655E-05	0.
272.5	AU	4.2310745E-01	-8.0303579E-03	-9.6847704E-05	1.0092628E-06
270.0	AU	2.6992164E-02	-7.2666732E-03	-1.6175818E-05	3.9946092E-07
267.5	AU	-4.6021431E-01	-5.3618477E-03	4.8300886E-05	0.
265.0	AU	-1.2159141E+00	7.1608311E-03	-9.5282503E-06	0.
262.5	AU	-1.7865826E+00	2.8373707E-02	-2.8246794E-04	1.0580146E-06
260.0	AU	-1.6932539E+00	1.1649355E-02	0.	0.
257.5	AU	-1.4009016E+00	7.5109500E-03	0.	0.
255.0	AU	-1.1978996E+00	7.5004651E-03	7.8940864E-05	-1.2543698E-06
252.5	AU	-8.5611008E-01	6.0385165E-03	2.5495940E-05	-8.6576808E-07
250.0	AU	-5.6189816E-01	7.3648542E-03	-8.5162293E-05	-5.6223813E-08
247.5	AU	-3.3211729E-01	9.2301812E-03	-1.7542484E-04	5.2834663E-07
245.0	AU	-1.3211864E-01	7.6294508E-03	-1.4337337E-04	2.2568677E-07
242.5	AU	4.5218216E-02	5.9392853E-03	-1.5168485E-04	4.2882736E-07
240.0	AU	1.9533658E-01	3.8059636E-03	-1.3840485E-04	4.3360561E-07
237.5	AU	3.5725601E-01	-3.2131356E-03	-5.7322482E-06	-3.3734192E-07
235.0	AU	4.8479348E-01	-9.2264750E-03	1.0982654E-04	-1.0074988E-06
232.5	AU	5.6317315E-01	-1.3308972E-02	1.8787515E-04	-1.4523064E-06
230.0	AU	5.8373566E-01	-1.3035501E-02	1.6764553E-04	-1.2777631E-06
330.0	AC	1.1642750E-01	5.9463492E-05	-1.3045979E-05	0.
327.5	AC	1.3379334E-01	-2.7502157E-04	-1.0715212E-05	0.
325.0	AC	1.5031995E-01	-5.7390949E-04	-8.8217530E-06	0.
322.5	AC	1.6875926E-01	-6.5289727E-04	-9.8086721E-06	0.
320.0	AC	1.8711170E-01	-4.3537065E-04	-1.4126405E-05	0.
317.5	AC	2.2323685E-01	-1.1878761E-03	-9.2647155E-06	0.
315.0	AC	2.5520493E-01	-1.8240307E-03	-4.1878027E-06	0.
312.5	AC	2.7910547E-01	-1.7199703E-03	-6.8759645E-06	0.
310.0	AC	3.1660439E-01	-2.2016451E-03	-3.9041628E-06	0.
307.5	AC	3.6534566E-01	-3.0767453E-03	4.6624923E-06	0.
305.0	AC	4.2412347E-01	-3.4275268E-03	4.6032417E-06	0.
302.5	AC	4.9014591E-01	-3.7345827E-03	2.1765415E-06	0.

		A	B	C	D
300.0	AC	5.9386399E-01	-4.7405553E-03	2.1775231E-06	0.
297.5	AC	6.8055207E-01	-1.4067852E-03	-1.1708547E-04	8.5809216E-07
295.0	AC	7.9732644E-01	-1.4241115E-03	-1.3600477E-04	5.9075100E-07
292.5	AC	9.8745748E-01	-9.1617077E-03	2.4165532E-05	0.
290.0	AC	1.1075016E+00	-8.8195313E-03	-5.7570176E-05	6.9997483E-07
287.5	AC	1.1928349E+00	-1.1080159E-02	-5.1270214E-05	7.6074237E-07
285.0	AC	1.2370969E+00	-1.5827622E-02	1.7868115E-05	4.3154172E-07
282.5	AC	1.1760736E+00	-1.9447540E-02	7.8010619E-05	1.5716861E-07
280.0	AC	8.9209215E-01	-1.8956923E-02	1.5223459E-04	-5.4346556E-07
277.5	AC	4.4737118E-01	-1.7914573E-02	2.0195067E-04	-8.0008358E-07
275.0	AC	-3.2546185E-01	-2.7751976E-03	3.8504471E-05	0.
272.5	AC	-8.7570804E-01	-1.8676810E-03	1.5857104E-04	-5.5800630E-07
270.0	AC	-1.6192576E+00	2.0087105E-02	-1.6882594E-04	8.5119172E-07
267.5	AC	-2.1307525E+00	2.5279249E-02	-1.4864805E-04	4.7888154E-07
265.0	AC	-2.5255116E+00	3.5346982E-02	-2.6711248E-04	1.0075731E-06
262.5	AC	-2.7417307E+00	4.6632153E-02	-4.7970879E-04	2.2119220E-06
260.0	AC	-2.6455715E+00	5.2048325E-02	-6.8194765E-04	3.7389218E-06
257.5	AC	-2.3705965E+00	4.5706558E-02	-5.6462737E-04	2.8668749E-06
255.0	AC	-2.0708125E+00	3.9364712E-02	-4.7456236E-04	2.3000917E-06
252.5	AC	-1.7250826E+00	2.9683024E-02	-3.2960859E-04	1.4686481E-06
250.0	AC	-1.4713637E+00	2.4542685E-02	-2.9067371E-04	1.4340275E-06
247.5	AC	-1.2437432E+00	1.9787119E-02	-1.8395127E-04	5.9758411E-07
245.0	AC	-1.0232747E+00	1.8037050E-02	-2.1532047E-04	8.6857834E-07
242.5	AC	-8.5967505E-01	1.8714886E-02	-3.0853031E-04	1.6765634E-06
240.0	AC	-6.3508823E-01	1.6601029E-02	-2.8263848E-04	1.3902564E-06
237.5	AC	-3.5404365E-01	1.7100852E-02	-3.6451519E-04	1.9323662E-06
235.0	AC	5.9572848E-02	4.8656946E-03	-9.8118204E-05	0.
232.5	AC	6.1359176E-01	-7.9649445E-03	-1.2854049E-05	0.
230.0	AC	9.5558482E-01	-1.8549216E-02	7.5021078E-05	0.
330.0	AG	1.0052524E-01	-1.3674488E-03	0.	0.
327.5	AG	9.9563000E-02	-1.3255957E-03	0.	0.
325.0	AG	1.0765428E-01	-1.4927879E-03	0.	0.
322.5	AG	1.1537927E-01	-1.6636074E-03	0.	0.

		A	B	C	D
320.0	AG	1.2233C96E-01	-1.78C4925E-03	0.	0.
317.5	AG	1.26C8308E-01	-1.8449535E-03	0.	0.
315.0	AG	1.4290556E-01	-1.9537305E-03	0.	0.
312.5	AG	1.5E64295E-01	-2.2366456E-03	0.	0.
310.0	AG	1.7141140E-01	-2.3874462E-03	0.	0.
307.5	AG	1.866C556E-01	-2.5791758E-03	0.	0.
305.0	AG	2.1889939E-01	-2.941664CE-03	0.	0.
302.5	AG	2.6625327E-01	-3.5027768E-03	0.	0.
300.0	AG	3.0763550E-01	-3.7820536E-03	0.	0.
297.5	AG	3.6826722E-01	-4.3546967E-03	0.	0.
295.0	AG	4.2424927E-01	-5.1913923E-03	0.	0.
292.5	AG	4.9514CC6E-01	-6.3548641E-03	0.	0.
290.0	AG	4.9737892E-01	-6.9303448E-03	0.	0.
287.5	AG	3.486770CE-01	-5.1857460E-03	0.	0.
285.0	AG	1.8193231E-01	-3.837C6C8E-03	0.	0.
282.5	AG	1.002451CE-01	-1.1352512E-02	9.6605245E-05	0.
280.0	AG	-3.32EE919E-01	2.1375016E-03	-1.3474551E-04	1.3637616E-06
277.5	AG	-6.6482635E-01	1.4946922E-03	5.4634563E-06	2.6311262E-07
275.0	AG	-1.1316924E+CC	1.2249450E-02	-9.9612215E-05	6.1878709E-07
272.5	AG	-1.5940117E+00	2.6753505E-02	-3.1185208E-04	1.7695646E-06
270.0	AG	-1.7653414E+00	3.0285555E-02	-3.2263751E-04	1.7346413E-06
267.5	AG	-1.735C547E+CC	3.255795EE-02	-3.6649829E-04	2.2736374E-06
265.0	AG	-1.4491250E+CC	2.6837CCEE-02	-3.9016479E-04	2.5373251E-06
262.5	AG	-8.2053220E-01	7.3795CC6E-03	1.3192826E-05	4.1759519E-08
260.0	AG	-3.5619190E-01	1.4193939E-02	-3.1155935E-04	2.3361081E-06
257.5	AG	2.1511CC6E-C1	-2.6994019E-03	2.9177634E-05	0.
255.0	AG	5.2126862E-01	-2.7375623E-03	0.	0.
252.5	AG	8.20C5119E-01	-5.4111252E-03	0.	0.
250.0	AG	9.5833496E-C1	-6.607C828E-03	0.	0.
247.5	AG	9.3368749E-01	-5.7785328E-03	0.	0.
245.0	AG	9.0349854E-C1	-5.6171319E-03	0.	0.
242.5	AG	8.2909877E-01	-4.8901258E-03	0.	0.
240.0	AG	9.4408061E-01	-2.0931242E-02	1.7722327E-04	0.

		A	B	C	D
237.5	AG	8.2671264E-01	-1.6198633E-02	1.3842162E-04	0.
235.0	AG	5.7649372E-01	-2.8906968E-03	0.	0.
232.5	AG	6.5155520E-01	-4.1017569E-03	0.	0.
230.0	AG	5.7218417E-01	-3.2682411E-03	0.	0.
330.0	UA	5.7623339E-03	1.8406251E-03	-2.0122181E-05	0.
327.5	UA	1.2384096E-02	1.4524554E-03	-1.5373296E-05	0.
325.0	UA	2.1845094E-02	8.8821039E-04	-9.2842379E-06	0.
322.5	UA	1.8693079E-02	1.0052477E-03	-1.0187003E-05	0.
320.0	UA	1.4905577E-02	1.0988950E-03	-1.1478131E-05	0.
317.5	UA	8.8666545E-03	1.0254858E-03	-1.1723260E-05	0.
315.0	UA	1.2014113E-02	9.4370639E-04	-1.1768878E-05	0.
312.5	UA	2.2438632E-02	8.3005054E-04	-1.0717560E-05	0.
310.0	UA	5.1068418E-02	6.8008352E-04	-9.5934982E-06	0.
307.5	UA	6.7417343E-02	3.6056534E-04	-7.1434073E-06	0.
305.0	UA	7.8103536E-02	1.3787161E-04	-5.5548533E-06	0.
302.5	UA	9.9877689E-02	-5.7099089E-04	2.6008898E-07	0.
300.0	UA	9.6713687E-02	-4.1533875E-04	-4.7108669E-06	0.
297.5	UA	1.0369801E-01	-1.0268420E-03	9.6367833E-07	0.
295.0	UA	1.3078829E-01	-1.1771079E-03	1.0038619E-06	0.
292.5	UA	1.7692685E-01	-1.8675156E-03	5.9055596E-06	0.
290.0	UA	2.4433669E-01	-3.2110738E-03	1.6204589E-05	0.
287.5	UA	3.1373016E-01	-3.7724712E-03	1.8845980E-05	0.
285.0	UA	3.7962192E-01	-4.4545629E-03	2.2461683E-05	0.
282.5	UA	4.3738036E-01	-5.7543443E-03	2.9706982E-05	0.
280.0	UA	4.9034489E-01	-8.2705401E-03	7.1160482E-05	-2.7631851E-07
277.5	UA	4.8029550E-01	-7.9681112E-03	5.2535510E-05	-1.5231944E-07
275.0	UA	3.6273817E-01	-4.3270309E-03	-7.8665193E-06	1.5496614E-07
272.5	UA	1.4545109E-01	-1.1330959E-03	-1.2554528E-05	0.
270.0	UA	-1.4287574E-01	3.4600256E-03	-4.2291248E-05	0.
267.5	UA	-5.0288283E-01	9.0745146E-03	-7.2839852E-05	0.
265.0	UA	-8.7945124E-01	1.9932428E-02	-2.8796536E-04	1.4564159E-06
262.5	UA	-1.2181238E+00	3.2663754E-02	-5.3140418E-04	2.8503651E-06
260.0	UA	-1.3104586E+00	3.1896776E-02	-5.4145099E-04	3.0654416E-06

		A	B	C	D
257.5	UA	-1.3050807E+00	2.9510468E-02	-5.0445357E-04	2.9096171E-06
255.0	UA	-1.2183338E+00	2.6292944E-02	-4.5443244E-04	2.7303549E-06
252.5	UA	-1.0976365E+00	2.3083202E-02	-3.7886857E-04	2.2234913E-06
250.0	UA	-9.3435066E-01	1.9082959E-02	-3.0624114E-04	1.7412898E-06
247.5	UA	-7.6661833E-01	1.5569685E-02	-3.3807719E-04	1.9759747E-06
245.0	UA	-4.9770319E-01	6.1026241E-03	-5.6188947E-05	0.
242.5	UA	-3.4626451E-01	4.4873932E-03	-4.9342174E-05	0.
240.0	UA	-2.5297330E-01	7.7594542E-03	-1.5626433E-04	1.6704214E-07
237.5	UA	-1.7547473E-01	4.1564901E-03	-4.8956229E-05	0.
235.0	UA	-1.5493412E-01	3.7967140E-03	-3.7388287E-05	0.
232.5	UA	-1.1976818E-01	3.5926853E-03	-3.4315340E-05	0.
230.0	UA	-7.8354756E-02	3.9916536E-03	-4.0972649E-05	0.
330.0	UU	-3.9997586E-04	4.1529020E-03	-1.6450154E-04	2.1439776E-06
327.5	UU	5.0663636E-03	4.8876837E-03	-1.9286699E-04	2.4109370E-06
325.0	UU	1.9873919E-02	4.1429985E-03	-1.5949843E-04	1.9851540E-06
322.5	UU	2.5764308E-02	5.1275866E-03	-2.0520779E-04	2.5096340E-06
320.0	UU	4.2721676E-02	4.6753866E-03	-1.9029540E-04	2.2996722E-06
317.5	UU	6.5551904E-02	6.2375653E-04	0.	0.
315.0	UU	7.9865665E-02	1.5807693E-03	-2.5534910E-05	0.
312.5	UU	9.8391485E-02	1.5746543E-03	-3.1162227E-05	0.
310.0	UU	1.1736426E-01	3.2259862E-03	-1.2954185E-04	1.2391339E-06
307.5	UU	1.4888876E-01	1.9887842E-03	-8.9419694E-05	7.7404061E-07
305.0	UU	1.8707133E-01	1.2922409E-03	-8.3137998E-05	7.6195959E-07
302.5	UU	2.2384475E-01	8.5547284E-04	-8.5461694E-05	9.4249293E-07
300.0	UU	2.7871023E-01	-1.5988058E-03	-3.4765920E-06	0.
297.5	UU	3.4075945E-01	-1.9312784E-03	-2.7040507E-05	3.7505384E-07
295.0	UU	4.1477633E-01	-3.3166580E-03	1.5015517E-05	0.
292.5	UU	5.2630780E-01	-3.9540456E-03	1.0122485E-05	0.
290.0	UU	6.7913211E-01	-5.7973214E-03	1.2492293E-05	0.
287.5	UU	8.5433466E-01	-1.0867285E-02	6.7576166E-05	0.
285.0	UU	9.6111050E-01	-1.2248094E-02	-1.1721524E-05	1.5279999E-06
282.5	UU	9.1574584E-01	-2.0169388E-02	3.9452417E-04	-2.9832447E-06
280.0	UU	7.4945408E-01	-2.1103195E-02	5.0013892E-04	-3.7217297E-06

		A	B	C	D
277.5	UU	5.166465CE-C1	-1.6777242E-02	3.8765542E-04	-2.8151441E-06
275.0	UU	1.8123630E-01	-8.8273587E-03	1.8464884E-04	-1.0765115E-06
272.5	UU	-2.7233873E-C1	-7.0515323E-03	3.6436506E-04	-3.3167032E-06
27C.C	UU	-8.1679412E-01	6.1232926E-03	1.4918087E-04	-1.6664375E-06
267.5	UU	-1.2C07838E+00	1.0920480E-02	1.8193457E-C4	-2.6617403E-06
265.0	UU	-1.4801626E+00	1.4059671E-02	2.2884167E-05	C.
262.5	UU	-1.6439834E+0C	6.6501952E-03	5.3831962E-04	-7.2336806E-06
26C.C	UU	-1.5974536E+C0	-2.6077497C-03	6.88C4727E-04	-7.9457981E-06
257.5	UU	-1.5219081E+C0	4.1940201E-03	1.0827723E-04	C.
255.C	UU	-1.3587E16E+00	-9.9831223E-03	7.0573415E-04	-6.9012148E-06
252.5	UU	-1.1742006E+00	-1.4087253E-02	8.1806148E-04	-8.0172905E-06
25C.C	UU	-9.73E6C29E-01	-1.4336972E-02	7.5265903E-04	-7.2924668E-06
247.5	UU	-7.8439E0EE-C1	-5.9664511E-03	2.8CC7071E-04	-1.7180190E-06
245.C	UU	-5.2615994E-C1	-1.4738468E-02	5.4576900E-04	-4.7114712E-06
242.5	UU	-3.225E815E-01	-1.7501234E-02	6.2170525E-04	-5.7146699E-06
24C.0	UU	-1.6710551E-C1	-1.4937579E-02	4.8CC7501E-04	-4.1406798E-06
237.5	UU	-2.9555482E-02	-1.3395SC4E-02	2.2021076E-C4	C.
235.C	UU	8.5141150E-C2	-1.7022883E-02	2.7627704E-04	C.
232.5	UU	2.0633772E-C1	-3.1227751E-02	9.2991804E-04	-7.9867292E-06
23C.C	UU	2.0929201E-01	-2.6307123E-02	7.3639801E-04	-5.8258837E-06
33C.C	UC	1.1140182E-C1	4.7221046E-03	-8.2094201E-05	3.44C5079E-07
327.5	UC	1.3476446E-01	3.8300582E-03	-6.6650340E-05	2.6566992E-07
325.0	UC	1.5962162E-C1	3.1496960E-03	-5.76C6046E-05	2.2848942E-07
322.5	UC	1.7152516E-C1	3.7663674E-03	-7.5907079E-05	3.5099120E-07
32C.0	UC	1.9348127E-C1	3.5195180E-03	-7.3989298E-05	3.4425821E-07
317.5	UC	2.1472933E-01	3.3043034E-03	-7.0863199E-05	3.2041448E-07
315.0	UC	2.3971773E-C1	2.8181515E-03	-6.1726297E-05	2.6C912C4E-07
312.5	UC	2.7097352E-C1	2.1853836E-03	-5.1770408E-05	1.9888562E-07
31C.0	UC	3.0281649E-C1	2.6347653E-03	-7.2985409E-05	3.8241095E-07
307.5	UC	3.8622521E-01	-1.5318071E-04	-2.2905728E-05	8.6506639E-08
305.0	UC	4.4284651E-C1	-5.1851723E-05	-3.8196483E-05	2.1442515E-07
302.5	UC	5.2562775E-01	-1.3361860E-03	-1.7468236E-05	9.6400778E-08
3CC.0	UC	6.3238734E-C1	-2.1805141E-03	-1.2844891E-05	7.1086894E-08

		A	B	C	D
257.5	UC	7.6251592E-01	-3.6095577E-03	-1.0142677E-05	1.3026607E-07
255.0	UC	9.4895961E-01	-7.4555746E-03	4.9422388E-05	-2.3617724E-07
252.5	UC	1.1564007E+00	-1.0524169E-02	6.8573601E-05	-2.6436874E-07
250.0	UC	1.3628558E+00	-1.6196846E-02	1.3500764E-04	-5.1739804E-07
247.5	UC	1.4106915E+00	-1.7307068E-02	1.4955746E-04	-5.9519593E-07
245.0	UC	1.2609384E+00	-1.1207115E-02	3.8460728E-05	3.4968394E-08
242.5	UC	9.7528388E-01	-3.8983204E-03	-6.0909332E-05	5.1893972E-07
240.0	UC	6.1617523E-01	-1.1618459E-03	-2.0477394E-05	0.
237.5	UC	1.7362081E-01	4.4792921E-03	-4.5150965E-05	0.
235.0	UC	-3.0159566E-01	1.1365481E-02	-8.5733768E-05	0.
232.5	UC	-8.8715190E-01	2.7586083E-02	-3.7916663E-04	1.8299436E-06
230.0	UC	-1.2800241E+00	2.8364727E-02	-3.2507534E-04	1.4456241E-06
227.5	UC	-1.5859613E+00	3.3482354E-02	-4.2174574E-04	2.0868636E-06
225.0	UC	-1.7696028E+00	3.5382552E-02	-4.5787582E-04	2.2739639E-06
222.5	UC	-1.8248664E+00	2.8882377E-02	-2.7966058E-04	5.8136002E-07
220.0	UC	-1.8127799E+00	2.3352052E-02	-1.5925299E-04	6.1536763E-07
217.5	UC	-1.6111347E+00	8.0975677E-03	0.	0.
215.0	UC	-1.6564717E+00	1.4176408E-02	-7.6126432E-05	0.
212.5	UC	-1.5875633E+00	1.4318126E-02	-9.0365396E-05	-4.7122038E-08
210.0	UC	-1.5640112E+00	1.9293703E-02	-1.9903849E-04	5.6925556E-07
207.5	UC	-1.3836692E+00	1.2887762E-02	-7.9544115E-05	-8.3081717E-08
205.0	UC	-1.1376194E+00	4.0911062E-03	0.	0.
202.5	UC	-1.0812248E+00	1.0101265E-02	-1.1363126E-04	4.7642178E-07
200.0	UC	-9.4036442E-01	9.3982209E-03	-1.3408059E-04	7.0962608E-07
197.5	UC	-8.9646545E-01	1.5566026E-02	-3.8934587E-04	2.3306820E-06
195.0	UC	-6.7599406E-01	6.2060475E-03	-5.8011854E-05	0.
192.5	UC	-5.5722668E-01	3.7174037E-03	-3.0698686E-05	7.7053531E-08
190.0	UC	-5.8571388E-01	2.6637274E-03	-1.0494790E-05	0.
330.0	UG	6.4285063E-02	3.7248582E-04	-8.4432053E-06	0.
327.5	UG	7.1759022E-02	4.6583268E-05	-4.1550418E-06	0.
325.0	UG	6.7231236E-02	7.3727210E-04	-2.4890898E-05	1.8391964E-07
322.5	UG	6.9589185E-02	5.9271289E-04	-1.4410544E-05	7.8927068E-08
320.0	UG	7.6503344E-02	7.1538633E-04	-1.4630163E-05	5.0813626E-08

		A	B	C	D
317.5	UG	9.3244882E-02	-9.3970381E-06	8.7365735E-07	-7.1428614E-08
315.0	UG	1.2673967E-01	-2.2176734E-03	5.4314820E-05	-4.6909068E-07
312.5	UG	1.3817556E-01	-3.1421758E-03	8.1498129E-05	-6.8264086E-07
310.0	UG	1.4604217E-01	-3.3975926E-03	8.3741319E-05	-6.4540562E-07
307.5	UG	1.5834579E-01	-2.9908352E-03	6.0913046E-05	-4.1438894E-07
305.0	UG	1.6667464E-01	-2.2873666E-03	3.5174743E-05	-2.5497127E-07
302.5	UG	2.3469779E-01	-5.4576057E-03	9.7045454E-05	-5.9304242E-07
300.0	UG	3.0214765E-01	-7.1244054E-03	1.1741950E-04	-6.9751836E-07
297.5	UG	3.4606621E-01	-5.7562507E-03	6.3941487E-05	-3.0154530E-07
295.0	UG	4.1344529E-01	-8.1330429E-03	1.0553939E-04	-5.5545202E-07
292.5	UG	4.5391754E-01	-8.1931047E-03	8.6729558E-05	-3.8386471E-07
290.0	UG	4.7487151E-01	-9.4604573E-03	1.1344543E-04	-5.4792575E-07
287.5	UG	4.1480709E-01	-8.7832927E-03	1.2913106E-04	-7.2426343E-07
285.0	UG	2.4660084E-01	-2.7808454E-03	2.7189228E-07	2.8550425E-07
282.5	UG	-4.8868130E-03	1.1079228E-03	-1.4671604E-05	2.3545501E-07
280.0	UG	-2.2545188E-01	2.9564855E-03	0.	0.
277.5	UG	-4.2066277E-01	4.3433418E-03	0.	0.
275.0	UG	-6.2134689E-01	6.2554049E-03	0.	0.
272.5	UG	-7.8876608E-01	7.4914139E-03	0.	0.
270.0	UG	-9.5597524E-01	1.4350288E-02	-2.7193054E-05	-6.3129017E-07
267.5	UG	-9.0268793E-01	1.2442047E-02	-6.5866141E-05	0.
265.0	UG	-6.6110062E-01	-7.0166406E-03	4.1492712E-04	-3.4919848E-06
262.5	UG	-4.9782246E-01	-7.1495029E-03	3.3059068E-04	-2.7310406E-06
260.0	UG	-2.6532670E-01	-8.4112068E-03	2.5978399E-04	-2.0331648E-06
257.5	UG	-1.0175255E-01	-8.7478759E-03	2.7181733E-04	-2.2883810E-06
255.0	UG	-8.7044444E-02	-1.0730776E-03	4.6183392E-05	-6.5671002E-07
252.5	UG	-1.1092735E-01	3.4572489E-03	-6.9674847E-05	1.7951675E-07
250.0	UG	-7.6201101E-02	3.0763508E-03	-7.1312044E-05	1.9848602E-07
247.5	UG	-1.1703209E-01	3.7331152E-03	-6.9115128E-05	1.2489521E-07
245.0	UG	-9.1551715E-02	-7.6232709E-03	3.1618578E-04	-2.8319843E-06
242.5	UG	-6.9054034E-02	-9.4220631E-03	3.2540344E-04	-2.6831314E-06
240.0	UG	-7.4839465E-02	-9.7849716E-03	3.4560311E-04	-2.6943509E-06
237.5	UG	-7.0147607E-02	-8.9213459E-03	3.4516301E-04	-2.6968844E-06

		A	B	C	D
235.0	UG	-1.2849345E-01	9.4740953E-04	1.7145920E-05	0.
232.5	UG	-1.0670732E-01	2.1156923E-03	2.8517349E-06	0.
230.0	UG	-4.9731226E-02	-5.6205755E-03	3.2427298E-04	-2.8512599E-06
330.0	CA	1.7266691E-01	-4.2773965E-03	8.6682401E-05	-5.4061547E-07
327.5	CA	1.8978026E-01	-5.1118481E-03	1.0196145E-04	-6.3006894E-07
325.0	CA	1.9855104E-01	-5.0073831E-03	9.1611820E-05	-5.4807432E-07
322.5	CA	2.1455172E-01	-4.3801341E-03	7.1476088E-05	-4.1745070E-07
320.0	CA	2.2226033E-01	-3.4924541E-03	4.8312616E-05	-2.6602207E-07
317.5	CA	2.4057870E-01	-3.9405604E-03	5.3745267E-05	-2.8210814E-07
315.0	CA	2.7955552E-01	-5.5861967E-03	9.5810022E-05	-5.6826287E-07
312.5	CA	3.0267553E-01	-6.3881470E-03	1.1667351E-04	-7.2347324E-07
310.0	CA	3.2219291E-01	-6.1882235E-03	1.0174374E-04	-5.9224908E-07
307.5	CA	3.6173384E-01	-7.5855869E-03	1.3209476E-04	-7.9076537E-07
305.0	CA	4.0271506E-01	-7.8272319E-03	1.5120752E-04	-9.9585354E-07
302.5	CA	4.9585417E-01	-8.7512444E-03	1.3924474E-04	-8.1328636E-07
300.0	CA	6.1047037E-01	-1.2425428E-02	2.0987076E-04	-1.2323465E-06
297.5	CA	7.1919516E-01	-1.4673227E-02	2.6375799E-04	-1.6297603E-06
295.0	CA	8.5527475E-01	-1.4238030E-02	2.0823222E-04	-1.1714595E-06
292.5	CA	1.0203461E+00	-1.7104681E-02	2.3443072E-04	-1.2923788E-06
290.0	CA	1.1736540E+00	-2.0026864E-02	2.4402389E-04	-1.2284342E-06
287.5	CA	1.2209529E+00	-1.9487652E-02	1.7327546E-04	-6.1810358E-07
285.0	CA	1.1651611E+00	-2.1613288E-02	2.5463749E-04	-1.3015211E-06
282.5	CA	5.7528813E-01	-1.6770925E-02	1.3731372E-04	-4.7474780E-07
280.0	CA	5.8643521E-01	-9.1970320E-03	4.8691147E-05	0.
277.5	CA	1.3627780E-01	-4.8348073E-03	5.9116036E-05	-2.5619667E-07
275.0	CA	-4.3173640E-01	5.1101063E-03	-2.4325643E-05	0.
272.5	CA	-5.4707322E-01	7.7062121E-03	0.	0.
270.0	CA	-1.4391174E+00	1.2097024E-02	0.	0.
267.5	CA	-1.6664585E+00	1.5815034E-02	0.	0.
265.0	CA	-2.3637891E+00	3.4745006E-02	-1.8653203E-04	0.
262.5	CA	-2.4336591E+00	3.5309903E-02	-2.1437723E-04	2.5245602E-07
260.0	CA	-2.3202046E+00	3.2836024E-02	-2.1819906E-04	3.7282048E-07
257.5	CA	-2.1519374E+00	3.4642576E-02	-3.4690919E-04	1.3156247E-06

		A	B	C	D
255.0	CA	-1.8682264E+00	2.6109003E-02	-2.3929418E-04	7.9624077E-07
252.5	CA	-1.6145700E+00	1.6414711E-02	-8.7287866E-05	0.
250.0	CA	-1.5165040E+00	1.6138866E-02	-8.6705488E-05	0.
247.5	CA	-1.4002705E+00	1.3806801E-02	-7.3436326E-05	0.
245.0	CA	-1.3276480E+00	1.0085077E-02	-4.0085155E-05	0.
242.5	CA	-1.2804383E+00	1.1230961E-02	-5.6265237E-05	0.
240.0	CA	-1.1811183E+00	9.6364053E-03	-5.0957717E-05	0.
237.5	CA	-9.0267070E-01	3.8740750E-03	-1.3042205E-05	0.
235.0	CA	-4.8630064E-01	-4.9872439E-03	4.4784122E-05	0.
232.5	CA	-1.1447834E-01	-1.8926597E-02	3.4621411E-04	-2.1200405E-06
230.0	CA	1.6585243E-01	-2.0787948E-02	3.0573057E-04	-1.6253875E-06
330.0	CU	3.7667039E-01	-7.8133800E-03	1.0331673E-04	-5.3999913E-07
327.5	CU	4.0388960E-01	-8.2949567E-03	1.0814002E-04	-5.6063397E-07
325.0	CU	4.2858535E-01	-8.6385056E-03	1.1141001E-04	-5.7815430E-07
322.5	CU	4.5271845E-01	-8.7314829E-03	1.0908551E-04	-5.4476559E-07
320.0	CU	4.7411627E-01	-7.8957581E-03	8.5011301E-05	-3.8391628E-07
317.5	CU	4.9011158E-01	-6.6026457E-03	5.0814423E-05	-1.5772128E-07
315.0	CU	5.2600169E-01	-6.8303257E-03	6.1632260E-05	-2.8487597E-07
312.5	CU	6.0111775E-01	-9.1998951E-03	9.8347093E-05	-4.6606408E-07
310.0	CU	6.5348188E-01	-9.7905582E-03	1.0518830E-04	-4.9324422E-07
307.5	CU	7.2677276E-01	-9.9068712E-03	8.6848701E-05	-3.2550452E-07
305.0	CU	8.2322735E-01	-1.1380865E-02	1.0346752E-04	-4.0608380E-07
302.5	CU	9.7719258E-01	-1.6233063E-02	1.5965530E-04	-1.0014057E-06
300.0	CU	1.1411786E+00	-1.6352412E-02	1.5737474E-04	-6.4641391E-07
297.5	CU	1.3387191E+00	-1.8246440E-02	1.6193482E-04	-6.4282279E-07
295.0	CU	1.6517161E+00	-2.4362834E-02	2.2966865E-04	-9.1316804E-07
292.5	CU	2.0304191E+00	-3.1925264E-02	2.8929732E-04	-1.0394715E-06
290.0	CU	2.2972257E+00	-4.0946670E-02	4.0453645E-04	-2.4169115E-06
287.5	CU	2.2870976E+00	-3.6376683E-02	3.3231670E-04	-1.2975782E-06
285.0	CU	2.0745598E+00	-3.6415857E-02	3.6360025E-04	-1.6400072E-06
282.5	CU	1.4405191E+00	-1.7892500E-02	9.8455128E-05	0.
280.0	CU	7.4121703E-01	-7.1862166E-03	3.5265096E-05	0.
277.5	CU	4.9844337E-02	3.0930523E-03	-7.8149798E-05	6.9060164E-07

		A	B	C	D
275.0	CU	-8.3529063E-01	2.2279774E-02	-3.3665353E-04	2.0573756E-06
272.5	CU	-1.5736084E+00	2.5056756E-02	-1.5459982E-04	3.0525637E-07
270.0	CU	-2.1625247E+00	3.3608257E-02	-2.3211437E-04	6.1315434E-07
267.5	CU	-2.8152822E+00	7.9694418E-02	-1.7533404E-03	1.4315296E-05
265.0	CU	-2.8046136E+00	4.3404334E-02	-4.1544413E-04	1.7013586E-06
262.5	CU	-2.7807835E+00	4.0412422E-02	-4.1718664E-04	1.8924422E-06
260.0	CU	-2.6992043E+00	3.3311316E-02	-3.1850578E-04	1.4825648E-06
257.5	CU	-2.5635206E+00	2.9738244E-02	-3.2566541E-04	1.7625472E-06
255.0	CU	-2.3861292E+00	2.1047713E-02	-1.6365869E-04	6.9654669E-07
252.5	CU	-2.2466771E+00	1.7508330E-02	-1.3252659E-04	5.6589254E-07
250.0	CU	-2.1380405E+00	1.4306365E-02	-9.9474004E-05	4.8730964E-07
247.5	CU	-1.9945005E+00	1.6072268E-02	-1.6863339E-04	1.1532968E-06
245.0	CU	-1.6872853E+00	5.7894368E-03	-3.4377481E-05	4.2276923E-07
242.5	CU	-1.5544628E+00	1.0465598E-02	-1.7810904E-04	1.3957939E-06
240.0	CU	-1.3555162E+00	1.4779805E-02	-3.1383296E-04	2.2202158E-06
237.5	CU	-1.0496743E+00	3.2788858E-03	-6.8531364E-05	5.9502625E-07
235.0	CU	-7.0774093E-01	-6.4455403E-03	8.8759187E-05	-3.7124858E-07
232.5	CU	-4.2201603E-01	-1.2431220E-02	1.3498927E-04	-2.3711241E-07
230.0	CU	-2.2883875E-01	-1.4591257E-02	1.7531079E-04	-7.0554954E-07
330.0	CC	2.8184472E-01	-4.0784036E-03	2.1828084E-05	-1.9103755E-08
327.5	CC	3.0336762E-01	-4.7485015E-03	4.6410857E-05	-2.5288444E-07
325.0	CC	3.4141069E-01	-5.5248806E-03	5.6868629E-05	-2.8807938E-07
322.5	CC	3.7115169E-01	-4.9654407E-03	2.6896574E-05	3.4696058E-08
320.0	CC	4.0906237E-01	-4.8783730E-03	1.5785559E-05	1.3077851E-07
317.5	CC	4.7360804E-01	-6.6076252E-03	3.2182717E-05	1.2813448E-07
315.0	CC	5.7513873E-01	-1.2147279E-02	1.9127218E-04	-1.2393189E-06
312.5	CC	6.3864805E-01	-1.4935748E-02	2.9407034E-04	-2.2332060E-06
310.0	CC	7.1507298E-01	-1.3302616E-02	2.1471689E-04	-1.3385648E-06
307.5	CC	8.1115744E-01	-1.3446582E-02	2.1005968E-04	-1.4141791E-06
305.0	CC	9.4602650E-01	-1.5212842E-02	2.0121194E-04	-1.1454455E-06
302.5	CC	1.1333091E+00	-1.5135968E-02	1.5893721E-04	-1.4307708E-06
300.0	CC	1.3938347E+00	-1.4551608E-02	6.2597027E-05	7.4723608E-08
297.5	CC	1.7176446E+00	-1.7124436E-02	3.1181969E-05	9.0883347E-07

		A	B	C	D
255.0	CC	2.0958627E+00	-2.2668439E-02	6.6666290E-05	3.2008866E-07
252.5	CC	2.4292593E+00	-2.7284989E-02	2.6839882E-05	1.1525675E-06
250.0	CC	2.4390546E+00	-2.5714138E-02	-9.7573234E-05	2.6253536E-06
247.5	CC	1.9807445E+00	-2.7587628E-02	2.0158561E-04	-2.5815858E-07
245.0	CC	1.3169143E+00	-2.5441514E-02	3.6760000E-04	-1.9538225E-06
242.5	CC	5.0662287E-01	-9.6052256E-03	1.6747534E-04	-1.0733278E-06
240.0	CC	-3.4767014E-01	2.7352175E-03	1.2048899E-04	-1.2073615E-06
237.5	CC	-1.1675835E+00	7.9074655E-03	2.4726489E-04	-2.2212404E-06
235.0	CC	-1.6763837E+00	1.5874252E-02	2.3243841E-04	-2.3165676E-06
232.5	CC	-2.4951527E+00	2.1140682E-02	3.8138632E-04	-4.6361091E-06
230.0	CC	-2.7332065E+00	1.4871318E-02	6.7311137E-04	-7.2913341E-06
227.5	CC	-2.6866366E+00	1.8685129E-02	4.0738104E-04	-4.7718249E-06
225.0	CC	-2.5135324E+00	1.0952259E-02	4.6952390E-04	-4.8750061E-06
222.5	CC	-2.3226473E+00	1.9616684E-02	-4.1208842E-05	C.
220.0	CC	-2.0836083E+00	1.4618466E-02	-2.6802655E-05	C.
217.5	CC	-1.9065797E+00	1.1195254E-02	-1.5914817E-05	C.
215.0	CC	-1.6838679E+00	-1.1836177E-03	2.2866642E-04	-1.8500763E-06
212.5	CC	-1.5597999E+00	5.3955701E-04	4.3627952E-05	C.
210.0	CC	-1.5777318E+00	-1.1971205E-03	7.0409958E-05	C.
207.5	CC	-1.5110711E+00	-1.2708364E-02	3.6037656E-04	-1.7730065E-06
205.0	CC	-1.5665813E+00	-1.1199447E-02	4.5545015E-04	-3.4797532E-06
202.5	CC	-1.5546888E+00	-9.6040342E-03	3.2494386E-04	-1.9500140E-06
200.0	CC	-1.6044691E+00	-4.3893385E-03	1.9826346E-04	-1.1398215E-06
197.5	CC	-1.5174716E+00	-1.6966514E-03	6.8074816E-05	1.6460908E-07
195.0	CC	-1.3197455E+00	-4.9837355E-03	1.3091942E-04	-5.7451761E-07
192.5	CC	-1.0819955E+00	-7.6006132E-03	1.6046728E-04	-7.7079102E-07
190.0	CC	-9.4728818E-01	7.6885715E-04	-1.5555215E-04	2.0677454E-06
330.0	CG	1.2047754E-01	-9.4939565E-04	0.	0.
327.5	CG	1.3822680E-01	-1.0537644E-03	0.	0.
325.0	CG	1.5902350E-01	-1.2091025E-03	0.	0.
322.5	CG	1.7678114E-01	-1.3136859E-03	0.	0.
320.0	CG	1.8432457E-01	-1.2304334E-03	0.	0.
317.5	CG	2.2293656E-01	-1.5553906E-03	0.	0.

		A	B	C	D
315.0	CG	2.7268369E-01	-2.0275256E-03	0.	0.
312.5	CG	3.0623666E-01	-2.2569950E-03	0.	0.
310.0	CG	3.6420224E-01	-5.5827954E-03	6.0517394E-05	-2.1095438E-07
307.5	CG	4.1350418E-01	-6.0854917E-03	5.2576784E-05	-1.4329062E-07
305.0	CG	4.7193882E-01	-6.5864789E-03	5.5634456E-05	-1.5449186E-07
302.5	CG	5.8502434E-01	-7.6136221E-03	5.1667720E-05	-6.3891877E-08
300.0	CG	7.0446357E-01	-9.9128706E-03	8.6680284E-05	-2.9135658E-07
297.5	CG	8.6038614E-01	-1.2775371E-02	1.2061689E-04	-4.6832171E-07
295.0	CG	1.0353781E+00	-1.7225421E-02	1.7938158E-04	-7.2914509E-07
292.5	CG	1.1008526E+00	-1.7493360E-02	1.7588775E-04	-7.4539134E-07
290.0	CG	9.9322590E-01	-1.4333526E-02	1.2978469E-04	-4.6718387E-07
287.5	CG	6.6366576E-01	-7.0015965E-03	3.6084864E-05	0.
285.0	CG	2.1807551E-01	2.3885913E-03	-1.0542462E-04	8.7109230E-07
282.5	CG	-2.4758071E-01	1.5319655E-02	-3.0294392E-04	1.9426522E-06
280.0	CG	-6.7858493E-01	2.4730159E-02	-4.1745196E-04	2.4456786E-06
277.5	CG	-1.0090179E+00	2.6557028E-02	-3.6400487E-04	1.8563020E-06
275.0	CG	-1.2372575E+00	2.0329450E-02	-1.5400822E-04	4.3930391E-07
272.5	CG	-1.3291577E+00	1.7902570E-02	-1.1138169E-04	2.3558097E-07
270.0	CG	-1.3554423E+00	1.5153034E-02	-8.5953822E-05	2.5326156E-07
267.5	CG	-1.3119091E+00	1.4976975E-02	-1.4674281E-04	7.2098349E-07
265.0	CG	-1.1523478E+00	7.7507652E-03	-7.4442765E-05	4.9724217E-07
262.5	CG	-1.0896105E+00	4.9173307E-03	-6.1025007E-05	5.2639007E-07
260.0	CG	-1.0299742E+00	6.1278032E-04	1.6674171E-05	5.2009824E-08
257.5	CG	-1.0305276E+00	1.7922661E-04	3.8910322E-05	-1.6778959E-07
255.0	CG	-1.0323151E+00	6.2499165E-03	-1.0876603E-04	7.8553288E-07
252.5	CG	-9.5483233E-01	8.2833757E-03	-2.0456111E-04	1.5593417E-06
250.0	CG	-8.4805046E-01	9.4090230E-03	-2.8568490E-04	2.2422602E-06
247.5	CG	-7.2642203E-01	8.1824496E-03	-2.8268492E-04	2.2459857E-06
245.0	CG	-6.5612783E-01	6.7875563E-03	-2.1707944E-04	1.5846722E-06
242.5	CG	-6.6597424E-01	2.7245393E-03	-1.5978715E-05	-1.3299520E-07
240.0	CG	-6.6072056E-01	-1.2577502E-03	9.7645585E-05	-5.7767958E-07
237.5	CG	-6.0176936E-01	2.8474003E-03	-1.0201005E-04	7.5730092E-07
235.0	CG	-5.4877675E-01	5.8581426E-03	-3.6557634E-04	2.9237565E-06

		A	B	C	D
232.5	CG	-4.3357846E-01	2.2103656E-03	-1.6805791E-04	1.6315188E-06
230.0	CG	-2.7222728E-01	-1.2948653E-02	1.8274560E-04	-7.2605101E-07
330.0	GA	2.1356305E-02	-1.6810241E-03	0.	0.
327.5	GA	2.7220969E-02	-1.6944672E-03	0.	0.
325.0	GA	9.2255E77E-02	-6.4382664E-03	5.2996018E-05	0.
322.5	GA	3.2450328E-02	-1.9100982E-03	0.	0.
320.0	GA	1.0368779E-01	-7.3726242E-03	6.0839619E-05	0.
317.5	GA	8.6212352E-02	-7.0211050E-03	5.9306458E-05	0.
315.0	GA	6.4237748E-02	-6.3990564E-03	5.3585987E-05	0.
312.5	GA	8.3665282E-02	-7.4137491E-03	6.0825284E-05	0.
310.0	GA	9.5472590E-02	-8.1590031E-03	6.7120517E-05	0.
307.5	GA	1.1029513E-01	-9.5900568E-03	8.0136598E-05	0.
305.0	GA	4.6977075E-03	-2.4350778E-03	0.	0.
302.5	GA	-1.1802140E-03	-2.6237416E-03	0.	0.
300.0	GA	-1.6686689E-02	-2.5516626E-03	0.	0.
297.5	GA	7.4241002E-02	-1.0045007E-02	8.4386017E-05	0.
295.0	GA	8.6309828E-02	-1.1076249E-02	9.3731165E-05	0.
292.5	GA	1.1610428E-01	-1.2728172E-02	1.0745054E-04	0.
290.0	GA	-2.3136810E-03	-3.5535022E-03	0.	0.
287.5	GA	8.0267126E-02	-4.7808408E-03	0.	0.
285.0	GA	2.2748138E-01	-6.7222066E-03	0.	0.
282.5	GA	4.2346018E-01	-7.6687765E-03	0.	0.
280.0	GA	6.0973573E-01	-9.5260325E-03	0.	0.
277.5	GA	6.5972541E-01	-9.7110614E-03	0.	0.
275.0	GA	6.0401554E-01	-8.7753066E-03	0.	0.
272.5	GA	4.5137966E-01	-7.3233949E-03	0.	0.
270.0	GA	2.3450313E-01	-5.4976838E-03	0.	0.
267.5	GA	-2.2461387E-02	-3.5440937E-03	0.	0.
265.0	GA	-2.5611085E-01	-7.5410083E-03	7.7353756E-05	0.
262.5	GA	-7.3511005E-01	1.2960168E-02	-3.7885543E-04	3.0765081E-06
260.0	GA	-9.5057402E-01	1.5736237E-02	-4.2321093E-04	3.3949986E-06
257.5	GA	-1.1700989E+00	1.8830948E-02	-5.0356368E-04	4.0880391E-06
255.0	GA	-1.1303159E+00	1.9709517E-02	-5.2334419E-04	4.1989986E-06

		A	B	C	D
252.5	GA	-8.8643177E-01	8.8808708E-03	-3.3473206E-04	3.1437853E-06
250.0	GA	-7.5655489E-01	1.0067637E-02	-4.1862946E-04	3.8811433E-06
247.5	GA	-4.3085105E-01	-3.3414602E-03	-1.4254683E-04	2.1498458E-06
245.0	GA	-3.7287729E-01	-6.2132034E-03	6.2251857E-05	0.
242.5	GA	-3.7736548E-01	-3.9965485E-04	-5.0749282E-06	0.
240.0	GA	-3.4601998E-01	-1.5746059E-03	0.	0.
237.5	GA	-1.4196838E-01	-9.6815823E-03	-1.7920432E-05	1.1942879E-06
235.0	GA	-7.7934617E-02	-1.6354167E-02	1.4447413E-04	0.
232.5	GA	-7.7680523E-02	-1.5233111E-02	8.4471437E-05	7.4135546E-07
230.0	GA	-1.5571609E-01	-1.2065950E-02	-7.9684317E-05	2.2375890E-06
330.0	GU	6.7344693E-02	-2.4456351E-03	4.4383674E-05	-2.1564720E-07
327.5	GU	7.1954831E-02	-2.2451656E-03	3.4929626E-05	-1.3981986E-07
325.0	GU	7.2398222E-02	-1.9071269E-03	2.5961791E-05	-8.0200571E-08
322.5	GU	7.3901315E-02	-1.2057540E-03	3.9562279E-06	8.0753343E-08
320.0	GU	7.5208446E-02	-7.9414720E-04	-8.5554615E-06	1.7109640E-07
317.5	GU	7.5345413E-02	-4.8723454E-04	-1.6071630E-05	2.1752537E-07
315.0	GU	7.9029800E-02	-3.4574667E-04	-1.9369853E-05	2.3475972E-07
312.5	GU	7.7270088E-02	5.5548231E-04	-4.0924896E-05	3.6291488E-07
310.0	GU	9.0942995E-02	3.1223802E-04	-3.6003412E-05	3.2308006E-07
307.5	GU	1.0485183E-01	5.9357429E-04	-5.3267133E-05	4.8325744E-07
305.0	GU	1.3457659E-01	-9.7754029E-04	-2.1737058E-05	3.0541483E-07
302.5	GU	1.6650709E-01	-1.2513504E-03	-3.2001316E-05	4.2501717E-07
300.0	GU	1.9936065E-01	-1.7906655E-03	-3.1875795E-05	4.6929666E-07
297.5	GU	2.2797056E-01	-1.6520065E-03	-4.2254800E-05	5.3641555E-07
295.0	GU	2.2255434E-01	6.1622227E-04	-9.4622712E-05	8.6019514E-07
292.5	GU	2.1416596E-01	3.0791872E-03	-1.5068712E-04	1.2092143E-06
290.0	GU	2.2135382E-01	2.6014364E-03	-1.3110232E-04	1.0586835E-06
287.5	GU	1.6015992E-01	7.2533480E-03	-2.2820895E-04	1.6855181E-06
285.0	GU	1.1602856E-01	8.8253406E-03	-2.4487295E-04	1.7592423E-06
282.5	GU	4.0466311E-02	9.2922851E-03	-2.3269129E-04	1.6772689E-06
280.0	GU	-8.5422533E-02	9.3674458E-03	-1.7344166E-04	1.1387337E-06
277.5	GU	-1.4627152E-01	7.2652967E-03	-8.1761965E-05	3.9109749E-07
275.0	GU	-1.4241052E-01	3.0105090E-03	0.	0.

		A	B	C	D
272.5	GU	-1.8369147E-01	6.9856020E-03	-6.0865895E-05	1.0741213E-07
270.0	GU	-1.2715129E-01	4.7460350E-03	-3.5266818E-05	-1.1735453E-08
267.5	GU	1.5882338E-02	2.8609917E-03	-7.8288632E-05	4.1398799E-07
265.0	GU	2.9144639E-01	-9.8243667E-03	1.1017192E-04	-5.8439948E-07
262.5	GU	5.5053059E-01	-2.5242276E-02	3.8624518E-04	-2.2339888E-06
260.0	GU	6.7134587E-01	-3.4691932E-02	5.7410969E-04	-3.4331297E-06
257.5	GU	6.7117743E-01	-3.6508376E-02	6.1893065E-04	-3.7617166E-06
255.0	GU	5.4667548E-01	-2.9717816E-02	5.0330881E-04	-3.2195041E-06
252.5	GU	3.5445261E-01	-2.2006369E-02	3.8232211E-04	-2.4883644E-06
250.0	GU	9.1033374E-02	-1.6693530E-02	3.6273803E-04	-2.4439244E-06
247.5	GU	-1.8797114E-01	-3.0575979E-03	1.2919830E-04	-1.0293335E-06
245.0	GU	-4.2572802E-01	8.2992246E-03	-5.0593710E-05	-5.0318718E-08
242.5	GU	-3.7821973E-01	3.6756364E-03	8.5122215E-05	-1.0647369E-06
240.0	GU	-4.8762954E-01	8.2715169E-03	6.6439582E-05	-1.2153670E-06
237.5	GU	-4.6238313E-01	4.8424814E-03	1.4984806E-04	-1.7667720E-06
235.0	GU	-4.0969913E-01	5.6996550E-03	0.	0.
232.5	GU	-4.7617359E-01	2.2042170E-02	-3.2934202E-04	1.7600532E-06
230.0	GU	-3.1219944E-01	1.7964525E-02	-3.2859745E-04	2.2570409E-06
330.0	GC	2.4254621E-01	-9.1084853E-03	1.5053485E-04	-8.2520426E-07
327.5	GC	2.4615081E-01	-8.1668425E-03	1.2220416E-04	-6.1343127E-07
325.0	GC	2.4518450E-01	-6.6353207E-03	8.2936973E-05	-3.5319607E-07
322.5	GC	2.6429281E-01	-6.6714513E-03	7.8735708E-05	-3.2531196E-07
320.0	GC	2.7970849E-01	-5.7171479E-03	3.8808712E-05	0.
317.5	GC	3.1632565E-01	-7.6228522E-03	7.9335433E-05	-2.7319196E-07
315.0	GC	3.2611156E-01	-6.5115921E-03	4.2659402E-05	0.
312.5	GC	3.0057717E-01	-2.8142167E-03	0.	0.
310.0	GC	3.8840328E-01	-7.9973180E-03	8.2774652E-05	-3.2464502E-07
307.5	GC	4.3809137E-01	-8.9321283E-03	9.0153372E-05	-3.2432191E-07
305.0	GC	4.7560308E-01	-7.7006364E-03	5.7020627E-05	-1.2111701E-07
302.5	GC	5.7572574E-01	-9.5076353E-03	8.0972003E-05	-2.1019254E-07
300.0	GC	6.8759946E-01	-1.3912231E-02	1.7744614E-04	-6.9783712E-07
297.5	GC	8.1330105E-01	-1.4695834E-02	1.5315374E-04	-6.2399812E-07
295.0	GC	8.9805500E-01	-1.7158813E-02	2.1126383E-04	-1.0335550E-06

		A	B	C	D
252.5	GC	8.8C49851E-C1	-9.7136125E-C3	1.8373584E-C5	2.7203457E-07
250.C	GC	8.3419851E-C1	-9.6076024E-03	4.4528243E-C5	C.
247.5	GC	6.8538342E-01	-6.6255466E-03	2.7126267E-05	C.
245.C	GC	4.8945676E-C1	-4.0127917E-03	1.7390537E-05	C.
242.5	GC	2.6019112E-C1	3.2921352E-03	-1.2129002E-C4	8.8C207C4E-07
240.0	GC	8.9199230E-02	7.7252502E-03	-2.3045841E-04	1.7212514E-06
237.5	GC	-9.9420905E-02	8.5431888E-03	-1.8770415E-04	1.2737053E-06
235.0	GC	-3.2178844E-01	1.8986692E-02	-4.4014788E-04	2.9704717E-06
232.5	GC	-3.0122500E-01	8.1624391E-03	-2.1353891E-04	1.5987049E-06
230.C	GC	-3.1504267E-01	-3.2019273E-03	4.1829889E-05	-9.8033376E-09
227.5	GC	-3.5467441E-01	-5.4127407E-03	8.6097195E-06	6.1408739E-07
225.C	GC	-5.0300388E-01	-3.6075564E-04	-9.4753058E-05	1.2477924E-06
222.5	GC	-5.9125823E-01	-5.1283784E-03	2.5305060E-05	5.2861857E-07
220.C	GC	-6.5110490E-01	-7.5342960E-03	8.3429530E-05	2.5267733E-07
217.5	GC	-6.8324877E-01	-1.0477275E-02	1.5728688E-04	-3.3873738E-07
215.0	GC	-7.9117826E-01	-3.3810255E-03	3.1866244E-05	2.8276863E-07
212.5	GC	-7.8901769E-01	-1.2476463E-03	-1.5867806E-05	5.3624122E-07
210.C	GC	-6.9264796E-01	-9.7445228E-04	-7.0589233E-05	1.0416638E-06
207.5	GC	-6.3306658E-01	-2.3907155E-03	-3.0702859E-05	6.8889072E-07
205.0	GC	-6.0836931E-01	-2.8684022E-03	5.1129961E-05	-9.3034571E-08
202.5	GC	-5.6858394E-01	-3.2466614E-03	4.8026903E-05	C.
200.C	GC	-6.5852093E-01	6.5485252E-03	-2.3649698E-04	2.1933024E-06
197.5	GC	-5.7239099E-01	1.0493902E-03	-7.5186425E-05	9.0089556E-07
195.C	GC	-5.9569191E-01	3.0090463E-03	-1.0179313E-04	9.3471312E-07
192.5	GC	-4.6748219E-01	-1.5353766E-03	3.2248176E-05	-3.0015238E-07
190.C	GC	-2.4942320E-02	-1.9852675E-02	3.0848213E-04	-1.6027759E-06
330.C	GG	-5.5329891E-02	6.7621210E-04	-2.9636056E-06	2.1809296E-09
327.5	GG	-5.5329891E-02	6.7621210E-04	-2.9636056E-06	2.1809296E-09
325.C	GG	-5.5329891E-02	6.7621210E-04	-2.9636056E-06	2.1809296E-09
322.5	GG	-5.5329891E-02	6.7621210E-04	-2.9636056E-06	2.1809296E-09
320.C	GG	-5.5329891E-02	6.7621210E-04	-2.9636056E-06	2.1809296E-09
317.5	GG	-6.9213349E-02	8.7271088E-04	-4.3618817E-06	6.5965958E-09
315.C	GG	-6.9213349E-02	8.7271088E-04	-4.3618817E-06	6.5965958E-09

		A	B	C	D
312.5	GG	-6.9213349E-02	8.7271088E-04	-4.3618817E-06	6.5965958E-09
310.0	GG	-6.9213349E-02	8.7271088E-04	-4.3618817E-06	6.5965958E-09
307.5	GG	-8.3722656E-02	1.1222413E-03	-7.4876640E-06	2.3930384E-08
305.0	GG	-8.3722656E-02	1.1222413E-03	-7.4876640E-06	2.3930384E-08
302.5	GG	-8.3722656E-02	1.1222413E-03	-7.4876640E-06	2.3930384E-08
300.0	GG	-9.7274703E-02	1.2702534E-03	-7.4819378E-06	1.8761456E-08
297.5	GG	-9.7274703E-02	1.2702534E-03	-7.4819378E-06	1.8761456E-08
295.0	GG	-9.7274703E-02	1.2702534E-03	-7.4819378E-06	1.8761456E-08
292.5	GG	-8.3722656E-02	1.1222413E-03	-7.4876640E-06	2.3930384E-08
290.0	GG	-5.5325691E-02	6.7621210E-04	-2.5636056E-06	2.1809256E-09
287.5	GG	-1.3883455E-02	1.9645878E-04	-1.3982761E-06	4.4156661E-09
285.0	GG	4.0992345E-02	-5.0983026E-04	2.7367188E-06	-6.3771078E-09
282.5	GG	1.1076439E-01	-1.4155653E-03	7.9169081E-06	-1.8252375E-08
280.0	GG	2.0912486E-01	-2.7523664E-03	1.6558843E-05	-4.4545670E-08
277.5	GG	3.4817764E-01	-4.5508158E-03	2.7050112E-05	-7.1056983E-08
275.0	GG	5.0164056E-01	-6.5784875E-03	3.9281348E-05	-1.0423713E-07
272.5	GG	5.2970231E-01	-6.9760301E-03	4.2401404E-05	-1.1640199E-07
270.0	GG	5.1575146E-01	-6.7559279E-03	4.0093929E-05	-1.0434687E-07
267.5	GG	4.7274272E-01	-6.1633870E-03	3.6837882E-05	-1.0004774E-07
265.0	GG	4.1569654E-01	-5.1937129E-03	2.6150686E-05	-4.5026888E-08
262.5	GG	2.0873108E-01	-2.7015835E-03	1.5635537E-05	-4.0020923E-08
260.0	GG	-1.3883459E-02	1.9645878E-04	-1.3982761E-06	4.4156661E-09
257.5	GG	-3.3373549E-01	4.3208529E-03	-2.4833529E-05	6.1362645E-08
255.0	GG	-6.5419959E-01	8.5685938E-03	-5.1279974E-05	1.3775329E-07
252.5	GG	-8.4981866E-01	1.1129307E-02	-6.6331460E-05	1.7529411E-07
250.0	GG	-9.5221850E-01	1.2771135E-02	-8.1327228E-05	2.3931773E-07
247.5	GG	-8.7772979E-01	1.1507346E-02	-6.9014903E-05	1.8614223E-07
245.0	GG	-7.2370778E-01	9.4462457E-03	-5.5965360E-05	1.4768342E-07
242.5	GG	-5.4319206E-01	7.1217459E-03	-4.2836374E-05	1.1569291E-07
240.0	GG	-3.4817764E-01	4.5506158E-03	-2.7050112E-05	7.1056983E-08
237.5	GG	-1.9231934E-01	2.2086514E-03	-9.6137969E-06	1.7514703E-08
235.0	GG	-1.3883459E-02	1.9645878E-04	-1.3982761E-06	4.4156661E-09
232.5	GG	1.5278608E-01	-1.9754479E-03	1.1412932E-05	-2.9210241E-08

		A	B	C	D
330.0	GG	2.3718621E-01	-3.1495090E-03	1.9718899E-05	-5.7110530E-08
330.0	U	8.0641315E-02	2.8981303E-04	-5.5335506E-06	0.
327.5	U	8.4770175E-02	2.6581960E-04	-5.4843773E-06	0.
325.0	U	8.5528937E-02	4.2154114E-04	-7.2068714E-06	0.
322.5	U	8.6472367E-02	5.8389632E-04	-8.8483161E-06	0.
320.0	U	9.0491147E-02	7.0585358E-04	-1.0647982E-05	0.
317.5	U	9.8297725E-02	6.3187187E-04	-1.0514593E-05	0.
315.0	U	1.0470025E-01	6.1303766E-04	-1.0612277E-05	0.
312.5	U	1.0276348E-01	1.5227922E-03	-4.4750011E-05	2.4285472E-07
310.0	U	1.0926671E-01	2.0081459E-03	-4.4777173E-05	2.3588586E-07
307.5	U	1.1786262E-01	1.6295628E-03	-3.1011414E-05	1.4272553E-07
305.0	U	1.3240607E-01	1.0895464E-03	-1.3555075E-05	2.0811922E-08
302.5	U	1.4934827E-01	1.0344584E-03	-1.4877225E-05	4.4522820E-08
300.0	U	1.7829569E-01	2.2905651E-04	-2.0164158E-06	0.
297.5	U	2.1034565E-01	1.6385756E-04	-8.9283423E-06	8.3283308E-08
295.0	U	2.5450763E-01	-4.0987753E-04	5.8669858E-06	-2.9714374E-08
292.5	U	3.0836718E-01	-9.3749633E-04	1.9345500E-05	-1.3641843E-07
290.0	U	3.6959472E-01	-1.7111518E-03	3.8713745E-05	-2.9321833E-07
287.5	U	4.3370891E-01	-1.0005900E-03	9.8357462E-06	-9.3347695E-08
285.0	U	4.9244229E-01	-1.3429819E-03	1.3896685E-05	-1.2350491E-07
282.5	U	5.4126336E-01	-2.1998130E-03	2.2063889E-05	-1.1564445E-07
280.0	U	5.4408481E-01	-4.0191701E-03	5.3834414E-05	-3.0228327E-07
277.5	U	4.4596716E-01	-1.4219937E-03	-1.5842259E-05	1.3863571E-07
275.0	U	3.2674140E-01	-2.7534905E-03	7.1157675E-06	0.
272.5	U	1.5851545E-01	-3.6153352E-03	1.8909568E-05	0.
270.0	U	-2.3185894E-02	-4.4225837E-03	4.5073036E-05	-1.9079080E-07
267.5	U	-2.2925146E-01	-3.4704217E-03	1.7056618E-05	-6.2924089E-09
265.0	U	-4.7456114E-01	-4.0855976E-04	-1.4823823E-05	0.
262.5	U	-7.0452079E-01	6.2155175E-04	-1.2629067E-05	0.
260.0	U	-8.8515641E-01	2.5810705E-04	2.2153708E-06	0.
257.5	U	-1.0642165E+00	6.1336188E-03	-1.2283148E-04	8.1434661E-07
255.0	U	-1.1574610E+00	7.5760211E-03	-1.1622515E-04	6.2096481E-07
252.5	U	-1.1990006E+00	7.7163758E-03	-9.6761810E-05	4.8859426E-07

		A	B	C	D
250.0	U	-1.1427705E+00	7.0618467E-03	-1.0706550E-04	7.1171158E-07
247.5	U	-1.0464765E+00	7.7046421E-03	-1.2226175E-04	7.8215123E-07
245.0	U	-8.8761364E-01	5.3406600E-03	-2.7990887E-05	0.
242.5	U	-6.8047905E-01	2.3395661E-03	0.	0.
240.0	U	-5.1306816E-01	2.0222629E-03	0.	0.
237.5	U	-3.6698518E-01	2.5040803E-03	-5.9369831E-06	0.
235.0	U	-2.2741765E-01	-1.3355261E-03	9.5639950E-05	-6.7250887E-07
232.5	U	-1.5754669E-01	1.4418503E-03	3.5571540E-05	-2.7462403E-07
230.0	U	-7.2919868E-02	2.4419151E-03	-6.1652265E-06	1.0608701E-08
330.0	C	6.2669510E-02	1.4660235E-02	-2.7886942E-04	1.3309540E-06
327.5	C	9.0960500E-02	1.3623273E-02	-2.6517284E-04	1.2888987E-06
325.0	C	1.1229123E-01	1.3254029E-02	-2.6573793E-04	1.3378843E-06
322.5	C	1.3749753E-01	1.2404364E-02	-2.5452700E-04	1.3081147E-06
320.0	C	1.6458038E-01	1.1674461E-02	-2.5053663E-04	1.3404142E-06
317.5	C	2.2776680E-01	4.1112012E-03	-5.1833027E-05	0.
315.0	C	2.5247111E-01	3.6336363E-03	-4.6708551E-05	0.
312.5	C	2.7603373E-01	3.2384863E-03	-4.1581763E-05	0.
310.0	C	2.8000032E-01	8.0615898E-03	-1.7919142E-04	9.5653403E-07
307.5	C	3.5267360E-01	2.3153960E-03	-3.2274585E-05	0.
305.0	C	3.9977340E-01	1.3988212E-03	-2.1655984E-05	0.
302.5	C	4.7253464E-01	1.1255016E-03	-2.0860118E-05	0.
300.0	C	5.4075297E-01	9.2791116E-04	-1.7387635E-05	0.
297.5	C	6.3732781E-01	5.3532363E-04	-1.6404526E-05	0.
295.0	C	7.5671431E-01	-6.1656456E-04	-7.6532207E-06	0.
292.5	C	8.8379759E-01	-2.8003030E-03	1.4611557E-05	0.
290.0	C	1.0170800E+00	-4.5983921E-03	2.3318180E-05	0.
287.5	C	1.0735380E+00	-6.3010022E-03	3.0446151E-05	0.
285.0	C	1.0027509E+00	-4.2616807E-03	0.	0.
282.5	C	9.1757204E-01	-4.7563359E-03	0.	0.
280.0	C	8.4570360E-01	-9.6255054E-03	5.1309370E-05	0.
277.5	C	6.5354430E-01	-8.9287223E-03	4.3713241E-05	0.
275.0	C	3.2806955E-01	-4.2856630E-03	0.	0.
272.5	C	1.3793738E-01	-9.1250241E-03	6.1118323E-05	0.

		A	B	C	D
270.0	C	-9.2129401E-02	-1.0264980E-02	1.1820986E-04	-4.3673398E-07
267.5	C	-3.3242674E-01	-7.5551180E-03	5.6191404E-05	-1.3495745E-08
265.0	C	-5.2578121E-01	-5.3439343E-03	-1.3055189E-05	5.1183608E-07
262.5	C	-7.1419649E-01	-1.8686388E-03	-1.1645029E-04	1.2390010E-06
260.0	C	-8.6401266E-01	-4.1602113E-03	-7.2841662E-05	1.1148370E-06
257.5	C	-9.9953779E-01	-5.3238583E-03	-3.2563286E-05	8.3236183E-07
255.0	C	-1.0844117E+00	-5.4256809E-03	-2.3360984E-05	7.2228687E-07
252.5	C	-1.1440373E+00	-7.3243003E-03	5.1166475E-05	2.1911191E-07
250.0	C	-1.1888177E+00	-9.5611974E-03	1.2055538E-04	-1.4008689E-07
247.5	C	-1.1584962E+00	-1.9326674E-02	3.7487242E-04	-1.7512012E-06
245.0	C	-1.1467869E+00	-1.9710873E-02	3.1789014E-04	-1.1590296E-06
242.5	C	-1.1575737E+00	-1.4945651E-02	1.6557372E-04	-2.3780586E-07
240.0	C	-1.1503034E+00	-1.0899754E-02	8.4111428E-05	0.
237.5	C	-1.1898171E+00	-9.5815604E-03	1.0088927E-04	0.
235.0	C	-1.2254525E+00	-8.9663573E-03	1.0174361E-04	0.
232.5	C	-1.1799237E+00	-1.1936827E-02	1.2504633E-04	0.
230.0	C	-9.6058147E-01	-1.8205829E-02	1.6809086E-04	0.
330.0	A	-8.4312161E-02	6.5915628E-04	0.	0.
327.5	A	-8.6829191E-02	6.7377542E-04	0.	0.
325.0	A	-9.3507656E-02	6.9295917E-04	0.	0.
322.5	A	-9.9951568E-02	7.4321115E-04	0.	0.
320.0	A	-1.0498563E-01	7.7244941E-04	0.	0.
317.5	A	-1.0750266E-01	7.8706855E-04	0.	0.
315.0	A	-1.1191501E-01	7.6102757E-04	0.	0.
312.5	A	-1.1241684E-01	6.9981639E-04	0.	0.
310.0	A	-1.1684555E-01	6.7423805E-04	0.	0.
307.5	A	-1.2308243E-01	4.9243445E-04	0.	0.
305.0	A	-1.2513303E-01	6.2581603E-04	0.	0.
302.5	A	-1.3190713E-01	4.4035250E-04	0.	0.
300.0	A	-1.3465787E-01	3.3528352E-04	0.	0.
297.5	A	-1.3334451E-01	1.9824241E-04	0.	0.
295.0	A	-1.4571020E-01	1.5915740E-04	0.	0.
292.5	A	-1.7108233E-01	3.1335522E-04	0.	0.

		A	B	C	D
290.0	A	-1.9742666E-01	4.0791695E-04	0.	0.
287.5	A	-2.3692877E-01	6.2546567E-04	0.	0.
285.0	A	-2.6604105E-01	7.0804093E-04	0.	0.
282.5	A	-2.8836644E-01	5.4815575E-04	0.	0.
280.0	A	-3.0707617E-01	4.8283229E-04	0.	0.
277.5	A	-3.1761255E-01	3.5055287E-04	0.	0.
275.0	A	-3.0593233E-01	3.2796408E-04	0.	0.
272.5	A	-2.6730158E-01	2.7377459E-05	0.	0.
270.0	A	-2.4700285E-01	1.6030669E-04	0.	0.
267.5	A	-2.0903834E-01	3.9693718E-04	0.	0.
265.0	A	-1.7006624E-01	5.9565250E-04	0.	0.
262.5	A	-1.1751775E-01	6.8381964E-04	0.	0.
260.0	A	-5.6327366E-02	7.3498660E-04	0.	0.
257.5	A	3.0550516E-02	5.9823256E-05	0.	0.
255.0	A	1.0146287E-01	-1.8273914E-04	0.	0.
252.5	A	1.6138359E-01	-3.8784905E-04	0.	0.
250.0	A	2.0719792E-01	-6.2146730E-05	0.	0.
247.5	A	2.2578307E-01	-1.3524239E-04	0.	0.
245.0	A	2.3622698E-01	-1.8549437E-04	0.	0.
242.5	A	2.3639662E-01	-3.5995868E-04	0.	0.
240.0	A	2.1833066E-01	-4.8066138E-04	0.	0.
237.5	A	1.8899615E-01	-2.7321944E-04	0.	0.
235.0	A	1.0163639E-01	1.7993252E-04	0.	0.
232.5	A	4.1446389E-02	3.5489947E-04	0.	0.
230.0	A	-3.2969463E-02	7.5377773E-04	0.	0.
330.0	G	-6.1935369E-02	3.8387682E-04	0.	0.
327.5	G	-6.4052563E-02	4.1546628E-04	0.	0.
325.0	G	-7.1905984E-02	4.6652823E-04	0.	0.
322.5	G	-7.8656168E-02	5.6414357E-04	0.	0.
320.0	G	-8.4146454E-02	6.3448129E-04	0.	0.
317.5	G	-9.3965504E-02	7.2339147E-04	0.	0.
315.0	G	-9.4210543E-02	6.9267761E-04	0.	0.
312.5	G	-9.5161313E-02	6.7247357E-04	0.	0.

		A	B	C	D
310.0	G	-1.0396550E-01	7.2335147E-04	0.	0.
307.5	G	-1.0954927E-01	7.4927371E-04	0.	0.
305.0	G	-1.1286227E-01	7.2986526E-04	0.	0.
302.5	G	-1.1476381E-01	6.8947717E-04	0.	0.
300.0	G	-1.2074507E-01	6.9835500E-04	0.	0.
297.5	G	-1.2712454E-01	6.5026180E-04	0.	0.
295.0	G	-1.3421054E-01	6.9267761E-04	0.	0.
292.5	G	-1.4028328E-01	6.5710115E-04	0.	0.
290.0	G	-1.4752105E-01	6.5628555E-04	0.	0.
287.5	G	-1.5829027E-01	7.4196432E-04	0.	0.
285.0	G	-1.6341224E-01	7.2655151E-04	0.	0.
282.5	G	-1.6451518E-01	7.0315646E-04	0.	0.
280.0	G	-1.7200078E-01	7.0557227E-04	0.	0.
277.5	G	-1.7252024E-01	5.4149314E-04	0.	0.
275.0	G	-1.7985088E-01	5.1315509E-04	0.	0.
272.5	G	-1.8202684E-01	3.3942173E-04	0.	0.
270.0	G	-1.9030935E-01	2.9095061E-04	0.	0.
267.5	G	-2.0115803E-01	2.1255025E-04	0.	0.
265.0	G	-2.0868333E-01	1.9802440E-04	0.	0.
262.5	G	-2.2641695E-01	4.1628362E-04	0.	0.
260.0	G	-2.3461134E-01	6.7576692E-04	0.	0.
257.5	G	-2.0870319E-01	1.2522068E-03	0.	0.
255.0	G	-1.7723515E-01	1.4365515E-03	0.	0.
252.5	G	-1.4429027E-01	1.5415661E-03	0.	0.
250.0	G	-5.3145541E-02	1.3871103E-03	0.	0.
247.5	G	-4.1675292E-02	1.3078634E-03	0.	0.
245.0	G	2.0264466E-02	9.2386266E-04	0.	0.
242.5	G	8.3495925E-02	3.7170464E-04	0.	0.
240.0	G	1.4402422E-01	8.7237653E-06	0.	0.
237.5	G	1.9918331E-01	-4.0025164E-04	0.	0.
235.0	G	2.3056429E-01	-5.2392171E-04	0.	0.
232.5	G	2.4516790E-01	-6.7265940E-04	0.	0.
230.0	G	2.1813997E-01	-4.6495060E-04	0.	0.

References

1. V. A. Ingram, The Biosynthesis of Macromolecules (W. A. Benjamin, Inc., New York, 1966).
2. H. G. Khorana, H. Büchi, H. Ghosh, N. Gupta, T. M. Jacob, H. Kössel, R. Morgan, S. A. Narang, E. Ohtsuka, and R. D. Wells, in Cold Spring Harbor Symposia on Quantitative Biology, 31, 39 (1966)
3. K. A. Marcker, R. F. C. Clark, and J. S. Anderson, in Cold Spring Harbor Symposia on Quantitative Biology, 31, 279 (1966).
4. P. Leder and H. Bursztyn, in Cold Spring Harbor Symposia on Quantitative Biology, 31, 297 (1966).
5. R. E. Thach, K. F. Dewey, J. C. Brown, and P. Doty, Science, 153, 416 (1966).
6. W. M. Stanley and S. Ochoa, Proc. Nat. Acad. Sci., U.S., 57, 1062 (1967).
7. F. H. C. Crick, J. Mol. Biol., 19, 548 (1966).
8. W. Fuller and A. Hodgson, Nature, 215, 817 (1967).
9. H. Hayashi and K. Miura, in Cold Spring Harbor Symposia on Quantitative Biology, 31, 63 (1966).
10. M. Deutscher, J. Biol. Chem., 242, 3601 (1967).
11. C. Lettendre, A. M. Michelson, and M. Grunberg-Manago, in Cold Spring Harbor Symposia on Quantitative Biology, 31, 71 (1966).
12. J. R. Fresco, A. Adams, R. Ascione, D. Henley, and T. Lindahl, in Cold Spring Harbor Symposia on Quantitative Biology, 31, 527 (1966).

References (Continued)

13. T. Lindahl, A. Adams, M. Geroch, and J. R. Fresco, Proc. Nat. Acad. Sci., U.S., 57, 178 (1967).

14. T. Lindahl, A. Adams, and J. R. Fresco, Proc. Nat. Acad. Sci., U.S., 55, 941 (1966).

15a. W. Gartland and N. Sueoka, Proc. Nat. Acad. Sci., U.S., 55, 948 (1966).

15b. T. Ishida and N. Sueoka, Proc. Nat. Acad. Sci., U.S., 58, 1080 (1967).

16. R. W. Holley, S. Apgar, G. A. Everett, J. T. Madison, M. Marquisse, S. H. Merrill, J. R. Penswick, and A. Zamir, Science, 147, 1462 (1965).

17. H. G. Zachau, D. Dütting, H. Feldmann, F. Melchers, and W. Karan, in Cold Spring Harbor Symposia on Quantitative Biology, 31, 417 (1966).

18. J. T. Madison, G. A. Everett, and H. K. Kung, in Cold Spring Harbor Symposia on Quantitative Biology, 31, 409 (1966).

19. T. H. Jukes, Biochem. Biophys. Res. Commun., 24, 744 (1966).

20. H. G. Zachau, D. Dütting, and H. Feldman, Angew. Chemie., 78, 392 (1966); Internatl. Ed., 5, 422.

21. U. L. RajBhandary, S. H. Chang, A. Stuart, R. D. Faulkner, R. M. Hoskinson, and H. G. Khorana, Proc. Nat. Acad. Sci., U.S., 57, 751 (1967).

References (Continued)

22. J. T. Madison, G. A. Everett, and H. K. Kung, Science, 153, 531 (1966).

23. J. N. Davidson, The Biochemistry of the Nucleic Acids (Methuen and Co., Ltd., London, 1965).

24. J. D. Watson, Molecular Biology of the Gene (W. A. Benjamin, Inc., New York, 1965).

25. Y. Hayashi, S. Osawa, and K. Miura, Biochim. Biophys. Acta., 129, 519 (1966).

26. G. L. Brown in Progress in Nucleic Acid Research, 2, 260 (J. N. Davidson and W. E. Cohn, Eds., Academic Press, New York, 1963).

27. C. G. Brownlee and F. Sanger, J. Mol. Biol., 23, 337 (1967).

28. B. G. Farget and S. M. Weissman, Science, 158, 1695 (1967).

29. J. R. Fresco, B. M. Alberts, and P. Doty, Nature, 188, 98 (1960).

30. A. S. Spirin, J. Mol. Biol. 2, 436 (1960).

31. A. S. Spirin, Macromolecular Structure of Ribonucleic Acids (Reinhold Publishing Corp., New York, 1964).

32. H. DeVoe and I. Tinoco, Jr., J. Mol. Biol., 4, 500 (1962).

33. D. M. Crothers and B. H. Zimm, J. Mol. Biol., 9, 1 (1964).

34. O. Sinanŏglu and S. Abdulnur, Photochemistry and Photobiology, 3, 333 (1964).

References (Continued)

35. C. R. Cantor and I. Tinoco, Jr., J. Mol. Biol., 13 69 (1965).

36. C. R. Cantor, S. R. Jaskunas, and I. Tinoco, Jr., J. Mol. Biol., 20, 39 (1966).

37. C. R. Cantor and I. Tinoco, Jr. Biopolymers, 5, 821 (1967).

38. I. Tinoco, Jr., J. Am. Chem. Soc., 82, 4785 (1960); Errata in J. Am. Chem. Soc., 84, 5047 (1961).

39. W. Rhodes, J. Am. Chem. Soc., 83, 3609 (1961).

40. H. DeVoe, J. Chem. Phys., 41, 393 (1964).

41. A. M. Michelson, The Chemistry of Nucleosides and Nucleotides (Academic Press, New York, 1963).

42. P. Doty, H. Boedtker, J. R. Fresco, R. Haselkorn, and M. Litt, Proc. Nat. Acad. Sci., U.S., 45, 482 (1959).

43. M. M. Warshaw and I. Tinoco, Jr., J. Mol. Biol., 13, 54 (1965).

44. M. M. Warshaw and I. Tinoco, Jr., J. Mol. Biol., 19, 29 (1966).

45. Y. Inoue, S. Aoyaga, and K. Nakanishi, J. Am. Chem. Soc., 89, 5701 (1967).

46. W. Stanley, Jr., Ph.D. Thesis, University of Wisconsin (1964).

47. J. Applequist and V. Damle, J. Am. Chem. Soc., 88, 3895 (1966).

References (Continued)

48. K. Van Holde, J. Brahms, and A. M. Michelson, J. Mol. Biol., 12, 726 (1965).

49. M. Leng and G. Felsenfeld, J. Mol. Biol., 15, 455 (1966).

50. A. Adler, L. Grossman, and G. D. Fasman, Proc. Nat. Acad. Sci., U.S., 57, 423 (1967).

51. J. Brahms, J. C. Maurizot, and A. M. Michelson, J. Mol. Biol., 25, 465 (1967).

52. M. M. Warshaw, C. A. Bush, and I. Tinoco, Jr., Biochem. Biophys. Res. Commun., 18, 633 (1965).

53. D. Poland, J. N. Vournakis, and H. A. Scheraga, Biopolymers, 4, 223 (1966).

54. J. N. Vournakis, H. A. Scheraga, G. W. Rushizky, and H. A. Sober, Biopolymers, 4, 33 (1966).

55. J. Brahms, A. M. Michelson, and K. E. Van Holde, J. Mol. Biol., 15, 467 (1966).

56. J. T. Yang, T. Samejima, and P. K. Sarkar, Biopolymers, 4, 623 (1966).

57. D. N. Holcomb and I. Tinoco, Jr., Biopolymers, 3, 121 (1965).

58. I. Tinoco, Jr., Radiation Research, 20, 133 (1963).

59. C. A. Bush and I. Tinoco, Jr., J. Mol. Biol., 23, 601 (1967).

60. R. Davis and I. Tinoco, Jr., Biopolymers, in press.

61. D. Glaubiger, Ph.D. Thesis, University of California, Berkeley (1965).

References (Continued)

62. D. Glaubiger, D. Lloyd, and I. Tinoco, Jr., Biopolymers, in press.

63. P. O. P. Tsʻo, I. S. Melvin, A. C. Olson, J. Am. Chem. Soc., 85, 1289 (1963).

64. M. P. Schweizer, S. I. Chan, and P. O. Tsʻo, J. Am. Chem. Soc., 87, 5241 (1965).

65. P. O. P. Tsʻo and S. I. Chan, J. Am. Chem. Soc., 86, 4176 (1964).

66. S. I. Chan, M. P. Schweizer, P. O. P. Tsʻo, and G. M. Helmkamp, J. Am. Chem. Soc., 86, 4182 (1964).

67. A. D. Broom, M. P. Schweizer, and P. O. P. Tsʻo, J. Am. Chem. Soc., 89, 3612 (1967).

68. S. I. Chan, B. W. Bangerter, and H. H. Peter, Proc. Nat. Acad. Sci., U.S., 55, 720 (1966).

69. V. Luzzati, A. Mathis, F. Masson, and J. Witz, J. Mol. Biol., 10, 28 (1964).

70. C. C. McDonald and W. D. Phillips, Science, 144, 1234 (1964).

71. G. D. Fasman, C. Lindblow, and L. Grossman, Biochemistry, 3, 1015 (1964).

72. J. R. Fresco in Informational Macromolecules (H. J. Vogel, V. Bryson, and J. O. Lampen, Eds., Academic Press, New York, 1963).

73. H. Boedtker, J. Mol. Biol., 2, 171 (1960).

74. H. Boedtker, Biochim. Biophys. Acta., 32, 519 (1959).

References (Continued)

75. R. Haschemeyer, B. Singer, and H. Fraenkel-Conrat, Proc. Nat. Acad. Sci., U.S., 45, 313 (1959).

76. R. A. Cox and U. Z. Littauer, Nature, 184, 818 (1959).

77. H. Boedtker, Biochemistry, 6, 2718 (1967).

78. G. D. Fasman, C. Lindblow, and E. Seaman, J. Mol. Biol. 12, 630 (1965).

79. D. B. Millar and R. F. Steiner, Biochemistry, 5, 2289 (1966).

80. M. N. Thang, W. Guschlbauer, H. G. Zauchau, and M. Grunberg-Manago, J. Mol. Biol., 26, 403 (1967).

81. D. M. Crothers, N. R. Kallenbach, and B. H. Zimm, J. Mol. Biol., 11, 802 (1965).

82. J. Marmur and P. Doty, J. Mol. Biol., 5, 109 (1962).

83. J. R. Fresco, Tetrahedron, 13, 185 (1961).

84. W. Kauzmann in Advances in Protein Chemistry, 14, 1 (1959).

85. J. R. Fresco and E. Klemperer, Ann. N. Y. Acad. Sci., 81, 730 (1959).

86. R. C. Warner, J. Biol. Chem., 229, 711 (1957).

87. C. Schildkraut and S. Lifson, Biopolymers, 3, 195 (1965).

88. J. R. Fresco, L. C. Klotz, and E. G. Richards, in Cold Spring Harbor Symposia on Quantitative Biology, 28, 83 (1963).

References (Continued)

89. J. N. Vournakis and H. A. Scheraga, Biochemistry, 5, 2997 (1966).

90. S. W. Englander and J. J. Englander, Proc. Nat. Acad. Sci., U.S., 53, 370 (1965).

91. M. Printz and P. H. von Hippel, Proc. Nat. Acad. Sci., U.S., 53, 363 (1965).

92. J. Brahms, J. C. Maurizot, and A. M. Michelson, J. Mol. Biol. 25, 481 (1967).

93. P. O. P. Tso, S. A. Rapaport, and F. J. Bollum, Biochemistry, 5, 4153 (1966).

94. W. Fuller, F. Hutchinson, M. Spencer, and M. H. F. Wilkins, J. Mol. Biol., 27, 507 (1967).

95. S. Arnott, F. Hutchinson, M. Spencer, M. H. F. Wilkins, W. Fuller, and R. Langridge, Nature, 211, 227 (1966).

96. M. Spencer, W. Fuller, M. H. F. Wilkins, and G. L. Brown, Nature, 194, 1014 (1962).

97. M. Spencer and F. Poole, J. Mol. Biol., 11, 314 (1965).

98. D. R. Davies in Annual Review of Biochemistry (P. D. Boyer, Ed., Annual Reviews, Inc., Palo Alto, California, 1967), 36, 321.

99. J. Witz, L. Hirth, and V. Luzzati, J. Mol. Biol., 11, 613 (1965).

100. H. Lake and W. W. Beeman, Science, 156, 1371 (1967).

101. W. Fiers, R. DeWachter, L. Lepoutre, and L. Vandendriessche, J. Mol. Biol., 13, 451 (1965).

References (Continued)

102. E. K. F. Bautz and L. Heding, Biochemistry, 3, 1010 (1964).

103. P. K. Sarkar and J. T. Yang, J. Biol. Chem., 240, 2088 (1965).

104. T. L. V. Ulbricht, R. J. Swan, and A. M. Michelson, Chemical Communications, 3, 63 (1966).

105. C. R. Cantor, Ph.D. Thesis, University of California, Berkeley (1966).

106. F. Pochon and A. M. Michelson, Proc. Nat. Acad. Sci. U.S., 53, 1425 (1965).

107. M. Chamberlin, Personal communication, 1965.

108. M. M. Warshaw, Ph.D. Thesis, University of California, Berkeley (1965).

109. R. C. Davis, Ph.D. Thesis, University of California, Berkeley (1967).

110. G. Felsenfeld and H. T. Miles, Annual Review of Biochemistry (P. D. Boyer, Ed., Annual Reviews, Inc., Palo Alto, California, 1967), 36, 407.

111. A. Rich, D. R. Davies, F. H. C. Crick, and J. D. Watson, J. Mol. Biol., 3, 71 (1961).

112. K. A. Hartman, Jr., and A. Rich, J. Am. Chem. Soc., 87, 2033 (1965).

113. B. Tomlinson, Personal communication, 1965.

114. D. N. Holcomb, Personal communication, 1966.

115. R. F. Steiner and R. F. Beers, Jr., Polynucleotides (Elsevier Publishing Co., 1961).

References (Continued)

116. I. Tinoco, Jr., J. Am. Chem. Soc., 86, 297 (1964).

117. C. A. Bush and H. A. Scheraga, Biochemistry, 6, 3036 (1967).

118. P. D. Ross and R. L. Scruggs, Biopolymers, 3, 491 (1962).

119. R. F. Steiner and C. Kitzinger, Nature, 194, 1172 (1962).

120. M. A. Rawitscher, P. D. Ross, and J. M. Sturtevant, J. Am. Chem. Soc., 85, 1915 (1963).

121. J. Massoulié and A. M. Michelson, Biochim. Biophys. Acta., 134, 22 (1967).

122. J. M. Sturtevant, S. A. Rice, and E. P. Geiduschek, Disc. Faraday Soc., 25, 138 (1958).

123. S. Ochoa, C. Weissmann, P. Borst, R. H. Burdon, and M. A. Billeter, Federation Proc., 23, 1285 (1964).

124. D. W. McMullen, S. R. Jaskunas, and I. Tinoco, Jr., Biopolymers, 5, 589 (1967).

125. G. Felsenfeld and G. L. Cantoni, Proc. Nat. Acad. Sci. U.S., 51, 818 (1964).

126. G. Felsenfeld and G. Sandeen, J. Mol. Biol., 5, 587 (1962).

127. M. R. Lamborg and P. C. Zamecnik, Biochem. Biophys. Res. Commun., 20, 328 (1965).

128. M. R. Lamborg, P. C. Zamecnik, T. Li, J. Kägi, and B. L. Vallee, Biochemistry, 4, 63 (1965).

129. T. Samejima and J. T. Yang, Biochemistry, 3, 613 (1964).

References (Continued)

130. P. K. Sarkar and J. T. Yang, Biochemistry, 4, 1238 (1965).

131. R. Haselkorn and C. F. Fox, J. Mol. Biol., 13, 780 (1965).

132. M. Chamberlin, R. L. Baldwin, and P. Berg, J. Mol. Biol., 7, 334 (1963).

133. S. I. Chan, Personal communiction, 1967.

134. S. R. Jaskunas, C. R. Cantor, and I. Tinoco, Jr., submitted to Biochemistry (1968).

135. D. Kalafofsky and T. Nakamoto, Proc. Natl. Acad. Sci., U.S., 56, 1786 (1966).

136. M. N. Lipsett, L. A. Heppel, and D. F. Bradley, J. Biol. Chem., 236, 857 (1961).

137. E. F. Bautz and E. A. Bautz, Proc. Natl. Acad. Sci., U.S., 52, 1476 (1964).

138. R. E. Thach in Procedures in Nucleic Acid Research, (G. Cantoni and D. Davies, Eds., Harper and Row, Inc., New York, 1966).

139. Methods in Enzymology XII, Part A (L. Grossman and K. Moldave, Ed., Academic Press, New York, 1967).

140. A. Tissières, J. D. Watson, D. Schlesinger, and B. R. Hollingworth, J. Mol. Biol., 1, 221 (1959).

141. H. Fraenkel-Conrat, B. Singer, and A. Tsugita, Virology, 14, 54 (1961).

References (Continued)

142. S. Mandeles and G. Bruening, Biochemical Preparations, 12, 111 (1968).

143. R. V. Tomlinson and G. M. Tener, Biochemistry, 2, 697 (1963).

144. G. W. Rushizky and H. A. Sober, Biochem. Biophys. Res. Comm., 14, 276 (1964).

145. S. Mandeles and H. O. Kammen, Analytical Biochem., 17, 540 (1966).

146. I. Gillam, S. Millward, S. Blew, M. von Tigerstrom, E. Wimmer, and G. M. Tener, Biochemistry, 6, 3043 (1967).

147. P. Leder, M. F. Singer, and R. L. C. Brimacombe, Biochemistry, 4, 1561 (1965).

148. R. E. Thach and P. Doty, Science, 148, 632 (1966).

149. M. F. Singer and B. M. O'Brien, J. Biol. Chem., 238, 328 (1963).

150. N. M. Thanassi and M. F. Singer, J. Biol. Chem., 241, 3639 (1966).

151. L. Meites, Ed., Handbook of Analytical Chemistry (McGraw-Hill, New York, 1963), sec. 6, p. 10.

152. A. Savitzy and J. J. E. Golay, Analytical Chemistry, 36, 1627 (1964).

153. J. Hearst and H. Gray, Personal communication, 1967.

154. K. E. Van Holde and R. L. Baldwin, J. Phys. Chem., 62, 734 (1958).

References (Continued)

155. H. G. Tennent and C. F. Vilbrandt, J. Am. Chem. Soc., 65, 424 (1944).

156. M. N. Lipsett, J. Biol. Chem., 239, 1256 (1964).

157. M. N. Lipsett, J. Biol. Chem., 239, 1250 (1964).

158. S. Podder, Personal communication, 1967.

159. M. N. Lipsett, Proc. Natl. Acad. Sci., U.S., 46, 445 (1960).

160. H. T. Miles, J. Frazier, and F. M. Rottman, quoted in Reference 110.

161. P. Job, Ann. Chim., 9, 113 (1928).

162. G. Felsenfeld and A. Rich, Biochim. Biophys. Acta., 26, 457 (1957).

163. A. E. V. Haschemeyer and H. M. Sobell, Nature, 202, 969 (1964).

164. A. E. V. Haschemeyer and A. Rich, J. Mol. Biol., 27, 369 (1967).

165. K. Watenpaugh, J. Dow, L. H. Jensen, and S. Furberg, Science, 159, 206 (1968).

166. V. Sasisekharen and D. R. Davies, quoted in Reference 98.

167. M. Gellert, M. N. Lipsett, and D. R. Davies, Proc. Natl. Acad. Sci., U.S., 48, 2013 (1962).

168. P. J. Flory, Principles of Polymer Chemistry (Cornell University Press, Ithaca, New York, 1963), Ch. 8.

169. D. C. Phillips, Proc. Natl. Acad. Sci., U.S., 57, 484 (1967).

References (Continued)

170. H. Jacobson and W. H. Stockmayer, J. Chem. Phys., 18, 1600 (1950).

171. J. C. Wang and N. Davidson, J. Mol. Biol., 19, 469 (1966).

172. G. Cassani and J. F. Bollum, J. Am. Chem. Soc., 89, 4998 (1967).

173. W. Guschlbauer, Nature, 209, 258 (1966).

174. S. Nishumura, D. S. Jones, and H. G. Khorana, J. Mol. Biol., 13, 302 (1965).

175. E. Ohtsuka, M. Moon, and H. G. Khorana, J. Am. Chem. Soc., 87, 2956 (1965).

176. R. D. Wells, E. Ohtsuka, and H. G. Khorana, J. Mol. Biol., 14, 221 (1965).

177. C. Byrd, E. Ohtsuka, M. W. Moon, and H. G. Khorana, Proc. Natl. Acad. Sci., U.S., 53, 79 (1965).

178. C. C. Richardson, C. L. Schildkraut, H. V. Aposhian, and A. Kornberg, J. Biol. Chem., 239, 222 (1964).

179. J. Josse and A. Kornberg, J. Biol. Chem., 237, 1968 (1962).

180. H. K. Schachman, J. Adler, C. M. Radding, I. R., Lehman, and A. Kornberg, J. Biol. Chem., 235, 3242 (1960).

181. S. W. Englander and D. Crowe, Analytical Biochemistry, 12, 579 (1965).

182. M. Laskowski in The Enzymes, V (P. D. Boyer, H. Lardy, and K. Myrback, Ed., Academic Press, N.Y., 1961), p. 125.

References (Continued)

183. W. E. Rozzell and H. G. Khorana, J. Biol. Chem., 234, 2105 (1959).

184. H. S. Shapiro and E. Chargaff, Biochim. Biophys. Acta, 26, 596 (1957).

185. R. B. Inman and R. L. Baldwin, J. Mol. Biol., 5, 172 (1962).

186. W. Doerfler and D. S. Hogness, J. Mol. Biol. 14, 237 (1965).

187. M. J. Chamberlin and P. Berg, Proc. Natl. Acad. Sci., U.S., 48, 81 (1962).

188. M. J. Chamberlin, Federation Proceedings, 24, 1446 (1965).

189. R. Wake and R. L. Baldwin, J. Mol. Biol., 5, 201 (1962).

190. P. O. P. Tsŏ, S. A. Rapaport, and F. J. Bollum, Biochemistry, 5, 4153 (1966).

191. C. B. Klee, J. Biol. Chem., 242, 3579 (1967).

192. M. W. Guschlbauer, C. R. Acad. Sc. Paris, 265, 1422 (1967).